The involvement of single-stranded DNA, replication protein A, and the DNA double-strand break dose in the damage checkpoint of *Saccharomyces cerevisiae*

By

Christian Zierhut

A thesis submitted for the degree of Ph.D.

at

The University of London

September 2006

Cancer Research UK
London Research Institute
Clare Hall Laboratories
South Mimms
Herts EN6 3LD

and

Department of Biology
University College London
WC1E 6BT

ProQuest LLC
789 East Eisenhower Parkway
P.O. Box 1346
Ann Arbor, MI 48106-1346

I, Christian Zierhut, confirm that the work presented in this thesis is my own. Where information has been derived from other sources, I confirm that this has been indicated in the thesis.

Abstract

In response to DNA damage, eukaryotic cells activate a checkpoint signalling cascade, resulting in cell cycle arrest, stabilisation of replication forks and activation of repair. While many players in these pathways have been identified, little is known about the original sensors, or of the DNA structures involved. Because it is present in all checkpoint-inducing lesions, single-stranded DNA (ssDNA) is a good candidate for a common structure recognised by the DNA damage response.

The role of ssDNA in checkpoint activation in the yeast *Saccharomyces cerevisiae* was investigated using three different approaches. Firstly, an attempt was made to produce ssDNA independently of strand breaks by inducing replication-independent plasmid unwinding. Secondly, the effects of depleting the major ssDNA-binding complex, replication protein A (RPA) were analysed. Lastly, an assay to quantify ssDNA generated at a defined DNA double-strand break (DSB) was developed.

Despite extensive efforts, the first approach proved unsuccessful, as the method used did not generate unwound plasmid. Using the second approach, it was found that depletion of RPA did not inhibit checkpoint activation during replication stress. Furthermore, replication with limiting amounts of RPA led to rapid cell death and checkpoint activation that was mediated independently of the response to stalled replication forks. Lastly, at a defined DSB it was found that less ssDNA was being generated than had previously been estimated from results based on non-quantitative methods. Additionally, an element of dose dependency was observed in the checkpoint response to DSBs, with stronger and more rapid responses being generated by higher numbers of breaks. Formation of four DSBs resulted in checkpoint activation even in G1 arrested cells. Together, these results raise the possibility of a DNA damage checkpoint pathway largely independent of long tracts of RPA-coated ssDNA and show that checkpoint activation to DSB-damage is possible in G1.

Table of Contents

List of Figures

List of Tables

List of abbreviations

4-NQO	4-nitro quinoline
5-FOA	5-fluoro orotic acid
AP-site	apurine/apyrimidine site
APC	anaphase promoting complex
ARS	autonomously replicating sequence
ATP	adenosine 5'triphosphate
BER	base excision repair
bp	base pairs
BRCT	BRCA1 C-terminal
CDK	cyclin-dependent kinase
ChIP	chromatin immunoprecipitation
Clb	B-type cyclin in *S. cerevisiae*
Cln	G1 cyclin in *S. cerevisiae*
cs	cut site
Ct	threshold cycle
DDK	Dbf4 dependent kinase
DHFR	dihydrofolate reductase
DHJ	double Holliday junction
DNA	deoxyribonucleic acid
dNTP	deoxynucleotide phosphate
DSB	double strand break
dsDNA	double-stranded DNA
E. coli	Escherichia coli
FACS	fluorescence activated cell sorting
FEAR	Cdc14 early anaphase release
FHA	forkhead associated
G1	gap 1 in the cell cycle
G2	gap 2 in the cell cycle
Gy	Grays
H2A	histone H2A
HA	haemagglutinin epitope
HDR	homology directed repair
HJ	Holliday junction
HOcs	HO cut site/HO recognition site
HR	homologous recombination
HU	hydroxyurea
IR	ionising radiation
kb	kilobase
M	mitotic phase
MCM	minichromosome maintenance
MEN	mitotic exit network
MMR	mismatch repair
MMS	methyl methane sulphonate
MRX	Mre11-Rad50-Xrs2 complex
NER	nucleotide excision repair
NHEJ	non-homologous end joining
NPE	nucleoplasmic extract
nt	nucleotide(s)

ORC	origin recognition complex
PCNA	proliferating cell nuclear antigen
PCR	polymerase chain reaction
PI3KK	phosphoinositol 3-kinase like kinase
pre-IC	preinitiation complex
pre-RC	prereplicative complex
Q-PCR	quantitative PCR
RFC	replication factor C
RNA	ribonucleic acid
RNAi	RNA-interference
ROS	reactive oxygen species
S phase	synthetic phase
S. cerevisiae	*Saccharomyces cerevisiae*
S. pombe	*Schizosaccharomyces pombe*
SCF	Skp1/Cullin/F-box complex
SDSA	synthesis dependent strand annealing
SPB	spindle pole body
SSA	single strand annealing
SSB	single strand break
ssDNA	single-stranded DNA
SV40	simian virus 40
T-Ag	large T-antigen
TLS	translesion synthesis
ts	temperature sensitive
UV	ultraviolet irradiation
wt	wild type
X. laevis	*Xenopus laevis*
YPGal	rich medium with galactose
YPRaff	rich medium with raffinose

Acknowledgements

There are a number of people that were directly or indirectly involved in the work on this thesis, and that I would like to show my gratitude to.

Firstly, I would like to thank my supervisor John Diffley for the opportunity to work and learn in his lab. I am also very grateful for his great support, his guidance and his wealth of ideas. The large amount of intellectual freedom I was given in the pursuit of my projects is also very much appreciated.

Secondly, I would like to thank the members of my thesis committee, Simon Boulton and Alain Verreault, and all members of our lab, for their support and helpful discussions at countless occasions. Especially, I would like to thank Jose Antonio Tercero and Helene Debrauwere for providing some of the strains and plasmids used in this thesis. Also, I am very grateful to Anne Early, Lucy Drury, Jonathan Baxter and Gemma Alderton for reading manuscripts of this thesis and for providing very helpful comments.

Thirdly, I would like to thank all friends and colleagues at Clare Hall or elsewhere for their support during the time I spent here. I would especially like to mention Jessica and Alberto, Barbara, Cristina, Dirk, Kristina, Luke, Monica and Peter who have been responsible for most of the happy memories of the time spent here.

Last but not least, special thanks go to my family, my parents Angelika and Herbert, and my sister Mary, who have made this life and profession possible for me.

1 Introduction

1.1 The eukaryotic cell cycle

In eukaryotic cells, the passage from one cell division to the next follows a defined and universal pattern of distinct stages, termed the cell cycle (Figure 1.1A, Nasmyth, 1996; Nasmyth, 2001b; Murray, 2004). The cell cycle is divided into four main stages, the "gap" before DNA replication (G1), the DNA synthetic phase (S), the "gap" after DNA replication (G2), and cell division, the mitotic phase (M).

Cell morphology closely correlates with cell cycle stage in the budding yeast *Saccharomyces cerevisiae* (Figure 1.1B). This has allowed the detection of mutants defective in the progression from one stage to the next (Hartwell et al., 1970). Extensive characterisation of these mutants has since led to a high degree of understanding of cell cycle regulation in yeast. Many fundamental processes in cell cycle regulation are highly conserved in evolution. Therefore, the study of model organisms such as *S. cerevisiae* is also highly relevant for furthering our understanding of these processes in human cells (Nasmyth, 2001b).

The regulated progression from one cell cycle stage to the next is a necessity for cell viability. Specific regulatory mechanisms, termed cell cycle checkpoints, function to ensure the proper order of these events (Hartwell and Weinert, 1989; Murray, 2004). Furthermore, checkpoint controls are essential for the maintenance of genomic stability, and are thus key components in safeguarding against cancer formation (reviewed in O'Driscoll and Jeggo, 2006). In the following sections, descriptions of these processes will be presented. Special emphasis will be put on *S. cerevisiae*, the organism used in this study, and on the function of checkpoint controls elicited by DNA damage, the main theme of this work.

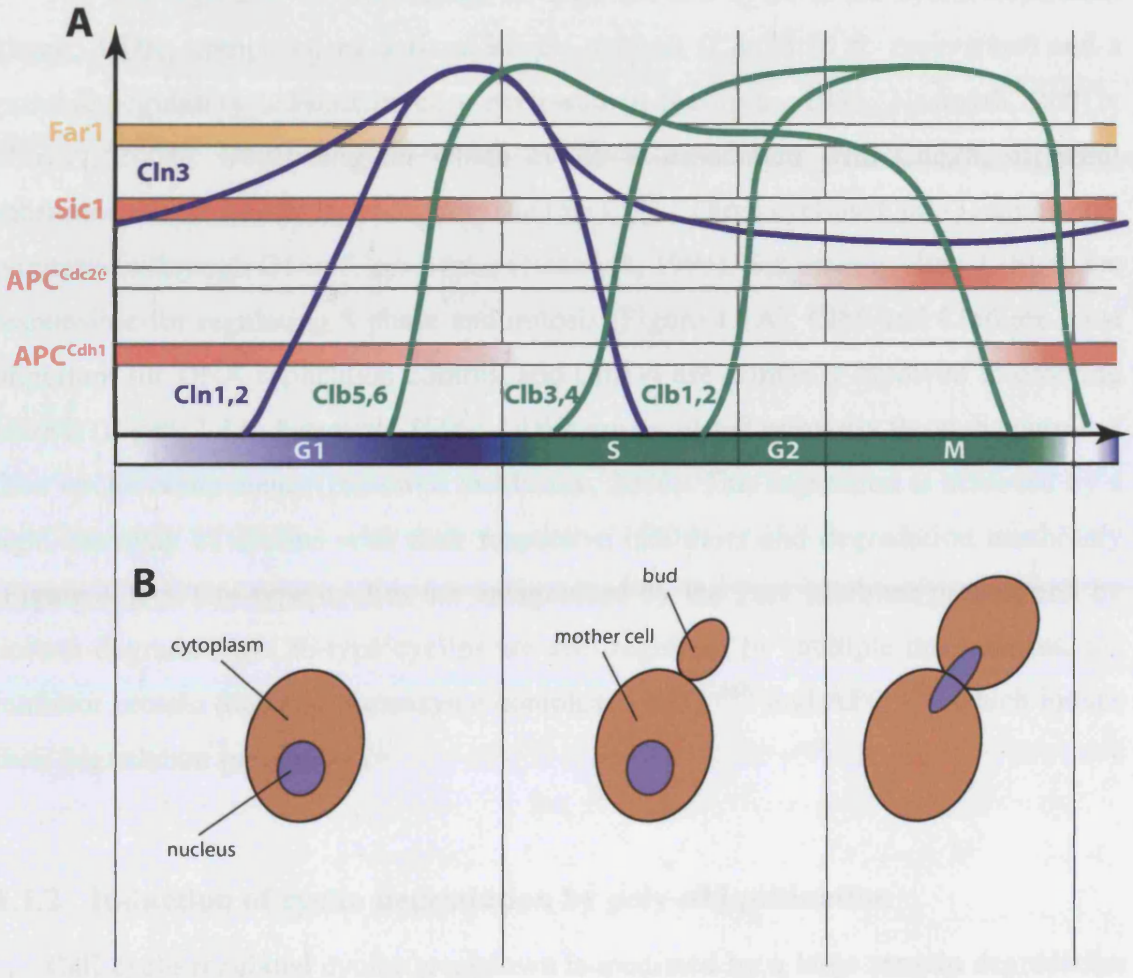

Figure 1.1: Simplified scheme of cell cycle regulation in *S. cerevisiae*. **A:** Diagram outlining the distribution of the different cyclin-CDK activities and their antagonists throughout the cell cycle. Curves represent the activity of the indicated cyclin-CDK complex, the bars in the background represent the distribution of the respective antagonists. Cln type cyclins are shown in blue; Clb type cyclins in green. The distribution of the Cln inhibitor Far1 is represented by the yellow bar; the distribution of the Clb inhibitor Sic1 and the Clb degradation complexes APC^{Cdc20} and APC^{Cdh1} are shown by red bars. **B:** Cell morphology during G1, S/G2, and M.

1.1.1 Regulation of cell cycle progression by cyclin-dependent kinases

The key regulator of progression through the cell cycle is the cyclin-dependent kinase, CDK, composed of a fixed kinase subunit (Cdc28 in *S. cerevisiae*) and a variable regulatory subunit (cyclin, reviewed in Nasmyth, 1996; Nasmyth, 2001b; Murray, 2004). Depending on which cyclin is associated with Cdc28, different substrates are preferentially phosphorylated by CDK. Three cyclins, Cln1-3, control the progression through G1 in *S. cerevisiae* (Nasmyth, 1996). Six other cyclins, Clb1-6, are responsible for regulating S phase and mitosis (Figure 1.1A). Clb5 and Clb6 are most important for DNA replication control, and Clb1-4 are primarily involved in ordering mitosis (Figure 1.1A, Nasmyth, 1996). CDKs are regulated primarily through control of their cyclin components (reviewed in Murray, 2004). This regulation is achieved by a tight interplay of cyclins with their respective inhibitors and degradation machinery (Figure 1.1A). Cln-type cyclins are antagonised by the Far1 inhibitor protein and by protein degradation. Clb-type cyclins are also regulated by multiple mechanisms, the inhibitor protein Sic1 and the enzyme complexes APC^{Cdc20} and APC^{Cdh1}, which induce their degradation (see below).

1.1.2 Induction of cyclin degradation by poly-ubiquitination

Cell cycle-regulated cyclin breakdown is mediated by a large protein degradation complex, the 26S proteasome (Glotzer et al., 1991). Recognition of proteins by the proteasome requires their modification by covalent attachment of multiple copies of a small (~8kDa) protein called ubiquitin (reviewed in Pickart and Eddins, 2004). At least three different enzymatic activities are required for ubiquitination. Individual ubiquitins are first attached to an E1 ubiquitin activating enzyme. The ubiquitin is then transferred to a conjugating enzyme (E2). E2 enzymes then associate with E3 ligases that directly transfer ubiquitins to target proteins. Substrate specificity is achieved mainly by the E3 enzymes, although conjugating enzymes can contribute to the specificity of the reaction (Pickart and Eddins, 2004). Ubiquitin moieties are attached to cysteine residues in the E1 and E2 enzymes, and to lysine residues in target proteins. Because the ubiquitin peptide itself contains a number or lysines, formation of multiubiquitin chains is possible (Pickart and Fushman, 2004). Depending on which lysine in ubiquitin is used for chain formation, differential outcomes on protein function and stability are achieved

(reviewed in Pickart and Fushman, 2004). The most common linkage, via K48, results in degradation by the proteasome.

Two different E3 ligases are responsible for ubiquitination of cyclins, the Skp1/Cullin/F-box complex (SCF) and the anaphase-promoting complex (APC), also known as the cyclosome (reviewed in (Harper et al., 2002; Willems et al., 2004). While all the G1 cyclins and Clb6 are SCF targets (reviewed in Willems et al., 2004; Jackson et al., 2006), all other cyclins (Clb1-5) are degraded following modification by the APC (reviewed in Harper et al., 2002).

1.1.2.1 The SCF

SCF complexes are composed of at least five subunits (protein names in brackets refer to the archetypical *S. cerevisiae* SCF): a cullin-like subunit (Cdc53), a ubiquitin-conjugating enzyme (Cdc34), a RING-finger E3 ligase (Rbx1/Roc1/Hrt1), a variable F-box adapter protein (most importantly Cdc4 and Grr1), and a linker-protein (Skp1) that connects the cullin with the F-box protein (reviewed in Willems et al., 2004). Substrates are recruited to SCF complexes by interaction with an F-box adapter protein that binds substrates on one side, and Cdc53 on the other side. Recognition of substrates is regulated by substrate phosphorylation (Skowyra et al., 1997; Willems et al., 2004). Two out of the total of 21 F-box proteins in the yeast genome, Cdc4 and Grr1, have so far been implicated in the turnover of cell cycle regulators. Cdc4 is required for the degradation of the Cln-inhibitor Far1 (Henchoz et al., 1997), the Clb-inhibitor Sic1 (Nash et al., 2001), and Clb6 (Jackson et al., 2006). Proteolysis of Cln1 and Cln2, on the other hand, appears to be mediated by Grr1 (Willems et al., 2004). Cln3 levels do not appear to be regulated by SCF-ubiquitination because no increased protein stability was observed upon shifting a temperature sensitive (ts) allele of *CDC34* to the restrictive temperature (Tyers et al., 1992).

1.1.2.2 The APC

The principal targets of the APC are Clb1-5. However, a number of other proteins involved in cell cycle control are also regulated by the APC (reviewed in (Harper et al., 2002).

APC and SCF complexes share some structural similarities. Both contain a cullin-like subunit, both contain a ubiquitin ligase subunit that is of the RING finger subclass

of ligases, and both require adapter proteins to allow substrate recognition (reviewed in (Reed, 2003). In the case of the APC, the cullin subunit is Apc2, and the ubiquitin ligase subunit is Apc11. Two different adapter proteins can interact with the APC during mitosis and are required for ubiquitination of substrates: Cdc20 and Cdh1 (reviewed in Harper et al., 2002). The timely activation of APC^{Cdc20} and the subsequent activation of APC^{Cdh1} are regulated by two differential mechanisms. Phosphorylation of the APC by CDK is required for association with Cdc20 (Rudner and Murray, 2000). Conversely, CDK-dependent phosphorylation of Cdh1 is inhibitory to its association with the APC (Zachariae et al., 1998).

1.1.3 G1 control

G1 is a period of cell growth in preparation of DNA replication and cellular division. It is also a period in which many external stimuli are recognised that can directly influence cell cycle control. For example, mating pheromone (a and α factor, see section 1.2.3.2) causes cells to arrest at this phase of the cell cycle. Furthermore, nutrient starvation also results in a cell cycle block in G1. In response to prolonged nutrient starvation, cells can also exit the cell cycle and enter a state that is known as G0 or quiescence (reviewed in Gray et al., 2004).

One of the characteristics of G1 is a very low amount of CDK activity. This is because Clb type cyclins were degraded as cells exited from mitosis in the previous cell cycle, and their transcription will not be reactivated until later in the cell cycle (Figure 1.1 A, B and Figure 1.2). Early in G1, the only cyclin gene that is transcribed is *CLN3*, in a mechanism depending on the transcription factor Mcm1 (McInerny et al., 1997). At the same time, however, the Far1 inhibitor of Cln3-CDK is produced (Jorgensen and Tyers, 2004). Throughout G1, Cln3 levels slowly increase, until Cln3-CDK can finally overcome Far1 inhibition through a double negative feedback loop (reviewed in (Jorgensen and Tyers, 2004), see Figure 1.2). Cell growth is thought to further enhance Cln3 activity and to repress Far1 function, allowing cells to achieve size homeostasis (Alberghina et al., 2004; Jorgensen and Tyers, 2004). Once a threshold level of Cln3 is reached, the G1/S transition, termed Start in yeast, is initiated. At this point, cells become committed to another round of DNA replication and mitosis.

Two parallel pathways mediate inhibition of Far1 by Cln3-CDK. Firstly, Cln3-CDK phosphorylates Far1, leading to its degradation in an SCF^{Cdc4} dependent fashion (Blondel et al., 2000). Secondly, Cln3-CDK activates transcription of *CLN1* and *CLN2*.

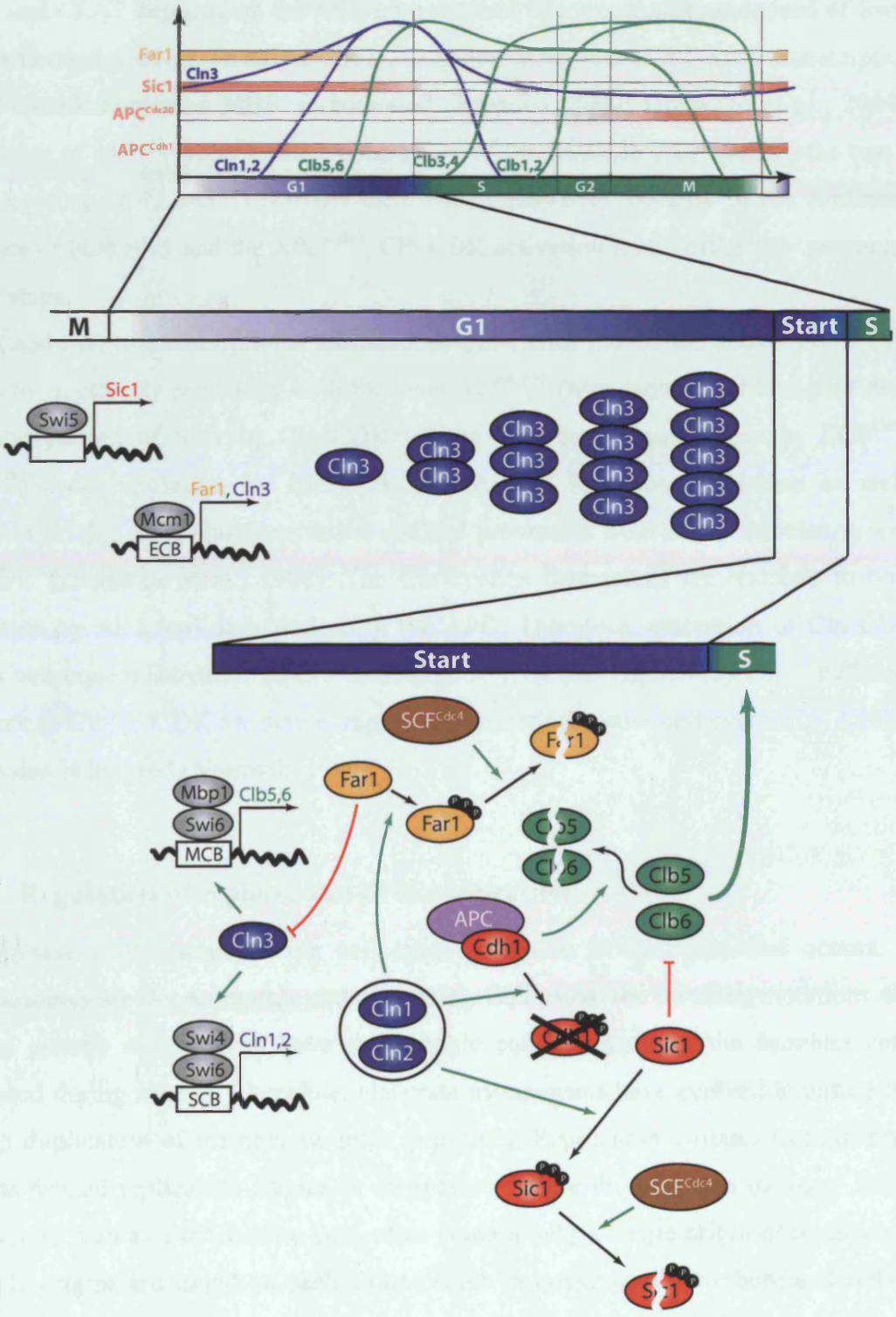

Figure 1.2: G1 control and the G1/S transition. Green arrows represent activating roles, red blunt arrows represent inhibition. Black arrows denote the transition of one state to another. Throughout G1, Cln3 levels gradually rise until they reach a threshold level (upper part). This triggers the transition through Start (lower part). See text for detailed explanations.

Cln1 and Cln2, in conjunction with Cdc28, further phosphorylate Far1. Transcription of *CLN1* and *CLN2* depends on the SBF transcription factor complex composed of Swi4 and Swi6 (reviewed in (Breeden, 2003). Concomitantly, the Mbp1-Swi6 transcription factor complex, termed MBF, is activated (Breeden, 2003; Costanzo et al., 2004). Activation of MBF results in the transcription of the first Clb type cyclins, the two S phase cyclins *CLB5* and *CLB6* (Breeden, 2003). However, because of the continued presence of both Sic1 and the APC^{Cdh1}, Clb-CDK activation is still efficiently prevented at this stage.

In addition to transcriptional stimulation, Cln-CDKs induce the activation of Clb-CDKs by negatively regulating both Sic1 and APC^{Cdh1} (Mendenhall and Hodge, 1998). Phosphorylation of Sic1 by Cln-CDK targets Sic1 for ubiquitination by SCF^{Cdc4}. APC^{Cdh1} downregulation by Cln-CDK is achieved by phosphorylation as well. However, in this case, phosphorylation of Cdh1 prevents it from stably associating with the APC (Zachariae et al., 1998). The Cln cyclins themselves are resistant to both inhibition by Sic1 and degradation by the APC. Therefore, activation of Cln-CDK allows subsequent activation of Clb-CDK (Figure 1.1A and Figure 1.2). Once sufficient amounts of Clb5,6-CDK are active, replication initiation ensues and eventually, Clb2-4 expression is induced (Nasmyth, 1996).

1.1.4 Regulation of S phase and DNA replication

S phase is the stage of the cell cycle in which DNA replication occurs. If chromosomes are not accurately and completely replicated, the resulting mutations and loss of genetic material can have catastrophic consequences for the daughter cells generated during mitosis. Therefore, elaborate mechanisms have evolved to ensure the correct duplication of the genome prior to mitosis. Replication initiates from distinct regions termed replication origins in all species. While the genomes of many lower organisms, such as *Escherichia. coli*, often contain only a single origin of replication, multiple origins are found on each chromosome in eukaryotes (Kornberg and Baker, 1992). *S. cerevisiae* is especially suited for studying DNA replication, because, in contrast to many other model organisms, replication origins are defined by essential sequence elements (reviewd in Diffley and Labib, 2002). Depending on the cell cycle stage, a number of other proteins that are required for replication initiation or elongation associate with origins (Diffley and Labib, 2002).

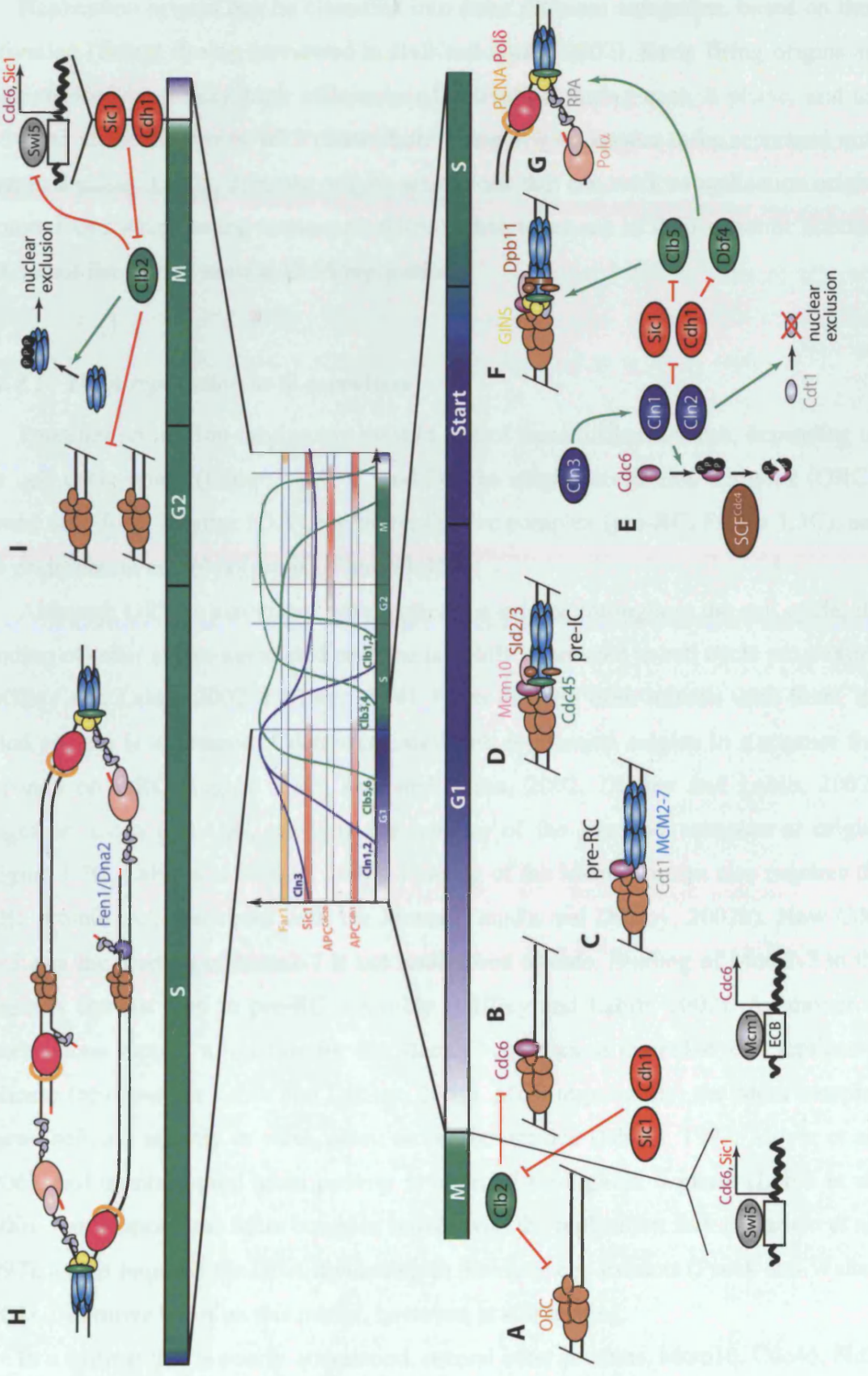

Figure 1.3: Regulation of DNA replication. See text for explanations. Note that in **H** the two lagging strands are shown to be slightly asynchronously processed. Whereas the one on the upper strand is still being replicated, the one on the lower strand is already being digested. RNA primers in **G** and **H** are shown in red.
The same colour scheme for arrows is used as in Figure 1.2.

Replication origins can be classified into three different categories, based on their activation (firing) timing (reviewed in Bell and Dutta, 2002). Early firing origins are characterised by a very high efficiency of activation during each S phase, and are activated at the beginning of S phase. Late firing origins appear to be repressed until later in S phase. Lastly, dormant origins are regions that can work as replication origins (autonomously replicating sequences, ARSs) when taken out of their genomic context, but do not fire during normal DNA replication.

1.1.4.1 DNA replication in S. cerevisiae

Potential replication origins can exist in one of three different states, depending on the cell cycle phase (Figure 1.3A, C, and D): the origin recognition complex (ORC)-bound only form (Figure 1.3A), the prereplicative complex (pre-RC, Figure 1.3C), and the preinitiation complex (pre-IC, Figure 1.3D).

Although ORC is associated with replication origins throughout the cell cycle, the binding of other origin-associated proteins is tightly connected to cell cycle progression (Diffley and Labib, 2002; Diffley, 2004). From the exit from mitosis until Start, the Cdc6 protein is expressed. Cdc6 associates with replication origins in a manner that depends on ORC (Figure 1.3B, Bell and Dutta, 2002; Diffley and Labib, 2002). Together, Cdc6 and ORC mediate the loading of the Mcm2-7 complex at origins (Figure 1.3C, Labib and Diffley, 2001). Loading of the Mcm complex also requires the Cdt1 protein that associates with the Mcms (Tanaka and Diffley, 2002b). How Cdt1 mediates the loading of Mcm2-7 is not understood to date. Binding of Mcm2-7 to the origin is the last step in pre-RC assembly (Diffley and Labib, 2002). A number of observations support a function for the Mcm2-7 complex as the eukaryotic replicative helicase (reviewed in Labib and Diffley, 2001). Most importantly, the Mcm complex shows helicase activity *in vitro*, albeit an inefficient one (Ishimi, 1997; Moyer et al., 2006), and uninterrupted Mcm activity is required throughout S phase (Labib et al., 2000). Furthermore, the Mcm complex moves with the replication fork (Aparicio et al., 1997), and is required for DNA unwinding in *Xenopus* egg extracts (Pacek and Walter, 2004). Definitive proof on this matter, however, is still lacking.

In a manner that is poorly understood, several other proteins, Mcm10, Cdc45, Sld2, Sld3, Dpb11, and the GINS complex (Sld5 and Psf1-3) associate with pre-RCs during G1 and together form the pre-IC (Figure 1.3D). Since complete pre-IC formation cannot be separated from replication initiation, detailed characterisation has not been possible

so far. Pre-IC proteins appear to associate with origins in two different ways. Both Dpb11 and the GINS complex require progression through Start for origin interaction, whereas all of its other components do not. No clear function has emerged for these proteins to date, although some functional indications exist (Bell and Dutta, 2002).

In addition to Clb-CDK, another protein kinase, Cdc7-Dbf4 (Dbf4-dependent kinase, DDK) is required for replication initiation (Figure 1.3E, reviewed in Bell and Dutta, 2002). Cdc7 is the kinase subunit of this complex, and Dbf4 has regulatory role. While Cdc7 protein levels are constant throughout the cell cycle, Dbf4 levels show strong variation. Dbf4 protein is only present from Start to mitosis, due to APC^{Cdh1}-mediated proteolysis during G1 (Ferreira et al., 2000). Although the essential substrates for DDK are not known, several lines of evidence indicate that alterations in the Mcm complex may be the ultimate outcome of DDK modification (Bell and Dutta, 2002).

By a mechanism that is very poorly understood, activation of both Clb-CDK and DDK eventually leads to origin firing, the first step of which is DNA unwinding (Hardy et al., 1997; Walter and Newport, 2000; Bell and Dutta, 2002; Diffley and Labib, 2002). Once origin DNA is unwound, polymerases are recruited and replisomes are assembled (Bell and Dutta, 2002).

Replication initiates with the synthesis of a short RNA primer (≤10nt) by the primase component of the Polα-primase complex (Diffley and Labib, 2002; Johnson and O'Donnell, 2005, Figure 1.3G). Subsequently, the DNA polymerase component of Polα takes over. In most systems, Polα-primase is recruited to replication forks via multiple protein protein interactions, such as with the replicative helicase and the single stranded DNA (ssDNA) binding complex RPA (replication protein A). Polα is an enzyme of low processivity, and is therefore soon replaced by the main replicative polymerase, Polδ (Diffley and Labib, 2002). Polδ, however, requires an auxiliary factor, proliferating cell nuclear antigen (PCNA), for optimal activity. PCNA, the sliding clamp of eukaryotic replication, forms a DNA encircling ring-like structure composed of three copies of Pol30 (Johnson and O'Donnell, 2005). PCNA binds to Polδ and tethers it to the DNA it is wrapped around, leading to increased processivity of the polymerase. Loading of PCNA on the primer end requires an additional protein complex, replication factor C (RFC, reviewed in Johnson and O'Donnell, 2005). RFC, composed of one large subunit and four smaller ones, binds to the 3'end of a primer/template junction and loads individual PCNA rings in an ATP hydrolysis dependent manner (Johnson and O'Donnell, 2005).

Polδ appears to be the main replicative helicase in eukaryotes. However, a second polymerase, Polε, may also contribute to processive DNA replication (Waga and Stillman, 1998). Some confusion exists concerning the exact function of this enzyme. This is because a full deletion of Polε is inviable, but a catalytically inactive mutant is viable (Waga and Stillman, 1998). The exact function of Polε in DNA replication is therefore not clear. In addition to their synthetic activity, Polδ and Polε contain proofreading activity that results in the removal and replacement of nucleotides that are incorrectly incorporated (Waga and Stillman, 1998).

As a consequence of the antiparallel nature of DNA, one strand is replicated continuously (leading strand synthesis) at each replication fork, whereas the other has to be replicated discontinuously (lagging strand synthesis, see (Diffley and Labib, 2002) and Figure 1.3H). Discontinuous synthesis leads to the formation of interrupted stretches of dsDNA, known as Okazaki fragments (reviewed in Hubscher and Seo, 2001). Since polymerases have the ability to displace strands when they meet a single strand/double strand junction, lagging strand synthesis will result in the formation of flap-like structures as the polymerase at one Okazaki fragment meets the 5' end of the previously replicated one (Figure 1.3H, upper part). This allows the replacement of the short RNA primers with DNA. Furthermore, this mechanism increases the fidelity of DNA replication because Polα, which is responsible for synthesising the beginning of each Okazaki fragment, does not contain proofreading activity and is thus more mutagenic than the main replicative polymerases. The flaps generated during lagging strand synthesis are processed by the flap endonucleases Fen1 (Rad27 in *S. cerevisiae*) and Dna2, resulting in the generation of nicked duplex DNA (reviewed in (Hubscher and Seo, 2001). Furthermore, the co-ordinated function of these nucleases requires RPA (Bae et al., 2001). In the final step of lagging strand synthesis, ligase I (Cdc9 in *S. cerevisiae*) mediates the ligation of successive Okazaki fragments (Hubscher and Seo, 2001).

1.1.4.2 The mechanism preventing rereplication

Replication must occur no more than once during each cell cycle. Because even a low amount of origin refiring can be a lethal event, a sophisticated mechanism has evolved to prevent origins that have fired during one S phase from being reactivated

until the initiation of the next S phase (reviewed in Diffley, 2004). The main purpose of this mechanism is to prevent the formation of new pre-RCs within that time.

The key player in preventing rereplication is CDK. CDK phosphorylation inhibits all three pre-RC components, ORC, Cdc6 and the Cdt1-Mcm complex (Labib et al., 1999; Drury et al., 2000; Nguyen et al., 2000; Nguyen et al., 2001; Tanaka and Diffley, 2002b; Blow and Dutta, 2005; Liku et al., 2005, see also Figure 1.3I). CDKs also regulate replication by co-ordinating the transcription profile of replication proteins (reviewed in Breeden, 2003), by regulating the degradation of Dbf4 (see above), and by inhibitory binding to Cdc6 (Mimura et al., 2004).

1.1.4.3 Insights into the biochemistry of DNA replication from other model systems

Two *in vitro* systems of replication, based on the gram negative bacterium *Escherichia coli* and simian virus 40 (SV40), are briefly described here because they directly relate to some aspects of the work described in this thesis.

E. coli

Much of our understanding of the basic principles of replication comes from work carried out on *E. coli* replication (Kornberg and Baker, 1992). *E. coli* chromosomal replication initiates from a single origin, *oriC* (Kornberg and Baker, 1992). Multiple copies of DnaA protein bind co-operatively to *oriC*. Association of DnaA with *oriC* results in the local melting of DNA adjacent to the DnaA binding sites, creating an open bubble structure. In a reaction that requires both DnaA and an accessory complex composed of DnaC proteins, this bubble structure is loaded with two copies of the replicative helicase, composed of hexameric rings of DnaB (Davey et al., 2002). Two heat shock protein like factors, DnaJ and DnaK, are also involved in this mechanism (Kornberg and Baker, 1992). Although their roles are not very clear in *oriC* replication, it appears that they prevent DnaA from forming inactive aggregates (Banecki et al., 1998). During phage lambda replication, however, their roles are well defined, and it was shown that they are required for releasing DnaB from the origin (Kornberg and Baker, 1992). During *oriC* replication, release of DnaB does not require DnaJ and DnaK (Kornberg and Baker, 1992), indicating that DnaJ and DnaK carry out different functions.

In the next step in *oriC* replication, the two DnaB hexamers migrate away from each other, allowing bidirectional DNA replication. DNA unwinding by DnaB is stimulated by the single stranded DNA binding protein, SSB (Baker et al., 1986; Biswas et al., 2002) and also requires the relief of superhelical tension generated in this process (Baker et al., 1986). Furthermore, DnaB is directly involved in recruiting DnaG, the *E. coli* primase (Kornberg and Baker, 1992). In the last step of initiation, DNA PolIII holoenzyme assembles at the synthesised RNA primer (Johnson and O'Donnell, 2005). The γ complex, composed of five subunits (three copies of the γ subunit, and the δ and δ' subunits) constitutes the apparatus that loads the polymerase processivity clamp, the β complex (Johnson and O'Donnell, 2005). Both sequence alignments and functional similarities indicate that the γ complex is the homologue of eukaryotic RFC (see above). Interestingly, alternative proteins can be synthesised from the gene encoding the γ subunits. These proteins, referred to as τ, contain all the γ sequences and an additional two domains at their C terminus. These two domains bind to DnaB and to the PolIII core, and thus allow for a connection between helicase and polymerase (Johnson and O'Donnell, 2005). No functional equivalents exist in eukaryotes, however. It is therefore unknown how polymerase and helicase are connected in eukaryotes.

Replication of SV40

SV40 replication has been used extensively as a model system to gain knowledge about the eukaryotic replication machinery (Kornberg and Baker, 1992). SV40 replication can be analysed in cell free extracts (Li and Kelly, 1984; Li and Kelly, 1985; Stillman and Gluzman, 1985) and in a reconstituted *in vitro* system with purified proteins (Waga et al., 1994; Waga and Stillman, 1994). However, because the SV40 genome encodes both the origin unwinding and the helicase activities, this system has not provided any insight into the regulation of these factors in eukaryotes. The two activities are contained on the same protein, large T-antigen (T-Ag, Fanning and Knippers, 1992). T-Ag binds to the origin of SV40 as double-hexameric structures. This results in the unwinding of an AT-rich region close to the origin in a reaction that requires ATP and RPA. Interestingly, work on an *in vitro* reconstituted system has shown that this step can be supported by heterologous RPA such as from *S. cerevisiae* (Brill and Stillman, 1989) and even by the *E. coli* single strand binding protein (Wold et al., 1987). In addition to RPA and ATP, topoisomerases are required in order to relieve

the superhelical stress generated during DNA unwinding (Kornberg and Baker, 1992). The next step, Polα-primase recruitment, requires regions on T-Ag and RPA. However, in this case, mammalian RPA is required for function and yeast RPA cannot support this step (Brill and Stillman, 1989) because this recruitment is mediated by species-specific protein protein interactions between T-Ag, RPA, and Polα-primase (Fanning and Knippers, 1992; Kornberg and Baker, 1992; Wold, 1997; Iftode et al., 1999).

Following priming, polymerases of higher processivity and fidelity than Polα take over. Polδ is essential for SV40 *in vitro* replication, and is thus thought to be the main polymerase at this stage of replication (Waga et al., 1994; Waga and Stillman, 1994). Interestingly, Polε is not required in this system (Waga et al., 1994; Waga and Stillman, 1994). Additional factors that are required for replication of SV40 *in vitro* are RFC and PCNA (Waga and Stillman, 1994)(see above).

T-Ag, being the defining component of SV40-specific replication, is highly regulated within the cell (Fanning and Knippers, 1992). Post-translational modifications affect its function both positively and negatively. One of the best-characterised stimulatory modifications is phosphorylation by CDK on T124 (McVey et al., 1989; McVey et al., 1993; Moarefi et al., 1993). Phosphorylation of this residue appears to activate the origin unwinding function of T-Ag (McVey et al., 1993; Moarefi et al., 1993). Additionally, two other kinases, CK2 and ATM have been suggested to positively regulate T-Ag by direct phosphorylation (Hubner et al., 1997; Shi et al., 2005). In the case of the CK2-dependent phosphorylation, this appears to enhance the efficiency of nuclear import of T-Ag (Shi et al., 2005). The mechanism by which the possible ATM-dependent phosphorylation works is not known so far. Phosphorylation is also used to negatively regulate T-Ag (Fanning and Knippers, 1992). Protein phosphatase 2A (PP2A) is required for SV40 replication, and is thought to promote the assembly of T-Ag double hexamers, at the origin (Virshup et al., 1989; Virshup et al., 1992).

1.1.5 Regulation of mitotic events

In many organisms, G2 is thought of as the period of time between the end of DNA replication and the onset of mitosis as judged by nuclear envelope breakdown and spindle formation (Smits and Medema, 2001). Since the nuclear envelope stays intact during mitosis and kinetochores are attached to microtubules throughout the cell cycle

(Winey and O'Toole, 2001), G2 is a relatively poorly defined stage in *S. cerevisiae*. A further aspect of the G2 phase of the cells of many species is a DNA damage induced checkpoint mechanism (see below, section 1.3) that results in the temporary downregulation of CDK activity and transient cell cycle arrest (reviewed in Smits and Medema, 2001). However, in response to DNA damage, *S. cerevisiae* cells arrest preferentially in metaphase, and maintain high levels of CDK activity (Foiani et al., 2000; Lowndes and Murguia, 2000). Therefore, the proteins that are important for the checkpoint response of other organisms by downregulation of CDK activity, either have no role in the budding yeast checkpoint (for example Cdc25/Mih1 and Wee1/Swe1), or are entirely absent from the genome (for example p53). A delay in G2 is only apparent when the morphogenesis checkpoint is activated in response to faulty nuclear positioning or cytoskeletal abnormalities (reviewed in Lew, 2000).

During mitosis, the cell's replicated genetic material is distributed between the prospective mother and daughter cells. Figure 1.4B outlines the main stages of mitosis that can be characterised cytologically (reviewed in Winey and O'Toole, 2001). During prophase, chromosomes, whose sister chromatids are connected by chromosomal cohesin, attach to the spindle apparatus. Metaphase is defined as the stage in which all chromosomes have been properly connected to the spindle and await their segregation. In early anaphase, triggered by the disruption of cohesion, sister chromatids are segregated to opposite poles of the nucleus (referred to as anaphase A). Later, the nucleus stretches to opposing ends of the mother and daughter cell (anaphase B). During the following telophase, the DNA masses are fully segregated. Lastly, mother and daughter cells become distinct entities by closing the budneck that connects the two (cytokinesis). Anaphase B, telophase and cytokinesis are closely connected to each other, and are sometimes hard to distinguish. As a consequence, the terms have sometimes been confusingly used in the literature.

1.1.5.1 Chromosome alignment on the mitotic spindle

Since chromosomes undergo equational division during mitosis (segregation of sister chromatids to opposite poles, see Figure 1.4B), sister kinetochores may not attach to the same spindle pole body (SPB). Correct attachment to opposite SPBs is referred to as chromosomal bi-orientation (Tanaka, 2002). Bi-orientation is thought to be achieved by a system that senses the tension generated between sister kinetochores (reviewed in Tanaka, 2002).

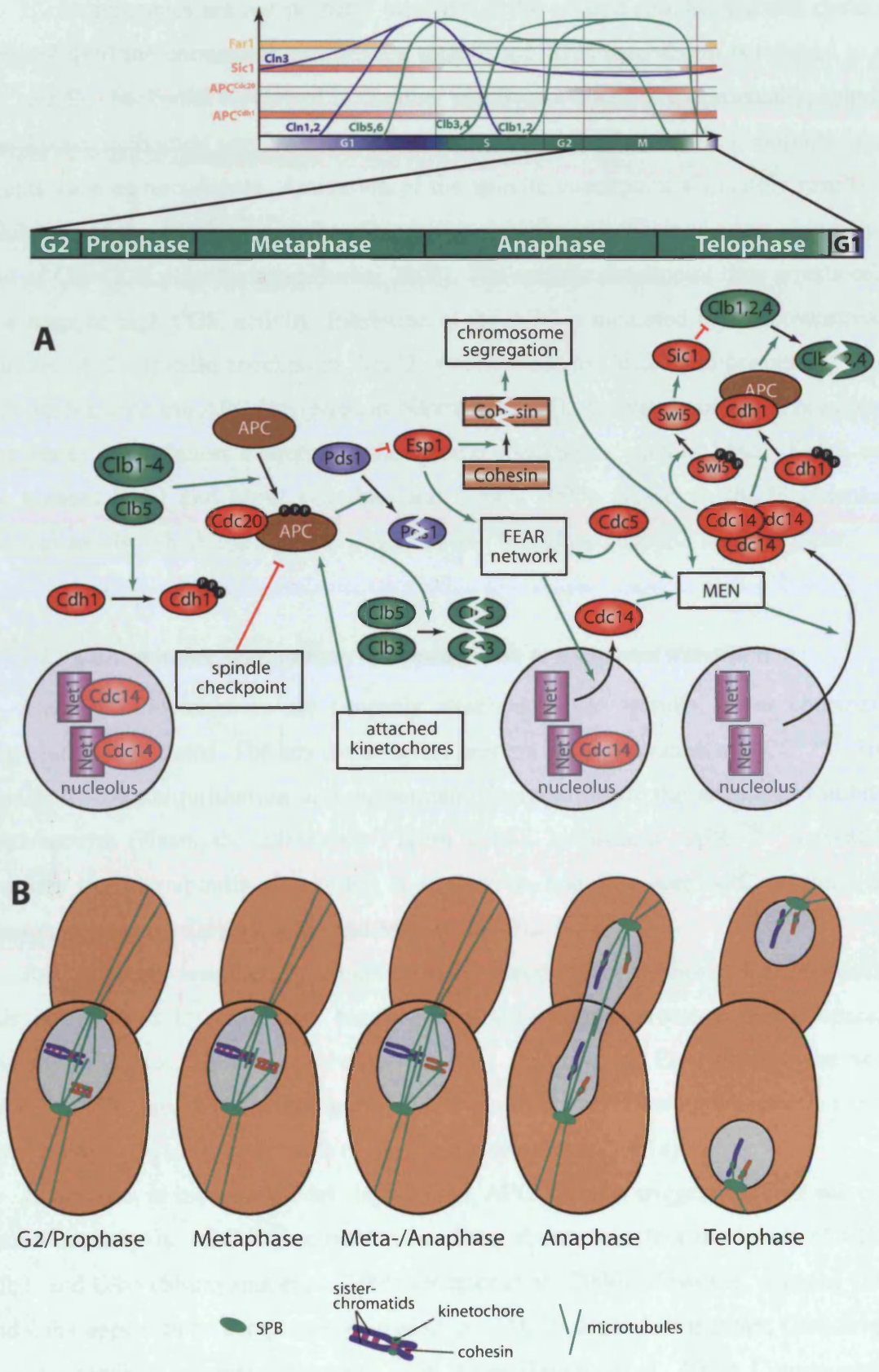

Figure 1.4: Regulation of mitotic events. **A:** Interplay between the key regulators of mitosis. Green arrows represent activating roles, red blunt arrows represent inhibition. Black arrows denote the transition of one state to another. **B:** Cellular anatomy from prophase until telophase.
See text for detailed explanations.

If chromosomes are not properly attached to the mitotic spindle, the cell cycle is delayed until the correct connections are established. This mechanism is referred to as the spindle checkpoint (reviewed in Gardner and Burke, 2000). Experimentally, spindle checkpoint activation can be induced by treatment with microtubule depolymerising agents such as nocodazole. Activation of the spindle checkpoint ultimately results in inhibition of the APC^{Cdc20} and therefore in the stabilisation of joined sister chromatids and of Clb-CDK (Gardner and Burke, 2000). The spindle checkpoint thus arrests cells at a stage of high CDK activity. Inhibition of the APC is mediated by the downstream effector of the spindle checkpoint, Mad2, which binds to Cdc20 and prevents it from functioning with the APC (reviewed in Nasmyth, 2005). Activation of Mad2 requires a number of other factors essential to the spindle checkpoint, such as Mad1, Bub3, and the kinases Bub1 and Mps1 (Gardner and Burke, 2000). However, the biochemical mechanisms by which the signal is generated and transduced are still not very clear.

1.1.5.2 Chromosome segregation: The metaphase to anaphase transition

Once all kinetochores are properly attached to the spindle, sister chromatid segregation is initiated. The key event in this process is the activation of APC^{Cdc20}. This results in the ubiquitination and subsequent degradation of the anaphase inhibitor Pds1/securin (Nasmyth, 2001a)(see Figure 1.4A). Importanly, APC^{Cdc20} activation requires that the spindle checkpoint is not active, and that core APC subunits are phosphorylated by CDK (Rudner and Murray, 2000).

Pds1 prevents anaphase by inhibiting sister chromatid separation. Mechanistically, this is achieved by inhibitory binding to a site-specific protease, Esp1/separase (Nasmyth, 2001a). Upon its activation by Pds1 degradation, Esp1 cleaves the Scc1 subunit of cohesin, thus disrupting the cohesin complex and allowing the spindle to pull sister chromatids to opposite ends of the nucleus (Nasmyth, 2001a).

In addition to mediating Pds1 degradation, APC^{Cdc20} also triggers the first wave of cyclin proteolysis. APC^{Cdc20} activation has been shown to affect the levels of Clb2, Clb3, and Clb5 (Shirayama et al., 1999; Baumer et al., 2000). However, whereas Clb5 and Clb3 appear to be completely degraded in a Cdc20-dependent manner, Clb2 levels are only partially affected (Shirayama et al., 1999; Baumer et al., 2000). Consequently, CDK remains active until mitotic exit (see below).

1.1.5.3 Exit from mitosis

Apart from activating anaphase onset by cleavage of Pds1, Esp1 is also required for other aspects of mitotic progression. In a non-proteolytic mechanism, Esp1 is responsible for the activation of the CDK antagonist Cdc14 during early anaphase (reviewed in D'Amours and Amon, 2004). Cdc14 is a phosphatase that specifically counteracts CDK (Visintin et al., 1998). During most of the cell cycle, Cdc14 is inactivated due to sequestration in the nucleolus by association with the nucleolar Cfi1/Net1 protein (Figure 1.4A, Shou et al., 1999; Visintin et al., 1999). Upon the metaphase to anaphase transition, Cdc14 is partially released from the nucleolus, resulting in the dephosphorylation of some CDK substrates. A network of proteins, termed the FEAR network (for Cdc Fourteen Early Anaphase Release), amongst which Esp1 is a key player, is required for this activation of Cdc14 (reviewed in D'Amours and Amon, 2004). Although Esp1 mediates this function in a non proteolytic manner, association with Pds1 is also inhibitory to this function (D'Amours and Amon, 2004). Degradation of Pds1 at the metaphase to anaphase transition thus allows both the separation of sister chromatids, and the release of Cdc14 from the nucleolus.

Amongst the substrates of Cdc14 at this stage are regulators of spindle stability, but also the Clb inhibitors Cdh1 and Sic1 (D'Amours and Amon, 2004)(see Figure 1.4A). Therefore, this partial release of Cdc14 early in anaphase allows proper spindle elongation, and also primes the cell for the complete CDK inactivation mediated during mitotic exit.

During late anaphase, a signal transduction cascade known as the mitotic exit network (MEN) triggers the complete release of Cdc14 from the nucleolus and thus initiates the second wave of Clb destruction (Bardin and Amon, 2001). Together, three different mechanisms appear to contribute to the activation of the MEN: the FEAR network, Cdc5, and nuclear positioning during anaphase (D'Amours and Amon, 2004).

The resulting increase in Cdc14 activity leads to the quantitative dephosphorylation of Cdh1 and allows the complete activation of the APC^{Cdh1} (Bardin and Amon, 2001). As a consequence, degradation of the remaining Clb cyclins is triggered. Another substrate of Cdc14 is the transcription activator Swi5 (Visintin et al., 1998). CDK-phosphorylated Swi5 is inactive because it is restricted to the cytoplasm (Moll et al., 1991). Therefore, dephosphorylation of Swi5 by Cdc14 allows Swi5 to enter the nucleus where, amongst others, it induces the transcription of *SIC1* and *CDC6* (Breeden, 2003; see also Figure 1.2, Figure 1.3A, B and I, and Figure 1.4A).

Induction of *SIC1* transcription by Swi5 allows the reaccumulation of Sic1, the Clb-CDK inhibitor (see above, sections 1.1.1-1.1.3). Sic1, by binding to Clb-CDK and inhibiting its function, further enhances CDK inactivation. Thus, the negative regulation of Cdh1 by CDK phosphorylation is restrained, and the equilibrium between CDK phosphorylation and Cdc14 dephosphorylation shifts further towards dephosphorylation. Concomitantly, Cdc14-dependent dephosphorylation of the newly produced Sic1 prevents it from being degraded by the SCF (see above, section 1.1.2.1). Depletion of the Clb pool by the APC further decreases Sic1 and Swi5 phosphorylation, and reaccumulation of Pds1 is also allowed because Cdc20 itself is a target for APC^{Cdh1}.

Once cells have passed through cytokinesis, two daughter cells (or rather, due to the asymmetric division in budding yeast, a mother and a daughter cell) are formed. In addition, the cyclin machinery is reset, thus allowing another cell cycle to commence.

1.2 The maintenance of genomic integrity I - DNA damage and repair

The faithful transmission of the genetic material does not only depend on the accurate replication and segregation of chromosomes. Cells must also be able to repair a large variety of DNA lesions. Elaborate mechanisms have evolved in order to coordinate the cell cycle and to allow the repair of damaged DNA.

Importantly, mutations in many genes that are involved in DNA repair and cell cycle control cause hereditary cancer predisposition in metazoans (reviewed in (Hoeijmakers, 2001; O'Driscoll and Jeggo, 2006). Therefore, the study of these basic mechanisms is important for our understanding of tumour biology, and may produce clues to cancer prevention and treatment.

1.2.1 DNA damage

DNA is constantly exposed to exogenous as well as endogenous sources of damage (reviewed in Friedberg, 2006). Both the bases and the sugar/phosphate backbone can be affected and this can lead to mutations and the loss of genetic material. Moreover, some lesions have the capacity to block the progression of DNA replication forks, and thus carry the potential danger of resulting in the segregation of under-replicated chromosomes.

Important exogenous sources of DNA damage are chemical mutagens taken up from the environment. One of these that is especially important for this study is methyl-methane sulfonate (MMS), which transfers methyl groups onto adenine, guanine and cytosine. If left unrepaired, these lesions can potentially lead to mutations by mispairing with other bases and/or cause stalling of DNA replication forks.

Other important exogenous sources of DNA damage are ultraviolet irradiation (UV) and ionising radiation (IR). Both UV and IR can either directly damage DNA or lead to lesions through the production of reactive oxygen species (ROS, Friedberg, 2006). Importantly, both single strand breaks (SSBs) and double strand breaks (DSBs) can be observed after IR treatment of cells. The proposed mechanism of SSB formation is by attack of the sugar/phosphate backbone of the DNA with OH radicals formed in IR water interactions (Friedberg, 2006). In alternative mechanisms, IR can also interact with bases and the sugar backbone directly, independently of ROS formation (Friedberg, 2006). DSBs are thought to be formed when two SSBs are induced close to each other on opposite strands. In addition, unrepaired SSBs will be transformed into

DSBs during DNA replication. Breaks that are induced by ionising radiation often do not contain the canonical 3'-OH at their termini, and may also contain damaged bases (Friedberg, 2006). This poses an additional problem for repair because these faulty nucleotides have to be excised before the breaks can be religated or repaired by other means. In addition to inducing DNA breaks, IR can also lead to the formation of faulty bases within otherwise undamaged DNA. The spectrum of DNA damage, induced mutagenesis and repair pathways activated upon IR treatment is therefore very diverse (Friedberg, 2006). IR treatment is often used to study the response to DSBs. However, one has to bear in mind that DSBs are only one of the many outcomes of IR treatment.

Similar to IR, treatment with UV results in a varied cocktail of lesions (Friedberg, 2006). The most frequent products are pyrimidine dimers (mostly T-T, but also T-C and C-C), but many other aberrations can also be the result of UV, albeit at a lower frequency. If left unrepaired, pyrimidine dimers will also inhibit the progression of replication forks.

Many anti-cancer treatments utilise DNA damaging agents. Importantly, localised treatment frequently makes use of IR, and alkylating agents such as MMS are often applied in systemic treatments. Moreover, mutations and DNA damage from both endogenous and exogenous sources are important and causative factors in tumour development. Therefore, comprehensive knowledge of the cellular responses to DNA damage is vital in understanding tumour biology and the mechanisms behind many anti-cancer treatments.

1.2.2 Repair of base and nucleotide damage

1.2.2.1 Base excision repair

Base excision repair is the primary repair pathway for oxidised, deaminated and alkylated bases, such as induced by MMS (Friedberg, 2006). A varied family of enzymes known as DNA glycosylases recognise modified bases and remove them from the deoxyribose that they are connected to by direct cleavage of the sugar-base bond, generating an AP site (Friedberg, 2006). In the following step, the damaged nucleotide is removed by AP-lyases or AP-endonucleases (reviewed in Boiteux and Guillet, 2004). In the final reactions, repair DNA synthesis fills the generated gap, and DNA ligase I (Cdc9) closes the remaining nick (Boiteux and Guillet, 2004). AP sites generated by

spontaneous hydrolysis of the N-glycosyl bond between base and deoxyribose are also processed in this manner.

1.2.2.2 Nucleotide excision repair (NER)

In contrast to base excision repair, in which case usually only the damaged nucleotide is being excised, nucleotide excision repair (reviewed in Prakash and Prakash, 2000) is characterised by the concerted removal of a ~30nt single stranded fragment containing the lesion. NER is a very versatile repair process that primarily recognises lesions that distort the DNA double helix, such as pyrimidine dimers, bulky adducts, and also intrastrand crosslinks.

Two different protein complexes have been suggested to be responsible for the initial damage detection, Rad14 and the Rad4-Rad23 complex (Prakash and Prakash, 2000). Furthermore, RPA has a function in this step as well, probably mediated in conjunction with Rad14. Following lesion recognition by these factors, the TFIIH complex is recruited. TFIIH contributes helicase activity to the NER machinery, resulting in the formation of a bubble structure produced by unwinding DNA around the lesion.

In the next step of NER, the Rad1-Rad10 and Rad2 endonucleases are recruited and specifically cleave the damaged strand on either side of the lesion at the dsDNA-ssDNA junction. Rad1-10 cleaves 5' of the lesion, and Rad2 introduces its cut 3' of the lesion (Prakash and Prakash, 2000). In the final stage of NER, the resulting gap is filled in by Polδ or Polε, and ligase I (Cdc9) joins the filled-in fragment with its surrounding strands.

1.2.2.3 Mismatch repair (MMR)

A mechanism known as mismatch repair (MMR) is responsible for replacing incorrectly inserted nucleotides (reviewed in Kunkel and Erie, 2005). MMR targets not only mismatches, but can also affect other lesions. Amongst these are certain base modifications and insertion deletion loops that arise from erroneous replication of repeat sequences (Kunkel and Erie, 2005).

In the first step of MMR, mismatches are recognised by a dimer of homologues of bacterial MutS protein (Msh2-Msh6 and Msh2-Msh3 in yeast). These then recruit a dimer of homologues of bacterial MutL (Mlh1-3 and Pms1 in yeast). Unfortunately, the

subsequent steps in MMR are less clear in eukaryotic cells. In prokaryotic systems, the MutH protein that gets recruited by MutS in conjunction with MutL, cleaves the newly replicated strand (that contains the erroneously inserted base, Kunkel and Erie, 2005; Friedberg, 2006). In *E. coli*, after cleavage formation, helicase and endo-/exonuclease activities remove a fragment of up to ~1000nt embedding the mismatch (Friedberg, 2006). The resulting gap is filled in by PolIII and DNA ligase (Friedberg, 2006).

No homologues of MutH have so far been identified in eukaryotes. Furthermore, no helicases have yet been shown to be involved in MMR. Some information exists, however, about the MMR nucleases that degrade the displaced strand containing the mutation. This process appears mainly to be carried out by Exo1 and Rad27/Fen1 (Kunkel and Erie, 2005).

1.2.2.4 Translesion synthesis (TLS)

As mentioned earlier, base lesions and abasic sites that are not repaired have the potential of stalling DNA replication forks because the replicative helicases Polα, δ and ε are usually unable to synthesise across non-conventional bases (reviewed in (Kunz et al., 2000). In order to rescue such replication forks, cells can utilise one of several polymerases that have the ability to synthesise across a wide number of DNA modifications (Kunz et al., 2000; Prakash et al., 2005). These polymerases, termed translesion polymerases, are usually characterised by decreased selectivity and processivity and the absence of proofreading activity (Prakash et al., 2005).

In addition, some TLS polymerases can not only bypass a number of lesions, but can also extend 3' ends that are not perfectly base paired (Prakash et al., 2005). Especially in the extension of nucleotides incorporated opposite damaged bases, which often are characterised by imperfect base pairing and other aberrant structures, is this function important (Prakash et al., 2005).

Three TLS polymerases have so far been described in *S. cerevisiae*, Polη (Rad30), Polζ (Rev3-Rev7) and Rev1 (Kunz et al., 2000).

1.2.2.5 Other mechanisms of lesion bypass

In *E. coli*, forks that have collapsed at sites of DNA damage can be rescued by a specialised mechanism of DnaB reloading mediated by the PriA and PriC proteins (Sandler and Marians, 2000; Heller and Marians, 2005; Lovett, 2005; Heller and

Marians, 2006). Furthermore, homologous recombination (HR), together with PriA, can be used for restarting replication forks (Cox et al., 2000; Marians, 2004).

In eukaryotes, the situation is less clear, however. So far, it has not been possible to show that HR contributes to the restart of collapsed replication forks. In *E. coli*, whose one chromosome contains only a single replication origin, the collapse of one or both forks is a potentially lethal event, if origin-independent restarting mechanisms did not exist. However, since eukaryotic genomes contain a large number of replication origins on each chromosome, a collapsed replication fork could relatively easily be rescued by another, converging, fork. Only when a replication fork encounters a SSB or a DSB could recombination be envisaged to be essential for fork restart.

1.2.3 DNA double strand breaks

1.2.3.1 DSBs caused by DNA lesions

DSBs are thought to represent the most lethal of DNA lesions. Segregation of chromosomes containing unrepaired DSBs leads to the loss of a large amount of genetic information. If essential genes are lost, cell death is the result.

A number of mechanisms can be responsible for the formation of DSBs. Physiologically most important, perhaps, is the conversion of single strand breaks (SSBs) into DSBs when encountered by a replication fork (Figure 1.5A). SSBs arise very frequently during normal growth and can, for example, be caused by ROS-mediated breakage of the sugar-phosphate backbone of DNA, or by BER-mediated cleavage of AP sites (see above, section 1.2.2). Type I topoisomerases, which generate a nicked intermediate covalently attached to the enzyme, are other possible sources of SSBs (Wang, 2002). The reaction mechanism of type II topoisomerases includes the formation of a DSB intermediate (Wang, 2002), and can thus lead to break formation directly (Figure 1.5B). Since broken DNA is a relatively short lived intermediate in both type I and type II enzyme mediated reactions, its contribution to the DSB threat is probably a relatively minor one during normal growth. Several anti-cancer drugs, however, target topoisomerases and specifically block the steps following break formation (Wang, 2002). Other means of DSB formation can be exogenous sources such as IR (see above).

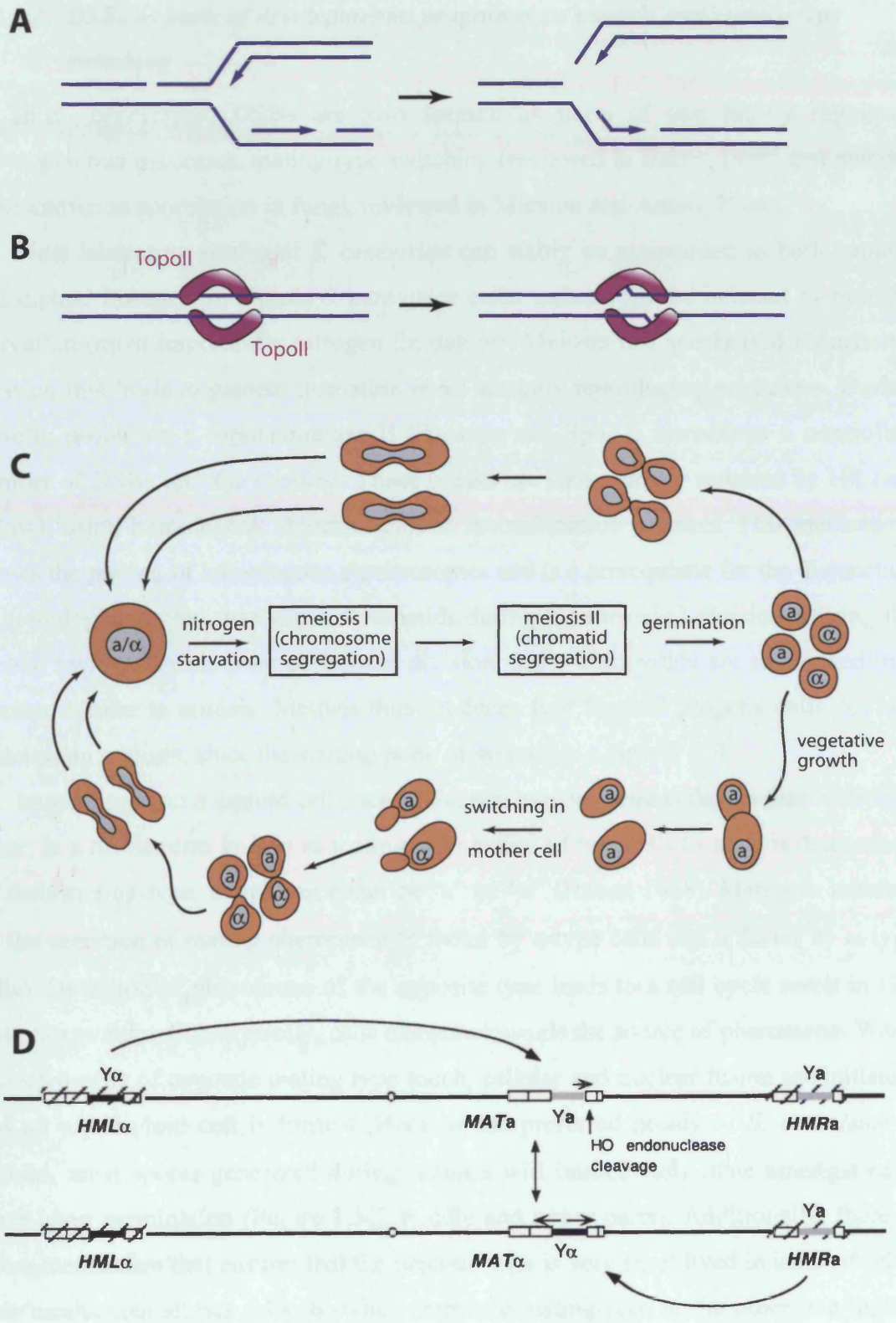

Figure 1.5: Mechanisms of DSB-formation and mating-type switching. See text for details.

1.2.3.2 DSBs as parts of developmental programmes: meiosis and mating-type switching

In *S. cerevisiae*, DSBs are also formed as parts of two highly regulated developmental processes, mating-type switching (reviewed in Haber, 1998) and meiosis (also known as sporulation in fungi, reviewed in Marston and Amon, 2004).

Most laboratory strains of *S. cerevisiae* can stably be maintained as both haploid and diploid lineages. In diploid *S. cerevisiae* cells, meiosis can be induced by nutrient starvation (most importantly nitrogen limitation). Meiosis is a specialised reductional division that leads to gamete formation in all sexually reproducing organisms. During meiotic prophase, a topoisomerase II-like enzyme, Spo11, introduces a controlled number of DSBs into the genome. These breaks are subsequently repaired by HR (see below), using homologous chromosomes as recombination partners. This mechanism allows the pairing of homologous chromosomes and is a prerequisite for the disjunction of homologues rather than sister chromatids during the meiosis I division. During the second meiotic division, an equational division, sister chromatids are segregated in a manner similar to mitosis. Meiosis thus produces four haploid progeny cells per cell undergoing meiosis, since the starting point of meiosis is a diploid cell.

In order to form a diploid cell once again, two haploid yeast cells can fuse with each other, in a mechanism known as mating. The ability of two cells to mate is determined by their mating-type, which can either be "a" or "α" (Haber, 1998). Mating is initiated by the secretion of mating pheromone (a factor by a-type cells and α factor by α-type cells). Detection of pheromone of the opposite type leads to a cell cycle arrest in G1, just prior to Start. Subsequently, cells elongate towards the source of pheromone. When two such cells of opposite mating type touch, cellular and nuclear fusion are initiated, and an a/α diploid cell is formed. Because the preferred ploidy of *S. cerevisiae* is diploid, most spores generated during meiosis will immediately mate amongst each other upon germination (Figure 1.5C, middle and upper parts). Additionally, there is also a mechanism that ensures that the haploid stage is very short lived in isolated cells. This mechanism allows cells to switch from one mating-type to the other in a highly regulated manner (Figure 1.5C, lower part). After a round of cellular division, mother cells undergo a switching event that is induced by expression of the *HO* gene (Haber, 1998). After the subsequent cell division, the four progeny cells generated from mother and daughter cell can mate and form two diploid cells.

Importantly, the protein encoded by *HO* is a site-specific endonuclease (Haber, 1998). HO has a very large recognition site that is uniquely accessible in the yeast genome. This site is localised in the region that determines a cell's mating type, the *MAT* locus on chromosome III (Figure 1.5D). Cleavage of the HO cut site (HOcs) at *MAT* triggers a gene conversion event (see below) in which a sequence at *MAT* is replaced with information stored in other regions of the genome, the silent mating-type loci *HML*α and *HMR*a (Figure 1.5D, see also Haber, 1998). Expression of these silenced loci and accessibility to HO is prevented by a stable heterochromatin state. Importantly, there is directionality in the recombination reaction, in that *MAT*a will preferentially recombine with *HML*α and vice versa (Haber, 1998). Since strains that are wild type for *HO* cannot stably be maintained as haploids, most laboratory strains carry inactive *HO* genes.

Mating-type switching has extensively been used as a model for DSB repair (reviewed in (Haber, 2002). Importantly, the use of galactose-inducible *HO* genes has allowed the analysis of synchronous break formation and repair in a whole population of cells. Furthermore, by deletion of *HML* and *HMR*, or by moving HOcs to different regions of the genome, analysis of other repair pathways and analysis of the response to irreparable DSBs has been made possible (Haber, 2002).

DSBs induced by HO type endonucleases are arguably the cleanest form of DSBs that can be analysed because they do not contain any other byproducts. Furthermore, standard 3'OH and 5'-PO_3 ends are generated in the cleavage process. However, one has to be aware that such clean breaks by themselves are a relatively extraordinary situation, and conclusions drawn from the response to such breaks may not be applicable to breaks generated by other means. Nonetheless, the analysis of HO-mediated DSBs has contributed more than any other experimental approach to our understanding of the response to and repair of DSBs.

1.2.3.3 Telomeres as DSBs: The cdc13-1 *mutant*

Since eukaryotic chromosomes are usually linear, it is vital that the specialised ends of each chromosome, the telomeres, are protected from erroneous repair and degradation (reviewed in Smogorzewska and de Lange, 2004). This is important, because the degradation of telomeres would result in the loss of genetic information, and the recognition of telomeres by DSB repair machineries carries the risk of inducing chromosomal rearrangements. Furthermore, it is vital that telomeres do not activate

DNA damage checkpoints since this would result in a block to cell proliferation. A large number of proteins function together to allow the stable maintenance of telomeres (reviewed in Smogorzewska and de Lange, 2004).

Much research has been carried out on a ts mutant that allows the conditional erosion of telomeres, *cdc13-1* (Garvik et al., 1995). Cdc13 is a constitutive component of yeast telomeres and binds preferentially to the 3' single stranded DNA tail that characterises eukaryotic telomeres (Smogorzewska and de Lange, 2004). Shifting *cdc13-1* cells to the restrictive temperature results in degradation of DNA from the telomere into the chromosome, with ssDNA accumulating at the 3' end (Garvik et al., 1995). Increased recombination at telomeric regions, chromosome end-to-end fusions and checkpoint activation are amongst the consequences of loss of Cdc13 function (Garvik et al., 1995; Sanchez et al., 1999).

In addition to its role in protecting chromosome ends from degradation, Cdc13 is also a recruiting factor for the telomere extending enzyme, telomerase (Smogorzewska and de Lange, 2004).

The *cdc13-1* mutation has frequently been used as a tool to study cellular responses to DSBs. However, while many aspects of unprotected telomeres may be applicable to proper DSBs, it has to be recognised that these telomeres are still very different from other regions of the genome.

1.2.3.4 Repair of DSBs by non-homologous end joining (NHEJ)

Two main pathways, non-homologous end joining (NHEJ) and homologous recombination (HR), are thought to compete for the repair of DSBs (Frank-Vaillant and Marcand, 2002, see below). Non-homologous end joining (reviewed in Dudasova et al., 2004; Daley et al., 2005) can, in principle, be viewed as a direct reversal of a DSB. It is a highly conserved process, and NHEJ machineries can be found throughout eukaryotes and even in bacteria (Wilson et al., 2003).

NHEJ can be studied by three different assays in yeast. Firstly, it can be monitored by analysing the transformation efficiency of linearised plasmids that do not contain homology to yeast sequences at the ends (Boulton and Jackson, 1996). Only religation of these ends *in vivo* allows the stable propagation of the plasmids. Secondly, the rejoining of chromosomal breaks induced by HO can be monitored (Moore and Haber, 1996; Haber, 2002). Lastly, *in vitro* assays with purified proteins have also been described (Chen et al., 2001).

In combination, these assays have lead to the formation of a model for NHEJ (Dudasova et al., 2004; Daley et al., 2005), which will be outlined in the following paragraphs, followed by more detailed descriptions of the involved factors.

Amongst the first factors that are thought to interact specifically with breaks during NHEJ are the Mre11-Rad50-Xrs2 (MRX) complex and the Yku70-Yku80 complex (Frank-Vaillant and Marcand, 2002; Lisby et al., 2004). In addition to end-binding activity, both complexes can form bridges between DNA molecules *in vitro* (Cary et al., 1997; Ramsden and Gellert, 1998; Chen et al., 2001). It is possible that such end-bridging functions are part of the role that these proteins carry out in NHEJ. Together, MRX and the Yku70-Yku80 complex (Ku complex) are thus thought to bring the two broken ends together. In the next step, a specialised ligase, ligase IV (Dnl4), is recruited (Schar et al., 1997; Teo and Jackson, 1997; Wilson et al., 1997). Dnl4 requires a cofactor, Lif1, both for protein stability and for functioning in end joining (Herrmann et al., 1998; Teo and Jackson, 2000). Lif1 is thought to mediate interactions with DNA, Xrs2, and another protein, Nej1 (Frank-Vaillant and Marcand, 2001; Tseng and Tomkinson, 2002; Palmbos et al., 2005). Nej1 is also required for NHEJ, but its contribution to the biochemistry of NHEJ is not clear (Frank-Vaillant and Marcand, 2001; Kegel et al., 2001; Ooi et al., 2001; Valencia et al., 2001). Lastly, the assembly of these core NHEJ proteins at the breaks eventually leads to the Dnl4-mediated ligation of the ends.

Yku70/80 and its homologues (Ku70/80 in higher eukaryotes) are essential to end joining in all known systems. They form a heterodimer that is thought to encircle dsDNA at the breaks (Daley et al., 2005). In addition to its possible end bridging role, Yku80 interacts with and is thought to be a recruiting factor for Dnl4. Deletion of either *YKU70* or *YKU80* results in a near complete loss of end joining (Milne et al., 1996). In higher eukaryotes Ku70-Ku80 also forms the non-catalytic DNA binding component of DNA-dependent protein kinase (DNA-PK). Similar to Ku70/80, the catalytic part of DNA-PK, DNA-PK_{cs}, is essential for end joining, although its essential phosphorylation targets are still not known. *S. cerevisiae* does not seem to contain a functional homologue of DNA-PK_{cs}, although it contains several kinases that belong to the same kinase sub family, the phospho-inositol-3 kinase like kinases . Two of these, Mec1 and Tel1 are important for DNA metabolism (see below, section 1.3). Interestingly, Mec1 is required for optimal NHEJ as measured by the plasmid transformation assay (de la

Torre-Ruiz and Lowndes, 2000). However, rather than indicating a direct role for Mec1 in NHEJ, this seems to be the consequence of the loss of DNA damage checkpoint control that is a result of deletion of *MEC1* (de la Torre-Ruiz and Lowndes, 2000; Haghnazari and Heyer, 2004).

The complex composed of Mre11, Rad50, and Xrs2 is similarly conserved in evolution, with the Mre11 and Rad50 subunits even having homologues in bacterial genera (Daley et al., 2005). However, only in *S. cerevisiae* has a role in end joining been established so far (Moore and Haber, 1996; Chen et al., 2001). The MRX complex has a wide range of functions in NHEJ and HR, and is also required for meiotic DSB formation (reviewed in D'Amours and Jackson, 2002). Complex formation appears to be essential for all MRX functions, as there are no clear indications for any of the three proteins carrying out functions on their own. Rad50 belongs to the SMC group of proteins that are characterised by two long coiled-coil domains linked by a hinge region, and globular N- and C terminal heads that form an ATPase domain (D'Amours and Jackson, 2002). Two Rad50 monomers can associate with each other by virtue of a Zn hook contained in the hinge region (Wiltzius et al., 2005). Both the Zn hook and the ATPase domains are essential for Rad50 function (Chen et al., 2005; Wiltzius et al., 2005). Mre11, which appears to bind the globular heads of Rad50, is a rather enigmatic protein. *In vitro*, it has been shown to contain nuclease activity, although this function does not appear to be required for NHEJ or HR (Moreau et al., 1999). No biochemical function has been attributed to Xrs2 so far. During NHEJ, Xrs2 appears to link the MRX complex with Dnl4 by interacting with Dnl4's partner protein Lif1 (Palmbos et al., 2005).

Dnl4 is specific for NHEJ, and does not appear to function in other ligation processes, such as the joining of Okazaki fragments (Schar et al., 1997; Teo and Jackson, 1997; Wilson et al., 1997). Similarly, ligase I (Cdc9) cannot substitute for Dnl4 in NHEJ, indicating that NHEJ intermediates are specifically accessible to Dnl4 (Schar et al., 1997; Teo and Jackson, 1997; Wilson et al., 1997).

In addition to their role in NHEJ, the Yku complex and MRX are also required for the maintenance of telomeric stability (reviewed in Dudasova et al., 2004). Deletion of any of these proteins results in telomere attrition.

1.2.3.5 Repair of DSBs by homology directed repair (HDR)

In contrast to NHEJ, HDR (reviewed in Paques and Haber, 1999) requires long tracts of homology between the break and a donor region that is used for repair. In addition, it is also necessary that the ends are processed to form 3' single stranded tails.

HDR can be subdivided into two main pathways, gene conversion and single strand annealing (SSA). The term gene conversion is almost always used synonymously with the term homologous recombination (HR), although strictly speaking HR is rather synonymous with HDR. However, because of its popular usage, HR is used instead of gene conversion in this study. Models for both HR and SSA will be described in the next sections, followed by a more detailed discussion of DSB processing, the reaction step most relevant for this study.

Overview of homologous recombination

Figure 1.6 outlines the main stages of two models of HR. In order to be a substrate for the HR machinery, a DSB first has to be processed by degradation of the 5' strand of each end of the DSB (Figure 1.6B, White and Haber, 1990; Sun et al., 1991). This process is known as 5'-3' resection, or just resection, and is believed to be mediated by 5' strand specific exonucleases. A number of factors have been shown to play a role in this, including the MRX complex and Exo1 (see below, section 1.2.3.6). The 3' single stranded tails that are thus produced are recognised by a number of proteins. Most importantly, the recombinase Rad51 forms a filament on these tails (reviewed in West, 2003). Rad51 filament formation is thought to be facilitated by two other factors, RPA and Rad52 (Sung, 1997). The Rad51-ssDNA structure then scans the genome for a region of sufficient homology to the break, usually a sister chromatid or a homologous chromosome. The homologous duplex DNA is subsequently invaded and one strand is replaced with the single stranded tail (Figure 1.6C). The resulting structure is known as a D loop (West, 2003). In addition to Rad51, three other proteins are required at this step, Rad54 and the Rad55-Rad57 complex (Sugawara et al., 2003; Wolner et al., 2003). Furthermore, RPA seems to be playing a role in this reaction, perhaps by stabilising the displaced strand (Wang and Haber, 2004). In a repair synthesis reaction, the invading strand is extended by a DNA polymerase activity (Figure 1.6D). It is not known which enzyme is responsible for this in *S. cerevisiae*, although recent evidence indicates Polη to be involved in higher eukaryotes (Kawamoto et al., 2005; McIlwraith et al., 2005). Two outcomes are possible following this step (Figure 1.6E-I and J-K). In

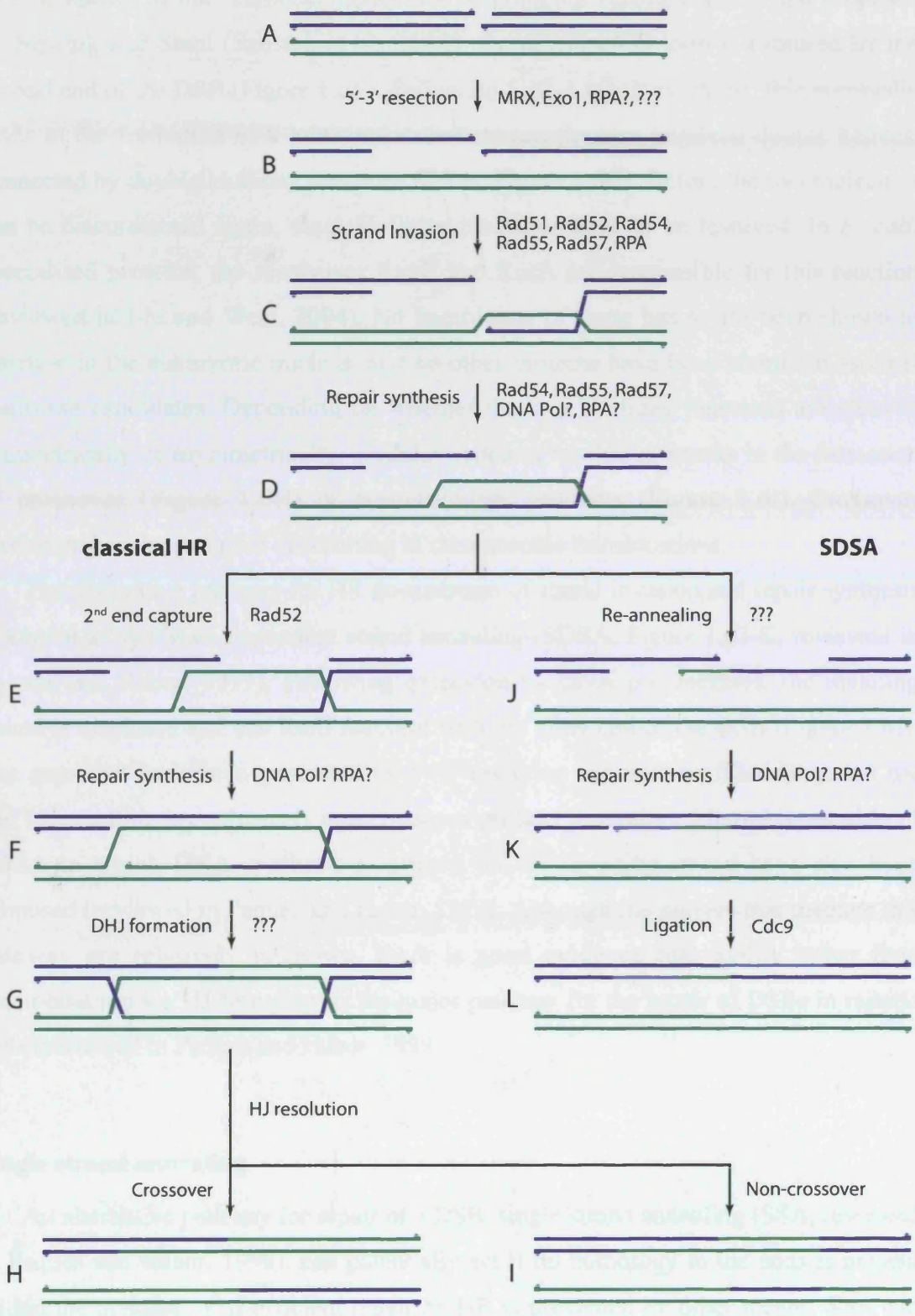

Figure 1.6: Mechanisms of homologous recombination. SDSA: Synthesis dependent strand annealing. DHJ: Double Holliday junctions. HJ: Holliday junction See text for explanations

what is known as the "classical model" for homologous recombination, first proposed by Szostak and Stahl (Szostak et al., 1983), the displaced D loop is captured by the second end of the DSB (Figure 1.6E). Following further repair synthesis, this eventually leads to the formation of a joint molecule between the two involved double helices, connected by double Holliday junctions (DHJs, Figure 1.6G). Before the two molecules can be disconnected again, these Holliday junctions have to be resolved. In *E. coli*, specialised proteins, the resolvases RuvC and RusA are responsible for this reaction (reviewed in Liu and West, 2004). No homologue of these has so far been shown to function in the eukaryotic nucleus, and no other proteins have been identified as clear resolvase candidates. Depending on whether the two Holliday junctions are cleaved symmetrically or asymmetrically, Holliday junction resolution results in the formation of crossover (Figure 1.6H) or non-crossover products (Figure 1.6I). Crossover resolution has the potential of resulting in chromosome translocations.

The alternative pathway for HR downstream of strand invasion and repair synthesis is known as synthesis dependent strand annealing (SDSA, Figure 1.6J-K, reviewed in Paques and Haber, 1999). Following extension by DNA polymerases, the invading strand is displaced and can itself reanneal with the other end of the DSB (Figure 1.6J). The gaps that have been generated by 5'-3' resection can now be filled (Figure 1.6K and L), resulting in exclusively non-crossover product formation. Alternative models of SDSA in which DNA synthesis is primed on the invading strand have also been proposed (reviewed in Paques and Haber, 1999). Although the players that mediate this pathway are relatively unknown, there is good evidence that SDSA rather than recombination via HJ formation is the major pathway for the repair of DSBs in mitotic cells (reviewed in Paques and Haber, 1999).

Single strand annealing

An alternative pathway for repair of a DSB, single strand annealing (SSA, reviewed in Paques and Haber, 1999), can potentially act if no homology to the ends is present within the genome, or if efficient repair by HR is prevented by other means. SSA can rejoin a DSB if there is some homology further inwards between the ends. Although usually analysed with artificial repeat sequences, SSA is thought to be relevant for *in vivo* repair because of the presence of dispersed repeated genetic elements such as transposons and retroviruses.

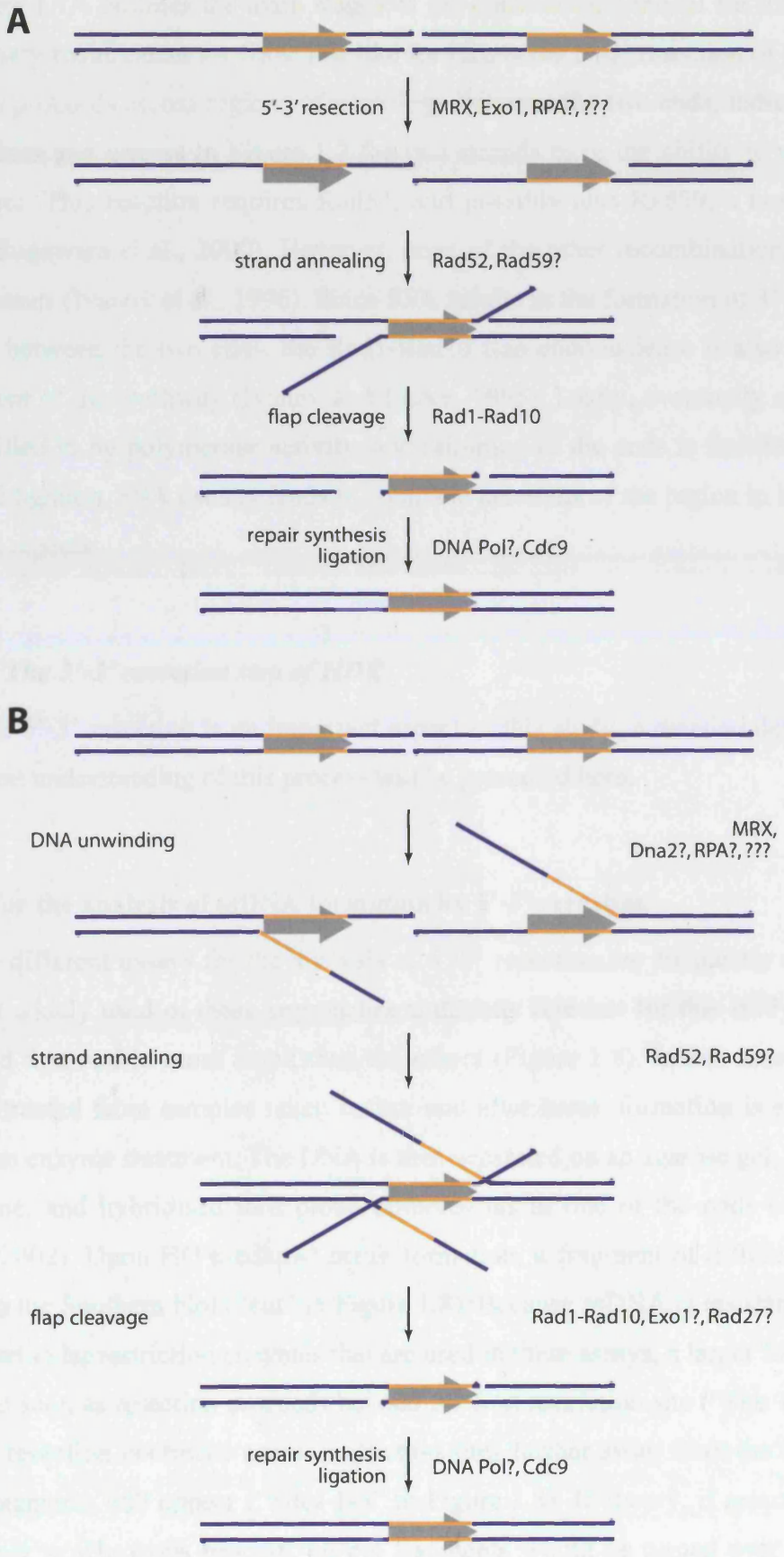

Figure 1.7: DSB repair by single strand annealing (SSA). Two models are presented (**A and B**). See text for explanations.

Figure 1.7A outlines the main stages of the conventional model for this pathway. The primary requirement for SSA, just like for HR, is the 5'-3' resection of the DSB. If resection proceeds across regions of homology between the two ends, indicated by the yellow lines and arrows in Figure 1.7 the two strands have the ability to anneal with each other. This reaction requires Rad52, and possibly also Rad59, a homologue of Rad52 (Sugawara et al., 2000). However, none of the other recombination Rad genes are necessary (Ivanov et al., 1996). Since SSA results in the formation of 3' flaps at the junction between the two ends, the Rad1-Rad10 flap endonuclease is also an integral component of this pathway (Ivanov and Haber, 1995). Lastly, eventually arising gaps can be filled in by polymerase activity, and rejoining of the ends is finished by Cdc9-mediated ligation. SSA usually leads to complete deletions of the region in between the annealed repeats.

1.2.3.6 The 5'-3' resection step of HDR

Since 5'-3' resection is an important aspect of this study, a detailed description of the current understanding of this process will be presented here.

Assays for the analysis of ssDNA formation by 5'-3' resection

Five different assays for the analysis of 5'-3' resection are frequently used. Since the most widely used of these approaches is directly relevant for this study, it will be described first and in more detail than the others (Figure 1.8). In this assay, genomic DNA extracted from samples taken before and after break formation is subjected to restriction enzyme treatment. The DNA is then separated on an agarose gel, blotted to a membrane, and hybridised to a probe homologous to one of the ends of the break (Haber, 2002). Upon HO-mediated break formation, a fragment of different size will appear in the Southern blot ("cut" in Figure 1.8). Because ssDNA is resistant to cutting by the particular restriction enzymes that are used in these assays, a larger fragment will appear as soon as resection proceeds beyond the first restriction site ("Site 1" in Figure 1.8). As resection continues across restriction sites further away from the break, even larger fragments will appear ("Sites 1-5" in Figure 1.8). In theory, if resection were a completely synchronous process, all cut fragments would be turned over into Site 1 fragments at about the same time. Accordingly, Site 1 fragments should disappear as Site 2 fragments make their appearance etc. As shown in the example in Figure 1.8B,

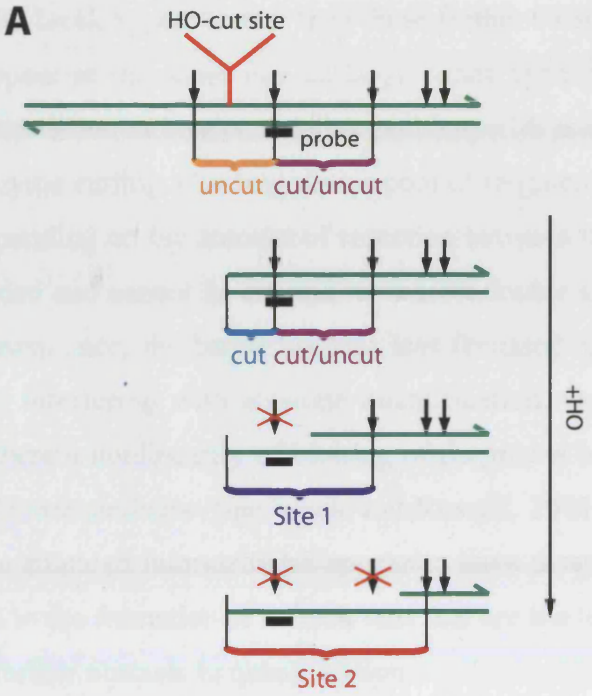

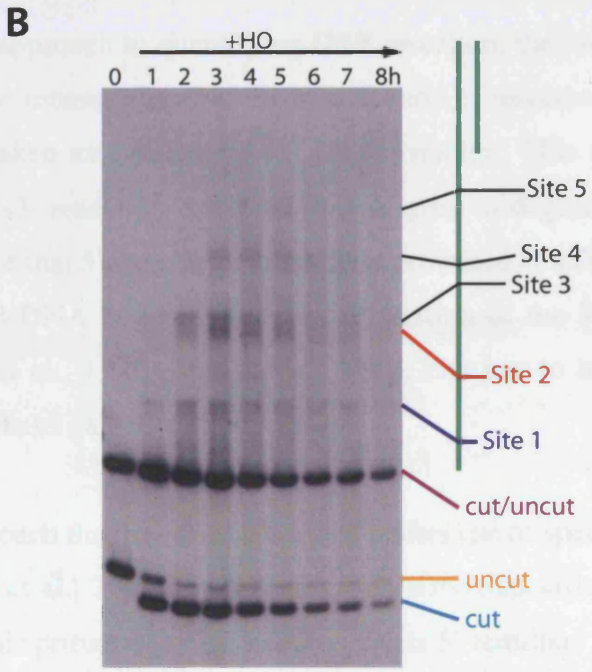

Figure 1.8: Classical approach for the detection of ssDNA. **A:** Schematic representation of the assay. Black arrows denote restriction enzyme sites. The black bar corresponds to the probe used. **B:** Typical Southern blot result for a given locus. See text for details.

however, this is usually not the case. Although fragments corresponding to restriction sites close to the HO break appear sooner than those further away, smaller fragments do not seem to disappear at the same rate as larger ones appear, indicating a lack of synchrony in the population of breaks. Another problem with assays like this is that that after restriction enzyme cutting a heterogeneous pool of fragments is generated for each restriction site, depending on the amount of resection between the last recognition site that is single stranded and cannot be cut and its nearest double stranded neighbour that gets cut. As a consequence, the bands become less focussed and have a tendency to smear downwards, interfering with accurate quantification. Quantification is further impeded by the inherent nonlinearity of blotting of fragments of vastly different sizes and states of single strandedness (Sambrook and Russell, 2001). Lastly, at later time points, most single stranded intermediates appear to have disappeared, a process that has been attributed to the formation of ssDNA tails that are too long to be resolved on a gel, resulting in a further obstacle to quantification.

In the second approach to quantifying DSB resection, the loss of signal for the cut-specific fragment is measured and taken as indication of resection (Ira et al., 2004). The loss of signal is taken as a value for ssDNA formation. This approach relies on the assumption that 5'-3' resection is the only mechanism of degradation at a DSB. While there is no evidence that 5' overhanging ends are produced at a DSB (Fishman-Lobell et al., 1992), some dsDNA degradation and degradation of the 3' overhang may occur (Fishman-Lobell et al., 1992), this study). Thus, one has to be very cautious in the interpretation of results gained with this assay.

The third approach that has been described makes use of specific PCR amplification of ssDNA (Booth et al., 2001). In this assay, a ssDNA-specific primer is annealed to template DNA. This primer contains a region on its 5' terminus that is not homologous to any other region in the genome. Following one round of primer extension, conditions are used in subsequent PCR rounds that exclusively allow the amplification of the product generated in the first cycle. This approach potentially allows a very accurate quantification of ssDNA at a given locus. However, since it relies on multistep PCR, which usually requires a long and tedious optimisation of conditions, it is not widely used.

The fourth assay for the quantification of ssDNA is based on dot blot procedures (Fishman-Lobell et al., 1992). Here, the hybridisation of a 3' strand specific probe to immobilised undenatured DNA samples is analysed. In principle, all signal coming from hybridisation to these native samples should stem from regions that have been resected. Comparison of the signal intensities resulting from hybridisation to undenatured samples with that of samples that have been denatured beforehand, should allow the determination of the percentage of ssDNA present. However, similar problems are associated with this approach as with the other southern membrane based ones described earlier.

Apart from these direct assays for ssDNA formation, an indirect fifth one is used sometimes (Fishman-Lobell et al., 1992). In this assay, the formation of SSA products between direct repeats is taken as readout for resection. This assay relies on the assumption that SSA requires both repeats to be resected, an assumption that has not formally been proven so far.

Because of the caveats that are associated with all these assays, it has so far not been possible to accurately quantify ssDNA generated at DSBs. Nonetheless, important findings have been made with these approaches.

The genetics and biochemistry of 5'-3' resection

Following studies using SSA as an assay for resection, it was calculated that degradation of the 5' strand occurs at a rate of ~4kb/hr (Fishman-Lobell et al., 1992; Vaze et al., 2002). The insertion of ~4kb of DNA in between two direct repeats increased the time required for repair by SSA by about one hour (Fishman-Lobell et al., 1992), and later experiments showed that multiples of ~4kb insertions increased the time required for SSA by multiples of ~1hr (Vaze et al., 2002).

So far, no clear picture has emerged on the enzymatic activities that mediate resection. Particularly confusing is the function of the MRX complex in this respect. Deletion of any of the three subunits results in reduced resection and delays in mating-type switching (Ivanov et al., 1994; Tsubouchi and Ogawa, 1998; Moreau et al., 1999). Furthermore, specific non-null mutations in *MRE11* and *RAD50*, *mre11S* and *rad50S*, resulted in a complete block to the resection of meiotic DSBs (Cao et al., 1990; Nairz and Klein, 1997). Later results also indicated that the *rad50S* mutation causes reduced

resection efficiencies even in mitotic cells (Clerici et al., 2005). Since Mre11 shows nuclease activity *in vitro* (reviewed in D'Amours and Jackson, 2002), these findings led to the idea that that the MRX complex itself constituted the enzymatic activity for 5'-3' resection. However, for two main reasons, it was soon realised that this model could not be true in its simplest form. Firstly, the exonuclease activity associated with Mre11 *in vitro* is of the wrong polarity (3'-5'). Moreover, although Mre11 can also act as a ssDNA-specific endonuclease, it did not appear to be able to cleave 5' branched structures (D'Amours and Jackson, 2002). This is important, because the cleavage of such structures is necessary if resection were mediated by the concerted action of helicase/endonuclease activities (see below). Secondly, nuclease negative mutants of *MRE11* did not appear to have any effect on resection or mating-type switching (Moreau et al., 1999; Llorente and Symington, 2004). In contrast, resection was impaired in meiotic cells carrying nuclease-defective alleles of *MRE11* (Moreau et al., 1999). This may indicate that different mechanisms affect resection in meiotic versus mitotic cells. In this respect it may be important that Spo11-mediated DSBs, in contrast to HO-mediated ones, involve covalent attachment of the enzyme to the breaks (Neale et al., 2005).

Another enzyme that is implicated in 5'-3' resection is Exo1, whose function is also connected to MMR (Tran et al., 2004). *In vitro*, Exo1 shows both 5'-3' exonuclease activity and cleavage of the 5' strand of branched substrates (Tran et al., 2002). By these criteria, Exo1 is a prime candidate for being involved in resection of DSBs. However, deletion of *EXO1* on its own does not result in apparent defects in the resection of HO- or Spo11-induced breaks (Tsubouchi and Ogawa, 2000; Moreau et al., 2001; Nakada et al., 2004). Moreover, the kinetics of mating-type switching are not affected (Tsubouchi and Ogawa, 2000; Moreau et al., 2001). However, *mre11*Δ *exo1*Δ double mutants are severely delayed in both resection and mating-type switching, although both processes are not completely abolished (Tsubouchi and Ogawa, 2000; Moreau et al., 2001; Nakada et al., 2004). It is possible to interpret these results such that both the MRX complex and Exo1 work as major 5'-3' resection enzymes, but in a manner that is nearly completely redundant. However, an alternative view in which MRX controls the activity of the actual nuclease (which may indeed be Exo1) is also possible. The reduced efficiency of resection of DSBs in the absence of MRX might thus be due to reduced accessibility of the ends to Exo1 or alternative nucleases. In such a scenario, the role of the MRX complex would be mainly structural. Combinations of

these two models, as well as alternative models in which a larger number of nucleases is involved in 5'-3' resection are also possible, however. Indeed, given that many DSBs contain non-standard DNA ends (such as modifications arising from IR and the covalent attachment of Spo11 or other topoisomerases), it is highly likely that differential enzymes are involved in different situations. Lastly, it is possible that resection is not only mediated by exonuclease digestion, but also by the activity of helicase unwinding from the DNA end with occasional cutting by 5' flap-specific endonucleases (Figure 1.7B). A similar mechanism, involving the RecBCD enzyme, is known to work in *E. coli* (reviewed in Kowalczykowski, 2000).

In addition to MRX and Exo1, a number of other proteins have been connected to DSB resection. In particular the Sae2/Com1 protein is of interest, because it is intimately connected to the MRX complex. Deletion of *SAE2* results in a near-complete phenocopy of the *rad50S* mutation (McKee and Kleckner, 1997; Prinz et al., 1997; Clerici et al., 2005). It is suspected that Sae2 interacts with MRX but such an interaction has not been proven so far. Furthermore, the biochemistry underlying the *sae2*Δ phenotype is just as poorly understood as the various MRX mutation phenotypes themselves. One of the problems, especially with work on the MRX complex and Sae2 is that the various studies rarely describe identical assays for the different mutations. Thus, recombination activity of *sae2*Δ cells has been analysed using an SSA assay requiring long stretches of ssDNA formation, whereas recombination in the various MRX mutants has been addressed by analysing mating-type switching, which requires very little ssDNA formation (only up to ~150nt). Unfortunately, until clearer data on these proteins is available, models of MRX and Sae2 function must remain very speculative.

An additional mechanism that potentially controls 5'-3' resection is the ability of cells to undergo NHEJ. Disruption of the Ku complex and deletion of *DNL4* result in an increase in ssDNA formation at an HO-induced DSB (Lee et al., 1998, this study). However, it is not clear whether alleviation of direct inhibition of resection by Yku70-Yku80 and Dnl4, or indirect effects such as making more ends available for resection, is responsible for this phenomenon. Most likely, a combination of both mechanisms is involved. Evidence for a possible direct inhibitory effect comes from studies on the NHEJ protein Nej1. Whereas deletion of *YKU70* or *DNL4* specifically increases DSB

resection (Lee et al., 1998, this study), deletion of *NEJ1* was reported to result in decreased ssDNA formation (Kegel et al., 2001). Perhaps in the absence of Nej1 an intermediate is stabilised that prevents access to the degradation machinery and also is deficient in mediating the transition to end joined products. More detailed comparisons between the various NHEJ mutants will be necessary to resolve this issue.

Much research has been carried out on the ssDNA formation that is observed at telomeres of *cdc13-1* mutants incubated at the restrictive temperature (see above, section 1.2.3.3). It has to be borne in mind, however, that such telomeres will still be structurally different to internal chromosomal regions. Therefore, one has to be careful in applying results obtained at *cdc13-1* telomeres to other kinds of DSBs.

Itwas recognised that DNA damage checkpoint proteins have some influence over ssDNA at such telomeres. In particular, deletion of the *RAD9* checkpoint gene (see below) resulted in an increase in ssDNA generation, and deletion of the *RAD24* checkpoint gene resulted in a decrease in ssDNA (Lydall and Weinert, 1995). Whereas Rad9 is thought to be a component of the checkpoint signal transduction machinery (Toh and Lowndes, 2003), Rad24 interacts with damage structures directly (Lowndes and Murguia, 2000; see below). Rad24 is a homologue of the large subunit of RFC (see section 1.1.4.1), and, in analogy to RFC, Rad24 together with the other four subunits of RFC loads a PCNA-like checkpoint factor onto DNA, the Ddc1-Mec3-Rad17 complex (Melo and Toczyski, 2002). Deletion of either *RAD17* or *MEC3* results in a very similar defect in telomere degradation as deletion of *RAD24* (Jia et al., 2004). Interestingly, Rad17 itself might contain a nuclease domain, perhaps suggesting a direct involvement in ssDNA formation at *cdc13-1* telomeres (Lydall and Weinert, 1995). The findings concerning the erosion of these telomeres, seem, however, not to be completely applicable to proper DSBs. No apparent DSB resection defects were observed *rad17*Δ mutants (Lee et al., 1998). In contrast, it was reported that *rad24*Δ cells showed decreased ssDNA formation (Aylon and Kupiec, 2003). It is therefore not clear, whether these checkpoint complexes directly affect DSB resection. Furthermore, no results obtained with mutants in the putative nuclease domain of Rad17 were reported. Another difference between the erosion of unprotected telomeres and proper DSBs is that deletion of *EXO1* is inhibitory to resection of telomeres (Maringele and Lydall, 2002) but does not appear to affect DSB processing (except when combined with MRX mutations, see above). Furthermore, deletion of *MRE11* increases ssDNA generation at

telomeres (Maringele and Lydall, 2002; Foster et al., 2006) but has the opposite effect on DSBs (see above).

1.2.3.7 The decision between NHEJ and HR

In *S. cerevisiae*, deletion of NHEJ specific genes does not result in enhanced cell death following treatment with IR. Deletion of HDR-specific genes, on the other hand, causes hypersensitivity to IR (Boulton and Jackson, 1996; Siede et al., 1996; Teo and Jackson, 1997). Only if HDR is compromised, such as by deletion of *RAD52*, does abrogation of NHEJ result in an additional increase in IR-sensitivity (Boulton and Jackson, 1996; Siede et al., 1996; Teo and Jackson, 1997). These findings have led to the view that HR is highly preferred over NHEJ for the repair of DSBs in budding yeast, and that NHEJ might only be allowed to function if HDR is impaired. More recent findings, however, have shown that this view is not entirely correct.

Under normal circumstances, NHEJ and HR appear to compete for the repair of DSBs (Frank-Vaillant and Marcand, 2002; Daley and Wilson, 2005). Two important studies have addressed this phenomenon experimentally. Frank-Vaillant and Marcand (1999) have shown that NHEJ is a major pathway for the repair of HO-mediated DSBs, at least in G1-arrested haploid cells. Interestingly, it was also found that deletion of *DNL4* resulted in an increase in HDR-mediated repair. On the other hand, deletion of *RAD51* did not appear to increase the efficiency of repair through NHEJ. Furthermore, unprocessed ends of HO breaks were preferentially co-immunoprecipitated with the Ku complex in ChIP experiments, whereas no such preference was observed for Rad52. Lastly, in a variation of the plasmid-rejoining assay (see section 1.2.3.4), it was found that allowing the *in vitro* resection of a linearised plasmid before transformation decreased the efficiency of plasmid end joining. Together, these results have led the authors to conclude that 5'-3' resection acts like a switch that prevents NHEJ from repairing a DSB. Daley and Wilson (2005) have extended these findings in a more detailed characterisation of the influence of the length of ssDNA at a linearised plasmid on transformation efficiency. In their assay, complementary oligonucleotides of increasing length were ligated onto both ends of linearised plasmids before transformation into wild type and various mutant strains. It was found that deletion of *DNL4* or *YKU70* did only affect transformation efficiencies of plasmids with short ($\leq$ 4nt) overhanging ends. In contrast, impairment of HDR by deletion of *RAD52*

specifically reduced the transformation of plasmids with longer overhanging ends (up to 20nt).

Unfortunately, it is not known which step in the NHEJ reaction is inhibited when longer regions of ssDNA are present at the ends of a DSB. This is mainly due to a lack of reported *in vitro* end joining experiments with substrates relevant to this issue.

Importantly, the decision between NHEJ and HDR is affected by the cell cycle stage in *S. cerevisiae* (Frank-Vaillant and Marcand, 2002; Aylon et al., 2004; Ira et al., 2004). When repair of an HO-induced DSB was analysed physically by Southern blotting, G1 arrested cells showed a high incidence of repair via NHEJ (Ira et al., 2004). In asynchronous, or G2/M arrested populations, on the other hand, NHEJ was nearly completely absent (Ira et al., 2004). HDR was found to be regulated in exactly the opposite way (Aylon et al., 2004; Ira et al., 2004). As described previously (section 1.1) one of the differences between G1 and later cell cycle stages is the absence of CDK activity in G1 as opposed to high CDK levels in S- and M phases. Indeed, cyclin-dependent kinase activity seems to be responsible for the differences in NHEJ and HDR, because CDK inhibition in asynchronous or G2/M arrested cells resulted in an increase in NHEJ up to levels identical to the ones observed in G1 arrested cells, and a decrease in HDR down to G1 levels (Ira et al., 2004). Interestingly, CDK activity seemed to be required for efficient DSB resection (Aylon et al., 2004; Ira et al., 2004). This has lead to the formation of the hypothesis that CDK directly activates DSB resection, thus preventing NHEJ and facilitating HDR (Ira et al., 2004). Alternatively, or in combination with such a mechanism, CDK activity might downregulate NHEJ directly, thus allowing more ends to be available for resection.

In a different study, ssDNA formation was analysed by looking at focus formation of RPA after IR treatment (Lisby et al., 2004). However, in this case, no such cell cycle regulation of ssDNA formation was observed, and RPA formed foci even in G1 arrested cells. It is not clear at present what is the cause of the discrepancy between these two studies. It is possible that HO-induced and IR-induced DSBs trigger different cellular responses. Moreover, other forms of DNA damage than DSBs could contribute to the response to IR (see above, section 1.2.1).

Conflicting results have also been reported on the ability of G1-arrested cells to carry out HR. No foci of recombination proteins were detected in G1 arrested cells after IR treatment, although they were readily observed in G2/M arrested cells (Lisby et al.,

2004). Moreover, mating-type switching was reported to be severely impaired in G1-arrested cells or after general inhibition of CDK activity (Ira et al., 2004). In contrast, other studies found that G1 cells were able to carry out mating-type switching, and that only interchromosomal recombination was restricted to G2/M (Raveh et al., 1989; Aylon et al., 2004). A combination of reasons might be accountable for the published discrepancies, such as the use of differential strain backgrounds, damage sources, damage doses and repair assays. Interestingly, however, Rad52, which is essential for HDR, was recently reported to be phosphorylated in a cell cycle dependent manner (Antunez de Mayolo et al., 2006). Thus, CDK could, in addition to regulating NHEJ and/or DSB processing, also regulate other aspects in DSB repair. More detailed analysis of these phenomena will be required before these issues can be resolved.

In addition to the mechanisms described above, the efficiency of NHEJ and HDR is also influenced by the ploidy state. This is mediated through the restriction of *NEJ1* expression to haploid cells (see above, Frank-Vaillant and Marcand, 2001; Kegel et al., 2001; Ooi et al., 2001; Valencia et al., 2001). Thus, NHEJ is repressed in diploid cells.

1.2.3.8 Concluding remarks regarding DSB processing and repair

The transmission of broken chromosomes is extremely lethal due to the loss of genetic information. Therefore, specialised mechanisms have evolved to ensure genomic integrity after DSB damage. Two different pathways appear to compete in DSB repair, NHEJ and HDR, whose relative efficiencies are thought to be determined by the processing state of the ends. Tracts of ssDNA at a DSB are detrimental to NHEJ, but essential for HDR. Although the enzymatic activities responsible for DSB processing are still elusive, some aspect of end turnover is regulated by cyclin-dependent kinase activity and thus depends on the cell cycle stage. These features are of direct relevance to the study presented here, and will often be referred to later on.

1.3 The maintenance of genomic integrity II - DNA damage checkpoint control

If irreparable damage is induced, or if the repair system is overloaded due to high damage doses, the DNA damage checkpoint is activated. Although the primary purpose of this machinery was at first perceived to be the attenuation of cell cycle progression (Hartwell and Weinert, 1989), it later on became clear that a variety of other functions are mediated as well. Checkpoint activation also results in the stabilisation of stalled DNA replication forks, the activation of repair processes and the induction of specialised transcriptional programmes (reviewed in Rouse and Jackson, 2002a; Longhese et al., 2003; Longhese et al., 2006). In the next paragraphs, a brief overview of the checkpoint will be given, followed by more detailed descriptions of the involved proteins and processes in the following sections.

In principle, the DNA damage checkpoint can be regarded as a signal transduction cascade, and many of its components are protein kinases (Table 1.1, Figure 1.9). Of central importance is the upstream protein kinase Mec1, whose activation is required for all known checkpoint responses (reviewed in Longhese et al., 2003; Longhese et al., 2006). Mec1 appears to accumulate at DNA damage structures in a way that depends on its partner protein Lcd1 (Rouse and Jackson, 2002b; Lisby et al., 2004; Nakada et al., 2005). Amongst the substrates of Mec1 during the response to general DNA damage is the adapter protein Rad9 (Gilbert et al., 2001). Phosphorylation of Rad9 is believed to allow its interaction with two other protein kinases, Rad53 and Chk1, the so-called effector kinases (Table 1.1). In a mechanism that involves phosphorylation of Rad53 and Chk1 by Mec1 and autophosphorylation of Rad53, binding to Rad9 leads to effector kinase activation (reviewed in (Pellicioli and Foiani, 2005). In response to DNA replication stress, another protein, Mrc1, is thought to mediate signal transduction similar to Rad9 (Alcasabas et al., 2001). In many situations, phosphorylation of Mec1 substrates also depends on a pair of alternative RFC- and PCNA-like complexes, Rad24-RFC and Ddc1-Mec3-Rad17 (see below). In addition, the MRX complex is involved in some hitherto enigmatic way (D'Amours and Jackson, 2001; Grenon et al., 2001; Nakada et al., 2004). Activated Rad53 and Chk1 are thought to mediate the downstream events in DNA damage signalling (reviewed in Lowndes and Murguia, 2000). In addition, a Rad53 like protein, Dun1, is a component of the checkpoint machinery. The activation of Dun1 depends on Rad53 (Bashkirov et al., 2003). Dun1 is

Table 1.1: Proteins involved in DNA damage signalling.

Protein class	Organism		
	S. cerevisiae	*S. pombe*	Mammals
PIKK	Mec1	Rad3	ATR
	Tel1	Tel1	ATM
ATR-binding partner	Lcd1/Ddc2	Rad26	ATRIP
RFC-like	Rad24	Rad17	RAD17
PCNA-like	Ddc1	Rad9	RAD9
	Rad17	Rad1	RAD1
	Mec3	Hus1	HUS1
Mediator/Adapter	Rad9	Crb2/Rhp9	53BP1
			MDC1
			BRCA1
	Mrc1	Mrc1	Claspin
Effector kinases	Rad53	Cds1	CHK2
	Chk1	Chk1	CHK1
	Dun1	(Cds1)	(CHK2)
MRX complex	Mre11	Rad32	MRE11
	Rad50	Rad50	RAD50
	Xrs2	Nbs1	NBS1
Histone	Hta1/Hta2	Hta1	H2AX
ssDNA binding	RPA	RPA	RPA

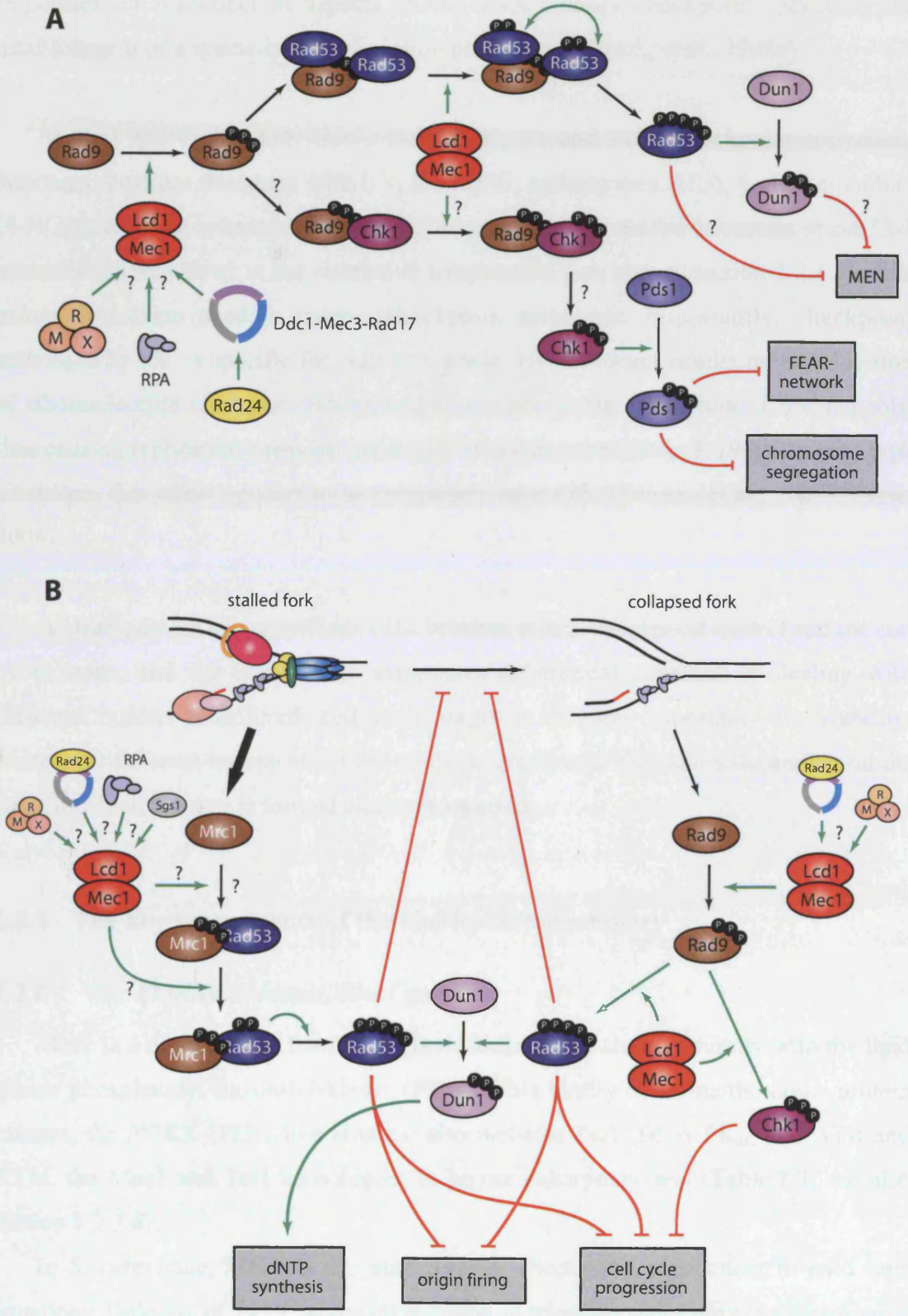

Figure 1.9: Putative models for DNA damage checkpoint signal transduction. **A:** G2/M checkpoint. **B:** DNA replication checkpoint. Green arrows represent activating roles, red blunt arrows represent inhibition. Black arrows denote the transition of one state to another.See text for details.

important for a number of aspects of the DNA damage checkpoint, including the establishment of a specialised transcription programme (Huang et al., 1998a).

Several approaches are widely used to trigger and study checkpoint activation. Amongst these are treatment with UV, IR, MMS, hydroxyurea (HU), 4-nitro-quinoline (4-NQO), and HO-induced DSBs. In addition to these, the eroded telomeres of *cdc13-1* mutant cells incubated at the restrictive temperature (see above, section 1.2.3.3) have extensively been used to trigger checkpoint responses. Importantly, checkpoint activation by HU is specific for cells in S phase. HU treatment results in the inhibition of ribonucleotide reductase (RNR), and in a consequential depletion of dNTP pools, thus causing replicative stress by stalling DNA polymerases (Elford, 1968). In wild type situations, this effect appears to be completely reversible (Tercero et al., 2003; Rouse, 2004).

A large number of connections exist between repair, checkpoint control and the cell cycle stage, and the correct and sometimes differential approach to dealing with different lesions at different cell cycle stages is of great importance for viability. Moreover, different lesions affect cell cycle progression differentially depending on the stage in which damage is formed and/or recognised.

1.3.1 The key components of the checkpoint machinery

1.3.1.1 The PI3K-like kinases, Mec1 and Tel1

Mec1 is a member of a family of protein kinases that share similarity with the lipid kinase phosphatidyl-inositol-3-kinase (PI3K). This family of serine/threonine protein kinases, the PI3KK (PI3K-like kinases) also includes Tel1, DNA-PK_{cs}, and ATR and ATM, the Mec1 and Tel1 homologues in higher eukaryotes, and (Table 1.1, see also section 1.2.3.4).

In *S. cerevisiae*, Mec1 is the main PI3KK checkpoint component in wild type situations. Deletion of *TEL1*, although resulting in telomere shortening (Smogorzewska and de Lange, 2004), does not result in any obvious defects in checkpoint signalling or increased sensitivity to DNA damage (Morrow et al., 1995; Vialard et al., 1998; Pellicioli et al., 1999). On the other hand, *MEC1* is required for virtually all known DNA damage responses (reviewed in Longhese et al., 2003; Longhese et al., 2006).

Interestingly, all residual checkpoint activity in *mec1*Δ cells requires Tel1 (Sanchez et al., 1996; Vialard et al., 1998; Lisby et al., 2004), indicating that Tel1 can carry out some checkpoint functions but that this activity is usually masked by Mec1.

Both Mec1 and Tel1 bind to regions of DNA damage, but with different cofactor requirements (Kondo et al., 2001; Melo et al., 2001; Rouse and Jackson, 2002b; Nakada et al., 2003; Lisby et al., 2004; Falck et al., 2005). Mec1 appears to be directly recruited to DNA by virtue of its partner protein, Lcd1, also known as Ddc2 and Pie1 (ATRIP in higher eukaryotes, see Table 1.1 and Paciotti et al., 2000; Rouse and Jackson, 2000; Cortez et al., 2001; Kondo et al., 2001; Melo et al., 2001; Wakayama et al., 2001; Falck et al., 2005). Neither Mec1 nor Lcd1 appear to have functions outside of the complex that they form with each other. Deletion of either gene gives near identical phenotypes of DNA damage sensitivity and checkpoint deficiency, and no additional phenotypes are observed in double mutants (Paciotti et al., 2000; Rouse and Jackson, 2000; Wakayama et al., 2001). ChIP and fluorescence microscopy experiments have shown that both proteins associate with an HO-induced DSB in an interdependent manner (Kondo et al., 2001; Melo et al., 2001; Rouse and Jackson, 2002b). No catalytic function has been attributed to Lcd1 and its function has been speculated to mainly consist of assuring the association of Mec1 with DNA damage sites (Rouse and Jackson, 2002b). In addition, it may be speculated that Lcd1 could be involved in recruiting other checkpoint factors and/or mediating interactions with Mec1 substrates.

Similar to Mec1, Tel1 was also shown to be recruited to regions close to an HO-induced DSB (Nakada et al., 2003; Lisby et al., 2004). In this case, the interaction was dependent on the C terminus of Xrs2 (Nakada et al., 2003; Lisby et al., 2004). No clear function for Tel1 association with lesions has yet been described in wild type cells (see below).

As discussed above, Tel1 does not appear to be essential for checkpoint responses under normal conditions. However, deletion of *SAE2* or introduction of the *rad50S* mutation in *mec1*Δ strains leads to an increase in Rad53 activation and cell cycle arrest efficiency that is dependent on Tel1 and the MRX complex (Usui et al., 2001; Nakada et al., 2003). It is believed that mammalian ATM, the homologue of Tel1, signals specifically in response to unprocessed DSBs (see below and Jazayeri et al., 2006; Longhese et al., 2006). In contrast, ATR, the homologue of Mec1, appears to be activated specifically by processed ends, intermediates in repair pathways, and replicative stress (Longhese et al., 2003; Jazayeri et al., 2006; Longhese et al., 2006).

Since Tel1 activity can be enhanced by the deletion of *SAE2* or the *rad50S* mutation, both resulting in delayed DSB resection (see above, section 1.2.3.6), similar mechanisms are thought to operate in *S. cerevisiae* (Usui et al., 2001; Ira et al., 2004; see below). However, the DSB resection defects in *sae2*Δ and *rad50S* mutants are not dramatic (Clerici et al., 2006), and recently it was shown that Sae2 appears to have some activity that is inhibitory to checkpoint activation (Clerici et al., 2006; see below). Thus, deletion of *SAE2* could permit checkpoint activation in *mec1*Δ cells by means other than reducing end processing. Due to a lack of clear evidence, this issue is not very clear.

Mec1 appears to be involved in other functions besides checkpoint regulation. Deletion of *MEC1*, or of *LCD1*, is lethal (Desany et al., 1998; Zhao et al., 1998; Paciotti et al., 2000; Rouse and Jackson, 2000; Wakayama et al., 2001). This lethality can be rescued by increasing dNTP levels by overexpression of ribonucleotide reductase or by deletion of its inhibitor *SML1* (Desany et al., 1998; Zhao et al., 1998; Paciotti et al., 2000; Rouse and Jackson, 2000; Wakayama et al., 2001). Importantly, suppression of lethality does not rescue any of the defects in checkpoint signalling associated with *mec1*Δ and *lcd1*Δ (Desany et al., 1998; Zhao et al., 1998; Paciotti et al., 2000; Rouse and Jackson, 2000; Wakayama et al., 2001). Similar mechanisms might be at work in higher eukaryotes since ATR is an essential gene as well (Shiloh, 2003).

1.3.1.2 Rad24, and the Ddc1-Mec3-Rad17 complex

Checkpoint signalling in response to most damage stimuli, with the exception of replicative stress (Pellicioli et al., 1999), also requires four other proteins Ddc1, Mec3, Rad17, and Rad24 (de la Torre-Ruiz et al., 1998; Vialard et al., 1998; Kondo et al., 2001). Interestingly, Ddc1, Mec3, and Rad17 form a heterotrimeric complex with similarity to PCNA (Thelen et al., 1999). Rad24 is a homologue of the large subunit of RFC that associates with the other four RFC components, Rfc2-5 (Green et al., 2000). Rad24 is required for the association of Ddc1 with HO-induced DSBs (Kondo et al., 2001; Melo and Toczyski, 2002). Furthermore, proper localisation of the alternative PCNA checkpoint complex requires the presence of all three subunits (Melo and Toczyski, 2002). A model in which, in analogy to RFC and PCNA, Rad24-RFC loads the Ddc1-Mec3-Rad17 complex, is therefore widely believed to be true (Rouse and Jackson, 2002a). Localisation of Ddc1 to sites of DNA damage depends on none of the

other checkpoint proteins except for the requirements described above (Kondo et al., 2001; Melo and Toczyski, 2002; Lisby et al., 2004). The function of these proteins is somewhat enigmatic. Deletion of any of these proteins results in reduced activation of Rad9 and Rad53 in response to DNA damage in G1 or G2/M arrested cells (de la Torre-Ruiz et al., 1998; Vialard et al., 1998; Kondo et al., 2001). On the other hand, however, phosphorylation of other Mec1 targets such as H2A and Lcd1, is not affected (Downs et al., 2000; Paciotti et al., 2000). A possible role for these proteins in processing unprotected telomeres and DSBs has already been discussed (see section 1.2.3.6).

The alternative RFC and PCNA-like checkpoint complexes appear not to be required for the initial checkpoint response to replication fork stalling induced by HU and MMS (Alcasabas et al., 2001), and deletion mutants are only mildly sensitive to these agents (Longhese et al., 1997; Parsons et al., 2004), indicating lesser importance in the replicative response to DNA damage.

1.3.1.3 Rad9, Mrc1, and the mode of effector kinase activation

Rad9 and Mrc1 belong to a class of checkpoint proteins that are thought to have an adapter role, mediating between the upstream kinase(s) Mec1 (and Tel1) and the effector kinases Rad53 and Chk1 (reviewed in Pellicioli and Foiani, 2005). While the mechanism in which Rad9 mediates Rad53 activation is relatively well understood, Chk1 activation by Rad9 is still rather enigmatic. Moreover, the mechanism of Rad53 activation by Mrc1 is not clear at present. More is known about *S. pombe* counterparts of Mrc1 and Rad53 (Table 1.1), and this mechanism will be referred to for lack of evidence in *S. cerevisiae*.

Importantly, both Mrc1 and Rad9 are phosphorylated in a Mec1 dependent manner (Vialard et al., 1998; Osborn and Elledge, 2003). In the case of Rad9, phosphorylation allows dimerisation of Rad9 via the phospho-epitope binding BRCT repeats in the Rad9 C-terminus (Soulier and Lowndes, 1999). Phosphorylated Rad9 can also be recognised by Rad53 through interaction between FHA domains of Rad53 and specific phosphoresidues on Rad9 (Sun et al., 1998; Schwartz et al., 2002). Activation of Rad53 requires two different phosphorylation events, its phosphorylation by Mec1, and autophosphorylation (Gilbert et al., 2001; Sweeney et al., 2005). It is thought that Rad9 mediates both of these events. Firstly, Rad9 is required to recruit Rad53 to sites of damage, allowing Mec1-mediated phosphorylation (Lisby and Rothstein, 2004; Sweeney et al., 2005). Secondly, binding of Rad53 to Rad9 complexes is thought to

increase its local concentration, thus allowing autophosphorylation (Gilbert et al., 2001; Sweeney et al., 2005). Fully phosphorylated Rad53 is then believed to be released from Rad9, and can subsequently mediate the phosphorylation of its substrates (Gilbert et al., 2001). It may also be possible that, in a positive feedback loop, Rad53 can activate other Rad53 molecules that have not been primed by Mec1 (Gilbert et al., 2001; Ma et al., 2006).

A similar mechanism is thought to operate in the activation of Rad53 by Mrc1 (Alcasabas et al., 2001; Osborn and Elledge, 2003). Mrc1 is phosphorylated in a Mec1 dependent manner upon treatment with HU or MMS (Alcasabas et al., 2001) and a mutant version of Mrc1, in which all putative Mec1 phosphorylation sites have been removed, fails to allow Rad53 activation in response to HU (Osborn and Elledge, 2003). However, very little is known about the biochemistry of this mechanism in *S. cerevisiae*. In *S. pombe*, phosphorylation of Mrc1 by Rad3 (Mec1) mediates binding to Cds1 (Rad53) by interacting with the FHA domain on Cds1 (Tanaka and Russell, 2004). Recent data support the idea that Mrc1-bound Cds1 is then itself phosphorylated by Rad3 (Xu et al., 2006). Two individual phosphorylated Cds1 proteins subsequently dimerise via FHA phosphoepitope interaction and phosphorylate each other, leading to the formation of active Cds1 (Xu et al., 2006). Importantly, in this case, amplification of the primary signal by Cds1 autophosphorylation is not predicted to happen, because both Cds1 molecules have to be prephosphorylated by Rad3 before they can interact with each other.

Although Chk1 activation also depends on Rad9 (Sanchez et al., 1999), very little is known about the biochemistry of this mechanism. Phosphorylation of Rad9 by Mec1 is expected to be important in this pathway, but different sites appear to be used than in the activation of Rad53. Mutation of the Mec1 sites on Rad9 important for Rad53 activation does not apparently affect Chk1 activation (Schwartz et al., 2002). Recently, a domain in Rad9 was identified that appeared to be required for Chk1 activation, but not for Rad53 activation in response to *cdc13-1* mediated telomere erosion (Blankley and Lydall, 2004). Lastly, HU treatment does not result in activation of Chk1, perhaps indicating that Mrc1 has specificity for Rad53 and cannot support Chk1 activation (Alcasabas et al., 2001).

1.3.1.4 The effector kinases Rad53, Chk1 and Dun1

As outlined above, activation of Mec1/Tel1 leads to the activation of the downstream effector kinases Rad53 and Chk1 (Lowndes and Murguia, 2000; Melo and Toczyski, 2002; Rouse and Jackson, 2002a). Rad53 furthermore activates another kinase, Dun1, which is also important for some of the downstream events in the checkpoint response (Bashkirov et al., 2003). Ultimately, these effector kinases mediate the various functions of the DNA damage checkpoint. These include the phosphorylation of cell cycle regulators, the stabilisation of stalled replication forks, the inhibition of late origin firing, the modification of dNTP pools, and the activation of damage-inducible transcription (reviewed in Lowndes and Murguia, 2000; Melo and Toczyski, 2002; Rouse and Jackson, 2002a). Interestingly, *RAD53* is an essential gene (Desany et al., 1998; Zhao et al., 1998). Similar to *mec1*Δ cells, viability can be restored by deletion of *SML1* or overexpression of ribonucleotide reductase without rescuing checkpoint defects (Desany et al., 1998; Zhao et al., 1998).

In terms of cell cycle arrest, it appears that Chk1 and Rad53 function in two pathways that are partially interdependent. Deletion of either protein usually results in only a partial alleviation of cell cycle arrest in response to many sources of DNA damage (Gardner et al., 1999; Sanchez et al., 1999; see below). In the response to DNA replication stress, however, Rad53 appears to be the much more important than Chk1 (Liu et al., 2000; Alcasabas et al., 2001; Schollaert et al., 2004; see below). Interestingly, in higher eukaryotes, Chk1 and Chk2 (the Rad53 homologue) appear to have switched some aspects of their functions, and Chk1 is more important for the response to replicative stress than Chk2 (reviewed in Sancar et al., 2004).

Many of the functions of Rad53 are mediated through Dun1 (Zhou and Elledge, 1993; Huang et al., 1998a; Gasch et al., 2001; Zhao and Rothstein, 2002). However, deletion of *DUN1*, however, is not lethal (Zhou and Elledge, 1993; Zhao et al., 1998). Moreover, *dun1*Δ strains, although sensitive to DNA damaging agents, are usually not as sensitive as *rad53*Δ strains (Schollaert et al., 2004).

Rad53 is also very important as an experimental marker for DNA damage checkpoint activation. Activated Rad53 is hyperphosphorylated, and runs with slower mobility during gel electrophoresis (see for example Figure 3.4A and Pellicioli et al., 1999; Gilbert et al., 2001; Tercero et al., 2003). Moreover, activated Rad53 shows autokinase activity that can be analysed in protein extracts immobilised on membranes after gel electrophoresis and western blotting (Pellicioli et al., 1999; see section

Materials and Methods section 2.10 for experimental details, and Figure 4.5B for an example). No situations are known in which checkpoint activation occurs but Rad53 remains in its inactive form. Therefore, Rad53 activation is frequently used as a marker for checkpoint activation.

1.3.1.5 Other components of DNA damage checkpoints

Histone modifications

An important factor in the response to DNA damage is thought to be the chromatin environment at the lesions. Much research has been carried out on how formation of an HO-induced DSB affects the surrounding chromatin state, and on how histone modifications can in turn influence the damage response (reviewed in Wurtele and Verreault, 2006).

Amongst the many histone modifications, the most important ones for the checkpoint response are phosphorylation of histone H2A by Mec1 and/or Tel1, and Dot1-dependent methylation of histone H3 (Wurtele and Verreault, 2006). H2A phosphorylation rapidly occurs on either side of an HO-induced DSB, and can be detected at regions up to 50kb away from the break (Shroff et al., 2004). Accumulation of Rad9 into damage-induced foci depends on H2A phosphorylation by Mec1/Tel1 (Toh et al., 2006). In a manner that is thought to be similar, the Rad9 homologues MDC1, 53BP1, and Crb2 require equivalent phosphorylation in *S. pombe* and higher eukaryotes for accumulation at damage sites (Ward et al., 2003; Nakamura et al., 2004; Stucki et al., 2005). Phosphorylation of H2A is not required for checkpoint activation and cell cycle arrest (Downs et al., 2000), but it appears to be involved in NHEJ repair, and its dephosphorylation following repair is necessary for recovery from checkpoint arrest (Downs et al., 2000; Keogh et al., 2006). It is thought that H2A phosphorylation dependent accumulation of adapter proteins at damage sites represents a mechanism of signal amplification (Lou et al., 2006).

Similar to H2A phosphorylation, methylation of histone H3 on lysine 79 by Dot1 is also required for retention of Rad9 in damage-induced foci (Toh et al., 2006). Interestingly, this modification is also necessary for cell cycle delay and Rad9 and Rad53 phosphorylation in response to IR and UV in G1, but not for the response to IR in G2/M (Giannattasio et al., 2005; Wysocki et al., 2005). Furthermore, the checkpoint response during S phase, induced by MMS, UV and HU treatment was reduced in

strains deficient for H3 lysine 79 methylation (Giannattasio et al., 2005; Wysocki et al., 2005). Activation of Mec1 kinase itself appeared to be largely unaffected in these situations, however, because Mec1-dependent phosphorylation of Ddc1 and Lcd1 that occur in response to DNA damage were detected (Giannattasio et al., 2005). This may indicate that H3 methylation is required specifically for the transduction of checkpoint signals downstream of the PI3K kinases. However, because histone modification mutants usually have a number of pleiotropic effects, it is not clear if these phenotypes are a result of direct involvement of H3 methylation in the DNA damage checkpoint. Some support for a direct involvement comes from the finding that Rad9-like proteins contain conserved Tudor domains that have been shown to directly bind to K79 methylated histone H3 (Huyen et al., 2004).

MRX, Sae2 and RPA

Efficient checkpoint activation in response to IR, HO-induced DSBs, and following treatment with low amounts of HU requires a functional MRX complex (D'Amours and Jackson, 2001; Grenon et al., 2001; Nakada et al., 2004). However, because the MRX complex is believed to be involved in both the processing of DSBs as well as in establishment of the proper protein organisation at breaks (see above), it is not clear whether these effects are direct or indirect.

Sae2 was recently shown to be involved in checkpoint control as well (Lisby et al., 2004; Clerici et al., 2006). Deletion of *SAE2* results in an inability of cells to adapt to the DSBs induced at a single HOcs and the persistence of MRX foci (Lisby et al., 2004; Clerici et al., 2006; see below). Overexpression of Sae2 has the opposite effect, resulting in the absence of detectable Rad53 activation in response to a low number of DSBs (Clerici et al., 2006). The mechanistic bases for these phenomena are unknown at present.

A proposed role for RPA in checkpoint activation (Lee et al., 1998; Zou and Elledge, 2003; Zou et al., 2003; Ira et al., 2004) will be discussed later (see section 1.3.5).

1.3.2 Checkpoint control during G2/M: Preventing CDK inactivation

In many organisms, including *S. pombe* and mammalian cells, a prominent stage of cell cycle arrest in response to DNA damage is G2 (Boutros et al., 2006). Cell cycle arrest is mediated by maintaining inhibitory phosphorylation of CDK (exemplified by the Y15 phosphorylation of CDK2). This is due to downregulation of the Cdc25-type phosphatases that normally reactivate CDK2 at the G2/M transition (Boutros et al., 2006). However, in *S. cerevisiae*, an equivalent mechanism appears to function only in meiotic cells (Leu and Roeder, 1999), and there is no indication of it being involved in mitotic DNA damage checkpoint control (Amon et al., 1992). Consequently, no delay in G2 is observed under conditions of DNA damage in vegetative cells. In contrast, many types of damage, most importantly DSBs, usually lead to metaphase arrest with high levels of CDK activity (Amon et al., 1992; Sanchez et al., 1999). The two effector kinases Rad53 and Chk1 are required for maintaining active CDK in two largely parallel pathways (Gardner et al., 1999; Sanchez et al., 1999; Figure 1.9A).

Chk1 appears to directly phosphorylate Pds1, and this phosphorylation is required to prevent its degradation by the APC^{Cdc20} (Cohen-Fix and Koshland, 1997; Sanchez et al., 1999; Wang et al., 2001; Agarwal et al., 2003). Thus, Chk1 largely works through inhibiting sister chromatid separation and preventing the activation of the FEAR network of early cyclin inactivation (Figure 1.4A and Figure 1.9A, see also section 1.1.5).

Rad53 appears to prevent CDK inactivation by preventing the activation of the mitotic exit network (Figure 1.4A and Figure 1.9A, see also section 1.1.5). The mechanistic details of this pathway, however, are not very clear. It appears that the polo kinase, Cdc5, is a component of this branch of the checkpoint (Cheng et al., 1998; Sanchez et al., 1999). Interestingly, DNA damage results in phosphorylation of Cdc5, and this phosphorylation is dependent on Rad53 (Cheng et al., 1998). However, the biological significance of this modification has not been addressed.

In addition to regulating MEN in response to DNA damage, Rad53 also appears to have an influence on Pds1 stability, by inhibiting its interaction with the APC in an as yet uncharacterised manner (Agarwal et al., 2003).

In terms of cell cycle arrest, most of the phenotypes of *rad53Δ* cells probably reflect the inability to activate Dun1, since *rad53Δ dun1Δ* double mutants only show mildly synergistic defects in cell cycle arrest in response to unprotected *cdc13-1* telomeres (Gardner et al., 1999).

1.3.3 Checkpoint control during G1: Preventing CDK activation

In response to DNA damage in early G1, cells undergo a Rad9- and Mec1-dependent delay in passage through Start, as detected by a delay in bud formation (Siede et al., 1993; Sidorova and Breeden, 1997). Partially, this delay appears to be due to Rad53-dependent downregulation of Swi6 (Sidorova and Breeden, 1997; Sidorova and Breeden, 2003). Consequently, transcription of SBF-dependent genes such as *CLN1* and *CLN2* is delayed, and Start-dependent reactivation of CDK is impeded (Sidorova and Breeden, 1997; Breeden, 2003; see Figure 1.2). Since Rad53 can directly phosphorylate Swi6 *in vitro* (Sidorova and Breeden, 1997; Breeden, 2003), this mechanism might not require Dun1. Unfortunately, it is not clear if downregulation of Swi6 is the only way in which Rad53 affects the G1/S transition. It is furthermore not known, whether Chk1 contributes to the G1 delay in response to DNA damage.

1.3.4 Checkpoint control during S phase: Preventing fork collapse and late origin firing

During S phase, in addition to preventing cell cycle progression, the checkpoint machinery is also required for the protection of replication forks and for blocking further origin firing (reviewed in Longhese et al., 2003). Interestingly, the tolerance of replicative stress appears to be more important for cell viability than cell cycle arrests. Cells deleted for *CHK1* have similar cell cycle arrest deficiencies as cells deleted for *RAD53* (see for example Gardner et al., 1999; Sanchez et al., 1999). However, Rad53 appears to be much more important than Chk1 in the tolerance of replicative stress (Sanchez et al., 1999; Alcasabas et al., 2001; Schollaert et al., 2004). Furthermore, while *chk1*Δ cells are only mildly sensitive to most sources of DNA damage (Sanchez et al., 1999; Schollaert et al., 2004), *rad53*Δ cells show a high incidence of lethality after DNA damage (Schollaert et al., 2004). Artificially delaying the cell cycle in *rad53*Δ (or *mec1*Δ cells) cells with nocodazole after treatment with the DNA damaging agent MMS does not rescue lethality (Tercero and Diffley, 2001). Together, these findings suggest that in response to replication stress inducing DNA damage, the replication-associated functions of the checkpoint machinery, rather than the cell cycle arrest functions, are essential for maintaining viability. To analyse this process and to induce replication stress and checkpoint activation in yeast, HU treatment is routinely used. In studies

carried out in higher eukaryotes, treatment with aphidicolin, a competitive inhibitor of DNA polymerases, is frequently encountered as well (Kornberg and Baker, 1992). In response to DNA damage that does not grossly interfere with replication (for example a low number of DSBs), the cell cycle arrest function of the checkpoint may be more important for maintaining viability.

Checkpoint activation during S phase affects DNA replication in two specific ways, both dependent on Mec1 as well as Rad53 (Figure 1.9B). Firstly, late origin firing is prevented (Santocanale and Diffley, 1998; Shirahige et al., 1998). Secondly, the irreversible breakdown of replication forks is prevented (Lopes et al., 2001; Tercero and Diffley, 2001). Interestingly, although *rad53*Δ and *mec1*Δ strains have near-identical phenotypes of hypersensitivity to replicative stress, deletion of *DUN1* results in only mild lethality (Schollaert et al., 2004). Thus, most of the responses to stalled replication forks appear to be mediated by Rad53 directly, or by downstream effectors other than Dun1. So far, the only functions that can be attributed to Dun1 in the response to replicative stress is the induction of the transcription programme associated with DNA damage and the stimulation of ribonucleotide reductase activity (Zhao and Rothstein, 2002; see also above and Figure 1.9B).

In the absence of Rad53 or Mec1, stalled replication forks have a high rate of collapsing (Lopes et al., 2001; Tercero and Diffley, 2001). Thus, in these checkpoint mutants, restart of DNA synthesis after repair or removal of HU occurs only in a very low fraction of replication forks. Because of the transmission of underreplicated chromosomes, this ultimately results in severe aneuploidy and lethality. In the presence of Mec1 and Rad53, fork breakdown is prevented, and replication can eventually resume. Presumably, the block to late origin firing induced by checkpoint activation represents a mechanism to allow the rescue of potentially collapsed forks by newly initiated forks after recovery from HU treatment or after DNA repair. Furthermore, reducing the number of forks available for breakdown may represent a mechanism to limit the potential amount of damage induced by stalled and collapsed forks.

It is not known which proteins are phosphorylated by Rad53 in order to mediate these two effects. Dbf4 appears to be an important component in preventing late origin firing because it is phosphorylated in a Rad53 dependent manner upon treatment with HU (Weinreich and Stillman, 1999; Duncker et al., 2002). However, definitive proof for such a regulation is still lacking.

Apart from being regulated by the checkpoint, replication forks can also be essential for activating the checkpoint in response to specific lesions, such as MMS-induced DNA alkylation and unrepaired UV photoproducts (Neecke et al., 1999; Lupardus et al., 2002; Tercero et al., 2003).

In the absence of Mrc1, it is thought that other structures are being generated that result in the activation of the Rad9-dependent branch of Rad53 activation (Alcasabas et al., 2001; Zegerman and Diffley, 2003; see Figure 1.9B). In such a situation, Rad53 activation in response to HU is delayed (Alcasabas et al., 2001). Furthermore, only in the absence of Mrc1 does HU treatment result in detectable phosphorylation of Rad9 and Chk1 (Alcasabas et al., 2001).

Apart from the proteins described, the MRX complex, the alternative RFC and PCNA-like checkpoint complexes and the RecQ-helicase Sgs1 have also been suggested to operate in the DNA replication checkpoint (Paulovich et al., 1997; Frei and Gasser, 2000; D'Amours and Jackson, 2001). However, these mechanisms are relatively poorly understood. Furthermore, only partial phenotypes are observed in mutants of any of these other factors when compared to *mec1*Δ and *rad53*Δ strains.

1.3.5 Is ssDNA the universal checkpoint signal?

While many of the key players in the checkpoint response are known, the mechanisms of lesion detection and signalling initiation are very poorly understood. Importantly, the DNA structures that are being recognised by the checkpoint machinery are unknown. Checkpoint activation as well as Mec1/ATR activation and its accumulation at DNA damage sites and stalled replication forks has been closely linked to ssDNA and RPA (Lee et al., 1998; Zou and Elledge, 2003; Zou et al., 2003; Ira et al., 2004; Lisby et al., 2004; Byun et al., 2005; Namiki and Zou, 2006).

Initial support for an involvement of ssDNA in eukaryotic checkpoint signalling came from the finding that checkpoint activation at unprotected *cdc13-1* telomeres correlated with telomeric erosion and ssDNA formation (Garvik et al., 1995; see also sections 1.2.3.3 and 1.2.3.6). The idea that checkpoint activation might be induced by the detection of ssDNA was very attractive, because ssDNA had been shown to be necessary for activation of the checkpoint-analogous process in prokaryotes, the SOS response (reviewed in Sutton et al., 2000). Furthermore, it was observed that the strength of Rad53 activation at irreparable HO-induced DSBs was increased in *yku70*Δ mutants, which show increased DSB resection (Lee et al., 1998). In contrast, deletion of

MRE11, resulting in delayed DSB processing, caused a decrease in the strength of checkpoint activation (Lee et al., 1998). In response to HO-induced DSBs, an *xrs2Δ exo1Δ* double mutant that is severely deficient for 5'-3' resection (see above, section 1.2.3.6) also shows defects in Rad53 activation (Nakada et al., 2004). Moreover, CDK inactivation resulted in a deficiency in checkpoint activation to HO-induced DSBs that correlated with defects in DSB processing (see sections 1.2.3.6 and 1.3.7).

During DNA replication in *Xenopus laevis* extracts and in mammalian cells, checkpoint activation can be induced by treatment with the DNA polymerase inhibitor aphidicolin. In a specific *X. laevis* extract system, the nucleoplasmic extract replication system (NPE, Walter et al., 1998), aphidicolin treatment appears to also result in uncoupling of helicase and polymerase activities (Walter and Newport, 2000; Byun et al., 2005). Interestingly, the strength of checkpoint response induced by aphidicolin was found to correlate with the amount of ssDNA produced (Byun et al., 2005).

At the same time as support for an involvement of ssDNA in the DNA damage response accumulated, evidence emerged that linked RPA with the transmission of the ssDNA signal to the checkpoint machinery. Firstly, a point mutant in *RFA1*, *rfa1-t11*, resulted in several checkpoint defects, including reduced recruitment of Lcd1 and Ddc1 to HO-induced DSBs, and reduced efficiency of checkpoint arrest in response to DSBs (Lee et al., 1998; Zou and Elledge, 2003; Zou et al., 2003). Furthermore, as described in more detail below, RPA was shown to be able to interact with both Lcd1-Mec1 and the alternative RFC- and PCNA-like complexes and its homologues in other organisms (see below). In mammalian cells, RPA downregulation by RNAi resulted in reduced ATR signalling after IR treatment and a loss of ATR foci (Zou and Elledge, 2003). Lastly, RPA depletion in *X. laevis* egg extracts resulted in abrogation of a checkpoint response to the topoisomerase II inhibitor etoposide and ssDNA gaps (Costanzo and Gautier, 2003; Costanzo et al., 2003).

For the reasons outlined above it is believed that large amounts of RPA-covered ssDNA are required in order to induce checkpoint activation. ssDNA is therefore widely accepted as the best candidate for a universal checkpoint inducing structure, if such a structure exists (Lee et al., 1998; Longhese et al., 2003; Ira et al., 2004; O'Connell and Cimprich, 2005; Longhese et al., 2006). However, it has to be kept in mind, that definitive proof for such a mechanism is still missing. Moreover, many discrepancies amongst the various results linking ssDNA formation with checkpoint activation have not yet been resolved.

1.3.5.1 Interactions of checkpoint proteins with DNA

A large number of studies have been reported aiming at identifying the potential mode of interaction between checkpoint proteins and DNA. These studies have largely concentrated on the alternative RFC and PCNA like complexes and on the Lcd1-Mec1 (ATR-ATRIP) complex.

DNA binding of the alternative RFC and PCNA-like complexes

Binding of the human homologue of the Rad24-RFC complex to various DNA substrates can be stimulated by using DNA coated with RPA (Zou et al., 2003). Interestingly, *E. coli* single strand binding protein cannot functionally substitute for RPA in these assays, indicating a specific interaction. Furthermore, RPA also appears to be able to stimulate the loading of the human 9-1-1 complex (the PCNA-like checkpoint complex) to the same substrates. Experiments carried out with the purified yeast proteins recently showed that RPA also lends specificity to the loading reaction of Ddc1-Mec3-Rad17. RPA-coated substrates as opposed to naked substrates show preferential loading of the PCNA-like complex onto 5' ends at ssDNA/dsDNA junctions (Majka et al., 2006).

Lastly, both the human and yeast the PCNA-like checkpoint complex appeared to be able to directly interact with RPA (Wu et al., 2005; Majka et al., 2006).

DNA binding of the PI3K-like kinases

Purified Lcd1 can bind to short DNA fragments (~70bp) of both ssDNA and dsDNA (Rouse and Jackson, 2002b). In cell extracts, however, the Lcd1-Mec1 complex efficiently bound only dsDNA fragments (Rouse and Jackson, 2002b). Furthermore, it appeared that Lcd1-Mec1 had a preference for linear molecules rather than circular ones, indicating a requirement for DNA ends (Rouse and Jackson, 2002b). Unfortunately, it is not known whether the DNA inserted into the extracts was processed or remained completely stable.

Conflicting results have been reported regarding the ability of the human ATR-ATRIP complex to bind DNA. One study reported that purified ATR-ATRIP complex specifically interacted with RPA coated ssDNA (Zou and Elledge, 2003). In contrast to

the results with yeast Lcd1, this interaction could not be prevented by the addition of linear or circular dsDNA as competitor (Zou and Elledge, 2003). However, it was found in another study that both ATR and ATRIP individually as well as the ATR-ATRIP complex were able to bind ssDNA (Unsal-Kacmaz and Sancar, 2004). This interaction could not be stimulated by the prior incubation of the DNA with RPA (Unsal-Kacmaz and Sancar, 2004). Undoubtedly, differing experimental conditions are accountable for this discrepancy. It is not known yet, which situation is more relevant physiologically. Purified *X. laevis* ATRIP (XATRIP) can bind both to ssDNA and dsDNA, and both these interactions can be stimulated by the addition of RPA (Kim et al., 2005). Interestingly, in egg extracts, no interaction with DNA fragments was observed after depletion of RPA, perhaps indicating that the RPA-dependent binding mode is more important biologically (Kim et al., 2005). However, in these studies, oligonucleotides were used to analyse DNA binding, structures that perhaps would normally not be expected to be intermediates in DNA damage signalling in response to physiological sources of DNA damage. Furthermore, XCHK1 activation in response to these fragments was not abrogated by depletion of RPA or the use of XATRIP mutant versions that rendered the XATR-XATRIP complex unable to interact with RPA or RPA-covered ssDNA *in vitro* (Kim et al., 2005), see below). Lastly, it is not known whether RPA directly recruits ATR-ATRIP, or whether other effects, such as elimination of secondary structures on ssDNA, stimulate ATR-ATRIP binding after treatment with RPA. Similar models have been proposed to explain the stimulation by RPA of *in vitro* strand invasion reactions carried out by Rad51 and Rad52 (Sung, 1997).

In contrast to the situation with Mec1/ATR, where there is some evidence for interaction with ssDNA and/or RPA, and for the importance of such a mechanism, no such indications exist for ATM/Tel1. No biochemical characterisation of Tel1 DNA binding has been reported, but purified ATM has the ability to bind to DNA and shows a preference for the ends of dsDNA over ssDNA and circular molecules (Smith et al., 1999). Further studies on purified ATM showed that, on immobilised dsDNA, ATM binding could be increased by prior treatment of the DNA with restriction enzymes or IR, but not by treatment with UV (Suzuki et al., 1999). Lastly, in cell extracts, ATM also preferentially associated with linear dsDNA (Suzuki et al., 1999). It is not clear, however, how much relevance these findings have for *in vivo* activation of ATM/Tel1. Detection of Tel1 at an HO-induced DSB by ChIP depends on Xrs2 (Nakada et al.,

2003). Moreover, in human cells, association of ATM with sites of DNA damage and ATM-dependent signalling requires a domain on NBS1 that interacts with ATM (Falck et al., 2005). These observations may suggest that the DNA binding activity of ATM is of much lesser importance than its recruitment by the MRX/MRN complex.

Nonetheless, together with the ATR results described above and the finding that ATM responds quickly to IR, while ATR responds relatively slowly (Bakkenist and Kastan, 2003; Jazayeri et al., 2006), this has led to the belief that ATM can be activated by unprocessed DSBs, whereas ATR activation requires DSBs to be processed. However, definitive evidence for both of these pathways is still missing.

1.3.5.2 Genetic approaches to deciphering the role of RPA in checkpoint signalling

Because of the essential nature of all individual RPA subunits it has so far not been possible to directly test the hypothesis of RPA regulating the damage response. Therefore, an extensive number of hypomorphic mutants were generated and analysed (Longhese et al., 1994; Firmenich et al., 1995; Santocanale et al., 1995; Smith and Rothstein, 1995; Longhese et al., 1996; Maniar et al., 1997; Parker et al., 1997; Huang et al., 1998b; Lee et al., 1998; Umezu et al., 1998; Smith and Rothstein, 1999; Smith et al., 2000; Kim and Brill, 2001; Kantake et al., 2003; Zou and Elledge, 2003; Lucca et al., 2004). Three mutants of *RFA1*, *rfa1-M2* (Longhese et al., 1994), *rfa1-t11* (Umezu et al., 1998), and *rfa1-S178A* (Kim and Brill, 2003) show partial defects in DNA damage checkpoint responses.

The *rfa1-M2* mutant, a two amino acid insertion at position 96, appeared to be partially defective in the checkpoint response to UV in G1 and during S phase, as well as in the response to MMS (Longhese et al., 1996). These conclusions were based on two different sets of experiments. Firstly, *rfa1-M2* mutants were found to have a defect in delaying budding after UV irradiation in G1 (Longhese et al., 1996). Because RPA is required for NER (Coverley et al., 1991; see above, section 1.2.2.2), it is possible that an inability to perform NER in this strain might lead to an indirect checkpoint defect. In this respect, it is of interest that that deletion of an early NER gene, *RAD14*, rendered the checkpoint blind towards UV damage outside S phase (Neecke et al., 1999). This is thought to result from an inability to produce checkpoint inducing repair intermediates (Neecke et al., 1999). However, the *rfa1-M2* mutant displays no apparent NER defects in a cell extract-based assay (Huang et al., 1998b), arguing against such indirect effects. To add to the confusion about the *rfa1-M2* phenotype, another report (Pellicioli et al.,

1999) found no defects in Rad53 activation in response DNA damage induced by 4-NQO, which, similar to UV-induced damage, requires NER for repair.

Secondly, in flow-cytometry experiments, DNA synthesis was found to be faster in the *rfa1-M2* mutant than in the wild type after UV irradiation and MMS treatment, although to an apparently lesser degree than in *mec1* or *rad53* mutants (Paulovich and Hartwell, 1995; Longhese et al., 1996). The increased speed of DNA synthesis in checkpoint mutants after DNA damage has been attributed to a defect in the inhibition of late origin firing normally observed in the wild type after DNA damage (Santocanale and Diffley, 1998; Shirahige et al., 1998). These findings might therefore indicate *rfa1-M2* mutants to be partially defective in the activation of the S phase checkpoint. Because of the requirement of RPA in replication initiation (Wold and Kelly, 1988; Walter and Newport, 2000), an alternative explanation would be the loss of a function downstream of checkpoint activation in the *rfa1-M2* mutant that prevented the inhibition of late origins. It is interesting in this respect to note that Rpa1 is a target of checkpoint kinases (Brush et al., 1996; Brush and Kelly, 2000; Brush et al., 2001). Yet another alternative explanation based on the involvement of RPA in replication initiation would be a defect in origin firing in the *rfa1-M2* mutant. Such a defect might inhibit checkpoint activation during S phase indirectly, in a manner similar to the situation in the *orc2-1* mutant (Shirahige et al., 1998; Shimada et al., 2002). If fewer origins were to fire in the *rfa1-M2* mutant, a threshold level of damaged forks required for full checkpoint activation might not be reached (Shimada et al., 2002), thus reducing the amounts of active checkpoint kinases and allowing late origins to be activated. However, arguing against such a scenario, Pellicioli et al. (1999) have found no obvious defects in Rad53 activation to either HU or MMS in the *rfa1-M2* mutant. It is therefore likely that the apparent defects of the *rfa1-M2* mutant in regulating the cell cycle in response to certain types of DNA damage are due to indirect effects.

A large number of papers have been published on the *rfa1-t11* allele. Originally isolated in a screen for *RFA1* point mutants (Umezu et al., 1998), *rfa1-t11* contains a lysine to glutamate substitution at position 48. *rfa1-t11* cells show increased sensitivity to DSBs, HU, UV and MMS (Umezu et al., 1998). In addition, they show severe defects in SSA and in HR during both mitosis and meiosis (Umezu et al., 1998; Soustelle et al., 2002; Kantake et al., 2003; Wang and Haber, 2004). NER was, however, found not to be affected in a cell extract based assay (Huang et al., 1998b). The HR and SSA defect

appears to be the consequence of an increased resistance to being displaced by Rad51 and Rad52 on ssDNA (Kantake et al., 2003; Wang and Haber, 2004).

Importantly, *rfa1-t11* mutants are partially defective in arresting the cell cycle when combined with the *cdc13* mutation and grown at the temperature restrictive for *cdc13* (Kim and Brill, 2001). However, it is not clear whether this deficiency directly is the result from checkpoint defects or caused by possible secondary effects, such as suppression of the telomere attrition in *cdc13* mutants that is responsible for the checkpoint arrest (Garvik et al., 1995).

Support for a direct effect on the DNA damage checkpoint conferred by *rfa1-t11* comes from the finding that *rfa1-t11* mutants show Rad53 activation defects upon UV irradiation in G1 and in asynchronous populations (Clerici et al., 2004). Furthermore, when compared to wild type cells, *rfa1-t11* cells show slightly slower activation of Rad53 after DSB formation by HO endonuclease (Pellicioli et al., 2001). However, because these experiments were carried out in asynchronous populations, alternative explanations such as different cell cycle stage distributions upon break formation are possible. Moreover, all cells were able to a undergo cell cycle arrest, despite these altered kinetics of Rad53 activation.

The *rfa1-t11* allele was also shown to have an effect on the curious phenomenon of checkpoint adaptation (Pellicioli et al., 2001). This is described in more detail below (section 1.3.6).

Conflicting results have been published as to whether recruitment of checkpoint proteins to sites of DNA lesions is affected in *rfa1-t11*. In chromatin-IP (ChIP) experiments it was found that antibodies against both Lcd1/Ddc2 and Ddc1 co-precipitated less DNA in *rfa1-t11* mutants than in the wild type when analysed with PCR primers close to an HO-induced DSB (Zou and Elledge, 2003; Zou et al., 2003). Similar results were obtained when HU-arrested cells were analysed for the capacity of Ddc1 and Lcd1/Ddc2 to co-precipitate DNA close to an origin of replication (Lucca et al., 2004). However, a recent study investigating HU treatment in more detail did only find Ddc1 localisation to be affected by the *rfa1-t11* mutation (Kanoh et al., 2006). Rpa1-t11 protein was found to severely impair the interaction of RPA with Rfc4, a factor required for Ddc1-Rad17-Mec3 loading (Kim and Brill, 2001), thus providing a possible molecular explanation for the reduced ChIP signals. It is possible that strain differences account for the conflicting results regarding Lcd1/Ddc2.

Together, it is therefore not clear whether the altered dynamics of the checkpoint response in *rfa1-t11* mutants result from defects in an active function for checkpoint activation/maintenance or are merely indirect effects. One possibility is that the reduced displacement of Rpa1-t11 by Rad51 (Kantake et al., 2003) results in an inaccessibility of ssDNA for other proteins required for checkpoint activation. Such a model would predict a negative role for RPA in checkpoint activation. Interestingly, in cell extracts, RPA is thought to compromise the DNA binding activity of Lcd1/Ddc2 (Rouse and Jackson, 2002b). Unfortunately, no data regarding RPA overexpression have been published.

In addition to *rfa1-M2* and *rfa1-t11*, the *rfa1-S178A* mutation, which abolishes a Mec1-dependent phosphorylation site, was postulated to cause some defects in checkpoint signalling (Kim and Brill, 2003). This conclusion was based on the fact that Rad53 phosphorylation appeared to be delayed when compared to the wild type upon release from G1-arrested cells into HU (Kim and Brill, 2003). Unfortunately, no data were presented as to whether release from G1 arrest was as synchronous in the mutant as in the wild type. Nor is it known, whether there are slight initiation defects in the *rfa1-S178A* mutant that might reduce the number of active replication forks, thus reducing the amount of checkpoint signal (Shimada et al., 2002). The *rfa1-S178A* mutant was further found to have no hypersensitivity to HU, MMS or UV irradiation, and to be able to delay S phase in response to MMS (Kim and Brill, 2003). Moreover, no defects in delaying budding in response to UV irradiation in G1 were observed (Kim and Brill, 2003). It is therefore not clear at present, whether the reduced Rad53 phosphorylation described above represents a *bona fide* checkpoint activation defect.

Lastly, some experiments have been carried out on a degron mutant of *RFA1* (*rfa1*^{td}) that allows temperature-dependent protein degradation (Zou and Elledge, 2003). After partial protein depletion, it was found that less DNA close to a DSB co-precipitated with Lcd1/Ddc2 (Zou and Elledge, 2003). However, because depletion of RPA could affect many processes at a DSB, including the generation of ssDNA itself, it is again not clear whether this represents a direct checkpoint-protein recruitment function of RPA. Furthermore, no results regarding checkpoint activation were presented alongside the ChIP data. In this respect it is of interest that degradation of an Rpa1^{td} allele was found to interfere only with IR-induced focus formation of GFP tagged Rad24, Ddc1, and Lcd1, but not with focus formation by Rad9-GFP and Rad53-GFP (Lisby et al., 2004). This would suggest that although accumulation of Lcd1-Mec1

and the alternative RFC and PCNA-like complexes to DNA damage is impaired under conditions limiting for RPA, this accumulation is not a prerequisite for the activation of the downstream effector kinases.

The regions responsible for interaction with RPA have been mapped to a high degree of detail in both human and *X. laevis* ATRIP (Ball et al., 2005; Kim et al., 2005). In human cells depleted for ATRIP by RNAi, Chk1 activation appeared normal in response to IR and HU when the RPA interaction mutant of ATRIP was allowed to be expressed (Ball et al., 2005). Accumulation of ATR-ATRIP at sites of damage, on the other hand, appeared to be abolished (Ball et al., 2005). Similar results were reported for *X. laevis* egg extracts treated with a short dsDNA model substrate for checkpoint activation (Kim et al., 2005). XCHK1 activation was reestablished upon addition of mutant XATRIP that could not interact with RPA to extracts depleted for ATR. Depletion of RPA did not appear to affect XCHK1 activation in response to these substrates, although XATR-XATRIP DNA binding was again abolished (Kim et al., 2005). Unfortunately, no other DNA substrates were analysed, and it is therefore not known whether this is a specific or general effect.

Interestingly, in the yeast Lcd1-Mec1 complex, an RPA-interacting region has been mapped to Mec1 (Nakada et al., 2005). Mutation of this region resulted in loss of Mec1 and Lcd1 association with an HO-induced DSB as measured by ChIP. However, other aspects of the Mec1-Lcd1 complex besides interaction with RPA may be affected, because these mutants were also deficient for their kinase activity (Nakada et al., 2005).

In summary, although much evidence for RPA modulating checkpoint responses exists, no clear picture of its actual function has emerged. Similarly, there is no clear understanding of the role of ssDNA in DNA damage checkpoint activation at present. The main problem in dissecting the role of ssDNA is that all checkpoint inducing lesions contain strand breaks in addition to ssDNA.

1.3.6 Checkpoint inactivation and adaptation

Relatively little is known about the mechanisms that turn off the checkpoint response after completion of DNA repair and loss of checkpoint stimulus. During recovery from HO-induced DSBs, however, it appears that at least two different mechanisms contribute to checkpoint inactivation. Firstly, the helicase Srs2 is required

for re-entry into the cell cycle after repair of a DSB by SSA (Vaze et al., 2002). This mechanism, which has been speculated to involve displacement of recombination and/or checkpoint proteins from DNA after completion of repair (Vaze et al., 2002), is not very well characterised to date.

Secondly, the dephosphorylation of checkpoint proteins was shown to be important for checkpoint inactivation after DNA damage as well. Three different phosphatases have been implicated in this process, the PP2C-like phosphatases Ptc2 and Ptc3, which are required for Rad53 dephosphorylation after repair of HO-induced DSBs (Leroy et al., 2003), and Pph3, which appears to mediate histone H2A dephosphorylation (Keogh et al., 2006). It is not clear, which proteins are involved in dephosphorylating other checkpoint components, or, indeed whether other dephosphorylation events are necessary for checkpoint inactivation. Furthermore, it is not known, whether other factors are involved in checkpoint inactivation following repair of DNA damage other than DSBs.

Inactivation of Rad53 and re-entry into the cell cycle can eventually also be triggered in cases in which DSBs have not been repaired. This curious phenomenon has been termed checkpoint adaptation (reviewed in Harrison and Haber, 2006). Adaptation occurs only after a prolonged period of time (≥14hrs), and is a strictly dose dependent process (Toczyski et al., 1997; Pellicioli et al., 2001). Increasing the amount of induced DSBs from two to four efficiently prevents adaptation (Pellicioli et al., 2001). Furthermore, deletions of *YKU70* or *TID1* (a sequence homologue of *RAD54*), as well as a specific mutation in *CDC5*, *cdc5ad*, all compromise adaptation (Toczyski et al., 1997; Lee et al., 1998; Lee et al., 2001). In addition, Rad51 is also required for adaptation, and this requirement can be overcome by deletion of *RAD52* (Lee et al., 2003). Additional requirements for adaptation are the Ptc2 and Ptc3 phosphatases, but not Srs2. Interestingly, deletion of MRX components or introduction of the *rfa1-t11* mutation suppresses the permanent arrest of *yku70*Δ and *tid1*Δ mutants (Lee et al., 1998; Lee et al., 2001), but not that of *cdc5ad* mutants (Lee et al., 1998). This may indicate that different pathways are involved in adaptation. Deletion of *YKU70* increases DSB resection (see above, section 1.2.3.6), and, together with the involvement of an RPA mutant in adaptation, this was taken as evidence in favour of RPA coated ssDNA being measured by the checkpoint (Lee et al., 1998). However, deletion of *TID1* does not appear to affect resection, yet its adaptation defect can also be rescued by *rfa1-*

t11 (Lee et al., 2001). Furthermore, by the time that adaptation actually happens, the differences in resection between wild type cells and *yku70Δ* cells appear to be minute (Lee et al., 1998). Similar to their hitherto elusive roles in checkpoint activation, the roles of ssDNA and RPA in adaptation are very poorly understood, therefore.

It remains possible that adaptation represents stochastic inactivation of the checkpoint machinery rather than it being actively enforced by a specifically evolved mechanism. The finding that most adaptation events appear to happen rather asynchronously after arrest for more than seven generation times may lend some support to the former possibility (Pellicioli et al., 2001).

1.3.7 Is checkpoint activation to DSB damage cell cycle regulated?

Expression of HO endonuclease in cells harbouring one HO recognition site leads to Rad53 activation in nocodazole arrested cells (G2/M phase), but not in alpha factor arrested cells (G1 phase, Pellicioli et al., 2001). Subsequent studies showed that abrogation of CDK activity in nocodazole arrested cells similarly compromised checkpoint activation (Ira et al., 2004). Since inactivation of CDK resulted in reduced DSB resection and an inefficiency to carry out HDR (Aylon et al., 2004; Ira et al., 2004; see also section 1.2.3.6), it was concluded that checkpoint activation in G1 was prevented because of a lack of ssDNA formation due to the low CDK activity in G1 (Ira et al., 2004; Longhese et al., 2006). Indeed, very little ssDNA was found to be detectable at a DSB introduced in G1 arrested cells (Aylon et al., 2004; Ira et al., 2004). Similar processes were recently also proposed to be at work in human cells (Jazayeri et al., 2006). IR was found to activate only ATM-dependent signalling in G1-enriched cell populations, whereas both ATM- and ATR-dependent signalling was induced by IR treatment at later stages of the cell cycle (Jazayeri et al., 2006). CDK appeared to play a role in these processes as well, because inactivation of CDK by treatment with roscovitine was inhibitory to ATR signalling and RPA focus formation after IR (Jazayeri et al., 2006).

However, conflicting results were reported in another study using IR to induce DSBs in yeast (Lisby et al., 2004). In this study, checkpoint activation was monitored by analysing focus formation of a number of checkpoint proteins fused to GFP variants. G1-arrested cells appeared competent for both ssDNA formation and checkpoint activation in this system, since Rpa1, Mec1, Lcd1, Tel1, Mre11, Ddc1, Rad9, Rad24,

and Rad53 were all able to form foci in irradiated G1 cells (Lisby et al., 2004; see above, section 1.2.3.7).

Since the two yeast studies utilised different experimental systems and cells of different strain backgrounds, this discrepancy cannot at present be resolved. One attractive possibility is, for example, that damage other than DSBs contributes to checkpoint activation after IR treatment.

1.4 Conclusions

Checkpoint mechanisms are important contributors to the maintenance of genomic stability. Although most of the key protein components of checkpoint signalling are likely to be known by now, very little understanding has emerged regarding the DNA structures that mediate checkpoint activation, and the mechanisms by which checkpoint pathways maintain viability after DNA damage and replicative stress.

Correlative evidence points towards a role for ssDNA in checkpoint activation. However, no definitive evidence has emerged for ssDNA to be able to induce a checkpoint response on its own. This is because the effects of strand breaks cannot be separated from those of ssDNA generated at sites of DNA damage. Moreover, convenient quantitative methods for the measurement of ssDNA amounts are still lacking.

Similarly, the RPA complex shows a clear interplay with the checkpoint machinery. However, the essential nature of RPA has made approaches to elucidating its role in the damage response very difficult.

A better understanding of the early steps and players in checkpoint activation would greatly improve our picture of this important process. In this study, it was attempted to obtain new evidence regarding the ability of ssDNA to induce a checkpoint response, the involvement of RPA in activating the checkpoint, and the correlation between checkpoint activation and DSB resection. In the following chapters the results regarding these approaches will be presented.

2 Material and Methods

2.1 Growth media and chemicals

Standard growth media were obtained from the media production services unit of Cancer Research UK. Deionised water was used for all media, and solid media additionally contained 1.6% agar. Prior to addition of sugar, amino acids and drugs, the media was autoclaved for 15min.

All chemicals, unless otherwise indicated, were purchased from Sigma.

2.1.1 Yeast media

2.1.1.1 YPD, YPGal, YPRaff

1% w/v yeast extract (DIFCO)

1% w/v peptone (DIFCO)

2% w/v glucose (YPD), galactose (YPGal), or raffinose (YPRaff)

Supplemented with adenine to a concentration of 40μg/ml.

2.1.1.2 Selective yeast drop-in media

6.7mg/ml Yeast nitrogen base without amino acids (DIFCO)

2% w/v glucose

40μg/ml adenine

40μg/ml uracil

80μg/ml leucine

40μg/ml tryptophan

40μg/ml histidine

The particular compound being selected for was not added to the media.

2.1.2 Bacterial media

2.1.2.1 LB (rich medium)

1% w/v bacto-tryptone (DIFCO)

0.5% w/v yeast extract (DIFCO)

1% w/v NaCl

pH adjusted to ~7

2.1.2.2 SOB and SOC

2% w/v bacto-tryptone

0.5% w/v yeast extract

10mM NaCl

2.5mM KCl

10mM $MgCl_2$

10mM $MgSO_4$

20mM glucose (only in SOC)

pH adjusted to ~7

2.1.2.3 Ψ broth

0.5% w/v yeast extract (DIFCO)

2% w/v tryptone (DIFCO)

10mM KCl

20mM $MgSO_4$

adjusted to pH ~7 with NaOH

2.1.3 Drug concentrations

Table 2.1 summarises the chemicals that were used for marker gene selection in yeast and *E. coli*, and for checkpoint induction in yeast.

2.2 General solutions

2.2.1 PBS (Phosphate Buffered Saline)

0.13M NaCl

7mM Na_2HPO_4

3mM NaH_2PO_4

pH adjusted to 7.5

Routinely, a 10x stock solution was prepared and diluted in water before use.

Table 2.1: Antibiotics and drugs used for growth selection and checkpoint induction.

Drug	Organism	Final concentration
ampicillin	*E. coli*	100μg/ml
5-FOA[a]	*S. cerevisiae*	1mg/ml
G418 (geneticin)	*S. cerevisiae*	200μg/ml
HU[b]	*S. cerevisiae*	0.2M
hygromycin	*S. cerevisiae*	250μg/ml
MMS[c]	*S. cerevisiae*	0.01% w/v

[a] 5-fluoro-orotic acid
[b] hydroxyurea
c methyl-methane sulphonate

2.2.2 TBS (Tris Buffered Saline) and TBST

10mM Tris-base

150mM NaCl

0.1% Tween-20 (only for TBST)

pH adjusted to 7.5 with HCl

Routinely, a 10x stock solution was prepared and diluted in water before use.

2.2.3 TE (Tris-EDTA)

1mM Tris-Cl pH 7.5

0.1mM EDTA pH 8.0

Routinely, a 10x stock solution was prepared and diluted in sterile water before use.

2.3 Yeast strains

Table 2.2 lists the yeast strains that were used in this study. All strains are isogenic to the w303 strain background (*MAT*a *ade2-1 can1-100 his3-11,15 leu2-3,112 trp1-1 ura3-1*).

Gene deletions were made using one step PCR product transformations. Marker genes were amplified from pRS vectors (Sikorski and Hieter, 1989) or pFA6a-based vectors (Wach et al., 1994; Wach et al., 1997; Bahler et al., 1998; Longtine et al., 1998; Knop et al., 1999). G418 (Merck Biosciences, Table 2.1) was used to select for *KanMX*. Hygromycin was used to select for *hph* (Table 2.1). Some genes were deleted using two-step transformations: after deletion with a *URA3* marker, *URA3* was deleted using parts of the pRS vector backbone (*pRS-1* and *pRS-2*) or parts of the pBR322 vector backbone (*pBR-1* and *pBR-2*). 5-fluoro orotic acid (5-FOA, Melford Labs, Table 2.1) was used to select for clones that had lost the *URA3* gene. Integrations of PCR products and plasmids were always analysed by colony PCR (see section 2.8.3) for correct integration. In addition, checkpoint and repair mutants were assayed for the phenotype of hypersensitivity to damaging agents.

The P_{CUP1}::rfa^{td} strains were made by replacing the respective *RFA*-promoters with a PCR product made from pPW66R (Dohmen et al., 1994) containing the degron cassette. The PCR products were transformed into YKL83 (Labib et al., 2000). YCZ20 was made by replacing the *CUP1*-promoter in front of $rfa1^{td}$ with the tetracycline regulatable promoter (Tanaka and Diffley, 2002b).

Table 2.2: Yeast strains used in this study.

Strain	Relevant genotype
w303-1b	*MATα*
YCZ2	*ubr1Δ::PGAL-Ubiquitin-M-lacI fragment-Myc-UBR1::HIS3 rfa1Δ::P_{CUP1}::rfa1^{td}::URA3*
YCZ3	*ubr1Δ::PGAL-Ubiquitin-M-lacI fragment-Myc-UBR1::HIS3 rfa2Δ::P_{CUP1}::rfa2^{td}::URA3*
YCZ4	*ubr1Δ::PGAL-Ubiquitin-M-lacI fragment-Myc-UBR1::HIS3 rfa3Δ::P_{CUP1}::rfa3^{td}::URA3*
YCZ5	*MATα leu2-3,112Δ::$P_{GAL1-10}$::T-Ag::LEU2 (pJT19, 4x)*
YCZ20	*ubr1Δ::PGAL-Ubiquitin-M-lacI fragment-Myc-UBR1::HIS3 leu2-3,112Δ::pCM244 (P_{CMV1}::tetR'-SSN6, LEU2, 3x) PRFA1Δ::KanMX::tTA::TetO2::rfa1^{td}*
YCZ42	*trp1-1::$P_{GAL1-10}$::P4gpαE214Q-2xNLS-MycHis::TRP1 (pCZ27)*
YCZ44	*pRS316-KanMX (pCZ7)*
YCZ45	*pRS316-KanMX-P4ori+P4crr1 (pCZ17)*
YCZ46	*pRS426-KanMX (pCZ15)*
YCZ47	*pRS426-KanMX-P4or1+P4crr1 (pCZ18)*
YCZ56	*trp1-1::$P_{GAL1-10}$::P4gpαE214Q-2xNLS-MycHis::TRP1 (pCZ27) pRS316-KanMX (pCZ7)*
YCZ57	*trp1-1::$P_{GAL1-10}$::P4gpαE214Q-2xNLS-MycHis::TRP1 (pCZ27) pRS316-KanMX-P4ori+P4crr1 (pCZ17)*
YCZ58	*trp1-1::$P_{GAL1-10}$::P4gpαE214Q-2xNLS-MycHis::TRP1 (pCZ27) pRS426-KanMX (pCZ15)*
YCZ59	*trp1-1::$P_{GAL1-10}$::P4gpαE214Q-2xNLS-MycHis::TRP1 (pCZ27) pRS426-KanMX-P4or1+P4crr1 (pCZ18)*
YCZ64	*ade3::P_{GAL}::HO ARS607::HOcs::KanMX DDC2-GFP::TRP1 bar1Δ::URA3*
YCZ65	*ade3::P_{GAL}::HO ARS607::HOcs::KanMX DDC2-GFP::TRP1 bar1Δ::URA3 mre11Δ::LEU2*
YCZ70	*ade3::P_{GAL}::HO ARS607::HOcs::KanMX DDC2-GFP::TRP1 bar1Δ::URA3 matHOcsΔ::hph*
YCZ100	*ade3::P_{GAL}::HO ARS607::HOcs::KanMX bar1Δ::URA3*
YCZ101	*ade3::P_{GAL}::HO ARS607::HOcs::KanMX bar1Δ::URA3 matHOcsΔ::TRP1*
YCZ102	*ade3::P_{GAL}::HO bar1Δ::URA3*
YCZ127	*ade3::P_{GAL}::HO ARS607::HOcs::KanMX bar1Δ::URA3 matHOcsΔ::TRP1 trp1Δ::LEU2::HOcs*
YCZ134	*ade3::P_{GAL}::HO ARS607::HOcs::KanMX bar1Δ::URA3 sml1Δ::URA3 rad53Δ::TRP1*
YCZ136	*ade3::P_{GAL}::HO ARS607::HOcs::KanMX bar1Δ::URA3 matHOcsΔ::TRP1 dnl4Δ::LEU2*
YCZ147	*ade3::P_{GAL}::HO ARS607::HOcs::KanMX bar1Δ::TRP1 hmlΔ::URA3*
YCZ154	*ubr1Δ::PGAL-Ubiquitin-M-lacI fragment-Myc-UBR1::HIS3 leu2-3,112Δ::pCM244 (P_{CMV1}::tetR'-SSN6, LEU2, 3x) PRFA1Δ::KanMX::tTA::TetO2::rfa1^{td} rad9Δ::TRP1 sml1Δ::URA3*

YCZ155	*ubr1Δ::PGAL-Ubiquitin-M-lacI fragment-Myc-UBR1::HIS3 leu2-3,112Δ::pCM244 (P_{CMV1}::tetR'-SSN6, LEU2, 3x) PRFA1Δ::KanMX::tTA::TetO2::rfa1^{td} sml1Δ::URA3*
YCZ156	*ubr1Δ::PGAL-Ubiquitin-M-lacI fragment-Myc-UBR1::HIS3 leu2-3,112Δ::pCM244 (P_{CMV1}::tetR'-SSN6, LEU2, 3x) PRFA1Δ::KanMX::tTA::TetO2::rfa1^{td} mrc1Δ::hph sml1Δ::URA3*
YCZ161	*ade3::P_{GAL}::HO ARS607::HOcs::KanMX bar1Δ::TRP1 hmrΔ::URA3*
YCZ163	*ubr1Δ::PGAL-Ubiquitin-M-lacI fragment-Myc-UBR1::HIS3 leu2-3,112Δ::pCM244 (P_{CMV1}::tetR'-SSN6, LEU2, 3x) PRFA1Δ::KanMX::tTA::TetO2::rfa1^{td} rad9Δ::TRP1 mrc1Δ::hph sml1Δ::URA3*
YCZ172	*ade3::P_{GAL}::HO ARS607::HOcs::KanMX bar1Δ::URA3 hmlΔ::pRS-1 hmrΔ::pRS-2 leu2Δ::TRP1::HOcs trp1Δ::LEU2::HOcs*
YCZ173	*ade3::P_{GAL}::HO ARS607::HOcs::KanMX bar1Δ::TRP1 hmlΔ::pRS-1 hmrΔ::pRS-2 matHOcsΔ::pBR-1*
YCZ180	*ade3::P_{GAL}::HO ARS607::HOcs::KanMX bar1Δ::TRP1 hmlΔ::pRS-1 hmrΔ::pRS-2 matHOcsΔ::pBR-1 URA3::PGAL-SIC1ΔntMyc::ura3 (pLD1, ≥2x)*
YCZ186	*ade3::P_{GAL}::HO ARS607::HOcs::KanMX bar1Δ::LEU2 hmrΔ::pRS-2 URA3::PGAL-SIC1ΔntMyc::ura3 (pLD1, ≥2x)*
YCZ189	*ade3::P_{GAL}::HO ARS607::HOcs::KanMX hmlΔ::pRS-1 hmrΔ::pRS-2 matHOcsΔ::TRP1 URA3::PGAL-SIC1ΔntMyc::ura3 (pLD1)*
YCZ190	*ade3::P_{GAL}::HO ARS607::HOcs::KanMX hmrΔ::pRS-2 URA3::PGAL-SIC1ΔntMyc::ura3 (pLD1)*
YKL83	*ubr1Δ::PGAL-Ubiquitin-M-lacI fragment-Myc-UBR1::HIS3*
YST114	*ubr1Δ::PGAL-Ubiquitin-M-lacI fragment-Myc-UBR1::HIS3 leu2-3,112Δ::pCM244 (P_{CMV1}::tetR'-SSN6, LEU2, 3x)*

To generate HO cut sites at various places in the genome, a ~140bp sequence including the HO recognition site at *MAT* was PCR amplified, cloned into pGEM-T (Promega) and sequenced. It was subcloned into pUG6 (Guldener et al., 1996), pRS304 (Sikorski and Hieter, 1989), and pRS305 (Sikorski and Hieter, 1989) to allow the construction of *ARS607::HOcs*, *leu2Δ::TRP1::HOcs* and *trp1Δ::LEU2::HOcs* strains, respectively. These strains were generated by targeted PCR product integration. The original Gal-HO *ARS607::HOcs* strain was constructed by H. Debrauwere (YHHD180). This strain was used in genetic crosses and for gene deletions or knock-in transformations.

2.4 Plasmids

Brief overviews of the cloning procedures for the plasmids used in this study are provided here. PCR products were always sequenced in the final vector.

pCZ7 was made by cloning the XbaI-SacI KanMX4 fragment from pUG6 (Guldener et al., 1996) into XbaI/SacI cut pRS316 (Sikorski and Hieter, 1989).

pCZ12 was made by cloning four tandem copies of the SV40 origin (obtained from pSV011; Gluzman et al., 1980) into the XbaI site on pCZ7 (see above).

pCZ13 was made by cloning four tandem copies of the SV40 origin (obtained from pSV011; Gluzman et al., 1980) into the SpeI site on pCZ15 (see below).

pCZ15 was made by cloning the NotI KanMX4 fragment from pUG6 (Guldener et al., 1996) into NotI-cut pRS426 (Christianson et al., 1992).

pCZ17 was made by cloning a PCR product of the *oriI* and *crr* regions from pRB4 (Tocchetti et al., 1999) into EcoRI–cut pCZ7 (see above).

pCZ18 was made by cloning a PCR product of the *oriI* and *crr* regions from pRB4 (Tocchetti et al., 1999) into EcoRI–cut pCZ15 (see above).

pCZ27 was constructed in the following way. A PCR product of the 2xNLS cassette from pJL1206 (Nguyen et al., 2000; Nguyen et al., 2001) was cloned into the BamHI site of pMHTGal (Ferreira et al., 2000) to make pCZ20. The $P_{GAL1\text{-}10}$*::2xNLS-MycHis* fragment was released from pCZ20 by cutting with EcoRI/NdeI and the ends of the fragment were filled in with T4 DNA polymerase (New England Biolabs). The fragment was ligated into pRS304 (Sikorski and Hieter, 1989) cut with EcoRI/NotI (ends filled in as before) to make pCZ24. Finally, the gpαE214Q ORF from pMS4Δ1

(Ziegelin et al., 1993) was cloned behind the Gal-promoter (BamHI site) on pCZ24. The resulting plasmid was pCZ27.

pJT19 (provided by JA Tercero) was made by cloning the T-Ag coding sequence from pT7 (Mohr et al., 1989) into the BamHI/XhoI cut galactose-inducible expression vector pST6 (Tanaka and Diffley, 2002a).

pLD1 has been described previously (Desdouets et al., 1998).

2.5 Antibodies

Table 2.3 lists the antibodies that were used in this study. All antibody incubations for immunoblotting were performed in TBST containing 5% w/v fat-free milk (Marvel milk powder).

2.6 Bacterial techniques

2.6.1 Generation of competent *E. coli*

An overnight culture of *E. coli* strain DH5α grown in Ψ broth was used to inoculate 100ml fresh Ψ broth. The culture was allowed to grow at 37°C until it reached an OD_{550} of ~0.4. The culture was cooled on ice for 10min and centrifuged at 4°C. The pellet was resuspended in 33ml RF1 (100mM rubidium chloride; 50mM manganese chloride; 30mM potassium acetate; 10.2mM calcium chloride dihydrate; 15% w/v glycerol pH 7.5) and incubated on ice and centrifuged as before. The pellet was resuspended in 8ml RF2 (10mM MOPS pH 6.8; 10mM rubidium chloride; 10mM potassium chloride; 74.8mM calcium chloride; 15% w/v glycerol) and incubated on ice as before. This cell suspension was aliquoted and frozen on dry ice. The aliquots were stored at –80°C.

2.6.2 Plasmid transformation into *E. coli*

100µl of competent cells were mixed with transformation DNA and incubated on ice for ca. 30min. The cells were then heat-shocked at 42°C for 90sec, and cooled on ice. 1ml of SOC was then added and the tubes were incubated at 37°C with shaking for ca. 30min. Lastly, the cells were spun down and plated onto selective plates.

Table 2.3: Antibodies used in this study

Primary antibody		Secondary antibody	
Antigen/Name	Concentration	Name	Concentration
HA-epitope (12CA5 monoclonal)	1:1,000	α-mouse-HRP (Amersham)	1:1,000
HA-epitope (16B12 monoclonal)	1:10,0000	α-mouse-HRP (Amersham)	1:2,000
Myc-epitope (9E10 monoclonal)	1:1,000	α-mouse-HRP (Amersham)	1:1,000
Orc6 (SB49 monoclonal)	1.4μg/ml	α-mouse-HRP (Amersham)	1:10,000
Rad53 (JDI48 rabbit polyclonal)	1:800	Protein A-HRP (Amersham)	1:10,000
Rpa1 (rabbit polyclonal)	1:1,000	Protein A-HRP (Amersham)	1:10,000
T-Ag (rabbit polyclonal)	1:1,000	Protein A-HRP (Amersham)	1:10,000

2.6.3 Plasmid miniprep

QiaGen miniprep kits were used for plasmid purification from *E. coli*. 5ml of overnight cultures grown in LB plus ampicillin were harvested and used for each plasmid preparation. The manufacturer's instructions were followed throughout.

2.7 Yeast techniques

2.7.1 Growth conditions and cell cycle synchronisations

Unless otherwise indicated, cells were usually grown at 30°C. Experiments were performed with cultures of a density of ~$1x10^7$ cells/ml. Cell density was measured by cell counting using microscopic analysis of cells within a haemocytometer.

Nocodazole (methyl-(5-[2-thienylcarbonyl]-H-benzimidazol-2-yl) carbamate) was used for arrest in mitosis (Jacobs et al., 1988). A stock solution of 2mg/ml in DMSO was added to cultures to obtain a final concentration of 5μg/ml. Cells were incubated thus for ~2hrs, until >90% percent of the cells were arrested (as measured by counting the number of large-budded cells).

α factor mating pheromone was used to arrest cells in G1 (Duntze et al., 1973). The final concentration of α factor for arrests of strains wild type for the mating response was 10μg/ml. Cells deleted for the mating pheromone adaptation gene *BAR1* (Chan and Otte, 1982) were arrested in 1μg/ml α factor. For prolonged G1 arrests, α factor was re-added in regular intervals of ~1 generation time. α factor was obtained from the peptide synthesis laboratory at Cancer Research UK. Its peptide sequence is THTLQLKPGQPMY. Cell cycle arrests were confirmed by counting the proportion of unbudded cells.

When cells were released from a cell cycle arrest, they were harvested and washed twice before being resuspended in fresh medium.

2.7.2 LiOAc transformation of yeast strains

An overnight culture of the desired strain grown in rich medium was used to inoculate fresh medium. This culture was grown until it reached a density of ~$1x10^7$ cells/ml of culture. The cells were washed once in sterile water and once in LiOAc/TE (100mM LiOAc; 10mM Tris-Cl; 1mM EDTA; pH 7.5). After pelleting, the cells were

resuspended in LiOAc/TE at a concentration of $2x10^9$ cells/ml. DNA for transformation (usually ~15µl of PCR product or ~1µl of mini-prep plasmid) was combined with 50µl of this cell suspension and 5µl of salmon sperm ssDNA (10mg/ml, denatured by boiling for 5min prior to use) were added. Finally, 300µl of 40% v/v PEG3350 in LiOAc/TE were added and the transformation mixes were incubated at 30°C with shaking for 30min. Following this, 40µl of DMSO were added and the cells were heat-shocked at 42°C for 15min. After cooling briefly on ice, the cells were plated onto selective medium.

In case of usage of the *KanMX* or *hph* marker genes, cells were grown in rich medium for ca. 2hrs prior to plating.

In case of selection against *URA3*, cells were allowed to grow overnight in 10ml rich medium without selective pressure. 400µl of this overnight culture were plated onto rich media plates containing 1mg/ml 5-FOA and again incubated overnight. The following day, the plates were replica plated onto minimal medium containing all the supplemented substances outlined in section 2.1.1.2 and 1mg/ml 5-FOA.

2.7.3 Flow cytometric analysis of yeast DNA content

1ml of a culture of a density of $1x10^7$ cells/ml was harvested and washed with 50mM Tris-Cl pH 7.8. Cells were pelleted and resuspended in 0.5ml of 70% ethanol 50mM Tris-Cl pH 7.8, briefly sonicated and stored overnight at 4°C. Cells were then spun down, washed twice in 50mM Tris-Cl pH 7.8, and finally resuspended in 0.5ml of 50mM Tris-Cl pH 7.8 containing 0.2mg/ml RNase A (Sigma). After incubation at 37°C for ~4hrs, cells were pelleted, resuspended in 0.25ml of 55mM HCl containing 5mg/ml pepsin (Sigma) and incubated at 37°C for another 30min. The cells were then washed with 0.5ml FACS buffer (211mM NaCl; 78mM $MgCl_2$; 200mM Tris-Cl pH 7.5) and resuspended in 0.5ml FACS buffer containing 50µg/ml propidium iodide (Sigma). The samples were stored at 4°C in the dark until use. 100µl of the cells were mixed with 1ml of 50mM Tris-Cl pH 7.8 and briefly sonicated before reading on a Becton Dickinson FACScan machine. The manufacturer's instructions were followed for data acquisition and analysis.

2.7.4 Fluorescence microscopy

$1x10^7$ cells were harvested and washed with PBS. Cells were then resuspended in 100µl water and 500µl 99% ethanol were added. The suspension was briefly sonicated and incubated for 5-10min at room temperature. Cells were then spun down and resuspended in ~100µl of PBS containing 2µg/ml DAPI (4,6-diamidino-2-phenylindole) to allow visualisation of the nucleus. Cells were stored at 4°C for up to five days.

Deltavision microscopy with a 60x 1.4 NA Planapochromat lens on an Olympus inverted microscope (IX71) was used to examine cells. Images were captured and manipulated using SoftWorx software (Applied Precision). For pictures taken with the GFP channel, 10sec exposure times were used. Multiple z-stacks of views with multiple cells were taken. Three-dimensional data sets were computationally deconvolved and projected into one dimension. Between 70 and 100 cells were analysed per time point.

2.7.5 Preparation of yeast protein extracts with TCA

$1x10^8$ cells were harvested, frozen on dry ice and stored at –80°C until use. After thawing, the cells were resuspended in 200µl of 20% trichlor-acetic acid (TCA) and ~400µl of glass beads were added (0.5mm, BDH). Cells were crushed by incubation for 4min on a Mixer 5432 (Eppendorf). The liquid was transferred to a fresh tube and the glass beads were washed twice with 200µl 5% TCA. The washes were recovered and added to original cell lysate. Precipitated proteins were recovered by centrifugation (13krpm, 3min) and the supernatant was discarded. The pellets were resuspended in 200µl 1x Laemmli buffer (62.5mM Tris-Cl pH 6.8; 0.5% SDS; 10% glycerol; 720mM β-mercaptoethanol) and 50µl 1M Tris base was added. The extract was boiled for 5min and subsequently centrifuged (13krpm, 3min). The supernatant was transferred to another tube and used for subsequent analysis by SDS-PAGE (see section 2.9).

2.7.6 Preparation of yeast crude chromatin extracts

Yeast chromatin was, with minor modifications, isolated as described (Donovan et al., 1997).

$2x10^8$ cells were harvested, resuspended in 6.25ml 100mM Pipes/KOH pH 9.4 10mM DTT, and incubated at 30°C for 10min with agitation. Cells were then centrifuged and resuspended in 2.5ml YPD containing 0.6M sorbitol; 25mM Tris-Cl pH 7.5 and 0.5mg/ml lyticase (L-5763, Sigma, 8000u/mg protein). This suspension was

incubated at 30°C with agitation for ca. 15min until nearly 100% of the cells were spheroplasted (as judged microscopically by lysis in 1% Triton X-100). The cells were spun at 1krpm for 3min and the pellet was washed three times with 1ml lysis buffer (0.4M sorbitol; 150mM potassium acetate; 2mM magnesium acetate; 20mM Pipes/KOH pH 6.8; 1mM PMSF; 10µg/ml leupeptin; 1µg/ml pepstatin A; 10mM benzamidine HCl). The cells were finally resuspended in an equal pellet volume of lysis buffer (~500µl). Triton X-100 was then added to a final concentration of 1%, and the tubes were incubated on ice with gentle mixing until all cells were lysed (determined experimentally). 90µl of this solution was removed, mixed with 45µl of 3x Laemmli buffer and boiled and centrifuged as described above (see section 2.7.5). This represented the whole cell extract sample. Another 100µl were taken for chromatin enrichment. This sample was spun at 14krpm, 4°C for 15min. The supernatant was taken and mixed with half its volume of 3x Laemmli buffer, and boiled and centrifuged as before. The chromatin enriched pellet was washed with 100µl of lysis buffer and afterwards resuspended in a volume of lysis buffer that was equal to the volume of the supernatant. 3x Laemmli buffer was added, and the mixture was treated as before.

2.8 DNA techniques

2.8.1 Restriction digests and ligation reactions

Restriction enzymes were purchased from New England Biolabs and used according to the manufacturer's instructions.

Ligation reactions were performed with T4 DNA ligase (New England Biolabs), used as recommended by the manufacturer. The only difference was that ligation reactions of cohesive ends were usually performed for 1hr at 24°C. Whole ligation reactions were used for transformation into *E. coli*.

2.8.2 DNA sequencing

Sequencing reactions were performed using the BigDye Terminator v.1.1 Cycle Sequencing Kit (Applied Biosystems) according to the manufacturer's instructions. The Cancer Research UK Sequencing Service was used for analysis of the sequencing reactions. In all cases, both strands were sequenced.

2.8.3 Polymerase chain reaction (PCR)

All traditional PCR reactions were performed on a PTC-200 temperature cycler (MJ Research). Standard PCR reactions for gene replacements were carried out with ExTaq (Takara). Reaction mixes had concentrations of 250µM for each of the four dNTPs; 200nM for each oligonucleotides; and 1x of the supplied buffer. 1u ExTaq was used for each 25µl of reaction volume. For plasmid templates ~25ng of plasmid were used for each 25µl of reaction volume. For tagging/deletion PCR amplification a standard temperature programme was usually used: 95°C 2:30min → 5x(95°C 40sec → 55°C 40sec → 72°C 1min/kb) → 20x(95°C 40sec → 59°C 40sec → 72°C 1min/kb) → 72°C 10min.

For generation of epitope-tagging constructs, Phusion polymerase (Finnzymes) was used as instructed by the manufacturer.

Colony PCR was used for standard genotyping of clones after transformation. Primers annealing up- and downstream of the replaced sequence were usually used. For plasmid transformations, both ends of the integration were tested, by using one primer outside the integrated plasmid, and one primer inside the plasmid. Furthermore, clones were tested for multiple integration and for the absence of a PCR product corresponding to the wild type sequence. Standard PCR mixes without enzyme were incubated with a toothpick full of yeast for 5min at 96°C. The samples were then allowed to cool on ice and Taq-polymerase was added. A slightly different temperature program was used in this case: 95°C 2min → 30x(95°C 1min → 56°C 1min → 72°C 1min/kb) → 72°C 10min.

For descriptions of the quantitative real-time PCR see below (section 2.11).

All oligonucleotides were obtained from Sigma Genosys and were routinely desalted.

2.8.4 Agarose gel electrophoresis

Horizontal agarose gels were routinely used for the separation of DNA fragments. All agarose gels were 0.8% w/v agarose (SseKem LE, Cambrex) in 1xTAE (40mM Tris-acetate; 1mM EDTA pH8.0). The samples were loaded in 1x loading dye (6x stock: 0.25% bromophenol blue; 0.25 xylene cyanol FF; 30% v/v glycerol). Gels also contained 1µg/ml ethidium bromide to allow visualisation of the DNA under UV light.

Gels were run at ~6V/cm of the distance between the two electrodes. Hyperladder I (Bioline) was used for fragment size determination.

2.8.5 Purification of DNA from agarose gels

DNA was purified from agarose gels using the High Pure PCR Product Purification Kit from Roche as instructed by the manufacturer.

2.8.6 Southern blotting

2.8.6.1 Gel electrophoresis, gel preparation and Southern transfer

Agarose gels were run as described above. Gels were then photographed, and prepared for the transfer reaction as follows: The gel was trimmed and acid depurinated for 10min with gentle agitation in 0.25M HCl. DNA was then denatured by incubating for 25min with gentle agitation in denaturing solution (1.5M NaCl, 0.5M NaOH). Finally, the gel was neutralised in 1.5M NaCl, 1M Tris-Cl pH 7.4 for 30min with gentle agitation. Following this, DNA was transferred from the gel to a Hybond-N^+ nylon membrane (Amersham) by the capillary transfer technique (Sambrook and Russell, 2001) using 10x SSC as transfer solution (150mM Na3-Citrate, 1.5 M NaCl). The following day, the blotting setup was disassembled, the nylon membrane was removed and allowed to dry for ~15min. Finally, DNA was crosslinked to the membrane with a UV crosslinking apparatus (UV-Stratalinker 2400, Stratagene, default settings for auto crosslinking).

2.8.6.2 Probe preparation, hybridisation, stringency washes and detection

Non-radioactive probes

Non-radioactive probes were generated using the Gene Images Random Prime Labelling Module (Amersham Pharmacia Biotech) according to the manufacturer's instructions. Hybridisation and stringency wash steps were also performed as described in the manual.

For detection, the Gene Images CDP-Star Detection Module (Amersham) was used as described by the manufacturer. Membranes were exposed to Kodak Biomax XAR films.

If bands had to be quantified, the ECF detection reagent (Amersham) was used as instructed by the manufacturer. Membranes were read using a Fujifilm FLA-5000 scanner.

Radioactive probes

Radioactive probes were prepared using the Prime-a-Gene labelling system (Promega) as instructed by the manufacturer. dCTP labelled with ^{32}P at the α position (Amersham) was used.

Membranes were pre-hybridised in hybridisation buffer (0.2M Na-phosphate buffer pH 7.2; 6% w/v PEG6000; 1% BSA; 1% SDS) at 60°C for ~3hrs. Denatured probe was then added to fresh prewarmed hybrisiation buffer and this was used to replace the prehybridisation solution. Hybridisation was allowed to occur overnight (60°C).

Stringency washes were performed at 50°C. First, the membrane was washed inside the hybridisation bottle in 2xSSC; 0.1% SDS. Following this, it was further washed inside a plastic box with 1xSSC 0.1% SDS and with 0.5xSSC 0.1% SDS. The membrane was then exposed to a storage phosphor screen. Screens were read after typical exposure times of ~5days on a Storm 860 scanner (Molecular Dynamics).

2.9 Protein analysis by SDS-PAGE and immunoblotting

Samples were run on SDS-PAGE gels as described before (Sambrook and Russell, 2001). Gels were transferred to nitrocellulose membranes (Hybond-ECL, Amersham) using the semi-dry blotting mechanism (Sambrook and Russell, 2001). The transfer buffer that was used was 40mM Tris-base; 32mM glycine; 0.1% SDS 20% methanol.

Membranes were stained with 2% w/v ponceau S in 3% w/v TCA to check for equal loading and transfer efficiencies.

For immunoblots, membranes were washed in TBST and then blocked for ~30min in TBST containing 5% fat free milk (Marvel milk powder). Antibody incubations (in TBST 5% milk, see Table 2.3 for concentrations) were either for 1h at room temperature or for ca. 12h at 4°C. After each antibody incubation, the membrane was washed ~5 times with TBST for ~10min each time.

Visualisation was carried out using ECL (Amersham) as described by the manufacturer. Membranes were exposed to Kodak Biomax XAR films.

2.10 Rad53 *in situ* kinase assay

Rad53 autokinase assays were performed essentially as described (Pellicioli et al., 1999). Protein samples (generated as described in section 2.7.5) were run on 10% SDS-PAGE gels until the blue dye just migrated out from the bottom of the gel. Western blotting was then performed as described above except that methanol was omitted from the transfer buffer, and a PVDF membrane (Amersham) was used instead of nitrocellulose. The membrane was then put into denaturing solution (7M Guanidine chloride; 50mM DTT; 2mM EDTA, 50mM Tris-Cl pH 8) and incubated with gentle agitation for 1hr at room temperature. The membrane was then washed two times with TBS (10min each) and finally transferred to renaturing solution (2mM DTT; 2mM EDTA; 140mM NaCl; 1% w/v BSA; 0.04% v/v Tween 20; 10mM Tris-Cl pH7.5) in which it was incubated for 12-18hrs at 4°C. The membrane was then washed in 30mM Tris-Cl pH 7.5 for 1h. Following this, it was preincubated with kinase reaction solution for 10min (1mM DTT; 0.1mM EGTA; 20mM $MgCl_2$; 20mM $MnCl_2$; 100μM Na_3VO_4; 40mM Hepes/NaOH pH 8.0). The kinase reaction solution was then replaced and 8μl of ATP labelled with ^{32}P at the γ position (Amersham) was added for each 10ml of kinase reaction solution. After one hour at room temperature, the membrane was washed 2 times in 30mM Tris-Cl pH 7.5, once in 30mM Tris-Cl pH 7.5 containing 0.1% v/v NP-40, once in 30mM Tris-Cl pH 7.5; once in 1M KOH, and lastly once in 10% TCA. The membrane was then rinsed with water, air dried and exposed to a storage phosphor screen (Amersham). Typical exposure times were 1-2 days. Screens were read on a Storm 860 scanner (Molecular Dynamics).

2.11 Setting up a new assay for 5'-3' resection at a defined DSB

2.11.1 Overview of the assay

In the course of this study, a new assay was set up to quantify ssDNA formation at a defined DSB (induced by HO at *ARS607::HOcs*, see section 2.3). The first steps in this assay are, in principle, similar to the ones in the first of the Southern blot based assays described in section 2.2.3.6, since it relies on the resistance of ssDNA to restriction endonuclease digestion.

Samples of a culture were taken before and during HO induction and DNA was extracted. The DNA was then subjected to digestion with BstUI restriction endonuclease. At the same time, DNA was mock-digested in an identical manner, with water being substituted for BstUI. The digested and the mock-digested DNA was then used as template in quantitative real-time PCR reactions (QPCR). The TaqMan^R fluorogenic probe system was utilised for detection of PCR product formation (Heid et al., 1996). Briefly, this system is based on PCR-mediated degradation of a dually labelled probe that anneals inside the amplified sequence. On one side, the probe is labelled with a fluorophor (VIC or FAM), whose fluorescence is inhibited by the presence of a quencher molecule that labels the other end of the probe (TAMRA). Only when a probe molecule gets degraded as the DNA polymerase passes through, will the fluorophor be released and be able to fluoresce. Therefore, the intensity of fluorescence is directly proportional to the product amounts generated.

Three different amplicons were analysed, located 0.3; 9; and 14kb distal from the break (Figure 2.1A, Table 2.4). Each of them spanned two BstUI restriction sites, and none of the probes overlapped with any of these restriction sites. At early time points, only background amounts of PCR product are generated at all three amplicons, when BstUI-digested DNA is used as template (Figure 5.1A). This is because the vast majority of molecules are still double-stranded and therefore are degraded by BstUI. However, over the following period of time, as 5'-3' resection occurs, PCR products will first be detected in BstUI-digested samples at amplicons close to the HO-induced break (Figure 5.1B), and later on for amplicons that are further away from the DSB (Figure 5.1C). By comparing the amount of PCR product generated from digested template with that generated from mock-digested template DNA, the percentage of ssDNA can be calculated that is present at each time point (see below). To correct for

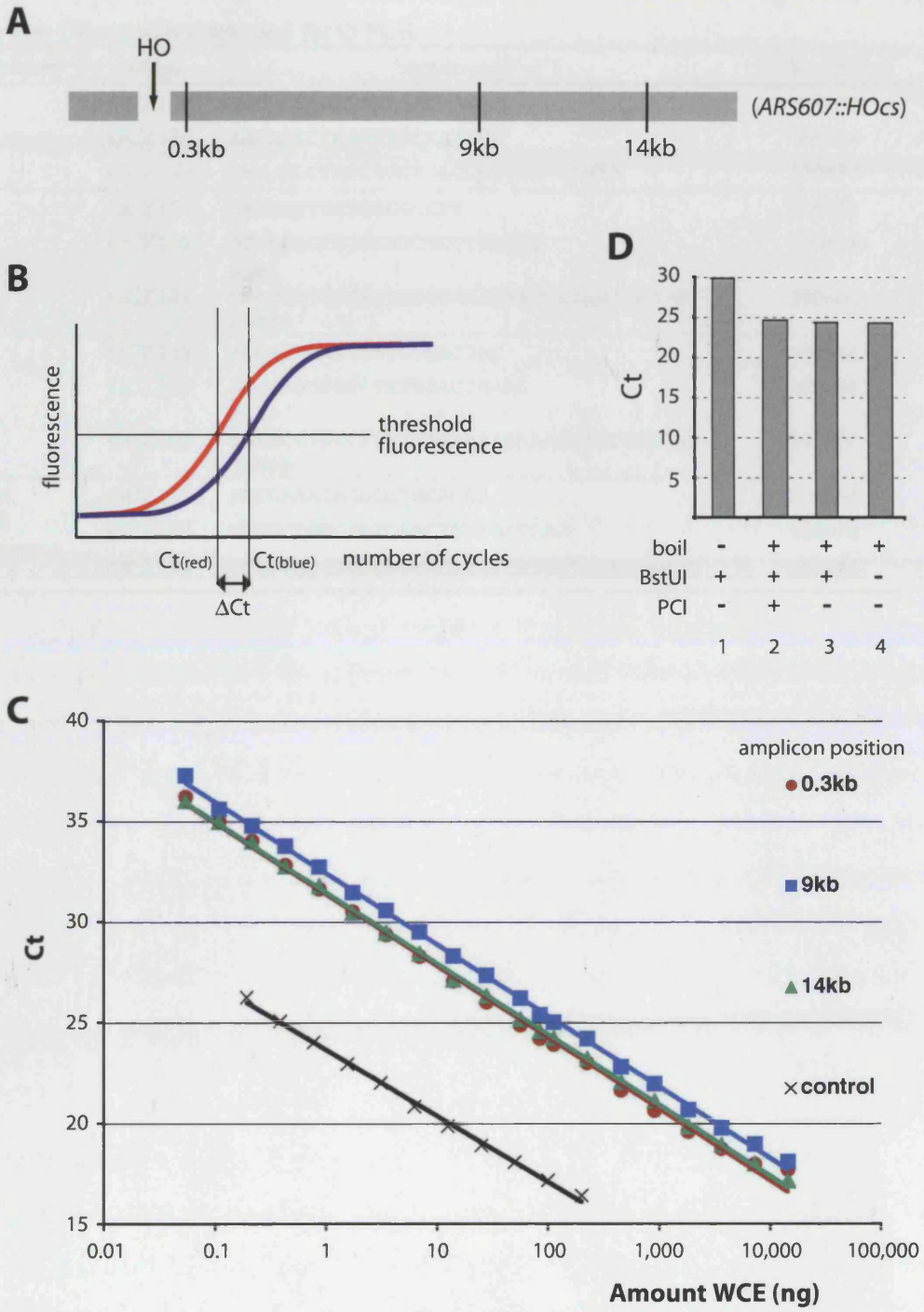

Figure 2.1: The QPCR approach. **A:** Schematic representation of the position of the sites analysed at *ARS607::HOcs*. **B:** The underlying principle of quantitative PCR. **C:** Extensive linear range of amplification of the used amplicons. **D:** No BstUI activity is retained during PCR and ssDNA is resistant to BstUI digestion. DNA extracted from YCZ64 was digested with BstUI (column 1). Another sample of the same extract was boiled and two thirds of this were digested with BstUI, whereas one third was mock-digested (columns 2-4). The digested sample was split in two and one half was extracted with phenol/chloroform/iso-amylalcohol (PCI). QPCR was then performed for all four samples using oligonucleotides OCZ125/OCZ126/OCZ140 (see Table 2.4).
Ct, threshold cycle. WCE, whole cell extract

Table 2.4: Oligonucleotides used for Q-PCR.

Amplicon	Oligo	Sequence (5'-3')	Concentration
0.3kb	OCZ125	GGCGCGAAGCAAAAATTAC	400nM
	OCZ126	AAGAACCTCAGTGGCAAATCC	400nM
	OCZ140	FAM-TCCTCGCTGCAGACCTGCGA-TAMRA	150nM
9kb	OCZ127	GAAACCTCCTGCCGCCTT	600nM
	OCZ128	GTTGTAGCTGGCATCTCCTTATGT	600nM
	OCZ141	FAM-TCATCCTTCGACTTAGGGAAGAATCTTAACAAATG-TAMRA	200nM
14kb	OCZ129	ACCATACAACTTTCGCACGAC	600nM
	OCZ130	AAGGAAGTGTCTATGGACCGAAC	600nM
	OCZ142	FAM-TGATCATATCTTTGCAGAAAATAAACGAACCAAGAC-TAMRA	200nM
internal control, chromosome XIII	OCZ135	AATCAAATAGGCGTGGAGCA	400nM
	OCZ136	TTCGCTGTCTATCAACTCTAGATCAG	400nM
	OCZ139	VIC-TGCGTCCTTTTCCAGATCATCTTCCA-TAMRA	200nM

possible variations in template input amounts, the data was normalised to an amplicon on a different chromosome that does not contain any BstUI sites (Table 2.4).

2.11.2 DNA extraction and BstUI digestion

DNA extractions

$2x10^7$ cells were harvested and frozen on dry ice. Cells were stored at –80°C until use. For DNA preparations, cells were thawed on ice and resuspended in 500µl extraction solution (1% SDS; 100mM NaCl; 10mM EDTA; 50mM Tris-Cl pH 8.0; 1% v/v β-mercaptoethanol; 1u/µl lyticase) and lysed by incubation with shaking at 37°C for 6min. Cells were then extracted twice with equal volumes of phenol/chloroform/iso-amylalcohol (25:24:1) and once with chloroform (Sambrook and Russell, 2001). Phenol saturated with Tris base was used (Rathburn) and phase lock gel tubes (Eppendorf) were used for extractions. Two volumes of 99% ethanol were added to the last aqueous phase, and nucleic acids were precipitated by incubation at –20°C for ~30min. Tubes were then centrifuged (13krpm ~8sec) and the supernatant was discarded. Care was taken to take out as much of the liquid as possible. Pellets were dried for 1min at 37°C and then resuspended in TE pH 8.0 containing 0.05µg/µl RNase A (40µl for samples from G1-arrested cells, 70µl for samples from M-arrested cells). RNA was digested by incubation for 45min at 37°C with shaking. DNA extraction and RNase digestion were confirmed by running 1µl on an agarose gel. Samples were then stored at –20°C until use.

BstUI digestion

4µl of the DNA extracts were digested in a total volume of 30µl containing 10u of BstUI in 1xbuffer 2 (both New Englands Biolabs). Reactions were allowed to proceed for 1hr at 60°C in a PTC-200 temperature cycler (MJ Research) with lid heating. In mock digests, BstUI was replaced with water. Samples were cooled on ice, centrifuged and then serially diluted three times in 1xTE pH 8.0, first 1:4 and then twice 1:2. The diluted samples, which were to be used as template in QPCR reactions, were stored at –20°C. Filter tips were used throughout, and samples were always kept on ice during the dilutions.

2.11.3 PCR analysis

QPCR was performed with the ABI7000 Sequence Detection System and corresponding software (Applied Biosystems). 1x ABsolute QPCR ROX Mix (ABgene) was used for the reactions. Table 2.4 lists the oligonucleotides for each amplicon and their respective concentrations within the PCR reaction mix. All labelled oligonucleotides (the TaqMan^R probes) were obtained from ABI. All other oligonucleotides were obtained from Sigma Genosys. Reaction volumes were 40µl, containing 4µl of the diluted samples each. The temperature cycling program was 95°C 15min → 45 x (95°C 15sec → 60°C 1min). Primer and probe concentrations were optimised as instructed by ABI QPCR manuals.

For PCR analysis, the base line was set to cycles 6-15, and the following fluorescence values determined the threshold cycle (see below):

Amplicon 0.3kb:	0.16
Amplicon 9kb:	0.2
Amplicon 14kb:	0.2
Control amplicon:	0.1

2.11.4 Analysis of break formation by southern blotting

Samples from the DNA extracts were digested with EcoRI and NotI (New England Biolabs) for 1hr at 37°C. The digested DNA was then separated on an 0.8% agarose gel and Southern transferred as described above. Probe generation and hybridisation were carried out as described above (section 2.8.6). Both radioactively labelled and non-radioactively labelled probes were used.

A 1.5kb PCR product corresponding to the region 1026-2532bp distal of the break at *ARS607::HOcs* was used for labelling. This PCR product was cloned into pGEM-T (Promega) to make pCZ29, and miniprep plasmid was used in PCR to generate template for labelling. Disappearance of a 4.3kb band corresponding to the intact locus was charted. Bands were quantified using Imagequant v.1.2 (Molecular Dynamics, radiolabelled probes) and AIDA v3.20.116 (Raytest, for non-radioactive probes).

2.11.5 Mathematical calculations

In real-time PCR, relative differences in template DNA are calculated by comparing the number of PCR cycles required to reach a specific fluorescence level, known as threshold fluorescence (Figure 2.1B). This value is referred to as threshold cycle, Ct, and the difference in Ct between two reactions is hence known as ΔCt (Figure 2.1B). Each cycle difference between two reactions is a consequence of a two-fold difference in template amounts. Threshold fluorescence is set in the mid-range of exponential detection of PCR product formation.

Rather than doing the usual triplicates of identical reactions during QPCR, it was decided to use three serial dilutions of BstUI digests and mock digests (see above). This step controlled for the linearity of PCR reactions. After subtraction of one cycle per dilution, averages of the three Ct values were calculated.

The following formula describes the percentage difference in template amounts between two reactions:

$$\% \text{ difference} = 100/(2^{\Delta Ct}) \qquad \text{(Equation 1)}$$

In the specific case of the assay described here, ΔCt describes the difference in average Ct values between undigested and digested template. ΔCt is thus computed from the following equation:

$$\Delta Ct = Ct_{(+BstUI,\ break)} - Ct_{(-BstUI,\ break)} \qquad \text{(Equation 2)}$$

(where $Ct_{(+BstUI,\ break)}$ is the Ct value for a given amplicon at the break region using digested DNA as template, and $Ct_{(-BstUI,\ break)}$ is the Ct value for its mock-digested counterpart)

To accommodate possible differences in the input amounts between digested and undigested samples, ΔCt was normalised to the control amplicon (Table 2.4). In this equation, $Ct_{(+BstUI,\ control)}$ is the Ct value of the control amplicon using digested DNA as template, and $Ct_{(-BstUI,\ control)}$ is the Ct value for its mock-digested counterpart:

$$\Delta Ct = (Ct_{(+BstUI,\ break)} - Ct_{(-BstUI,\ break)}) - (Ct_{(+BstUI,\ control)} - Ct_{(-BstUI,\ control)}) \qquad \text{(Equation 3)}$$

Equation 1 only describes the difference in template amounts between two reactions. Since all the template DNA that remains after BstUI digestion is single-stranded, Equation 1 furthermore has to be modified as follows to describe the percentage of resected molecules at a given locus at a given time:

$$\% \text{ resected} = 100/[(1+2^{\Delta Ct})/2] \qquad \text{(Equation 4)}$$

Lastly, the fraction of molecules cut by HO (f) has to be taken into account:

$$\% \text{ resected} = \{100[(1+2^{\Delta Ct})/2]\}/f \qquad \text{(Equation 5)}$$

The equations described above allow the calculation of the proportion of ssDNA as a percentage of the total DNA that is present at each time point. However, although not represented in this thesis, it is also possible, to determine the number of resected molecules present at each time point (t_i) relative to the number of molecules that were present before HO induction (t_0). In this case, ΔCt is described by the following equation:

$$\Delta Ct=[(Ctt_{0(\text{-BstUI, control})}\text{-}Ctt_{i(\text{+BstUI, control})})+Ctt_{i(\text{+BstUI, break})}]\text{-}Ctt_{0(\text{-BstUI, break})}$$

(Equation 6)

Here, ΔCt describes the difference between undigested template at t_0 and digested template at a given time point t_i.

The percentage of ssDNA is then calculated by using following equation:

$$\%resected=(100/2^{\Delta Ct\text{-}1})/f$$ (Equation 7)

Lastly, information obtained from QPCR can also be used to quantify whole template levels throughout a time course. As with the previous paragraph, such data is not presented in this study. However, for completeness's sake it is outlined here. In principle, if resection were allowed to occur to completion, this should result in a 50% drop in template levels at the most. If template were lost beyond 50%, this would be indicative of degradation of the 3' strand as well. Equation 1 can be used to calculate template levels when ΔCt is expressed by following formula.

$$\Delta Ct=[(Ctt_{0(\text{-BstUI, control})}\text{-}Ctt_{i(\text{-BstUI, control})})+Ctt_{i(\text{-BstUI, break})}]\text{-}Ctt_{0(\text{-BstUI, break})}$$

(Equation 8)

2.11.6 Control experiments

Template titration experiments were carried out to determine the linear range of amplification of each of the four PCR products (Figure 2.1C). DNA extracted from strain YCZ64 grown in YPD was quantified using the fluorescent dye PicoGreen (Molecular Probes) as instructed by the manufacturer. An RF-1501 spectrofluorophotometer (Shimadzu) was used to read DNA-PicoGreen fluorescence levels. Serial dilutions of the extracted DNA were used in QPCR reactions, without having been digested by BstUI beforehand. All four different sets of PCR primers had a linear detection range of PCR product over several orders of magnitude of template

DNA amounts (Figure 2.1C). Typical Ct values in actual experiments were in between 20 and 33 cycles for all amplicons used to detect ssDNA, and around 20 cycles for the control locus. These values are well within the linear detection range.

Although there are no indications that BstUI is able to cut ssDNA, it was tested whether treatment of heat-denatured DNA with BstUI had an effect on the outcome of QPCR if used as template. If BstUI shows no activity on ssDNA, heat denatured DNA should be completely resistant to enzyme treatment. No difference in QPCR efficiency between BstUI-treated and mock-treated template is expected in such a scenario. DNA was boiled for 5min and snap-cooled on ice. It was then used in restriction digests as before. QPCR was then performed for the amplicon closest to the HO site at *ARS607* (0.3kb). As shown in Figure 2.1D, column 3 and 4, no relevant difference in amplification was detected when boiled and BstUI treated DNA was compared with its boiled and mock-treated counterpart. In contrast, treatment of non-denatured DNA with BstUI resulted in an increase of Ct by ~6 cycles, thus confirming BstUI activity (a ~64-fold difference in PCR efficiency, column 1 in Figure 2.1D). Together, these findings confirm that ssDNA is indeed resistant to BstUI-digestion.

BstUI shows optimal cutting efficiency at 60°C, and can thus be expected to be relatively thermostable. It is of vital importance, however, that the enzyme does not remain active during PCR. Therefore, a part of the boiled and BstUI-treated DNA used in the previous experiment was extracted with phenol/chloroform/isoamylalcohol (see above) to remove the restriction enzyme. After extraction, DNA amounts were quantified as before to correct for any possible losses during the extraction. When this sample was used as template in QPCR of the amplicon closest to the HO site at *ARS607* and compared to its counterpart that had not been extracted, no relevant difference in PCR efficiency was detected (Figure 2.1D, compare column 2 with column 3). Since remaining BstUI activity in the non-extracted sample should result in an increase in Ct, this finding allows the conclusion that no such activity remains during QPCR.

The next question that was addressed was whether both strands were amplified with similar efficiencies. Bacteriophage T7 exonuclease (New England Biolabs) was used to mimic 5'-3' resection *in vitro*. This enzyme specifically degrades the 5' strand from dsDNA termini, and should thus result in the generation of similar structures as 5'-3'

resection *in vivo* (Kerr and Sadowski, 1972b; Kerr and Sadowski, 1972a; Shinozaki and Okazaki, 1978).

Strain YCZ101 was arrested in nocodazole and HO expression was induced for 1hr. At this point, >90% of the break sites were cut by HO (data not shown). A sample was taken and extracted as described above. 12µl of the DNA extract were digested with 20u T7 exonuclease in a total volume of 20µl. The recommended buffer was used at 1x concentration and digestion was allowed to proceed for 1.5h at 25°C. In parallel, mock digests using water instead of exonuclease were performed. 7.5µl of each mix were digested and mock-digested with BstUI as described above. Samples were diluted as described and used as template in QPCR-amplification of all the three different amplicons at *ARS607::HOcs*.

QPCR was performed with template DNA that had been digested with T7 exonuclease. In parallel, QPCR was performed using template that had not been treated with T7 exonuclease. Neither DNA had been digested with BstUI. The two Ct values were then compared with each other. As expected, PCR reactions with template that had been digested with T7 exonuclease required ~1 additional cycle to reach threshold fluorescence (Figure 2.2A). Thus, the loss of the 5' strand results in the predicted reduction in template amounts by 50%. These findings therefore confirm that both strands are amplified with similar efficiencies.

It was also determined whether T7 exonuclease-generated ssDNA was resistant to BstUI digestion. dsDNA (mock-treated with BstUI) was sensitive to BstUI digestion, and a large increase in Ct was observed when used as template and compared with its undigested counterpart (Figure 2.2B). In contrast, no relevant difference in Ct was detected when BstUI-treated or mock-treated DNA that had been digested with T7 exonuclease beforehand was used as template (Figure 2.2C). Therefore, these findings confirm the results obtained with boiled DNA described above and indicate that ssDNA is indeed resistant to BstUI digestion.

Together, these control experiments show that the assay described above is well suited to the demands of detecting and quantifying ssDNA formation *in vivo*. Chapter 5 describes how this assay was used in an experimental approach to gaining information about the regulation of DSB resection.

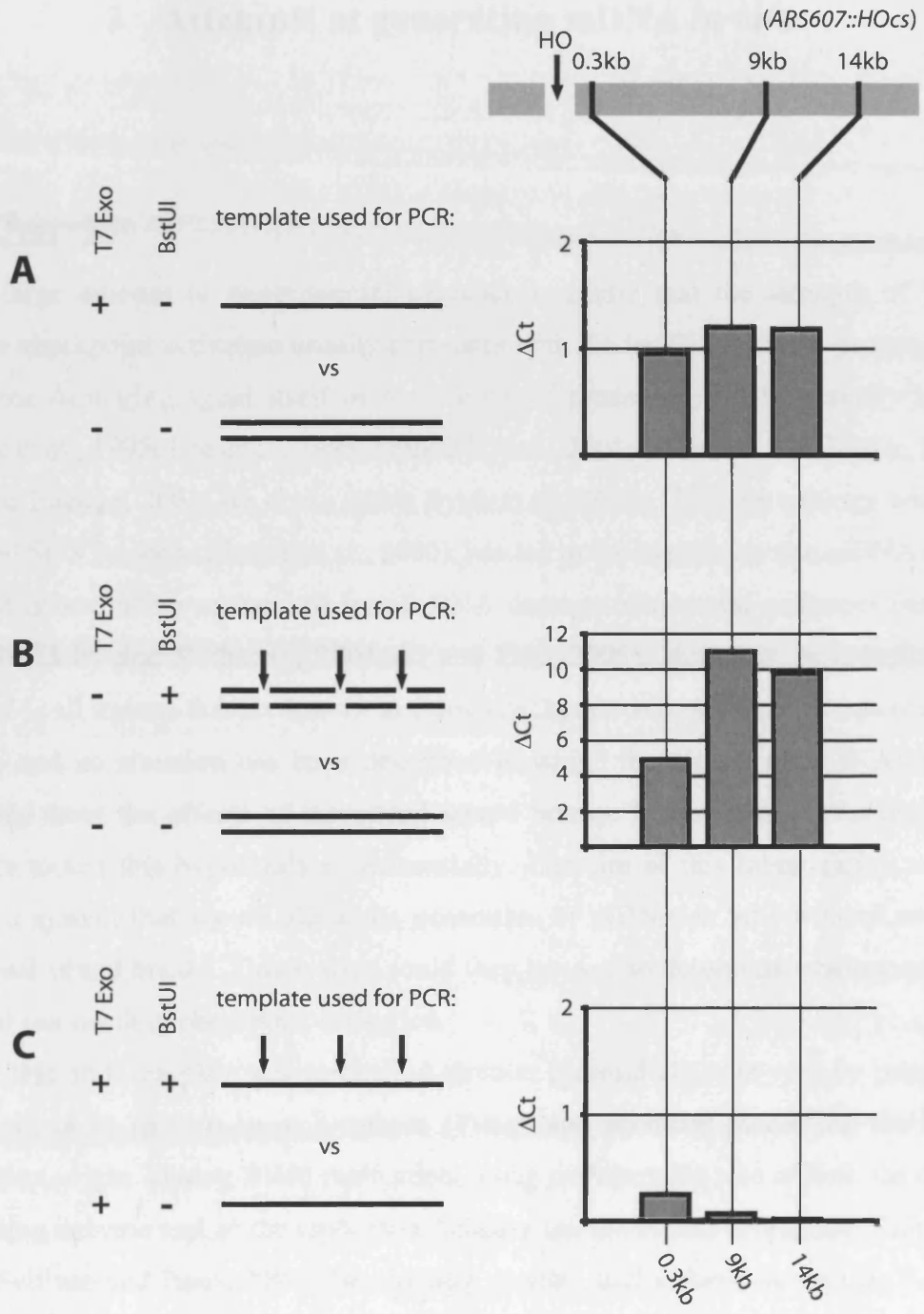

Figure 2.2: Analysis of *in vitro* resection using T7 exonuclease. DNA was extracted from strain YCZ64 after 1hr of HO induction. **A:** Both strands are amplified with similar efficiencies. DNA was either digested or mock-digested with T7 exonuclease and used as template in QPCR. The graphs show the difference in Ct values between the two reactions. **B:** BstUI digestion of dsDNA interferes with PCR amplification. DNA was mock-digested with T7 exonuclease and subsequently digested or mock-digested with BstUI. Graphs represent comparisons of Ct values of the BstUI and the mock-digested samples. **C:** ssDNA is resistant to BstUI digestion. DNA was digested with T7 exonuclease and subsequently either digested or mock-digested with BstUI. The graphs show comparisons of Ct values of BstUI digested versus mock-digested template.

3 Attempts at generating ssDNA *in vivo*

3.1 Overview

A large amount of experimental evidence suggests that the strength of DNA damage checkpoint activation usually correlates with the levels of ssDNA produced by either the damaging agent itself or as a result of processing of the primary lesion (Garvik et al., 1995; Lee et al., 1998; Pellicioli et al., 2001; Costanzo and Gautier, 2003; Zou and Elledge, 2003; Ira et al., 2004; Byun et al., 2005). This, by analogy with the bacterial SOS response (Sutton et al., 2000), has led to the hypothesis that ssDNA is the DNA structure being recognised by all DNA damage checkpoint pathways (see for example Lisby and Rothstein, 2004; Li and Zou, 2005). However, as described in Chapter 1, all lesions that are known to cause checkpoint activation also contain strand breaks, and no situation has been described in which the effects of ssDNA can be separated from the effects of associated strand breaks. It has, thus, so far not been possible to test this hypothesis experimentally. The aim of this investigation was to design a system that should allow the generation of ssDNA *in vivo* without causing additional strand breaks. This system could then be used to determine whether ssDNA by itself can result in checkpoint activation.

To this end, the plan was to unwind circular plasmid DNA *in vivo* by using the simian virus 40 (SV40) large T-antigen (T-Ag) and plasmids containing the SV40 replication origin. During SV40 replication, T-Ag performs the role of both the origin unwinding enzyme and of the replicative helicase (reviewed in Fanning and Knippers, 1992; Sullivan and Pipas, 2002). Importantly, *in vitro* studies have shown that T-Ag is able to co-operate with yeast RPA for origin unwinding and helicase activities, but not in any of the further steps in SV40 replication (such as primase recruitment; Brill and Stillman, 1989). Thus, expression of T-Ag in yeast containing SV40 origin plasmids should lead to origin melting and plasmid DNA unwinding without inducing DNA synthesis or causing DNA breaks to be formed.

3.2 Results

3.2.1 Expression of T-Ag in yeast does not result in checkpoint activation

Yeast strains were constructed containing multiple (≥4) copies of the ORF encoding T-Ag under the control of the GAL_{1-10} promoter stably integrated into the chromosomal *leu2* locus. Expression of T-Ag from these constructs can be induced by the addition of galactose to the growth medium. No expression of T-Ag was observed in cultures grown in the absence of galactose (Figure 3.1A). As expected, shifting cultures to medium containing galactose resulted in the rapid expression of T-Ag (Figure 3.1A).

Two different plasmids were constructed that contained four tandem repeats of the SV40 origin of replication (see Materials and Methods). One plasmid was based on the low-copy centromeric vector pRS316 (Sikorski and Hieter, 1989) (referred to as pCEN-4xori); the other was based on the multi-copy vector pRS426 (Christianson et al., 1992) that does not contain a centromere (referred to as p2μm-4xori). Since no induction of T-Ag was observed upon galactose-induction in minimal medium (used to select for the *URA3* marker on the plasmids), the plasmids were modified to additionally contain the *KanMX4* marker gene. This allowed selection for the plasmids in rich medium by adding the drug G418 to the growth medium (Wach et al., 1994). Under these conditions, T-Ag induction was possible (see below).

Cultures of the parent strain or the strain expressing T-Ag transformed with either plasmid were grown to mid-exponential phase in YPRaff and subsequently shifted to YPGal to induce expression of T-Ag (Figure 3.1A). Although T-Ag production was clearly detected, no phosphorylation of Rad53 was observed (Figure 3.1A), indicating that the checkpoint was not activated. Additionally, the cell cycle profile and density of each culture was monitored (Table 3.1). Cell morphology in *S. cerevisiae* closely correlates with the cell cycle stage: unbudded cells are in the G1 stage of the cell cycle, small-budded cells are in S-phase, and large-budded cells signify a position in either G2 or M phase. Since checkpoint activation results in an inhibition of cell proliferation and cell cycle arrest mostly in the G2/M stage (Weinert and Hartwell, 1988; Weinert and Hartwell, 1993; Sanchez et al., 1999), activation of the checkpoint should lead to an over-representation of large budded cells and/or an attenuation of cell proliferation. However, as shown in Table 3.1, no arrest or inhibition of growth was observed when strains expressing T-Ag were compared with their parent strain. Together with the absence of Rad53 activation (Figure 3.1A) this argues that the expression of T-Ag in

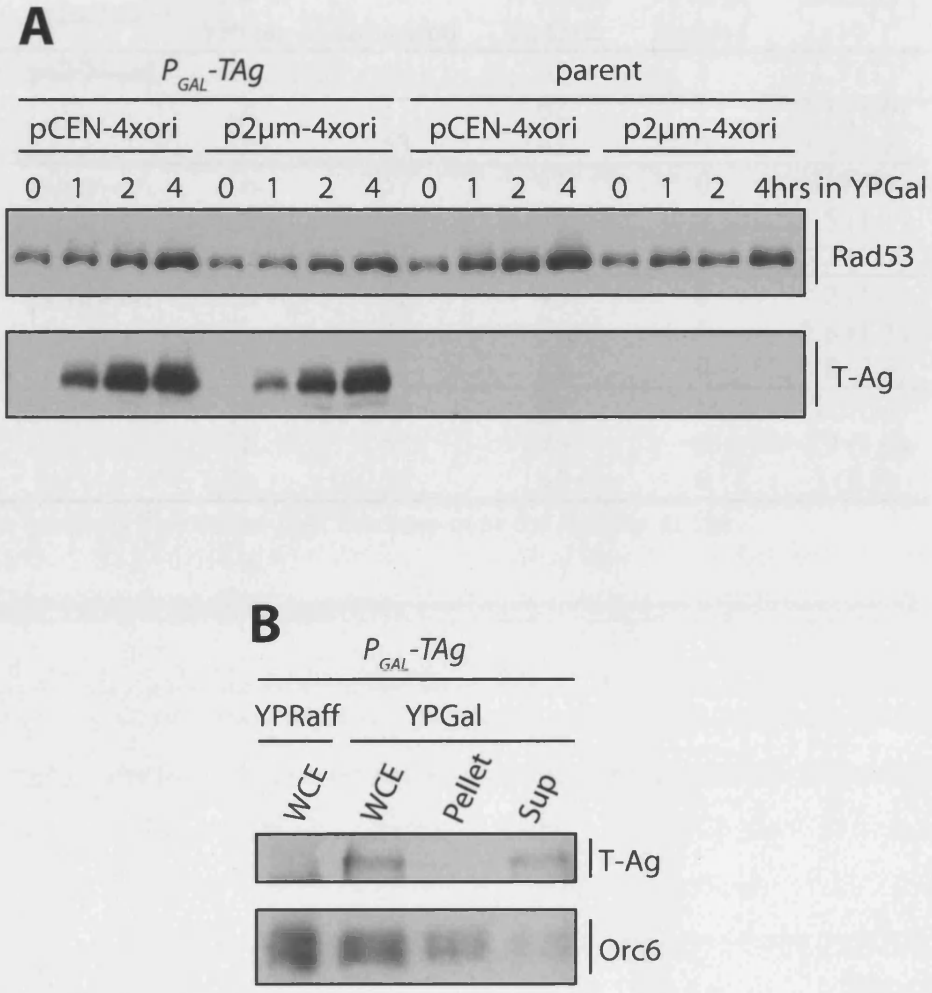

Figure 3.1: Expression of T-Ag in yeast does not result in checkpoint activation. **A:** Cells of strain YCZ5 (P_{GAL}-*TAg*) and w303-1b (parent) transformed with either pCEN-4xori (pCZ12) or p2µm-4xori (pCZ13) were grown inYPRaff G418 and shifted to YPGal G418. TCA extracts were analysed by western blotting. **B:** Chromatin fractionation of samples of strain YCZ5 (P_{GAL}-*TAg*) grown either in YPRaff or YPGal. WCE: whole cell extract; Pellet: chromatin enriched pellet; Sup: supernatant.

Table 3.1: Expression of T-Ag in yeast does not inhibit cell-cycle progression.

strain	plasmid	Time in YPGal	% unbudded	% small budded	% large budded	Density ($x10^7$)[a]
P_{GAL}-TAg	pCEN-ori	1h	47	52	1	1.3 (1)
		2h	37	62	1	2.1 (1.6)
		3h	55	45	0	3.2 (2.5)
	p2μm-ori	1h	57	43	0	1.4 (1)
		2h	45	55	0	1.5 (1.1)
		3h	64	35	1	3.2 (2.3)
parent	pCEN-ori	1h	55	45	0	2 (1)
		2h	45	54	1	2.6 (1.3)
		3h	51	49	0	4.8 (2.4)
	p2μm-ori	1h	50	49	1	1.2 (1)
		2h	54	46	0	1.9 (1.6)
		3h	59	41	0	3 (2.5)

[a] Values in brackets denote the fold increase over the density at 1hr

yeast containing SV40 origin plasmids does not result in checkpoint activation. Furthermore, no obvious growth inhibition was detected on YPGal G418 plates incubated over several days, indicating an absence of chronic effects of T-Ag expression.

3.2.2 Expression of T-Ag in yeast does not affect topology of SV40 origin plasmids

The lack of checkpoint activation described above raised the possibility that T-Ag was inactive in yeast. Previously, it was shown that in *in vitro* experiments, T-Ag is able to co-operate with yeast RPA in origin unwinding and helicase activity, but not in the recruitment of primase (Brill and Stillman, 1989). If T-Ag were active in yeast, unwound plasmid DNA should be present and detectable. Therefore, plasmid topology was followed throughout the experiment.

During plasmid unwinding, each helical turn that is being unwound leads to the formation of a compensatory positive supercoil ahead of the helicase (Hiasa and Marians, 1996; Walter and Newport, 2000; Postow et al., 2001). These positive supercoils are, however, almost immediately relaxed by topoisomerases. *In vivo*, the re-annealing of the separated strands is inhibited by the single-strand binding complex RPA (see also Chapters 1 and 4). However, in a deproteinised DNA extract, the separated strands are able to re-anneal. Since this occurs in the absence of topoisomerases, each helical turn that re-anneals results in the formation of a compensatory negative supercoil. Thus, the re-annealing of a partially or completely unwound circular plasmid generates molecules with a higher number of negative supercoils than were present in the starting molecules (see for example Baker et al., 1986; Walter and Newport, 2000).

On standard agarose gels, these highly supercoiled plasmids cannot be resolved from the regularly supercoiled form. However, the addition of DNA intercalating agents such as chloroquine or ethidium bromide to the gel and running buffer allows detection of these different topoisomers (Bates and Maxwell, 1993). These agents cause local unwinding of the double helix and a decrease in the twist of the molecule (number of helical turns) by binding in between the base stacks. The decrease in twist is accommodated for by the relaxation of negative supercoils, resulting in reduced gel mobility of the plasmid. At a certain concentration of intercalator, the DNA will run at an identical position as the relaxed (nicked) plasmid. If the intercalator concentration is

increased even further, positive supercoils will be induced, resulting in an increased mobility of the plasmid. Because of the resolution limits of gel electrophoresis, a highly negatively supercoiled plasmid will appear to be resistant in its gel mobility to low concentrations of chloroquine (Walter and Newport, 2000).

Plasmid topology of both pCEN-4xori and p2μm-4xori extracted from samples taken at regular intervals during galactose induction was analysed by Southern blotting. Membranes were hybridised with probes generated by random prime labelling of each plasmid (see Material and Methods). After optimisation of the concentration of chloroquine, agarose gels containing 3.5μM chloroquine were used for the assay. As control experiments, gels were run in parallel that contained no chloroquine.

Either plasmid, when extracted from *E. coli* or yeast not expressing T-Ag, showed reduced gel mobility and shifted towards the position of the relaxed (open) circle in gels containing chloroquine (Figure 3.2; Figure 3.3 and data not shown). Because the superhelicity throughout the population of a given plasmid is not identical in all the individual molecules, a distribution of topoisomers can be detected on both the gels containing chloroquine and lacking chloroquine (Figure 3.2 and Figure 3.3). These topoisomers cannot be separated in standard ethidium bromide gels because of the high concentration of intercalator used (Bates and Maxwell, 1993). In addition to the bands resulting from different supercoiled topoisomers, several other bands can be observed (Figure 3.2 and Figure 3.3). One band, labelled OC, represents the open (relaxed) circular form, resulting from single-strand breaks (nicks) introduced during DNA extraction (Bates and Maxwell, 1993). Other forms, labelled RI for replication intermediates, represent transient forms produced during the process of DNA replication (Sundin and Varshavsky, 1980; Sundin and Varshavsky, 1981).

No changes in the distribution of plasmid topoisomers were detected when expression of T-Ag was induced by shifting the culture to medium containing galactose (Figure 3.2 and Figure 3.3). Importantly, no plasmid forms were detected that appeared to be resistant to the effects of chloroquine. Since, as described above, such forms would have been the consequence of plasmid unwinding, this allows the conclusion that T-Ag was not functional in yeast. Interestingly, T-Ag was not found to associate with chromatin precipitates in cell fractionation experiments (Figure 3.1B; see Material and Methods for details about this assay). Whereas Orc6, a component of the origin recognition complex that stays associated with DNA throughout the cell cycle (Diffley et al., 1994; Donovan and Diffley, 1996), was specifically enriched in chromatin pellets,

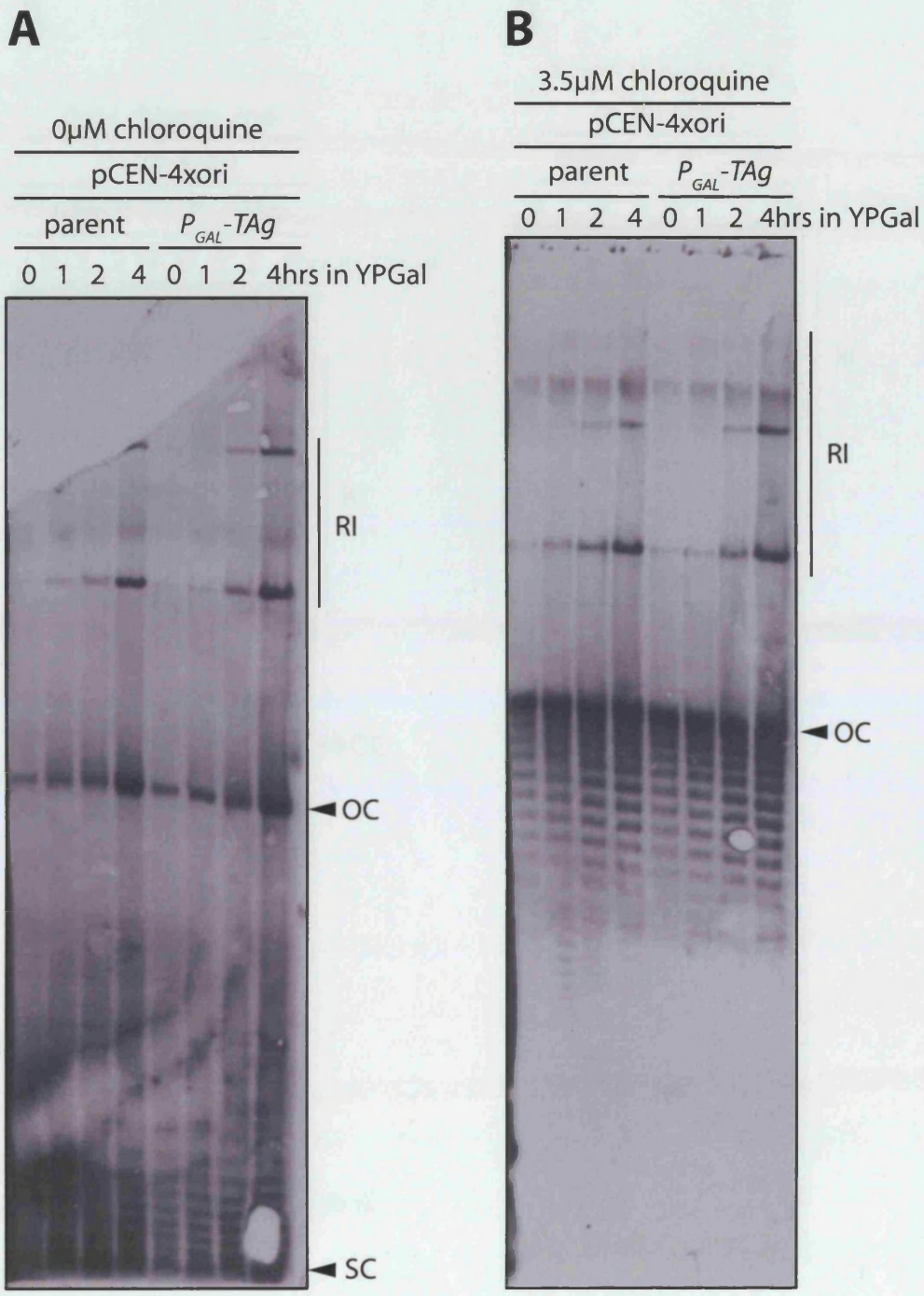

Figure 3.2: Expression of T-Ag does not result in any obvious topological changes in the pCEN-4xori plasmid. **A:** cells of strain YCZ5 (P_{GAL}-*TAg*) and w303-1b (parent) transformed with pCEN-4xori (pCZ12) were grown in YPRaff G418 and shifted to YPGal G418 to induce expression of T-Ag. DNA samples were run on an agarose gel in the absence of chloroquine.
B: Aliquots of the same samples as in A were run on an agarose gel containing 3.5μM chloroquine. SC: supercoiled plasmid; OC: open circle; RI: replication intermediates.

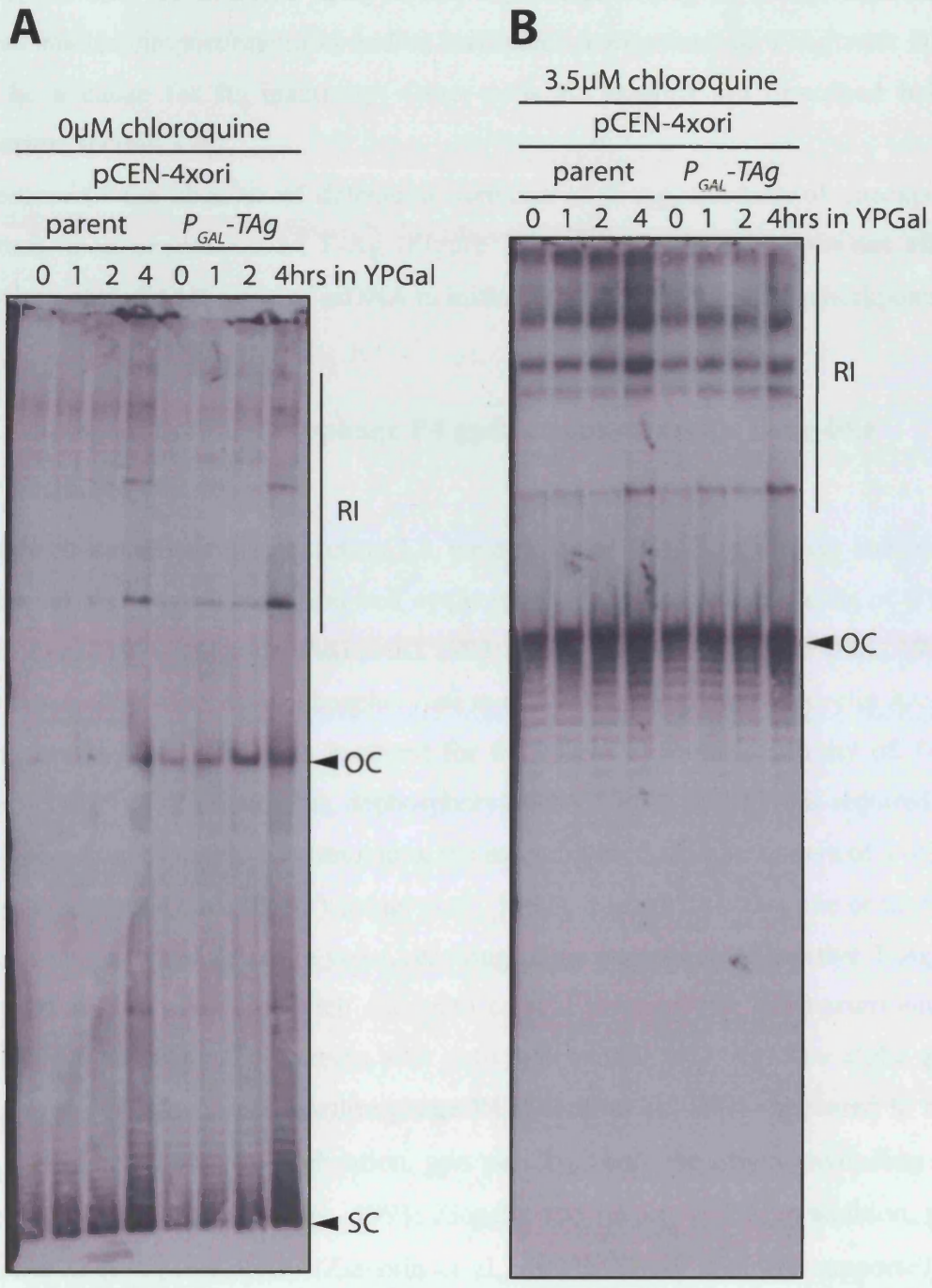

Figure 3.3: Expression of T-Ag does not result in any obvious topological changes in the p2μm-4xori plasmid. **A:** Cells of strain YCZ5 (P_{GAL}-*TAg*) and w303-1b (parent) transformed with p2μm-4xori (pCZ13) were grown in YPRaff G418 and shifted to YPGal G418 to induce expression of T-Ag. DNA samples were run on an agarose gel in the absence of chloroquine.
B: Aliquots of the same samples as in A were run on an agarose gel containing 3.5μM chloroquine. SC: supercoiled plasmid; OC: open circle; RI: replication intermediates.

T-Ag could only be detected in cytosolic supernatants (Figure 3.1B). Therefore, impaired nuclear import/retention and/or inefficient interactions of T-Ag with DNA might be a cause for its inactivity. Other possible reasons are described below (Discussion, section 3.3).

Because of the absence of detectable function of T-Ag, the lack of checkpoint activation upon expression of T-Ag (Figure 3.1A and Table 3.1) does not allow conclusions regarding the role of ssDNA in initiation of the DNA damage checkpoint.

3.2.3 Expression of bacteriophage P4 gpα, an enzyme with T-Ag-like activities

As discussed more fully in section 3.3, the activity of T-Ag is intimately connected with the cellular environment and cell cycle stage of the natural host cells of SV40 (McVey et al., 1989; Adamczewski et al., 1993; McVey et al., 1993; Xiao et al., 1998). In particular, CDK-dependent phosphorylation of T-Ag, presumably by cyclin A/cdc2 (Adamczewski et al., 1993), is required for the origin unwinding activity of T-Ag (McVey et al., 1993). In addition, dephosphorylation of T-Ag by PP2A is required for SV40 replication, probably by stimulating the assembly of double hexamers of T-Ag at the origin (Virshup et al., 1989; Virshup et al., 1992). It is possible that one or more of these mechanisms are lacking in yeast, resulting in the expression of inactive T-Ag. In order to avoid the effects of such elaborate control mechanisms, the bacteriophage literature was searched for proteins with activities similar to T-Ag. The alpha gene product (gpα) of the *E. coli* satellite phage P4 (Briani et al., 2001) appeared to be a useful candidate. During P4 replication, gpα performs both the origin unwinding and helicase functions (Ziegelin et al., 1993; Ziegelin and Lanka, 1995). In addition, gpα also contains primase activity (Ziegelin et al., 1993). These data are supported by several lines of experimental evidence in addition to helicase and primase assays. *In vivo* experiments have shown that the host initiator protein DnaA, and DnaC, the loading factor for the host helicase DnaB, are not required for P4 replication (Ziegelin and Lanka, 1995). Importantly, other studies have also shown that the host helicase DnaB itself is dispensable for P4 *in vitro* replication (Diaz Orejas et al., 1994). Furthermore, the DnaA chaperones DnaJ and DnaK and the host primase DnaG are not required for *in vitro* replication (Diaz Orejas et al., 1994).

Since it was essential not to initiate DNA replication during plasmid unwinding, a point mutation in gpα shown to abolish primase activity was utilised (Strack et al., 1992; Ziegelin et al., 1995). Similar to the T-Ag expressing strains, yeast strains were generated that carried $P_{GAL1\text{-}10}$::*gpα* fusions stably integrated into the genome at the *trp1* locus. To allow gpα to migrate into the nucleus and to be able to detect the protein by western blotting, two copies of the SV40 T-Ag nuclear localisation signal (NLS) (Nguyen et al., 2000; Nguyen et al., 2001) and Myc and His tags were fused to the gpα ORF. Two different fusion genes, 2xNLS-gpα-MycHis and gpα-2xNLS-MycHis, were constructed. Strains expressing either of these proteins behaved in an identical manner in all assays. For brevity, however, only the results obtained with the gpα-2xNLS-MycHis version are described.

Two different plasmids were constructed, based on the SV40 origin plasmids described earlier (see section 3.2.1). The two plasmids contained both the *oriI* and *crr* regions of P4 shown to be required for P4 replication both *in vitro* and *in vivo* (Flensburg and Calendar, 1987). A centromeric version, pCEN-ori, and a multicopy version without a centromere, p2μm-ori, were constructed. Furthermore, the analogous plasmids lacking *oriI* and *crr* (referred to as pCEN and p2μm) were used as controls.

As shown in Figure 3.4B, no gpα expression was detected when cells were grown in the absence of galactose. Moreover, no cross-reacting band was detected with the anti-Myc antibody in the parental strain (Figure 3.4A). Upon shifting the strains from YPRaff to YPGal, rapid induction of gpα expression was observed (Figure 3.4B). However, production of gpα did not lead to hyperphosphorylation of Rad53, even when the strains contained origin plasmids (Figure 3.4B).

As for the experiments described above for T-Ag expressing cells, cell proliferation and cell cycle stage distribution were followed throughout the experiment (Table 3.2). Again, no evidence of cell cycle arrest or growth inhibition was detected upon expression of gpα (Table 3.2). Furthermore, no obvious growth defects on YPGal G418 plates were observed (data not shown). Together, these findings imply that expression of gpα does not result in checkpoint activation, irrespective of whether cells contain origin-plasmids or not.

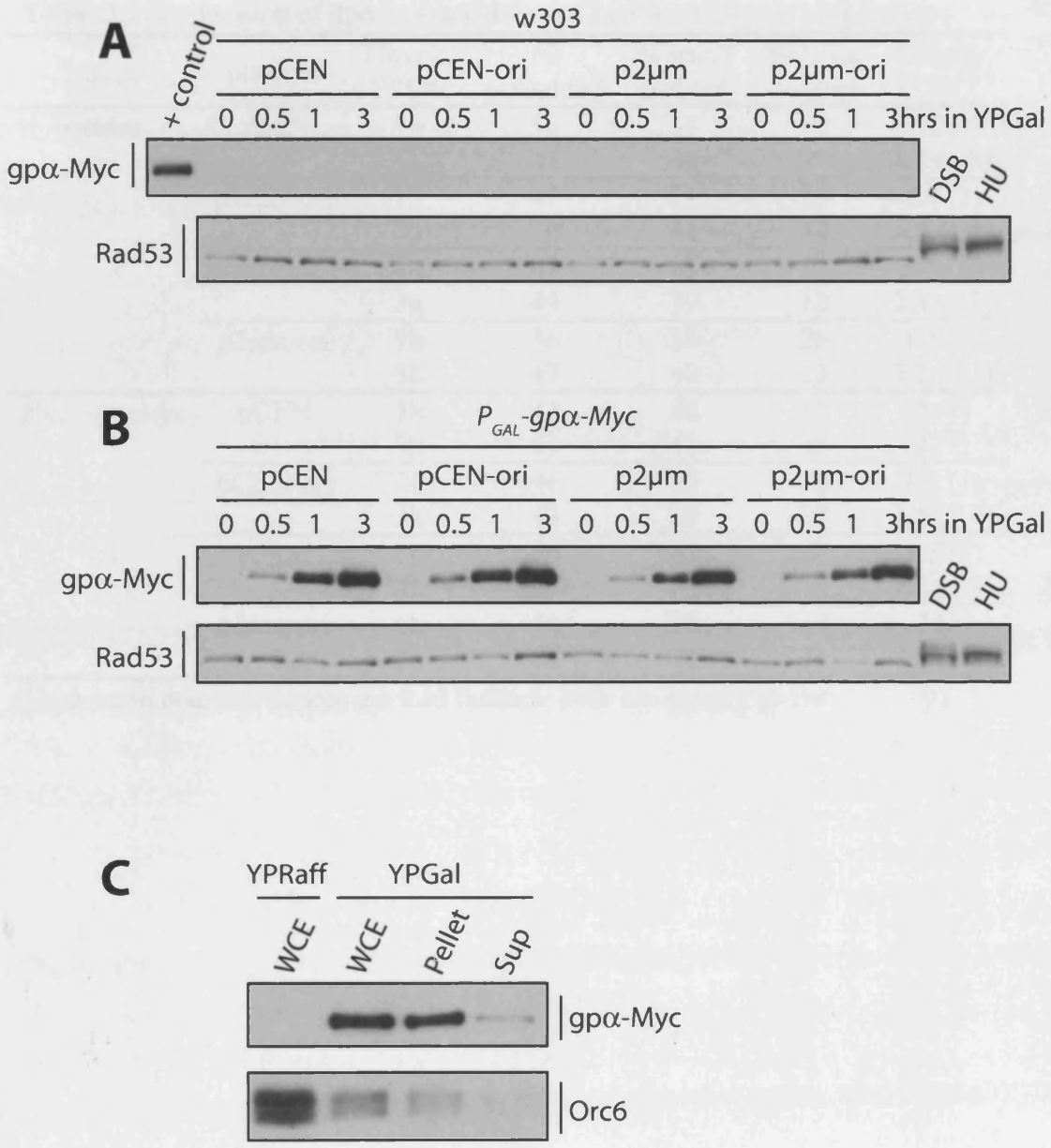

Figure 3.4: Expression and chromatin association of bacteriophage P4 gpα in yeast does not result in checkpoint activation. **A:** Cells of strains YCZ44 (pCEN), YCZ45 (pCEN-ori), YCZ46 (p2µm), and YCZ47 (p2µm-ori) were grown in YPRaff G418 and shifted to YPGal G418. TCA extracts were analysed by western blotting. DSB: samples from cells with DSBs (strain YCZ64); HU: samples from cells arrested with HU (strain YCZ64). **B:** Cells of strain YCZ56 (pCEN P_{GAL}-*gpαMyc*), YCZ57 (pCEN-ori P_{GAL}-*gpαMyc*), YCZ58 (p2µm P_{GAL}-*gpαMyc*), and YCZ59 (p2µm-ori P_{GAL}-*gpαMyc*) were treated as in A. **C:** Chromatin fractionation of samples of strain YCZ42 (P_{GAL}-*gpαMyc*) grown either in YPRaff or YPGal. WCE: whole cell extract; Pellet: chromatin enriched pellet; Sup: supernatant.
Plasmids used were pCZ7 (pCEN); pCZ17 (pCEN-ori); pCZ15 (p2µm) and pCZ18 (p2µm-ori).

Table 3.2: Expression of gpα in yeast does not inhibit cell-cycle progression.

strain	plasmid	Time in YPGal	% unbudded	% small budded	% large budded	Density ($x10^7$)[a]
parent	pCEN	1h	50	31	19	1.8 (1)
		3h	44	48	8	3.2 (1.8)
	pCEN-ori	1h	47	28	26	1.4 (1)
		3h	36	41	23	2.7 (1.9)
	p2μm	1h	47	43	10	1.1 (1)
		3h	49	39	12	2.5 (2.3)
	p2μm-ori	1h	36	38	26	1.5 (1)
		3h	47	40	13	3.2 (2.1)
P_{GAL}-gpαMyc	pCEN	1h	43	46	11	2 (1)
		3h	51	41	8	4 (2)
	pCEN-ori	1h	46	42	12	1.8 (1)
		3h	43	29	28	3.5 (1.9)
	p2μm	1h	50	43	7	1.3 (1)
		3h	50	35	15	2.3 (1.8)
	p2μm-ori	1h	50	36	14	2 (1)
		3h	48	29	23	3.5 (1.8)

[a] Values in brackets denote the fold increase over the density at 1hr

3.2.4 Expression of gpα does not affect the topology of P4-origin containing plasmids

The next question that was addressed was whether gpα was able to produce any ssDNA in yeast. To this end, plasmid topology was followed in assays similar to those described for the SV40-origin plasmids (see section 3.2.2), after determining the optimum concentration of chloroquine. Southern blotted membranes of gels run in either the absence or in the presence of 2μM chloroquine were hybridised with probes generated by random prime labelling of plasmid DNA (see Material and Methods). As for T-Ag, no changes in the distribution of plasmid topoisomers were detected upon expression of gpα (Figure 3.5). Importantly, no fraction of any of the plasmids appeared to become resistant to the reduced gel mobility caused by chloroquine (Figure 3.5C and D). Moreover, no difference was detected between plasmids containing the P4 origin and those lacking it (Figure 3.5C and D). Lastly, all plasmids behaved identically in the parent strain that did not carry the $P_{GAL1\text{-}10}$::*gpα* construct (Figure 3.5A and B). It was therefore concluded that gpα does not induce plasmid unwinding of P4 origin plasmids in yeast.

It is possible that the nuclear localisation signals fused to gpα are not functional in this context. If this were the case, no plasmid unwinding would be expected because of the lack of nuclear accumulation of gpα. To address whether gpα was able to associate with chromatin, chromatin-enriching cell fractionation experiments were carried out (see Materials and Methods for details). As shown in Figure 3.4, gpα was found to behave in a manner very similar to Orc6, which remains associated with DNA throughout the cell cycle (see section 3.2.2). Therefore, the lack of plasmid unwinding observed is not due to gpα not entering the nucleus or not being able to interact with DNA. Together, these findings indicate gpα to be inactive in yeast. Possible reasons for this are described in section 3.3.2.

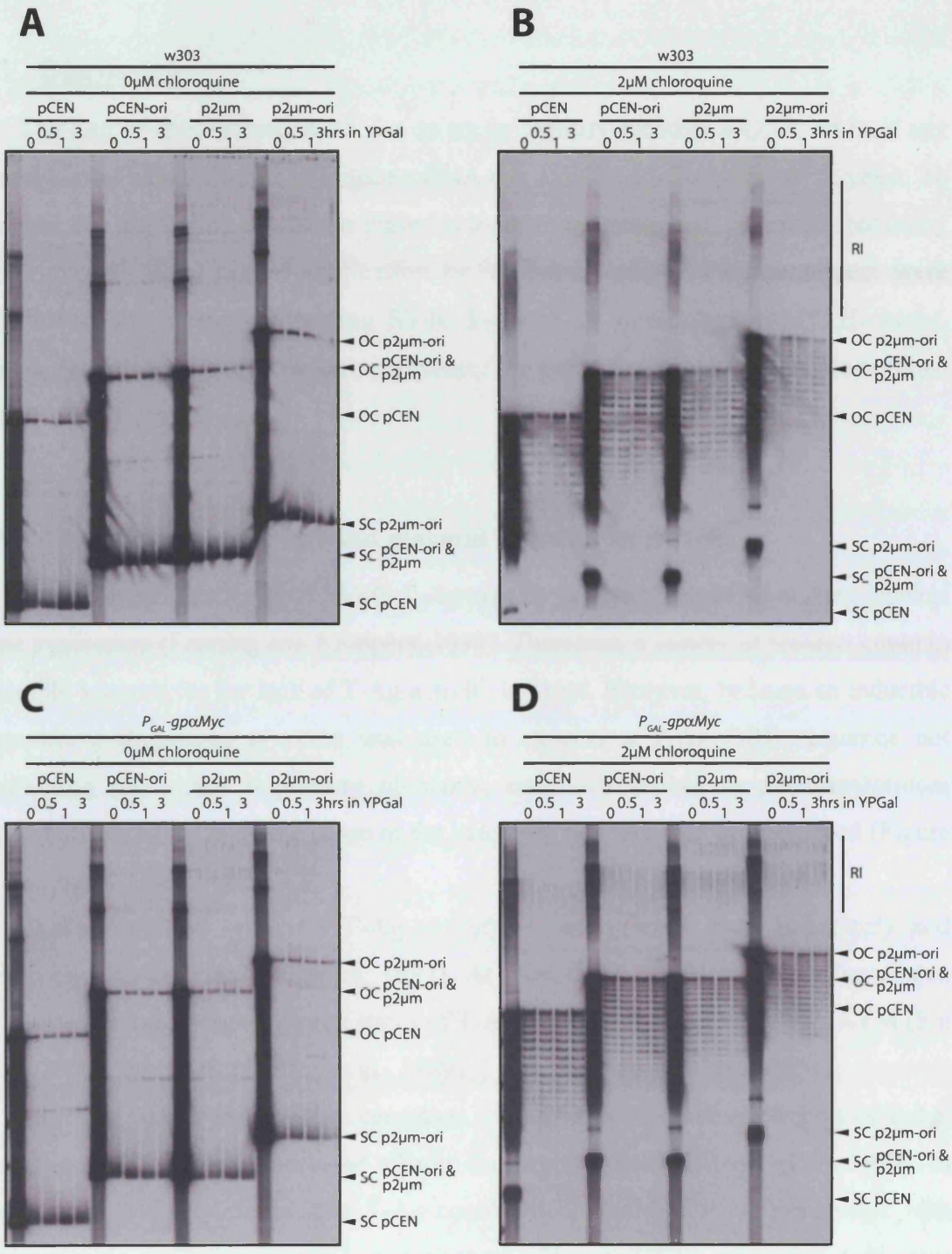

Figure 3.5: Expression of gpα does not lead to obvious topological changes in the pCEN or p2μm plasmids. Cultures of the indicated strains were grown in YPRaff G418 and shifted to YPGal G418. DNA extracted from samples taken at the indicated time-points was run on agarose gels lacking chloroquine (A and C) or containing 2μm chloroquine (B and D). **A and B:** Cells of strain w303-1a transformed with pCEN (YCZ44); pCEN-ori (YCZ45); p2μm (YCZ46) and p2μm-ori (YCZ47) were used. **B and D:** Cells of strain YCZ42 (P_{GAL}-*gpαMyc*) transformed with the same plasmids as in A and B were used (YCZ56-59). See Figure 3.4 for plasmid names.

3.3 Discussion

The aim of this investigation was to try to identify whether ssDNA without any strand breaks would be able to induce a DNA damage checkpoint response in yeast. To this end, the unwinding of circular plasmids *in vivo* was attempted. Plasmids containing either the SV40 origin of replication or its bacteriophage P4 counterpart were introduced into strains expressing SV40 T-Ag or P4 gpα, respectively. However, neither protein appeared to be active in yeast. The possible reasons for this are outlined in the following sections.

3.3.1 T-Ag is unable to unwind plasmid DNA in yeast cells

In the natural host cells of SV40, T-Ag activity is tightly regulated at each level of gene expression (Fanning and Knippers, 1992). Therefore, a variety of reasons could in principle account for the lack of T-Ag activity in yeast. However, because an inducible promoter endogenous to yeast was used to express a T-Ag ORF sequence not containing any other regulatory elements, only differences in posttranslational regulation are likely to be the cause of the inactivity of T-Ag that was observed (Figure 3.1, Figure 3.2, and Figure 3.3).

Phosphorylation regulates T-Ag activity in many ways, both negatively and positively (Fanning and Knippers, 1992). At least three different kinases have been implicated in the phosphorylation status of T-Ag: CK2 (Hubner et al., 1997), ATM (Shi et al., 2005), and CDK (McVey et al., 1989).

Phosphorylation at CK2 sites correlates with an improved nuclear import of T-Ag, probably mediated by an increased affinity for import-factors (Hubner et al., 1997). In this context it is of interest that T-Ag could not be detected to co-precipitate with chromatin in cell fractionation experiments (Figure 3.1B). A caveat with this experiment was, however, that the strains used did not contain the SV40 origin of replication and it is possible that nuclear retention and/or chromatin association of T-Ag depends on origin binding in yeast. Therefore, improper post-translational modifications that result in an inability to associate with origin DNA (see below) might also result in reduced nuclear retention of T-Ag.

Recently, it was postulated that phosphorylation of T-Ag by ATM represents yet another mechanism of SV40 replication regulation (Shi et al., 2005). Phosphorylation at S120, a site that is required for efficient replication *in vivo* (Schneider and Fanning,

1988), is dependent on ATM (Shi et al., 2005). Although PI3K like kinases are thought to have similar phosphorylation site preferences (Kim et al., 1999), it is not clear whether yeast Mec1 or Tel1 would be able to phosphorylate T-Ag.

Another requirement for T-Ag activity is phosphorylation by CDK (McVey et al., 1989). At least one essential site, T124, has been identified (McVey et al., 1989). Lack of phosphorylation by CDK results in a block to DNA unwinding by T-Ag (McVey et al., 1993; Moarefi et al., 1993). Because Cyclin A/CDK2 associates with T-Ag during replication (Adamczewski et al., 1993; Cannella et al., 1997), it is probably this particular CDK complex that mediates phosphorylation of T-Ag. Again, it is not clear whether the yeast CDK is able to substitute for its mammalian counterpart.

In addition to these cases of positive regulation of T-Ag by phosphorylation, phosphorylation of some residues is detrimental to T-Ag function (Fanning and Knippers, 1992). In particular, phosphorylation at S679 was found to inhibit SV40 replication (Schneider and Fanning, 1988). Unfortunately, neither the mechanism of inhibition, nor the kinase mediating this particular phosphorylation is known. The fact that a glutamate residue follows S679, however, suggests the involvement of PI3K-like kinases. As for the other modifications of T-Ag, it is not known whether any of these inhibitory sites on T-Ag are phosphorylated in yeast.

Another pathway of activating T-Ag by dephosphorylation appears to involve the phosphatase PP2A (Virshup et al., 1989; Virshup et al., 1992). Dephosphorylation of T-Ag by PP2A is required for SV40 replication in cell extracts (Virshup et al., 1989; Virshup et al., 1992). Since this step promotes the loading of a second T-Ag hexamer onto origin DNA that has already bound the origin, it is possible that PP2A regulates the formation of a double hexamer, the active helicase version of T-Ag (Virshup et al., 1992; Gai et al., 2004).

Inactivity of T-Ag might not necessarily be a result of deficiencies in post-translational modification control. It is theoretically also possible that protein cofactors required by T-Ag cannot be substituted in yeast. However, because T-Ag can co-operate with yeast RPA, and even *E. coli* single strand binding protein, in plasmid unwinding *in vitro* (Wold et al., 1987; Brill and Stillman, 1989), this explanation is not very likely.

Since replication origins usually show highly regulated placement of nucleosomes (Lipford and Bell, 2001; Weinreich et al., 2004) and chromatin assembly had been shown to be inhibitory to SV40 replication (Ishimi, 1992; Alexiadis et al., 1998), it is possible that interaction of T-Ag with the origin is prevented by higher order DNA

structures in yeast. To minimise the chance of origin inaccessibility, all the plasmids that were used contained 4 tandem copies of the SV40 origin. However, it still is possible that none of the origins allow interaction with T-Ag.

In summary, the most plausible explanation for the inactivity of T-Ag in yeast is an incorrect pattern of post-translational modifications, although other reasons might also play a part.

3.3.2 gpα is inactive when expressed in yeast

In an attempt to set up a less complicated approach for plasmid unwinding *in vivo*, *E. coli* bacteriophage P4 gpα (Ziegelin and Lanka, 1995) was used in a similar way as T-Ag. It was thought that gpα, originating from a much simpler system, would not be under as tight and cell environment specific regulation as T-Ag.

However, upon expression of gpα in cells containing P4 origin plasmids, no activity could be detected (Figure 3.3 and Figure 3.4). Immunoblot analysis of whole-cell extracts and cell fractionations showed that gpα was expressed and specifically enriched in chromatin-associated fractions (Figure 3.4). A lack of expression or nuclear accumulation of gpα can therefore be excluded as a cause for gpα's inactivity. Several other reasons could still account for it, however. It could be that the epitope tags and NLSs that were fused to gpα rendered the protein non-functional. In the hope of avoiding such a negative effect, two different versions of the fusion protein had been constructed, 2xNLS-gpα-MycHis and gpα-2xNLS-MycHis. Unfortunately, expression of neither construct resulted in detectable plasmid unwinding (see section 3.2.3).

Another possible reason for gpα not being functional is that necessary cofactors present in *E. coli* are absent in yeast. Arguing against such a possibility, however, gpα is able to carry out its helicase activity *in vitro* without any accessory proteins (Ziegelin et al., 1993). A number of experiments carried out *in vivo* and in cell extracts have implied that the host replication factors DnaA, DnaB, DnaC, DnaG, DnaJ, and DnaK are not required for P4 replication (Diaz Orejas et al., 1994; Ziegelin et al., 1995). These findings suggest that neither the host origin melting nor the DNA unwinding machinery are essential. Since P4 replication has, however, not been reported with reconstituted proteins, it is not known what the exact protein requirements are.

Eukaryotic DNA is densely packed into nucleosomes and higher order structures (Chakravarthy et al., 2005). This level of organisation is absent in bacterial and phage

genomes. It is therefore relatively likely that gpα is unable to interact with the origin and/or to carry out its unwinding function when the DNA is packaged into chromatin.

Because distinguishing between the possibilities outlined above (and several other possible ones) would require a large amount of experimental effort that would not likely result in a solution to the problems encountered in this investigation, no further experiments were carried out on this issue.

Since neither the T-Ag nor the gpα systems worked, this study does not give any further insight into the role of ssDNA in checkpoint activation.

4 Degradation of RPA leads to Rad9-dependent checkpoint activation during S phase

4.1 Overview

As described in chapters 1 and 3, ssDNA is widely believed to be the best candidate for a unifying DNA damage checkpoint inducing structure (Garvik et al., 1995; Lee et al., 1998; Pellicioli et al., 2001; Rouse and Jackson, 2002b; Costanzo and Gautier, 2003; Tercero et al., 2003; Zou and Elledge, 2003; Ira et al., 2004; Byun et al., 2005; Cortez, 2005). However, ssDNA, probably never exists in its naked form within the cell, but is usually covered by the heterotrimeric replication protein-A (RPA) complex (Wold, 1997; Iftode et al., 1999). RPA consists of three different subunits, Rpa1 (~70kD), Rpa2 (~36kD), and Rpa3 (~14kD), encoded by the *RFA1*, *RFA2*, and *RFA3* genes, respectively (Wold, 1997; Iftode et al., 1999). RPA is the functional homologue of prokaryotic single-strand binding protein (Wold, 1997; Iftode et al., 1999). As would be expected, therefore, RPA has been found to function in a large number of DNA-related processes, such as replication, transcription and repair (Wold, 1997; Iftode et al., 1999).

If ssDNA does play a role in the checkpoint response, it would not be unreasonable to assume a function for RPA in this process. Indeed, several lines of genetic evidence appear to support such an assumption (see Chapter 1 for more in-depth discussion of this matter). However, the dissection of the *in vivo* roles of RPA is hampered by the fact that all three subunits are essential for cell viability (Brill and Stillman, 1991). Therefore, most studies have utilised hypomorphic mutations (see Chapter 1). However, there are a number of problems associated with hypomorphs, the most obvious being that such mutations do not represent null phenotypes. Furthermore, apparent defects in checkpoint signalling in a particular mutant might not necessarily only reflect the loss of a function required. It is also possible that primary defects due to the mutation cause misleading secondary phenotypes. The aim of this investigation was therefore to construct mutants that could be expected to mimic the effects of complete gene deletions. To this end, the heat-inducible degron approach was used (Dohmen et al., 1994; Labib et al., 2000; Sanchez-Diaz et al., 2004) that allows the rapid degradation of

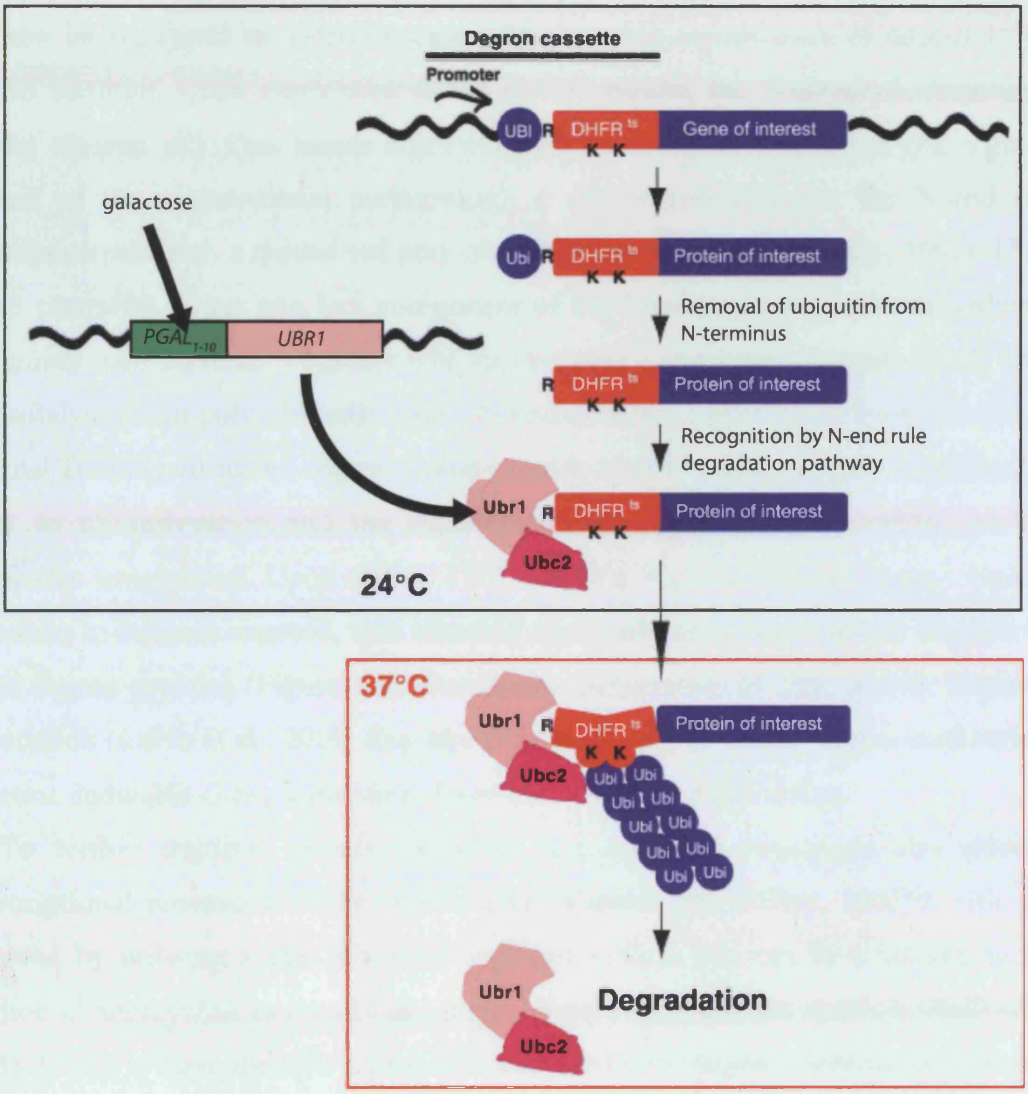

Figure 4.1: The heat-inducible degron approach for protein depletion *in vivo*. Upon expression of the degron-cassette fusion protein, the ubiquitin moiety is cleaved off from the N-terminus. This leaves a protein with an aberrant N-terminus, a strong substrate for the N-end rule degradation pathway. Ubr1 recognises such proteins and, with the help of Ubc2, catalyses their poly-ubiquitination once the culture is shifted from 24°C to 37°C. Ubiquitination at 24°C is inhibited because the conformation of the DHFR part of the degron cassette is such that none of its lysines are accessible to Ubr1. Overexpression of Ubr1 from the $GAL_{1\text{-}10}$ promoter greatly improves degradation.
Figure modified from Sanchez-Diaz et al., 2004.

a chosen protein *in vivo* in a temperature-dependent manner (Figure 4.1.). In this method, a degron-cassette, consisting of a ubiquitin moiety followed by a part of the dihydrofolate reductase (DHFR) gene, is fused to the region coding for the N-terminus of a given protein. In addition, the gene's promoter is replaced with the *CUP1* promoter that can be regulated to a certain extent by the addition/omission of copper to the growth medium. Upon expression of the fusion protein, the N-terminal ubiquitin is rapidly cleaved off. This leaves a protein with an aberrant N-terminus (an arginine instead of the conventional methionine), a strong substrate for the N-end rule degradation pathway, a specialised poly-ubiquitination mode (Varshavsky, 1997). Ubr1, an E3 ubiquitin ligase and key component of the N-end rule degradation pathway, recognises such proteins. Together with its ubiquitin conjugating enzyme, Ubc2, Ubr1 then catalyses their poly-ubiquitination. However, at 24°C, none of the lysines in the N-terminal DHFR part of the degron fusion-protein are accessible to Ubr1, resulting in a block to ubiquitination and the maintenance of degron-protein stability at this permissive temperature. Upon shift to 37°C, the DHFR conformation changes, causing its lysines to become exposed, thus allowing rapid poly-ubiquitination and degradation of the degron proteins (Figure 4.1). Because overexpression of Ubr1 greatly improves degradation (Labib et al., 2000; Sanchez-Diaz et al., 2004), all the strains used had the galactose-inducible $GAL_{1\text{-}10}$ promoter fused in front of the *UBR1* locus.

To further improve protein depletion, some degron constructs also allowed transcriptional repression of the chosen gene (Tanaka and Diffley, 2002b). This was achieved by utilising a dual activator/repressor system that can be regulated by the addition of tetracycline or its related compound doxycycline to the medium (Belli et al., 1998). In this system, the *CUP1* promoter from which the degron construct is expressed is replaced with $tetO_2$ promoter sequences, the binding site for the bacterial Tet-repressor (*tetR*, (Belli et al., 1998). Additionally, two transcription factor fusion proteins are expressed that are both based on *tetR* (Belli et al., 1998). A fusion protein of *tetR* to the transactivation domain VP16, works as an activator of transcription whose binding to the promoter is only possible in the absence of doxycycline. Furthermore, an inhibitor of transcription, Ssn6 is expressed in fusion with a modified form of the Tet-repressor that only allows promoter binding in the presence of doxycyline (*tetR'*-Ssn6)(Belli et al., 1998). Therefore, in the absence of doxycycline, only tTA will be able to interact with the promoter, resulting in activation of transcription. Upon addition of doxycycline, tTA will be replaced by *tetR'*-Ssn6, leading to transcriptional repression

(Belli et al., 1998). This system allows much tighter expression regulation than the standard *CUP1* promoter used in the original degron system (Tanaka and Diffley, 2002b).

4.2 Results

4.2.1 RPA degradation does not appear to interfere with maintaining an active DNA replication checkpoint

In order to address the function of RPA in the DNA damage response during replication, *CUP1*-degron mutants of *RFA1*, *RFA2*, and *RFA3* were constructed (referred to as $rfa1^{td}$, $rfa2^{td}$, and $rfa3^{td}$). None of the strains exhibited any obvious growth defects at the permissive temperature, or when grown at 37°C in the presence of glucose instead of galactose (i.e. in the absence of Ubr1). Moreover, as expected, no growth defects were detected when the strains were grown in galactose containing medium at the permissive temperature. Growth was, however, severely reduced when the strains were grown at 37°C in the presence of galactose. These findings are in agreement with the expectations of a degron mutant allele that is functional under permissive conditions but not at restrictive conditions. In order to allow detection of each degron protein by western blotting, all proteins also contained a haemagglutinin (HA) epitope tag on their N-terminus. As outlined below, a shift to 37°C in the presence of galactose resulted in the rapid degradation of each degron protein (see also Figure 4.2B and C).

The first question that was addressed was whether depletion of any of the individual subunits would interfere with maintaining a DNA replication checkpoint that had previously been activated. Two different drugs were used to induce a checkpoint response: hydroxyurea (HU), which inhibits ribonucleotide reductase, thereby depleting the intracellular dNTP pool (Elford, 1968); and methyl methanesulphonate (MMS), a DNA alkylating agent (Drablos et al., 2004). Both drugs had previously been shown to induce a DNA replication checkpoint response (Weinert et al., 1994; Navas et al., 1996; Sanchez et al., 1996; Sun et al., 1996; Tercero et al., 2003).

Figure 4.2A shows the experimental design that was followed. Cells were grown overnight at the permissive temperature in the absence of galactose with raffinose as the only carbon source. Subsequently, the cultures were synchronised in G1 by treatment with α factor (Bucking-Throm et al., 1973). At this stage, galactose was substituted as

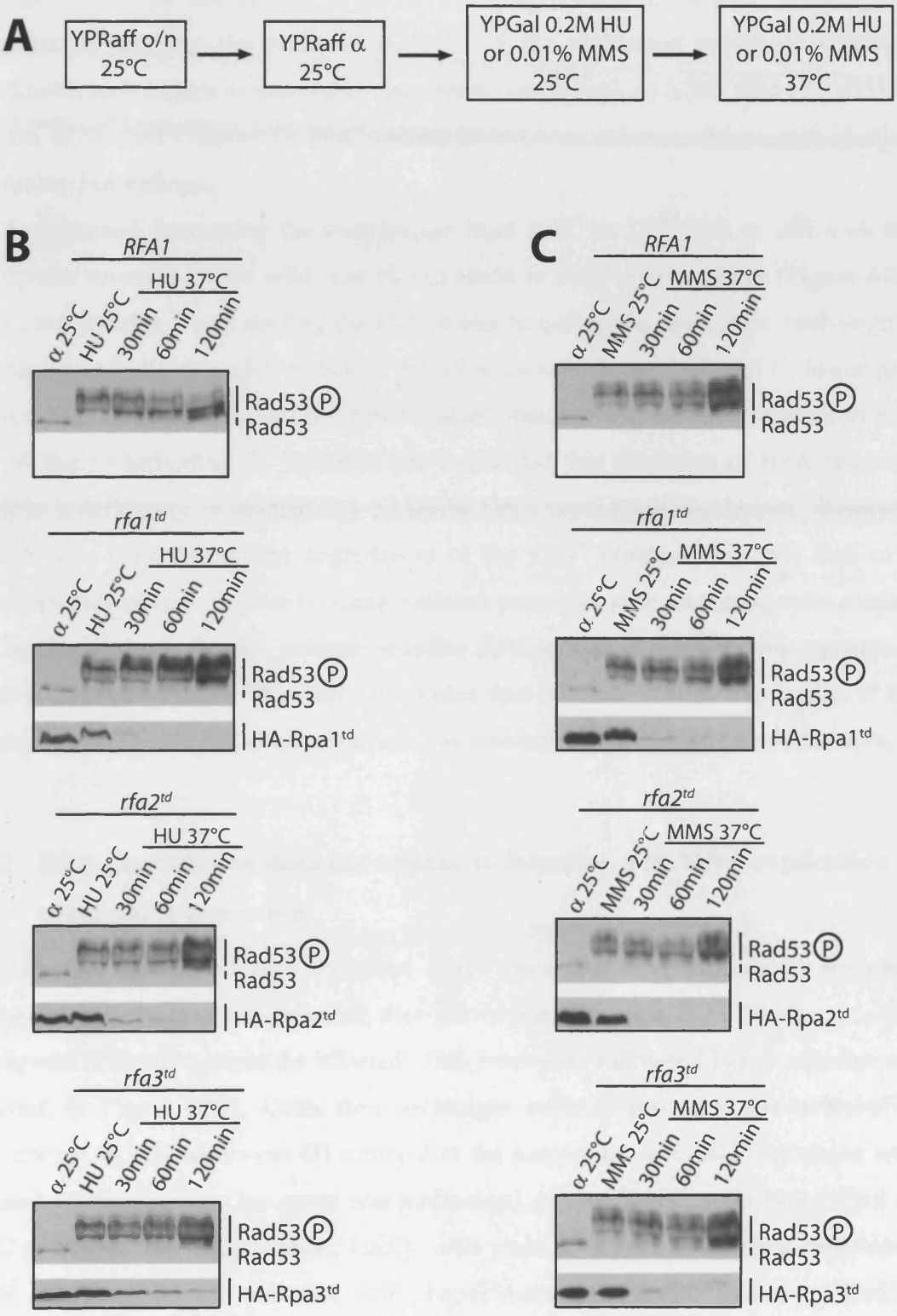

Figure 4.2: Decreasing the amounts of individual RPA subunits does not affect maintenance of the replication checkpoint. **A:** Experimental design. **B and C:** Cultures of YKL83 (*RFA1*), YCZ2 (*rfa1*^{td}), YCZ3 (*rfa2*^{td}) and YCZ4 (*rfa3*^{td}) were grown as outlined in A. TCA extracts were used for western blotting analysis. The individual RPA subunits were detected with 12CA5 anti-HA antibody.

carbon source, resulting in rapid induction of Ubr1 expression. The cells were then released from the arrest into medium containing either 0.2M HU or 0.01% MMS in order to activate the checkpoint. In the last step, degradation of the Rpa^{td} proteins was triggered by shifting the cultures to 37°C, in the continued presence of drugs. Checkpoint activation was assayed by monitoring the phosphorylation state of Rad53 in western blots, (see Chapter 1); Rpa^{td}-protein levels were followed by western blotting against the HA epitope.

As expected, increasing the temperature from 25°C to 37°C had no effect on the checkpoint response of the wild type parent strain to either HU or MMS (Figure 4.2B and C, top panels). Upon shifting the *rfa*^{td} strains to restrictive conditions, each degron protein was rapidly degraded to below detection levels (Figure 4.2B and C, lower part of each panel). Degradation of the Rpa^{td} mutant proteins, did, however, not result in a loss of Rad53 activation. It was therefore concluded that depletion of RPA does not result in a deficiency in maintaining an active DNA replication checkpoint. However, since it was later found that degradation of the Rpa^{td} proteins does not lead to a complete null phenotype due to some residual protein levels remaining (see section 4.2.3), these results do not indicate whether RPA *per se* is required for replication checkpoint maintenance. The only conclusion that can safely be drawn is that if the checkpoint required RPA, even extremely low amounts are sufficient for this function.

4.2.2 RPA degradation does not appear to interfere with DNA replication checkpoint activation

Although the experiments described above show that RPA degradation does not compromise checkpoint maintenance, they provide no indication as to whether *de novo* checkpoint activation might be affected. This issue was addressed in the experiments outlined in Figure 4.3A. Cells from overnight cultures grown at the permissive temperature in raffinose were G1-arrested at the same time as *UBR1* expression was induced. Following this, the arrest was maintained, but the temperature was shifted to 37°C to trigger Rpa^{td} degradation. Lastly, cells were released into medium containing 0.2M HU at 37°C. As for the experiments described above, Rad53 hyperphosphorylation and Rpa^{td} degradation were followed by immunoblotting (Figure 4.3B). Again, the elevated temperature did not affect checkpoint activation in the wild type parent strain (Figure 4.3B, top panel). No defects were observed in any of the three *rfa*^{td} strains, although the degron proteins were degraded to below detection limits

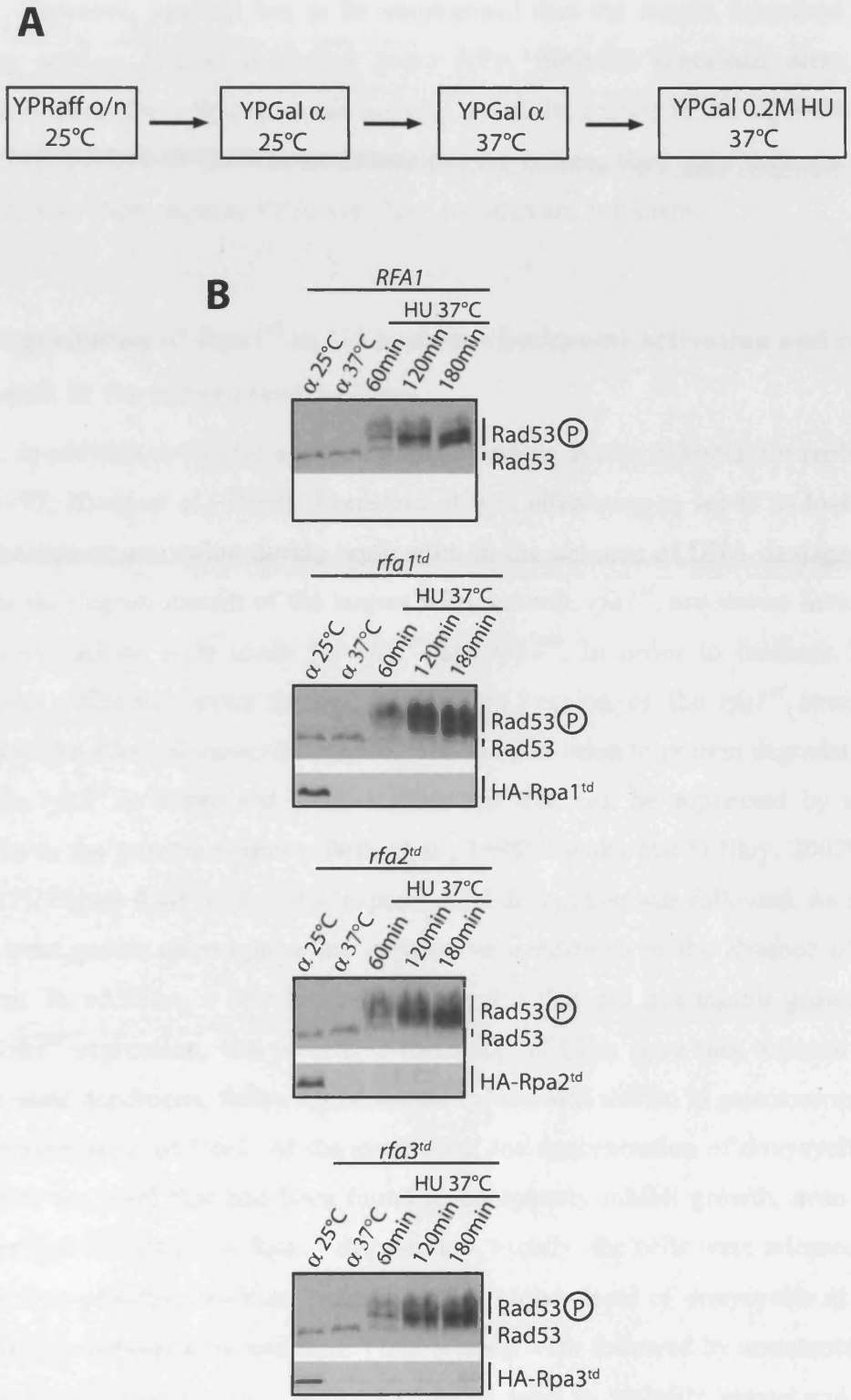

Figure 4.3: Decreasing the amounts of individual RPA subunits does not affect activation of the replication checkpoint. **A:** Experimental design. **B:** Cultures of YKL83 (*RFA1*), YCZ2 (*rfa1*^{td}), YCZ3 (*rfa2*^{td}) and YCZ4 (*rfa3*^{td}) were grown as outlined in A. TCA extracts were used for western blotting analysis. The individual Rpa^{td} subunits were detected using anti HA antibodies.

(Figure 4.3B bottom three panels). Therefore, degradation of the individual RPA subunits does not compromise the establishment of the DNA replication checkpoint response. However, again it has to be emphasised that the results described in the following section (4.2.3) indicated some RPA function remained after Rpa^{td} degradation. Thus, these findings to do not give a definite answer to the requirement for RPA during replication checkpoint activation. As before, they only indicate that if checkpoint activation requires RPA, very low amounts are sufficient.

4.2.3 Degradation of Rpa1^{td} in G1 leads to checkpoint activation and cell death in the subsequent S phase

RPA, in addition to its role in checkpoint activation, is also essential for replication (Wold, 1997; Iftode et al., 1999). Therefore, it was interesting to see if its loss could induce checkpoint activation during replication in the absence of DNA damage. Only results for the degron mutant of the largest RPA subunit, *rfa1^{td}*, are shown here. Very similar observations were made for *rfa2^{td}* and *rfa3^{td}*. In order to increase Rpa1^{td} degradation efficiency even further, a different version of the *rfa1^{td}* strain was constructed that allowed transcriptional repression in addition to protein degradation. In this strain, *rfa1^{td}* is expressed from a promoter that can be repressed by adding doxycyclin to the growth medium (Belli et al., 1998; Tanaka and Diffley, 2002b), see section 4.1). Figure 4.4A outlines the experimental design that was followed. As before, cultures were grown overnight under permissive conditions in the absence of Ubr1 expression. In addition, a low level of doxycyclin that did not inhibit growth, but reduced *rfa1^{td}* expression, was present in the medium. Cells were then arrested in G1 under the same conditions, following which the culture was shifted to galactose medium to induce expression of Ubr1. At the same time, the concentration of doxycyclin was increased to the level that had been found to completely inhibit growth, even under conditions that did not allow Rpa1^{td} degradation. Finally, the cells were released from G1 arrest into galactose medium containing this higher level of doxycyclin at 37°C. Rad53 hyperphosphorylation and Rpa1^{td} degradation were followed by immunoblotting as before. In addition, samples were taken to be used in viability assays and flow-cytometric analysis of DNA content. After 90min, α factor was added to the cultures to prevent cells that had undergone mitosis entering a second round of DNA synthesis.

Whereas Rad53 remained in its hypo-phosphorylated, faster migrating, form in the wild type strain throughout the experiment, hyper-phosphorylation of Rad53 was

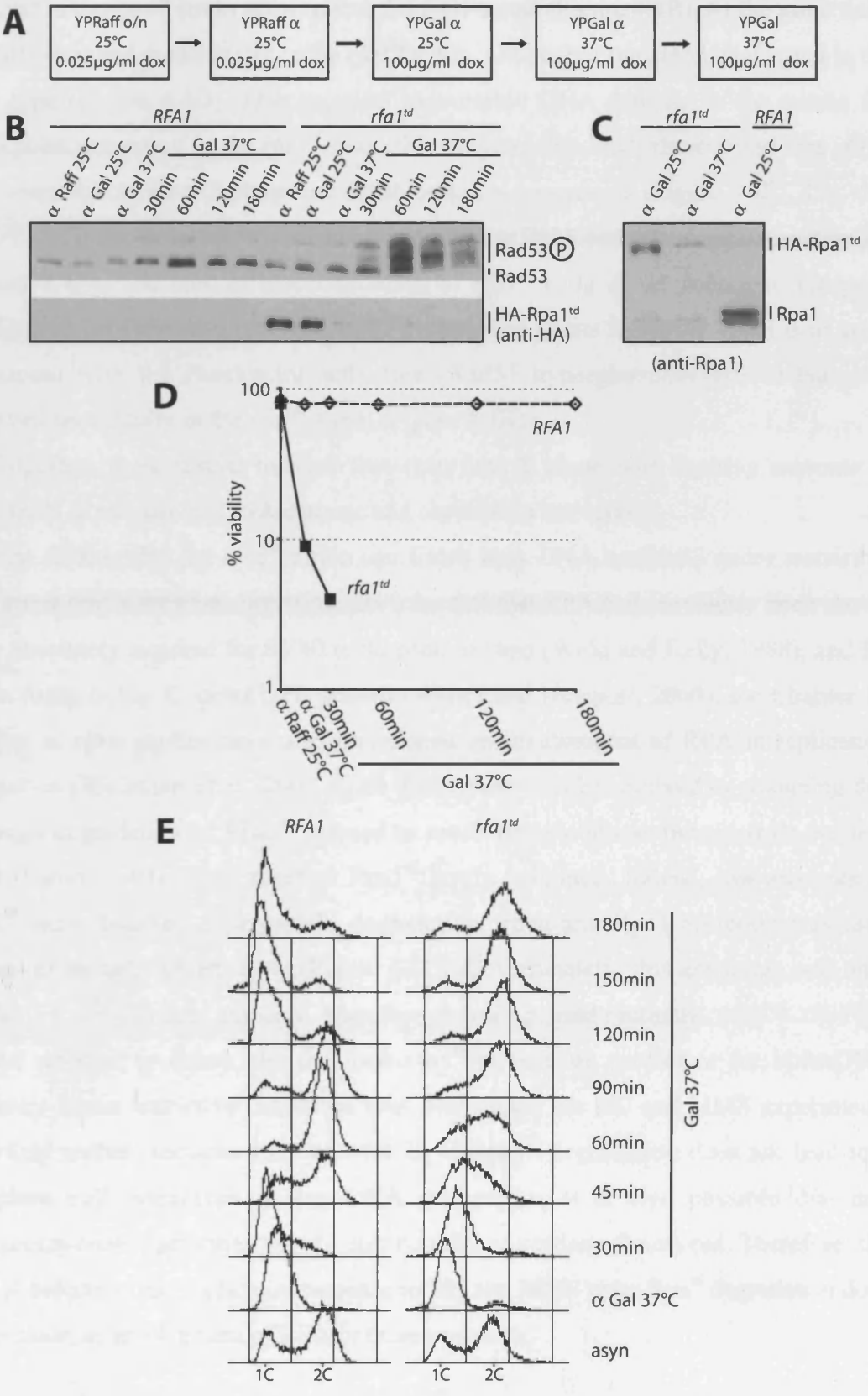

Figure 4.4: Depletion of RPA leads to checkpoint activation and loss of viability during S phase. **A:** Experimental design. Cultures of YST114 (*RFA1*) and YCZ20 (*rfa1^{td}*) were grown as outlined. To prevent entry into another cell cycle, alpha factor was added to the cultures 90min after release from the initial alpha factor arrest. **B:** Western blotting of TCA protein extracts. Rpa1^{td} was detected using 12CA5 anti HA antibody. **C:** Western blot of samples from the same samples as in (B) analysed with an anti-Rpa1 antibody. **D:** Viability during the experiment. **E:** FACS profiles of the cultures throughout the experiment.

detected in the *rfa1*^{td} strain upon release from G1 arrest (Figure 4.4B). At the same time, viability dropped dramatically in the *rfa1*^{td} strain, although it remained unaffected in the wild type (Figure 4.4D). This suggests irreversible DNA damage as the source for checkpoint activation in the *rfa1*^{td} strain. Flow-cytometric analysis revealed that *rfa1*^{td} cells were able to enter S phase and finish bulk DNA synthesis (Figure 4.4E). The vast majority of cells, however, remained arrested with a DNA content of approximately 2C (Figure 4.4E). The lack of reaccumulation of *rfa1*^{td} cells in G1 (compare the peak distribution between wild type and *rfa1*^{td} at late time points in Figure 4.4E) is in good agreement with the checkpoint activation (Rad53 hyperphosphorylation) that was observed specifically in the *rfa1*^{td} strain (Figure 4.4B).

Together, these results indicate that entry into S phase with limiting amounts of RPA leads to irreparable DNA damage and checkpoint activation.

The finding that the *rfa1*^{td} strain can finish bulk DNA synthesis under restrictive conditions was somewhat surprising given the fact that RPA had previously been shown to be absolutely required for SV40 replication *in vitro* (Wold and Kelly, 1988), and for origin firing in the *X. laevis* NPE system (Walter and Newport, 2000), see Chapter 1). Further *in vitro* studies have also established an involvement of RPA in replication elongation (Weisshart et al., 2004). This discrepancy can be resolved by assuming that although degradation of Rpa1^{td} seemed to reach completion as judged from western blots (Figure 4.4B), some residual Rpa1^{td} levels remained. Indeed, low amounts of Rpa1^{td} were detected after protein degradation when anti-Rpa1 antibody was used instead of an anti-HA antibody (Figure 4.4C). Unfortunately, this antiserum was only available in very limited amounts. Therefore, it was not used routinely.

As referred to above, the fact that *rfa1*^{td} strains are proficient for bulk DNA synthesis under restrictive conditions cast doubt upon the HU and MMS experiments described earlier (sections 4.2.1 and 4.2.2). If Rpa1^{td} degradation does not lead to a complete null phenotype during DNA replication, it is also possible that any checkpoint-related activities may be still be fully or partially functional. Therefore, the lack of defects in the checkpoint response to HU and MMS upon Rpa^{td} degradation does not exclude an involvement of RPA in these processes.

4.2.4 The checkpoint response to Rpa1^{td} degradation operates via Rad9

As described in Chapter 1, different checkpoint stimuli rely on different proteins to transduce a checkpoint signal from Mec1 to Rad53 (Alcasabas et al., 2001; Longhese et al., 2003). While general DNA damage appears to work through Rad9 (Longhese et al., 2003), this protein appears to play only a minor role in the response to replication stress such as induced by HU or MMS (Paulovich et al., 1997; Pellicioli et al., 1999; Alcasabas et al., 2001). During the response to replication stress, Mrc1, a protein that shows distant homology to Rad9, appears to carry out this function (Alcasabas et al., 2001; Tanaka and Russell, 2001). Conversely, Mrc1 does not appear to be involved in the DNA damage response triggered by other sources than replicative stress, such as telomere erosion in the *cdc13* mutant (Alcasabas et al., 2001).

In order to gain some insight into the nature of the checkpoint activation in the *rfa1*^{td} strain, *rad9*Δ, *mrc1*Δ, and *rad9*Δ *mrc1*Δ mutants were tested for their proficiency in mediating Rad53 hyperphosphorylation during S phase with degraded Rpa1^{td}. Strains deleted for both *RAD9* and *MRC1* require increased activity of ribonucleotide reductase for viability (Alcasabas et al., 2001). Therefore, all strains additionally carried a deletion of the ribonucleotide reductase inhibitor *SML1* (Zhao et al., 1998). Deletion of *SML1* also suppresses the lethality of *MEC1* and *RAD53* null alleles (Zhao et al., 1998). Importantly, this rescue of viability does not result from a re-establishment of checkpoint responses (Desany et al., 1998; Zhao et al., 1998), see Chapter 1).

Similarly to the previous experiments, Rpa1^{td} degradation was triggered before each of the strains was released from G1 arrest (Figure 4.5A). In addition to monitoring Rad53 hyperphosphorylation, Rad53 activation was also determined by *in situ* autokinase assays (Pellicioli et al., 1999; see also Chapter 1). In this assay, Rad53 autokinase activity is detected in protein extracts immobilised on western blot membranes. Checkpoint activation is a prerequisite for this activity (Pellicioli et al., 1999).

Deletion of *SML1* did not compromise Rad53 activation during replication following Rpa1^{td} degradation in an otherwise wild type background (Figure 4.5B). Rad53 activation also appeared fully functional in the *mrc1*Δ *sml1*Δ strain. In contrast, deletion of *RAD9* reduced Rad53 activation to levels barely above the detection limit. In the *rad9*Δ *mrc1*Δ double mutant background, which is completely defective for all tested checkpoint responses (Alcasabas et al., 2001; Gibson et al., 2004; Grandin et al., 2005), not even trace amounts of Rad53 activation were detected (Figure 4.5B).

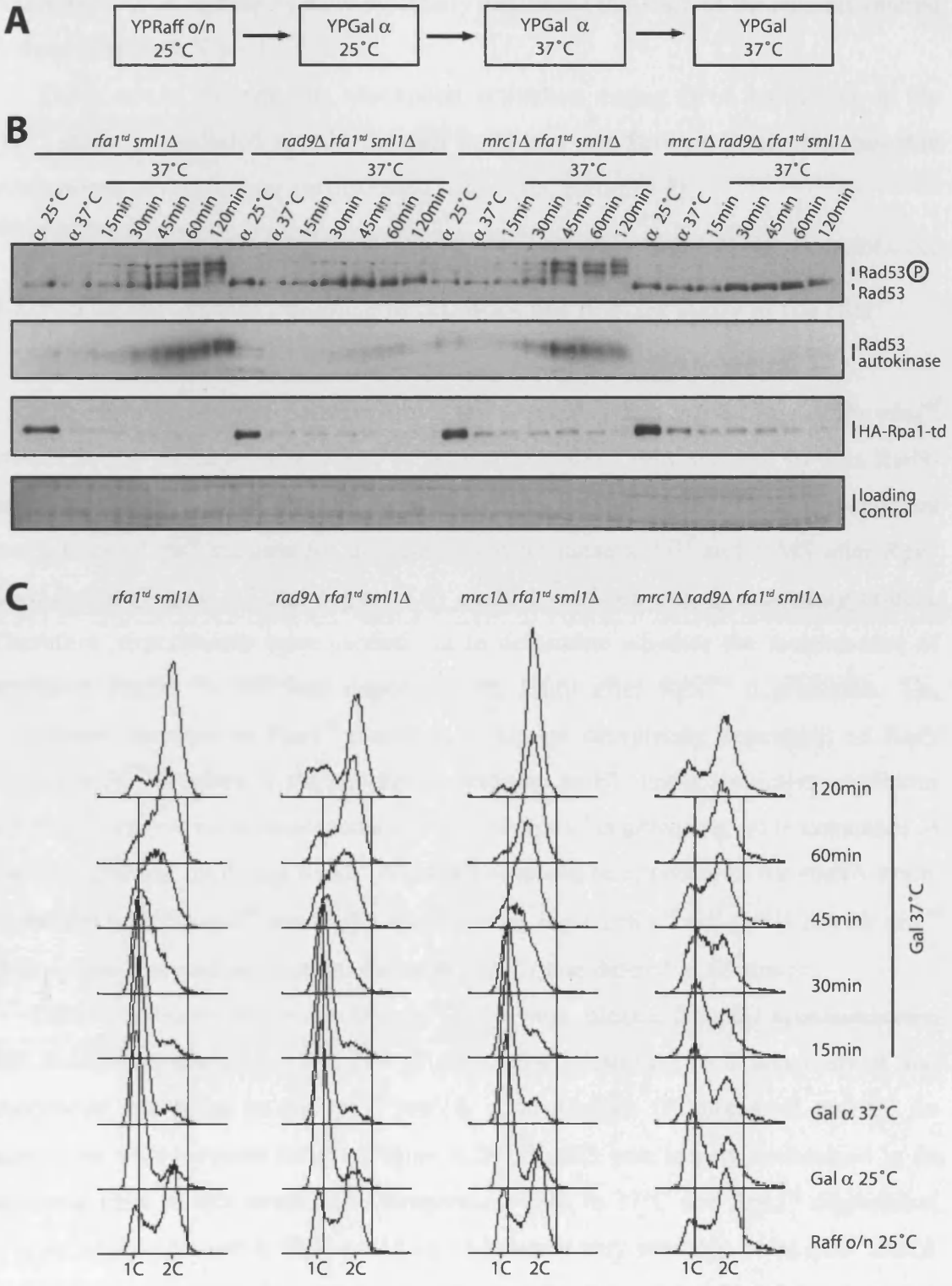

Figure 4.5: Rad9, but not Mrc1, is required for the checkpoint response following Rpa1^{td} degradation. **A:** Experimental design. Cultures of YCZ155 (*rfa1^{td} sml1Δ*), YCZ154 (*rad9Δ rfa1^{td} sml1Δ*), YCZ156 (*mrc1Δ rfa1^{td} sml1Δ*), YCZ163 (*mrc1Δ rad9Δ rfa1^{td} sml1Δ*) were grown as outlined. To prevent re-entry into another cell cycle, alpha factor was added to the cultures 90min after release fom the initial G1-arrest. **B:** Western blot analysis of Rad53 and HA-Rpa1^{td}, kinase assay for Rad53 activation and ponceau-S stained membrane as loading control. 16B12 anti HA antibody was used for HA-Rpa1^{td} detection. **C:** FACS profiles of the cultures throughout the experiment.

Analysis of DNA content by flow-cytometry confirmed that each of the cultures entered S phase (Figure 4.5C).

These results indicate that checkpoint activation during DNA replication in the *rfa1*^{td} strain is mediated mainly through Rad9 and not through Mrc1. The possible implications of this finding are discussed below (see section 4.3).

4.2.5 The checkpoint response to HU does not require Rad9 in the *rfa1*^{td} strain

The observations just described raise the possibility that any defects of the *rfa1*^{td} mutant in the checkpoint response to replication stress were masked by this Rad9-dependent response that resulted from Rpa1^{td} degradation itself. Thus, the apparent proficiency of *rfa*^{td} mutants for the checkpoint response to HU and MMS after Rpa^{td} degradation (Figure 4.2 and Figure 4.3) could have been due to secondary effects. Therefore, experiments were carried out to determine whether the maintenance of activated Rad53 in HU was dependent on Rad9 after Rpa1^{td} degradation. The checkpoint response to Rpa1^{td} depletion is almost completely dependent on Rad9 (Figure 4.5). Therefore, if the checkpoint response to HU under restrictive conditions for *rfa1*^{td} were only due to secondary effects of Rpa1^{td} degradation, no maintenance of Rad53 activation following Rpa1^{td} degradation would be expected in the *rad9*Δ strain. In parallel with the *rfa1*^{td} and *rad9*Δ *rfa1*^{td} strains, *mrc1*Δ *rfa1*^{td} and *rad9*Δ *mrc1*Δ *rfa1*^{td} strains were analysed as controls. As before, *SML1* was deleted in all strains.

Under conditions permissive for *rfa1*^{td}, cells were released from G1 synchronisation into medium containing 0.2M HU (Figure 4.6A), resulting in S phase arrest and checkpoint activation in the *rfa1*^{td} *sml1*Δ control strain (Figure 4.6B and C). In agreement with previous results (Figure 4.2B), Rad53 was largely maintained in its activated form in this strain upon temperature shift to 37°C and Rpa1^{td} degradation (Figure 4.6B). The *rad9*Δ *rfa1*^{td} *sml1*Δ strain behaved very similarly to the *rfa1*^{td} *sml1*Δ control strain (Figure 4.6B and C), indicating that Rad9 is not required for maintaining the checkpoint response to HU after degradation of Rpa1^{td}. This suggests that the proficiency of cells to maintain a checkpoint response to HU after Rpa1^{td} degradation (Figure 4.2) is not instead due to the activation of a secondary checkpoint response caused by the depletion of RPA.

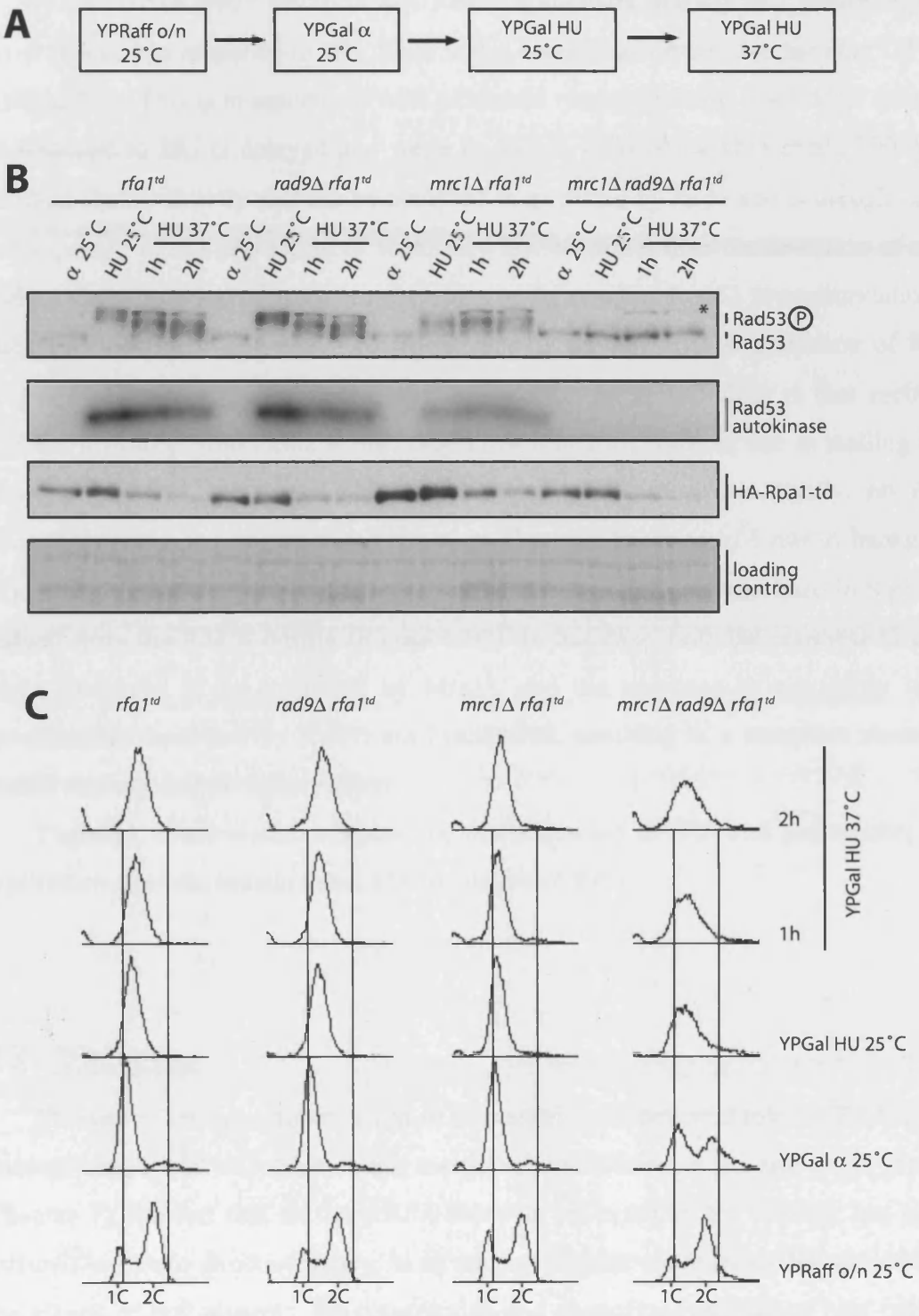

Figure 4.6: Maintenance of HU-induced checkpoint activation after Rpa1^{td} degradation does not require Rad9. **A:** Experimental design Cultures of YCZ155 (*rfa1^{td} sml1Δ*), YCZ154 (*rad9Δ rfa1^{td} sml1Δ*), YCZ156 (*mrc1Δ rfa1^{td} sml1Δ*), YCZ163 (*mrc1Δ rad9Δ rfa1^{td} sml1Δ*) were grown as outlined. To prevent cells with an inactive checkpoint from undergoing mitosis, nocodazole was added to the cultures upon temperature shift to 37°C. **B:** Western blot analysis of Rad53 and HA-Rpa1^{td}, kinase assay for Rad53 activation and ponceau-S stained membrane as loading control. 16B12 anti HA antibody was used for HA-Rpa1^{td} detection. **C:** FACS profiles of the cultures throughout the experiment.

In the *mrc1*Δ *rfa1*^{td} *sml1*Δ strain, Rad53 autokinase activity and phosphorylation were reduced in response to HU, even under conditions permissive for *rfa1*^{td} (Figure 4.6B and C). This is in agreement with published results showing that Rad53 activation in response to HU is delayed and weak in *mrc1*Δ cells (Alcasabas et al., 2001). The residual Rad53 activity that can be observed is mediated by Rad9 and is thought to be a consequence of the generation of secondary lesions rather than the detection of stalled forks (Alcasabas et al., 2001). No reduction in the residual Rad53 phosphorylation and autokinase activity was observed in the *mrc1*Δ mutant after degradation of Rpa1^{td} (Figure 4.6B and C). The most likely explanation for this finding is that secondary lesions, resulting from either Rpa1^{td} degradation or fork collapse due to stalling in the absence of Mrc1 are responsible for this checkpoint response. Lastly, no Rad53 phosphorylation or autokinase activity were observed in the *mrc1*Δ *rad9*Δ background at any stage of the experiment (Figure 4.6B), although cells accumulated in S phase as judged from the FACS profile (Figure 4.6C). In this case, both the response to stalled forks (believed to be mediated by Mrc1), and the response to secondary lesions (presumably mediated by Rad9) are inactivated, resulting in a complete absence of Rad53 activity and phosphorylation.

Together, these results suggest that the responses to HU, and presumably other replication stresses, remain intact after depletion of RPA.

4.3 Discussion

The aim of this investigation was to characterise the potential role for RPA in DNA damage checkpoint activation. While many indirect indications for such a role exist (see Chapter 1), the fact that all three RPA subunits are essential for viability has made it difficult to obtain direct evidence. In an attempt to generate mutants that should mimic the effects of null mutants, the construction and phenotypic analysis of heat-inducible degron mutants in *RFA1*, *RFA2* and *RFA3* was reported in the sections above.

4.3.1 Phenotypic similarity between *rfa1*^{td}, *rfa2*^{td}, and *rfa3*^{td}

RPA forms a tight heterotrimeric complex *in vivo* (Fairman and Stillman, 1988; Wold and Kelly, 1988; Wold, 1997). However, *in vitro* studies have suggested that a separate heterodimer between Rpa2 and Rpa3 can also form (Henricksen et al., 1994;

Wold, 1997). Because all three subunits contain ssDNA binding domains (Bochkarev et al., 1997; Brill and Bastin-Shanower, 1998; Bochkarev et al., 1999), it is formally possible that the Rpa2/Rpa3 dimer and the Rpa1 monomer could carry out some RPA-specific functions by themselves. However, neither the Rpa2/Rpa3 dimer nor Rpa1 on its own are able to support SV40 replication (Erdile et al., 1991; Henricksen et al., 1994). Additional support for a situation in which only the heterotrimer is active comes from the finding that complex formation can affect subunit stability *in vivo* (Maniar et al., 1997).

Hypomorphic mutations that have been isolated in each of the three subunits of RPA, however, show a wide range of overlapping and non-overlapping phenotypes (Longhese et al., 1994; Santocanale et al., 1995; Maniar et al., 1997; Umezu et al., 1998; discussed in detail in Chapter 1, Introduction). In contrast to the vast number of different possibilities with hypomorphic mutations, a similar kind of deficiency for each subunit should result from induced protein degradation. It was therefore interesting to determine whether the degron mutants of the individual RPA subunits constructed in this investigation showed identical or non-identical phenotypes.

In all assays, virtually identical phenotypes were observed upon degradation of Rpa1^{td}, Rpa2^{td}, or Rpa3^{td}. Degradation of each of the subunits had no obvious effect on maintaining Rad53 activation after treatment with HU or MMS (Figure 4.2), nor was there any difference in the ability to activate the checkpoint when any of the subunits were degraded before release from G1 arrest into HU (Figure 4.3). Lastly, when any of the RPA subunits was degraded before release into an otherwise unperturbed S phase, checkpoint activation and cell cycle arrest were observed in all three cases (Figure 4.4 and data not shown). As judged by flow cytometry and microscopic analysis, cells depleted for any of the RPA subunits arrested at a similar stage with almost all cells showing large buds and a DNA content around 2C (Figure 4.4 and data not shown).

Although one has to bear in mind that *rfa*^{td} degradation does not lead to a complete RPA null phenotype (see below), these data therefore corroborate previous results (reviewed in Wold, 1997; Iftode et al., 1999) that the individual RPA subunits are not functional outside the heterotrimeric RPA complex.

4.3.2 *rfa1*^{td} mutants are proficient for bulk DNA synthesis after Rpa1^{td} degradation

When Rpa1^{td} (or Rpa2^{td}, or Rpa3^{td}, data not shown) were degraded prior to release into an otherwise unperturbed S phase, flow-cytometric analysis of DNA contents revealed that cells were able to carry out bulk DNA synthesis (Figure 4.4E). This finding was surprising, given the known requirement for RPA in both initiation and elongation of SV40 replication (Dean et al., 1987; Wold et al., 1987; Fairman and Stillman, 1988; Wold and Kelly, 1988; Fanning and Knippers, 1992; Walther et al., 1999; Weisshart et al., 2004), and in initiation in *X. laevis* egg extracts (Walter and Newport, 2000). All three subunits of RPA are essential genes in yeast (Brill and Stillman, 1991), and temperature-sensitive point mutants in *rfa2* have been isolated that arrest with a 1C DNA content and prevent DNA synthesis in synchronised populations (Maniar et al., 1997). These findings strongly suggest that RPA is essential for DNA replication in yeast. The *rfa*^{td} results therefore suggest that degradation is not complete, even though in most cases, the Rpa^{td} proteins were degraded to below detection limits of the anti-HA antibody used. Indeed, some residual protein could be detected after Rpa1^{td} degradation when an anti-Rpa1 antibody was used instead (Figure 4.4C). Image analysis of immunoblots suggested that ~10% of the protein remained after degradation. Given the poor linearity of immunoblot signals, it has to be emphasised that this value only represents a rough estimate. Together, however, these considerations strongly suggest that Rpa^{td} degradation does not lead to a complete null phenotype. The proficiency of *rfa*^{td} strains to carry out bulk DNA synthesis (Figure 4.4E) and to activate Rad53 in response to drug treatment (Figure 4.2 and Figure 4.3) therefore do not allow the conclusion that RPA is not involved in the respective processes.

DNA replication appeared to be a slower process after Rpa1^{td} degradation (Figure 4.4E). While it only took ~15min for the wild type strain to replicate, the *rfa1*^{td} strain required ~60min (Figure 4.4E). There are two possible reasons to account for this phenomenon. Firstly, because checkpoint activation was observed during S phase after Rpa1^{td} degradation (Figure 4.4B), the slower S phase could be a result of checkpoint-mediated inhibition of late origin firing (Santocanale and Diffley, 1998; Shirahige et al., 1998). Secondly, because of the involvement of RPA during replication elongation (see Chapter 1), it is possible that limiting amounts of RPA interfere with the replication process directly. One outcome if only the former model is correct is that compromising checkpoint activation should result in the reduction of time spent in S phase to a length

similar to the wild type. However, deletion of *RAD9*, which resulted in a close to complete loss of Rad53 activation (Figure 4.5B), did not appear to significantly decrease the time required for DNA synthesis (Figure 4.5C). It is therefore unlikely that late origin firing inhibition is the major process delaying DNA synthesis after RPA depletion. It appears to be more likely that RPA depletion slows down S phase by interfering with the replication process itself. Depletion of RPA could affect one or more steps in S phase: initiation, DNA unwinding, Polα recruitment, the switch from Polα to Polδ, and Okazaki fragment maturation (Dean et al., 1987; Wold et al., 1987; Fairman and Stillman, 1988; Wold and Kelly, 1988; Walther et al., 1999; Bae et al., 2001; Weisshart et al., 2004).

RNAi-mediated partial depletion of RPA1 or RPA2 in human cells leads to a very similar phenotype of cells being apparently able to carry out bulk DNA synthesis (Dodson et al., 2004). Moreover, similar to the case in yeast, replication after RPA depletion leads to accumulation of DNA damage, checkpoint activation and cell death (Dodson et al., 2004). This similarity of phenotypes is consistent with the high evolutionary conservation of RPA functions.

4.3.3 How much ssDNA is generated during replication?

So far, few studies have endeavoured to quantify ssDNA formation during DNA replication, and no definitive results have been obtained (see below). In this section, an attempt will be made to provide an estimate of the amounts of ssDNA generated during S phase based on evidence from studies on other aspects of DNA replication. However, it has to be emphasised that these numbers are very speculative since no hard evidence on ssDNA formation is available.

While data from *E. coli* replication studies suggest that little ssDNA separates the leading strand polymerase from the replicative helicase (Johnson and O'Donnell, 2005), lagging strand synthesis results in defined patches of ssDNA. A rough estimate of origin usage predicts ~600 replication forks during an S phase in *S. cerevisiae* (Lengronne et al., 2001). Because yeast Okazaki fragments are ~130bp long on average (Bielinsky and Gerbi, 1999), up to ~78kb of ssDNA could be present during mid S phase. This value is even higher when one takes into account the flaps generated during lagging strand synthesis (Hubscher and Seo, 2001) and the short gap between leading strand polymerase and helicase. *In vitro* studies suggest that one RPA heterotrimer binds to ~30bp of ssDNA (Wold, 1997; Iftode et al., 1999), indicating ~2600 molecules of RPA

are required if the side-by-side binding mode suggested from *in vitro* studies (Wold, 1997; Iftode et al., 1999) is assumed to be correct *in vivo*. Quantification of tagged proteins showed that Rpa1, Rpa2, and Rpa3 are present in roughly equal amounts of ~5000 molecules/cell in asynchronously growing populations (Ghaemmaghami et al., 2003). Other studies performed on Rpa1 and Rpa2 showed that RPA amounts do not vary throughout the cell cycle (Mitkova et al., 2002). Therefore, wild type cells should be able to cover all the ssDNA generated during S phase. Assuming that *rfa*^{td} strains grown under restrictive conditions fire early origins only due to inhibition of late origin firing by activation of the DNA damage checkpoint, this would suggest ~400 active replication forks (Lengronne et al., 2001) and ~52kb of ssDNA. This value is still significantly higher than the amount of ssDNA that could be covered by ~10% of RPA (~15kb, again assuming a roughly side-by-side binding mode of RPA).

A study based on electron microscopy evidence (Sogo et al., 2002) suggested even longer tracts of ssDNA generation at each replication fork (~200nt), resulting in estimates of ~120kb of ssDNA present during unperturbed replication and ~80kb of ssDNA when late origin firing is inhibited. However, this method has to be treated with some caution since it employed a process of enrichment of replication intermediates that could be biased for some fork structures. Moreover, a relatively high standard deviation (~100nt) was associated with this measurement.

Recently, an attempt was made to characterise ssDNA formation on a genome-wide scale (Feng et al., 2006). However, due to the low signal/noise ratio, no accurate quantification was possible, although the authors were able to use the detection of ssDNA generation to identify and confirm replication origins (Feng et al., 2006).

Perhaps the slow S phase observed after depletion of RPA is a consequence of a reduced availability of low amounts of RPA to stimulate helicase activity (Baker et al., 1986; Walter and Newport, 2000). One prediction of such a situation would be a reduction in the size of Okazaki fragments under conditions restrictive for RPA. Further experiments on Okazaki fragment length and measurements of fork progression rates by density-substitution (Tercero et al., 2000) would be required to address this issue further.

4.3.4 Replication with limiting amounts of RPA leads to DNA damage and Rad9-dependent checkpoint activation

Releasing cells from G1 arrest after degradation of any one of the RPA subunits resulted in Rad53 activation and G2/M arrest (Figure 4.4B, E and data not shown), indicating an active DNA damage checkpoint. Rad53 activation required entry into S phase because it was not observed in the G1 arrested population and occurred before entry into G2/M (Figure 4.4B). Because none of the experiments carried out during this investigation has addressed the nature of the DNA damage that presumably is generated (see below), it remains formally possible that Rad53 activation and cell cycle arrest are caused by means distinct from DNA damage. However, three lines of evidence argue against such a possibility. Firstly, no situation has been described in which Rad53 activation was observed under conditions other than DNA damage (Bartek et al., 2001). Secondly, deletion of genes upstream of *RAD53* in the DNA damage checkpoint resulted in a complete loss of Rad53 activation in response to degraded RPA (Figure 4.5). Lastly and most importantly, the loss of viability that was observed (Figure 4.4E), strongly suggested the formation of irreversible DNA damage.

As described in Chapter 1, transduction of the checkpoint signal from Mec1 to Rad53 depends on one of two proteins, Rad9 and Mrc1, depending on the nature of damage stimulus (Alcasabas et al., 2001; Longhese et al., 2003). Mrc1 appears to function mainly in response to replication stress (Alcasabas et al., 2001; Tanaka and Russell, 2001) whereas Rad9 appears to transduce signals generated by general DNA damage (Paulovich et al., 1997; Pellicioli et al., 1999; Alcasabas et al., 2001; Tanaka and Russell, 2001). In addition to its role in activating the checkpoint, Mrc1 is also required to maintain a stably associated replisome after HU treatment (Katou et al., 2003).

Checkpoint activation in response to Rpa1^{td} degradation was found to depend for the most part on Rad9; Mrc1, on the other hand, did not appear to be required (Figure 4.5B). Such checkpoint activation does not seem to be unique to the *rfa^{td}* alleles generated in this investigation. Several temperature-sensitive mutants of *RFA1* and *RFA2* that had previously been isolated undergo checkpoint arrest in G2/M when grown at the restrictive temperature (Santocanale et al., 1995; Maniar et al., 1997; Umezu et al., 1998). In some cases this arrest was found to be relieved by deletion of *RAD9* (Santocanale et al., 1995). In addition, degron mutants of *CDC45* and of components of the MCM complex were found to cause Rad9-dependent checkpoint activation (Rajat

Roy, unpublished results). Thus, this kind of checkpoint activation might be a common theme for loss of function of some replication fork proteins. It will be of interest to determine whether other components of the replication fork, such as DNA polymerases will behave in a similar manner. Two different mechanisms might be at work. Firstly, checkpoint activation due to uncoupling of the helicase and polymerase parts of the replisome may cause Rad53 activation in an Mrc1-dependent pathway. Such an uncoupling of helicase and polymerase parts of the replication fork is thought to be the consequence of polymerase inhibition by treatment with aphidicolin in the *X. laevis* NPE replication system (Byun et al., 2005; see Chapter 1, Introduction). In yeast, the situation is less clear, however. For example, after treatment with HU, large-scale uncoupling cannot be detected in wild type cells (Katou et al., 2003), although there is evidence for some uncoupling to happen at a lower scale (Sogo et al., 2002). Interestingly, deletion of *MRC1* results in increased uncoupling (Katou et al., 2003).

Secondly, inhibition of helicase function might result in secondary processing of replication forks and subsequent activation of Rad9-dependent signalling. Limiting the amount of RPA might result in inhibition of helicase activity, given that replicative DNA unwinding requires the single strand binding protein in *E. coli* and RPA in *X. laevis* egg extracts and SV40 replication (Baker et al., 1986; Dean et al., 1987; Wold et al., 1987; Fairman and Stillman, 1988; Wold and Kelly, 1988; Walter and Newport, 2000).

4.3.5 What is the nature of the DNA damage induced by Rpa1 degradation?

Having limiting amounts of RPA present during DNA replication might generate DNA damage and activate the checkpoint in several different ways. Here, three possibilities are discussed in more detail.

Firstly, it is possible that replication forks containing limiting amounts of RPA are being recognised as DNA damage directly. If, for example, RPA were inhibitory to checkpoint activation, such a consequence would be possible. In this regard it is of interest that the gene product of the *rfa1-t11* mutant that is partially defective for DNA damage checkpoint activation is less efficiently displaced from ssDNA (Kantake et al., 2003). Moreover, recognition of aberrant replication forks might not depend on aberrant DNA structures. Replication proteins might undergo conformational changes upon fork stalling to expose interaction sites that mediate the recruitment of checkpoint proteins.

Interestingly, Mrc1 and Tof1, another protein implicated in the S phase checkpoint response, were shown to travel with replication forks (Katou et al., 2003). However, because Mrc1 is not required for Rad53 activation in response to Rpa1^{td} degradation (Figure 4.5), such a process would have to be mediated by other factors. Arguing against checkpoint activation without the actual generation of DNA damage, Rpa1^{td} degradation was found to result in a dramatic loss of viability (Figure 4.4D). Although checkpoint activation can be detrimental to cell viability (Wysocki and Kron, 2004), it is hard to envisage how transient checkpoint activation can result in complete loss of viability in yeast.

Secondly, RPA might be a factor that inhibits processing of aberrant replication forks. Replication forks loaded with sub-optimal amounts of RPA might thus be a substrate for flap endonucleases, resulting in DSB formation. In favour of this hypothesis, several flap endonucleases were shown to be detrimental to growth of *rad53*Δ cells treated with low amounts of HU (Mónica Segurado, unpublished results). However, the fast kinetics of checkpoint activation upon RPA depletion (Figure 4.4B), are somewhat in contrast to the relatively slow checkpoint activation observed in response to DSB formation (Pellicioli et al., 2001), see also Chapter 5). Moreover, deletion of Exo1, a flap endonuclease shown to be involved in the processing of collapsed replication forks (Cotta-Ramusino et al., 2005), was found not to affect checkpoint activation in an *mcm4^{td}* strain (Rajat Roy, unpublished).

Thirdly, limiting amounts of RPA might result in aberrant processing of Okazaki fragments. In an *in vitro* reconstituted system for this process, RPA has been shown to play an essential role by regulating the concerted action of Dna2 and Fen1 endonucleases (Bae et al., 2001). If proper processing of Okazaki fragments were impaired *in vivo* after Rpa1^{td} degradation, the flaps and gaps generated during lagging strand synthesis could account both for checkpoint activation and loss of viability.

4.3.5.1 rfa^{td} *strains are proficient for checkpoint activation in response to HU*

The observation that depletion of RPA resulted in Rad53 activation during S phase (Figure 4.4) cast doubt on the previous findings regarding the apparently normal checkpoint response to HU and MMS (Figure 4.2 and Figure 4.3). If the checkpoint response in HU and MMS under conditions restrictive for *rfa1^{td}* were only a consequence of the signal generated by depletion of RPA, then deletion of *RAD9* should abolish Rad53 activation. However, this was not observed (Figure 4.6). It was therefore

concluded that checkpoint activation to replication stress was apparently functional after RPA degradation.

Checkpoint activation in response to replication stress is weak and delayed in *mrc1*Δ mutants (Alcasabas et al., 2001). It is believed that secondary lesions generated from processing of collapsed replication forks mediate this residual checkpoint activation in *mrc1*Δ cells (Alcasabas et al., 2001). Evidence for such a mechanism comes from the finding that Rad9 is required for Rad53 activation in response to HU in *mrc1*Δ mutants, although it is not essential for this process in wild type cells. Interestingly, degradation of $Rpa1^{td}$ during an HU arrest did not increase Rad53 activation in *mrc1*Δ (Figure 4.6B, autokinase assay). This might indicate that the generation of structures that mediate checkpoint activation in response to HU precedes and compromises the formation of structures that mediate checkpoint activation in response to RPA depletion. Further studies will, however, be required to resolve this issue.

4.3.6 Rad9-dependent checkpoint activation independent of long tracts of RPA-covered ssDNA?

It was intriguing to observe efficient checkpoint activation during replication under conditions limiting for RPA, and possibly therefore also for the production of ssDNA. The findings obtained in the investigation reported here thus raise the possibility of structures other than long tracts of RPA covered ssDNA to be able to induce a checkpoint response. Support for such a situation comes from studies carried out in parallel (Rajat Roy, unpublished), indicating that inhibition of the replicative helicase by degradation of MCM subunits results in checkpoint activation as well. In such a situation, ssDNA formation by itself is inhibited due to the absence of DNA unwinding at the replication fork.

UV irradiation of G1 arrested cells can result in checkpoint activation at doses as low as $5Jm^{-2}$ (Neecke et al., 1999). At such a dose, an estimated ~70 pyrimidine-dimers are being formed per cell (Douki et al., 2000). During repair of these, the NER machinery generates gaps of ~30nt for each photoproduct (Prakash and Prakash, 2000). Assuming synchronous repair, ~2100nt of ssDNA would be generated. If such a low amount of ssDNA can induce a checkpoint response, how can the estimated tens of thousands of ssDNA nucleotides generated during DNA replication (see above, section

4.3.3) escape notice by the checkpoint? Studies carried out in the *X. laevis* NPE system (Walter et al., 1998) have established that ssDNA generation by itself is not sufficient for checkpoint activation (Byun et al., 2005). Rather, a junction to dsDNA is required in addition to ssDNA (Byun et al., 2005). Further results indicated that a freely available 5' end (e.g. a 3' overhang structure) was necessary for checkpoint activation (K. Cimprich, personal communication). Such structures are the preferred substrate for loading of the PCNA-like checkpoint complex (Ellison and Stillman, 2003). It is not known whether this alternative PCNA checkpoint complex can efficiently be loaded at Okazaki fragments, which contain RNA instead of DNA at their 5' ends. If loading were compromised, this might be a mechanism to prevent checkpoint activation during normal replication. Interestingly, activation of the checkpoint in non-replicating cells treated with UV and after DSB formation, depends on these factors (de la Torre-Ruiz et al., 1998; Kondo et al., 2001). Rad53 activation in response to HU or MMS, however, requires neither the Rad17-Ddc1-Mec3, nor the Rad24-RFC complex (Pellicioli et al., 1999). It is therefore possible that stalled replication forks signal to the checkpoint machinery in a way that differs from regular DNA damage responses. Such a mechanism might well work independently of long tracts of ssDNA.

5 Checkpoint activation to DSBs is a dose-dependent process and works independently of long resection tracts

5.1 Overview

As described in detail in the Introduction (Chapter 1), the first step in DSB repair by homologous recombination (HR) is the nucleolytic degradation of the 5' strands at both sides of the DSB (Paques and Haber, 1999). This process, termed DSB resection, generates free 3' ssDNA tails that are then used for strand invasion of homologous sequences. Because non-homologous end joining (NHEJ), when compared to HR, is a rather inefficient process in yeast (see section 1.2.3.7, Clikeman et al., 2001), the majority of breaks will be channelled into the HR route of repair. Therefore, if no homology is present within the genome, or if HR is otherwise inhibited, cells will largely be unable to repair DSBs. In such a case, checkpoint activation can be observed (Pellicioli et al., 2001). For reasons outlined in detail in the Introduction, it is believed that the damage response depends on ssDNA formation at DSBs. Resection was calculated to occur at a rate of ~4kb/hr (Fishman-Lobell et al., 1992; Vaze et al., 2002) and checkpoint activation can first be observed ~1-2hrs after formation of irreparable DSBs (Pellicioli et al., 2001). This has led to the wide belief that DSB resection is a relatively fast and synchronous process, and a prerequisite for checkpoint activation. Extensive tracts of ~16kb ssDNA are thought to be required for checkpoint activation (Lee et al., 1998; Vaze et al., 2002; Zou and Elledge, 2003; Ira et al., 2004). Yeast provides a powerful model system for studying the responses to DSB damage. By using the HO system, it is possible to induce DSBs in defined positions in the genome in a synchronous way within a population of cells (see section 1.2.3.2, reviewed in Haber, 2002).

The aim of this investigation was to characterise the correlation between ssDNA formation and checkpoint activation upon HO-dependent DSB formation to a high degree of detail. Since most existing assays for ssDNA do not allow an accurate quantification, a new method was set up based on quantitative real-time PCR (Q-PCR). In addition, the apparent inability of G1 arrested cells to activate the DNA damage checkpoint in response to DSB damage and to produce ssDNA at a DSB was analysed (Pellicioli et al., 1999; Ira et al., 2004).

5.2 Results

5.2.1 A new assay for the quantification of ssDNA

As described in Chapter 1, resection at a DSB has so far been measured by several different approaches. However, as has been pointed out, none of these assays readily allow an accurate quantification of the ssDNA that is produced. Since one of the aims of this investigation was the precise analysis of DSB resection, a new assay was set up to accurately measure ssDNA. This method is described in detail in the Material and Methods section but will briefly be outlined here (Figure 5.1). DNA extracted from samples taken before and at regular intervals during HO expression is treated or mock-treated with BstUI restriction endonuclease. The DNA is then used for quantitative PCR (QPCR) analysis with pairs of primers that amplify across the chosen restriction sites (Figure 5.1A). Because ssDNA is resistant to restriction enzyme digestion, comparison of product generation between digested and mock-digested template allows the determination of the percentage of ssDNA at each restriction site present at each time point. Three amplicons were analysed, situated 0.3kb, 9kb, and 14kb distal from an HO cut site (HOcs) inserted close to *ARS607* on chromosome VI (Figure 5.2). In addition, data was normalised to an amplicon on a different chromosome. Directly after break formation by HO, all DNA is double-stranded, and only background amounts of PCR product are generated at all three loci after BstUI digestion (Figure 5.1A). At later time points, however, some of the breaks will have been resected, and PCR products will be generated first for regions close to the break point (Figure 5.1B), and then for regions further away (Figure 5.1C).

Although, for reasons described below, strains with several HO cut sites introduced at different loci were used in the course of this investigation (Figure 5.2), resection was always analysed at *ARS607::HOcs*. To ensure rapid and synchronous break formation, all strains contained a $P_{GAL1\text{-}10}$*::HO* construct stably integrated into the genome.

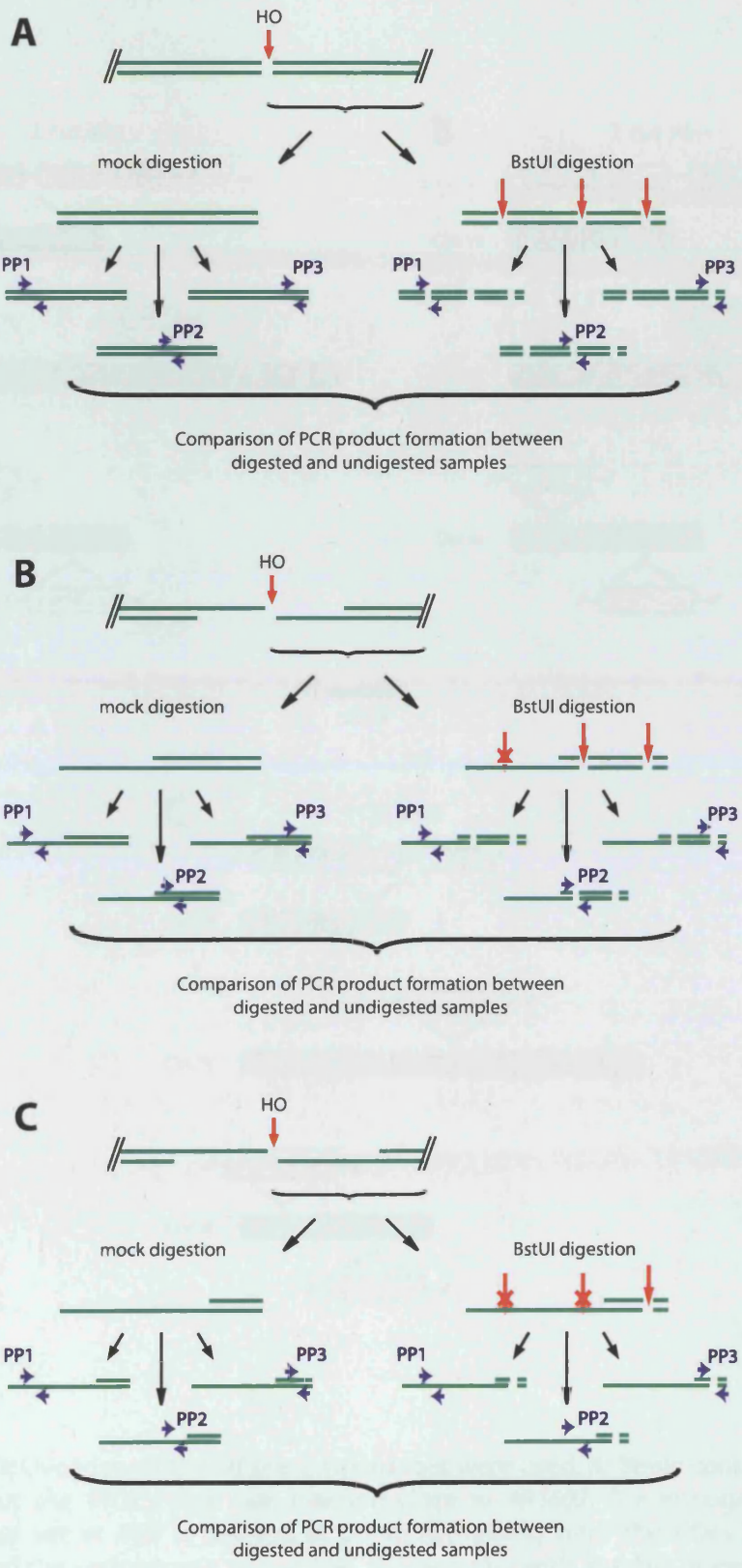

Figure 5.1: Schematic representation of the Q-PCR approach for the quantification of ssDNA at a DSB. PP1-PP3: Primer pairs 1-3. See text in Chapters 2 and 5 for details.

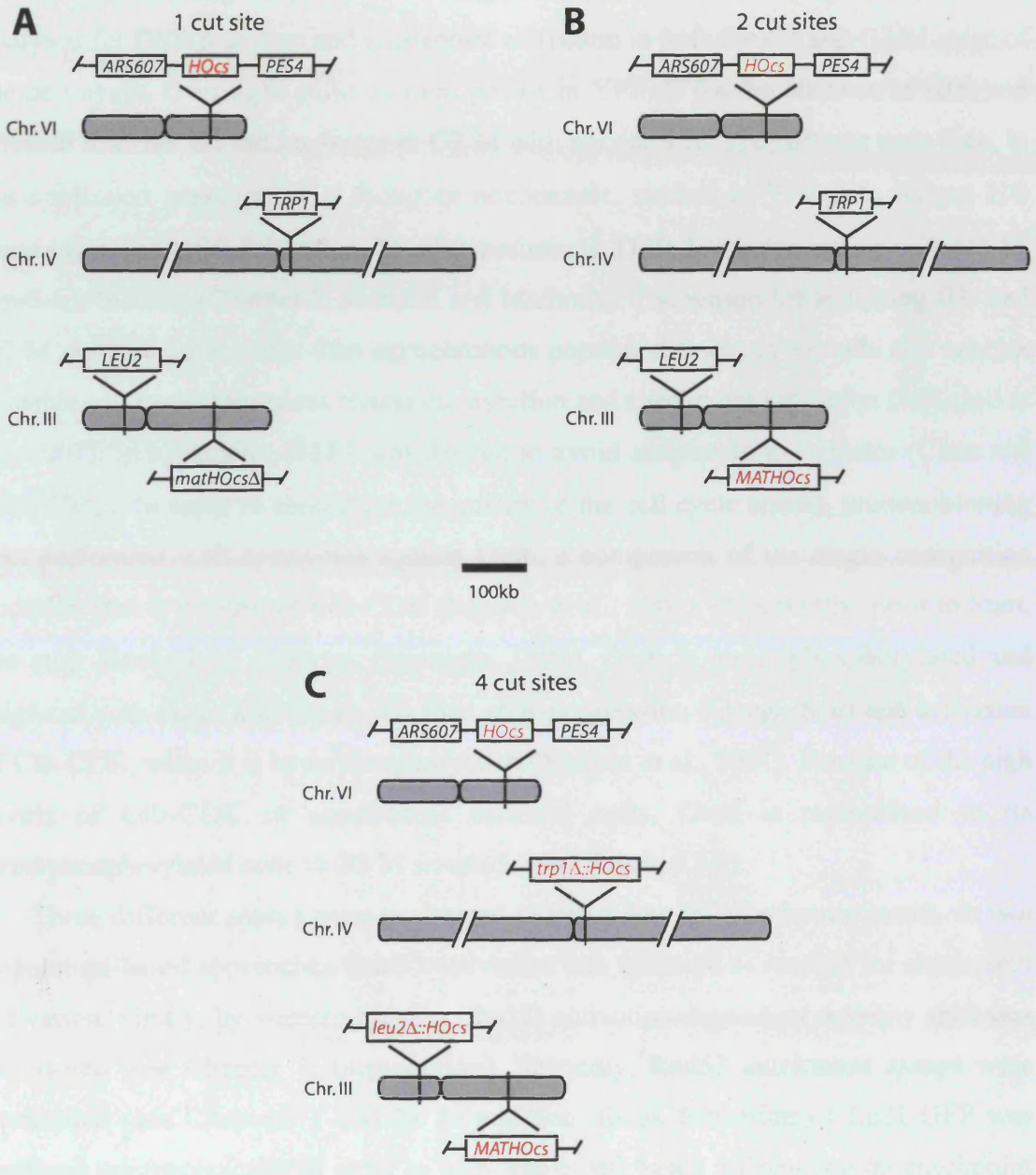

Figure 5.2: Overview of the different strains that were used. **A:** Strain containing only the HO cut site (HOcs) that was inserted close to *ARS607*. The endogenous HO-recognition site at *MAT* is deleted. **B:** Strain containing both the HOcs inserted at *ARS607* and the endogenous one at *MAT*. **C:** The strain with four HO recognition sites contains the endogenous one at *MAT*, the one inserted close to *ARS607*, and two additional ones at *leu2* and *trp1*.
The scale bar (centre) represents 100kb. See Section 2, Material and Methods for descriptions of strain constructions.

5.2.2 Checkpoint activation does not appear to require long resection tracts

Cells containing only the HO recognition site at *ARS607* (Figure 5.2A) were analysed for DSB resection and checkpoint activation in both the G1 and G2/M stage of the cell cycle. Overnight cultures were grown in YPRaff (in the absence of HO) and arrested in either G1 with α factor or G2/M with nocodazole. The cultures were then, in the continued presence of α factor or nocodazole, shifted to YPGal to induce HO expression and DSB formation. In all experiments, DSB formation was monitored by Southern blotting (Chapter 2, Material and Methods). The reason for analysing G1- and G2/M arrested cells rather than asynchronous populations was to exclude and analyse possible cell cycle dependent effects on resection and checkpoint activation (Pellicioli et al., 2001). In all strains, *BAR1* was deleted to avoid adaptation to α factor (Chan and Otte, 1982). In order to control for the quality of the cell cycle arrests, immunoblotting was performed with antibodies against Orc6, a component of the origin recognition complex that is a target of Clb-CDK (Nguyen et al., 2001). Importantly, prior to Start, the step blocked by α factor (Nasmyth, 1996), Orc6 is under-phosphorylated and migrates with faster kinetics in gels than after progression through Start and activation of Clb-CDK, when it is hyperphosphorylated (Nguyen et al., 2001). Because of the high levels of Clb-CDK in nocodazole arrested cells, Orc6 is maintained in its hyperphosphorylated state in G2/M arrested cells (Figure 5.3A).

Three different assays were performed to determine the checkpoint status. In two population-based approaches, Rad53 activation was followed as readout for checkpoint activation. Firstly, by western blotting, Rad53 activation-dependent mobility shift was monitored (see Chapter 1, Introduction). Secondly, Rad53 autokinase assays were performed (see Chapters 1 and 2). In addition, focus formation of Lcd1-GFP was analysed microscopically in order to gain single-cell based information on checkpoint activation. It had previously been shown that upon formation of DSBs as well as other kinds of DNA damage, Lcd1 forms a nuclear focus, thought to represent the accumulation of Lcd1-Mec1 at sites of damage (Melo et al., 2001).

In agreement with published results (Pellicioli et al., 2001), Rad53 activation after break formation in strains containing one HOcs was only observed in G2/M arrested cells but not when cells were arrested in G1 (Figure 5.3A). Furthermore, a similar restriction was detected to Lcd1-GFP focus formation (Figure 5.3B). After ~4h the majority of G2/M arrested cells had an active checkpoint as judged by Lcd1-GFP

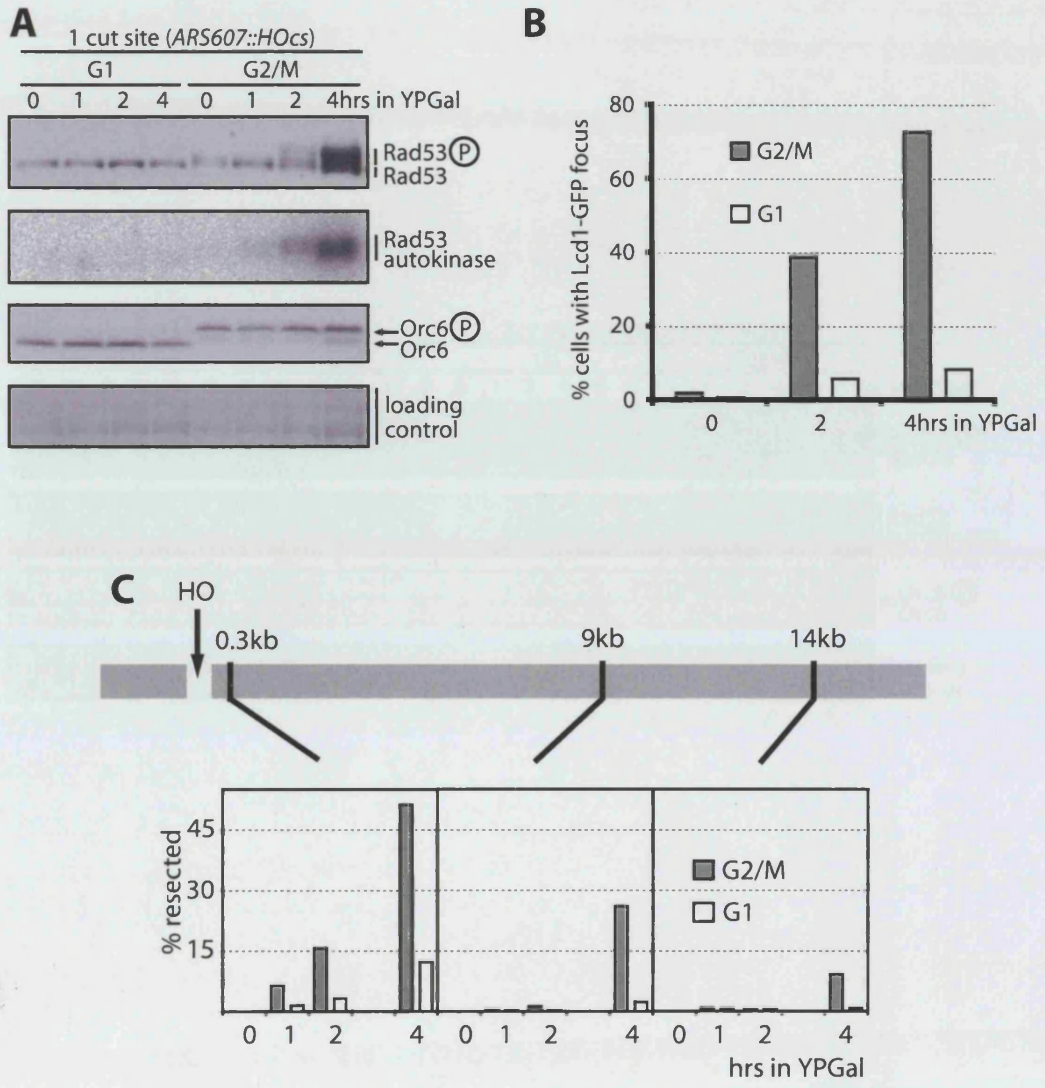

Figure 5.3: Checkpoint activation in response to DSB damage does not correlate with long resection tracts. Cells of strains YCZ101 (*ARS607::HOcs*, A and C) and YCZ70 (*ARS607::HOcs LCD1-GFP*, B) were arrested in YPRaff using either alpha factor (G1) or nocodazole (G2/M). The cultures were then shifted to YPGal while maintaining the cell cycle arrest. Samples were taken at the indicated time points. **A:** TCA extracts were used for immunoblotting or Rad53 autokinase assay. Ponceau-S staining was used as loading control. **B:** Samples were analysed for Lcd1-GFP focus formation. **C:** DSB resection at the HOcs close to *ARS607* was monitored by Q-PCR. Resection is plotted as the percentage of ssDNA relative to the total amount of DNA present at each time point. The three panels show ssDNA at the three loci indicated in the bar above them.

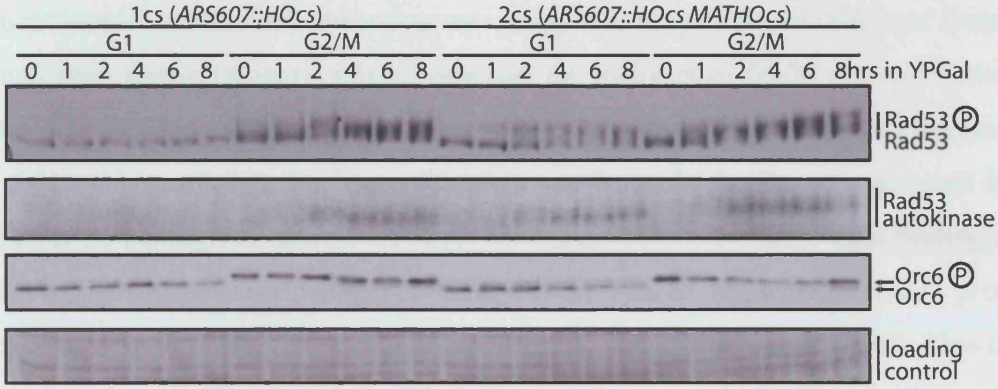

Figure 5.4: Checkpoint activation in strains containing one or two HO recognition sites. Cells of strain YCZ70 (1cs, *ARS607::HOcs*) and YCZ64 (2cs, *ARS607::HOcs MATHOcs*) were grown as described in Figure 5.3. TCA extracts were used for immunoblotting or Rad53 autokinase assay. 1cs, one HOcs. 2cs, two HOcs.

microscopy. However, not all of the Rad53 molecules appeared to be hypershifted. Analysis of Rad53 activation over a longer period of time showed that it reached a plateau after this time and no further increase was detected afterwards (Figure 5.4). This indicates that at this level of DNA damage not all of the Rad53 molecules within the cell are activated. The alternative explanation that some cells failed to activate the checkpoint and contained only inactive Rad53 does not appear to be likely, given that most cells showed Lcd1-GFP foci (Figure 5.4B). Moreover, during HO induction in asynchronous cultures, virtually all cells are arrested after ~1-2hrs (Pellicioli et al., 2001, data not shown).

Surprisingly, when DSB resection was analysed, very little ssDNA was found to have had been formed (Figure 5.3C). Although the majority of G2/M arrested cells had activated the DNA damage response after ~4h, only ~50% of the breaks were resected up to 0.3kb (Figure 5.3C). Positions further away from the break were resected in an even lower percentage of cases (~30% for 9kb and ~10% for 14kb). This finding is in contrast to the estimation of resection being a very synchronous and efficient process occurring at a rate of ~4kb/h (Fishman-Lobell et al., 1992; Vaze et al., 2002). However, it is similar to quantifications of ssDNA at eroded telomeres in the *cdc13-1* mutant (Maringele and Lydall, 2002).

When ssDNA was compared between G1 and G2/M arrested cells, much less resection was found to have had occurred in G1 arrested cells. This is in agreement with published results indicating that DSB resection is under cell cycle control (Ira et al., 2004).

5.2.3 Checkpoint activation in response to DSBs appears to be a dose-dependent process in G1

Because G2/M arrested cells contain two sister chromatids, but G1 arrested cells only contain one, twice as many breaks will be induced upon HO expression in G2/M than when HO is expressed in cells of the same strain arrested in G1. Therefore, rather than reflecting genuine cell cycle regulation, the absence of Rad53 activation in G1 arrested cells might result from the lower number of breaks induced in G1. To address this issue, a strain was used that, in addition to *ARS607::HOcs*, also contained the endogenous HOcs at *MAT* (Figure 5.2B). HO expression in cells of this strain arrested in G1 causes the formation of two DSBs. Thus, by comparing cells of this strain arrested in G1 with cells of the one HOcs (1cs) strain arrested in G2/M, situations with

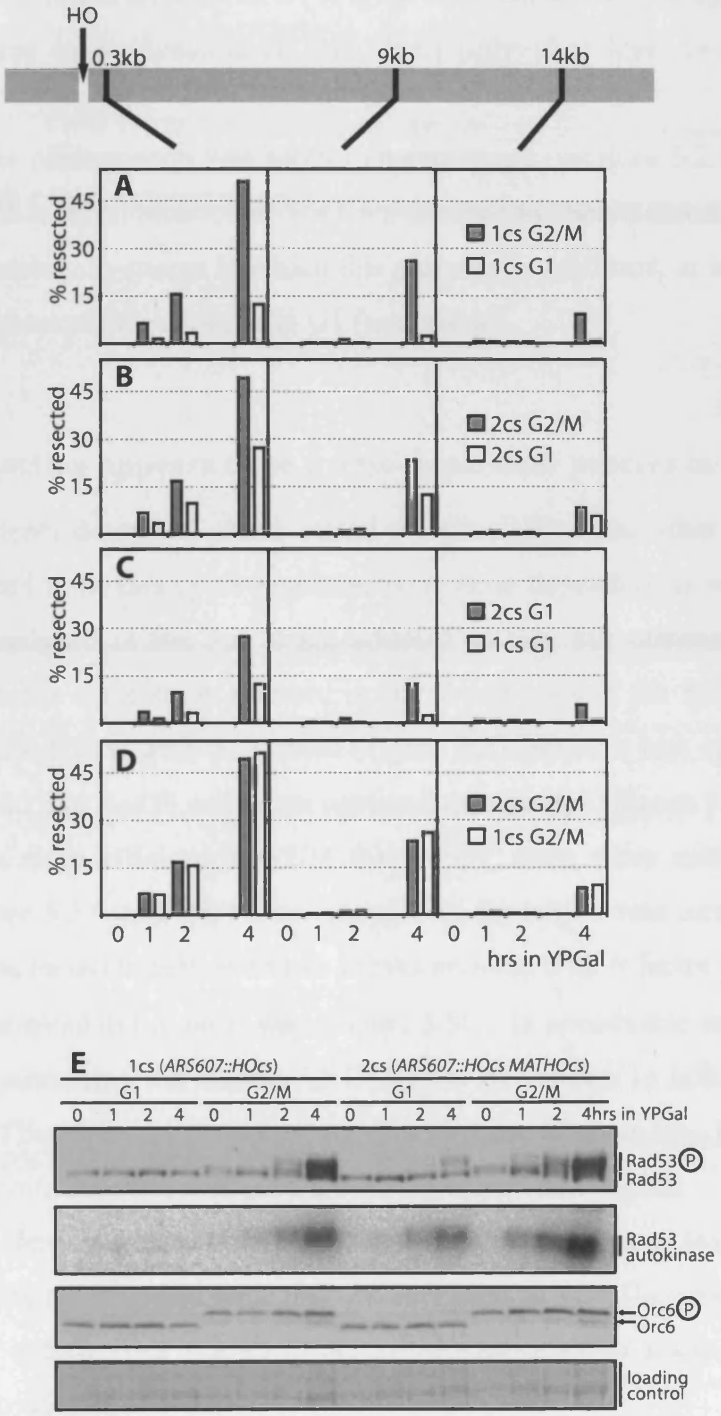

Figure 5.5: Checkpoint activation and DSB resection in strains containing one or two HO recognition sites. Cells of strain YCZ101 (1cs, *ARS607::HOcs*) and YCZ64 (2cs, *ARS607::HOcs MATHOcs*) were grown as described in Figure 5.3. **A-D:** Resection at the DSB close to *ARS607*. The graphs show comparisons between the indicated strains and cell cycle stages. **E:** TCA extracts were used for immunoblotting or Rad53 autokinase assay. Ponceau-S staining was used as loading control. 1cs, one HOcs. 2cs, two HOcs.

equal amounts of breaks are analysed. Interestingly, Rad53 activation was observed in the two HOcs (2cs) strain arrested in G1 (Figure 5.4). Therefore, checkpoint activation to DSBs appeared to be possible in G1, albeit only if at least two breaks were introduced.

Although this phenomenon was further characterised (sections 5.2.4 and 5.2.5), it was later found that recombination at *MAT* contributed to checkpoint activation in the 2cs strain (see below). In strains in which this pathway is inhibited, at least four DSBs are required for checkpoint activation in G1 (see below).

5.2.4 DSB resection appears to be a dose-dependent process in G1

The experiments described above raised the possibility that other processes at a DSB that appeared to be cell cycle-regulated were dose-dependent as well. Therefore, resection was analysed in the 2cs strain arrested in G1. For comparisons, parallel experiments with the same strain arrested in G2/M and cells of the 1cs strain arrested under the same conditions were performed (Figure 5.5). Western blot and kinase assay analysis confirmed that Rad53 activation occurred as expected (Figure 5.5E). Resection was found to be more efficient in G2/M than in G1, even when another break was introduced (Figure 5.5A and B). However, ssDNA formation was increased 2-5 fold (depending on the locus) in cells with two breaks arrested with α factor relative to cells with one break arrested in the same way (Figure 5.5C). In nocodazole arrested cells, on the other hand, increasing the number of DSBs did not appear to influence resection (Figure 5.5D). These results therefore suggest that, at least in G1, DSB resection, similar to checkpoint activation, may be a dose-dependent mechanism.

However, again it has to be emphasised that if recombination at *MAT* is prevented, at least four DSBs are required for enhanced resection in G1. Therefore, some of the results obtained with the 2cs strain just described may relate to a somewhat artificial situation (see below, section 5.2.8).

No mutants are known that show a complete absence of resection. However, mutations in subunits of the MRX complex cause resection to be delayed and less efficient (Ivanov et al., 1994; Lee et al., 1998). The *mre11*Δ mutant was therefore used as a near-negative control (Figure 5.6). In agreement with the published results (Ivanov et al., 1994; Lee et al., 1998), deletion of *MRE11* resulted in less ssDNA being generated in both G1 and G2/M (Figure 5.6A-D). In parallel with ssDNA

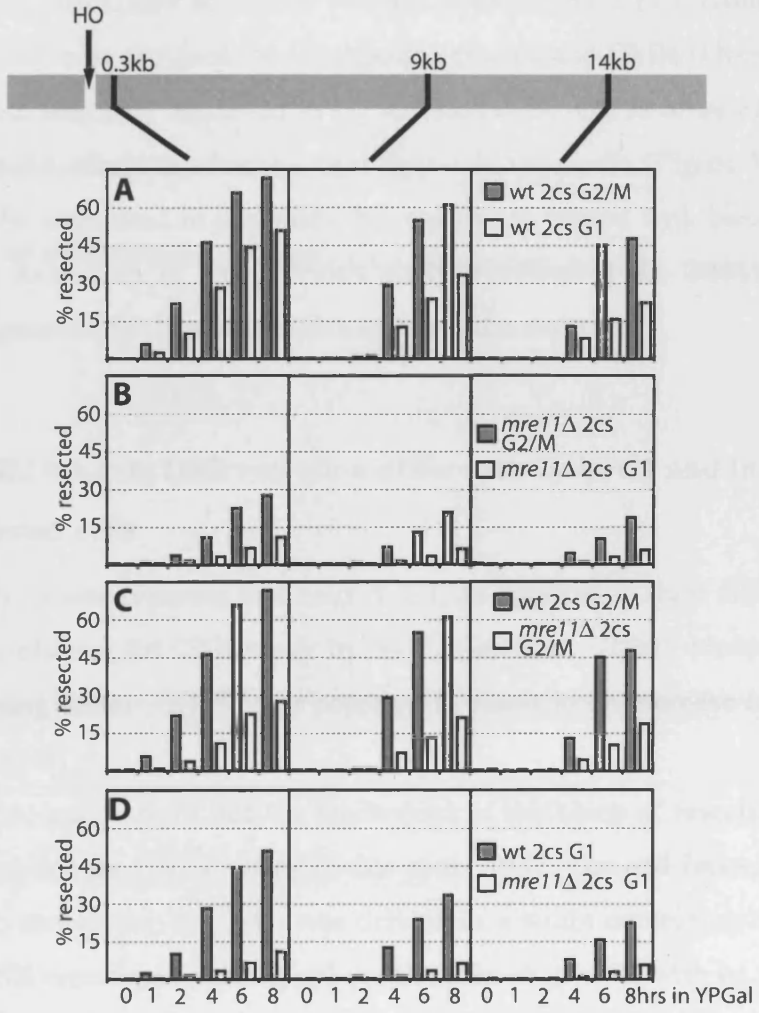

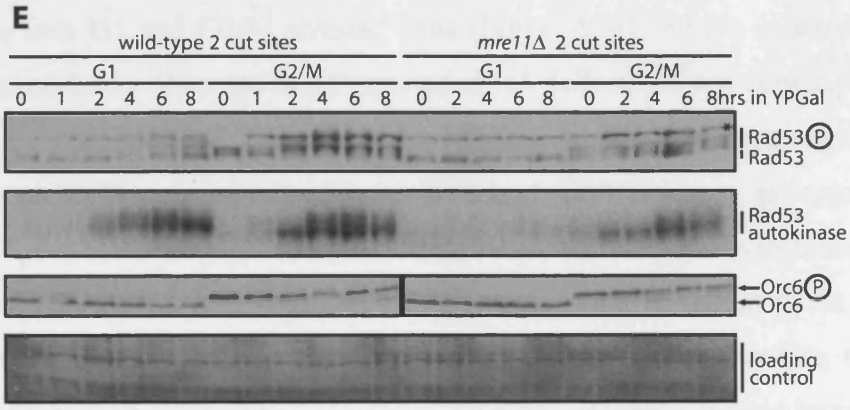

Figure 5.6: Checkpoint activation and DSB resection are partially dependent on *MRE11*. Cells of strain YCZ64 (wild-type, wt) and YCZ65 (*mre11Δ*) were grown as described in Figure 5.3. Both strains contain two HO recognition sites (2cs, *ARS607::HOcs MATHOcs*). **A-D:** Resection at the DSB close to *ARS607*. The graphs show comparisons between the indicated strains and cell cycle stages. **E:** TCA extracts were used for immunoblotting or Rad53 autokinase assay. Ponceau-S staining was used as loading control. 2cs, two HOcs.

quantification, checkpoint activation was analysed (Figure 5.6E). Although Mre11 had been published to be required for checkpoint activation to DSBs (Grenon et al., 2001), such an effect was only observed in G1 arrested cells. G2/M arrested cells contained activated Rad53, albeit to a lesser extent than wild type cells (Figure 5.6E). Since HO-induced DSBs were used in this study, but cells were treated with bleomycin and IR to cause DSB formation in the previous study (Grenon et al., 2001), differences in damaging agents might account for this apparent discrepancy.

5.2.5 NHEJ inhibits DSB resection differentially in G1 and in G2/M arrested cells

Recently, it was reported that cells in G1, as opposed to their G2/M counterparts, are highly proficient for DSB repair by NHEJ (Ira et al., 2004). Moreover, deletion of the end-joining factor *YKU70* was reported to result in an increase in DSB resection (Lee et al., 1998).

In order to gain insight into the mechanism of inhibition of resection by NHEJ, the ligase responsible for NHEJ, *DNL4* (Schar et al., 1997; Teo and Jackson, 1997; Wilson et al., 1997, see section 1.2.3.4), was deleted in a strain containing an HOcs only at *ARS607*. DSB resection was analysed in this strain in parallel with its parent strain that is wild type for *DNL4* (Figure 5.7A and B). Deletion of *DNL4* resulted in an increase in resection in both G1 and G2/M arrested cells (Figure 5.7C and D). Interestingly, the strongest increase was observed in G1 arrested *dnl4*Δ cells at the site closest to the DSB (0.3kb). Here, deletion of *DNL4* resulted in an increase in resection to levels comparable to G2/M arrested cells (Figure 5.7B and E). In contrast, at regions further away from the break (9kb and 14kb), resection was only marginally increased (Figure 5.7B and E). These findings suggest that CDKs regulate resection by at least two different mechanisms. Firstly, by downregulation of NHEJ, thus making more ends available for resection. Secondly, by increasing the rate of resection once initiated.

In G2/M arrested cells, NHEJ is very inefficient (Ira et al., 2004). Accordingly, deletion of *DNL4* resulted in only a slight increase in resection in G2/M (Figure 5.7C). In contrast to G1 arrested cells, a similar increase in resection was detected at all three sites in G2/M arrested *dnl4*Δ cells (Figure 5.7C). This suggests that all the breaks that become available for resection due to the absence of religation are efficiently processed in G2/M.

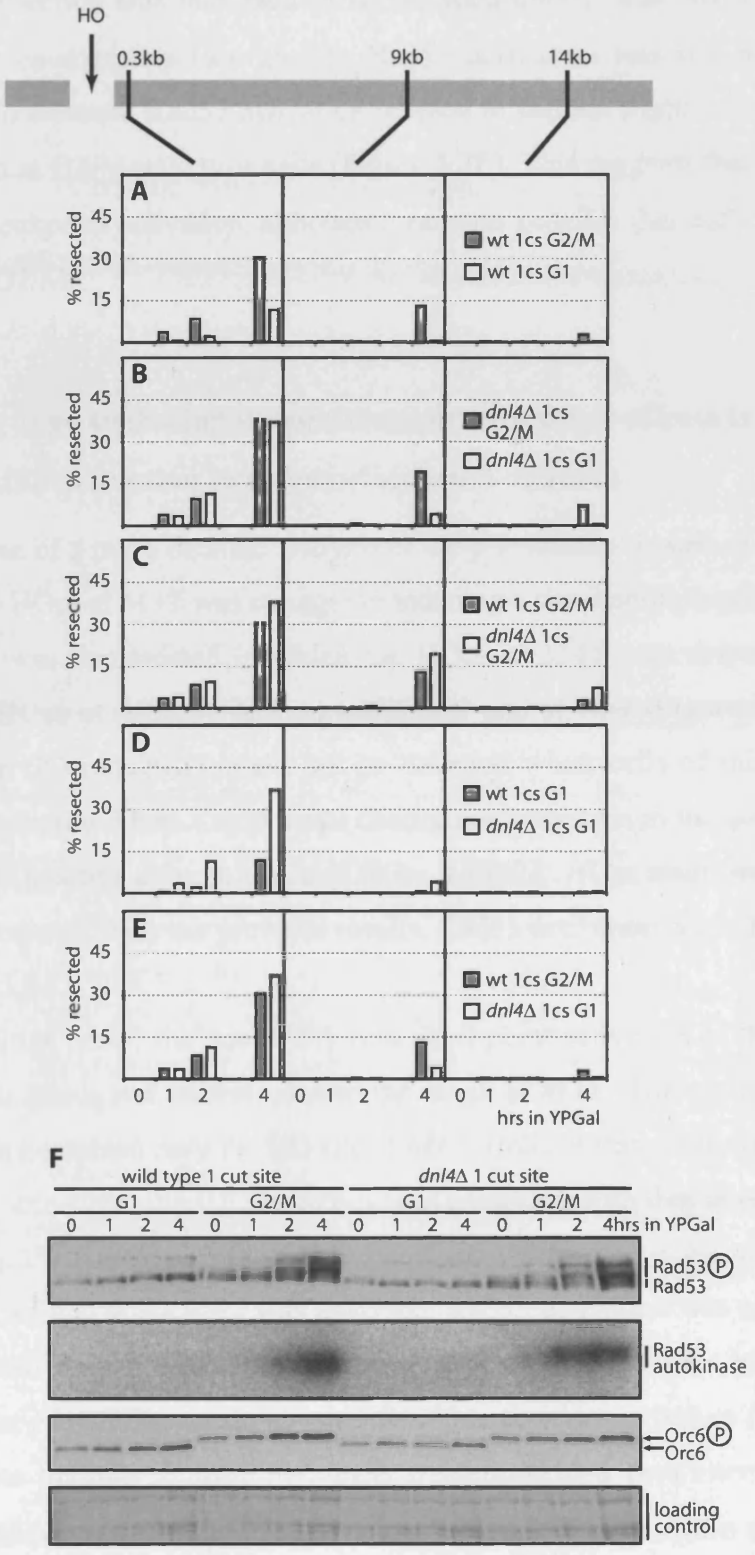

Figure 5.7: Effects of the deletion of *DNL4* on DSB resection and checkpoint activation. Cells of strain YCZ101 (wild type) and YCZ136 (*dnl4Δ*) were grown as described in Figure 5.3. **A-E:** Resection at the DSB close to *ARS607*. The graphs show comparisons between the indicated strains and cell cycle stages. 1cs, one HOcs. **F:** TCA extracts were used for immunoblotting and Rad53 autokinase assay. Ponceau-S staining was used as loading control.

Although resection was increased in G1 arrested *dnl4*Δ cells when compared to their wild type counterparts (see above), Rad53 activation was still not detectable (Figure 5.7F). In contrast, Rad53 activation seemed to happen slightly earlier in G2/M *dnl4*Δ cells than in G2/M wild type cells (Figure 5.7F). This suggests that NHEJ can be inhibitory to checkpoint activation, although it remains possible that such an effect may be confined to G2/M.

5.2.6 Mating-type switching in combination with other effects is responsible for Rad53 activation in α factor arrested cultures

In the course of a more detailed analysis of the phenomena described above, it was noticed that the HOcs at *MAT* was stronger in inducing a checkpoint response than other sites. A strain was constructed in which the HOcs at *MAT* was deleted but which contained the HOcs at *ARS607* and an additional one at *trp1* (Figure 5.2C). Rad53 activation after HO induction could not be detected when cells of this strain were arrested in G1 (Figure 5.8A). G2/M stage checkpoint activation in the same strain was not affected. As positive control, the *MATHOcs ARS607::HOcs* strain was analysed in parallel. In agreement with the previous results, Rad53 activation could be detected as before (Figure 5.8A).

These findings raised the possibility that checkpoint activation in the *MATHOcs ARS607::HOcs* strain was entirely due to the break at *MAT*. Therefore, a strain was constructed that contained only the HO site at *MAT*. Cells of this strain were arrested in G1 and Rad53 activation after HO induction was compared with that of cells of a strain only containing the HO site at *ARS607*. As positive control, the strain containing both the HOcs at *MAT* and at *ARS607* was analysed. Rad53 activation was not detected in either of the two strains containing only one HOcs (Figure 5.8B). In contrast, the *ARS607::HOcs MATHOcs* strain showed Rad53 activation as before (Figure 5.8B). Therefore, these findings indicate that under conditions of α factor arrest, a break at *MAT* is not sufficient for checkpoint activation, although it represents a stronger signal for the checkpoint.

Interestingly, although either break was sufficient for checkpoint activation in G2/M arrested cells, the break at *MAT* resulted in stronger Rad53 autokinase activity (Figure 5.8B). This suggests that also in G2/M, this break might be a stronger checkpoint signal than others.

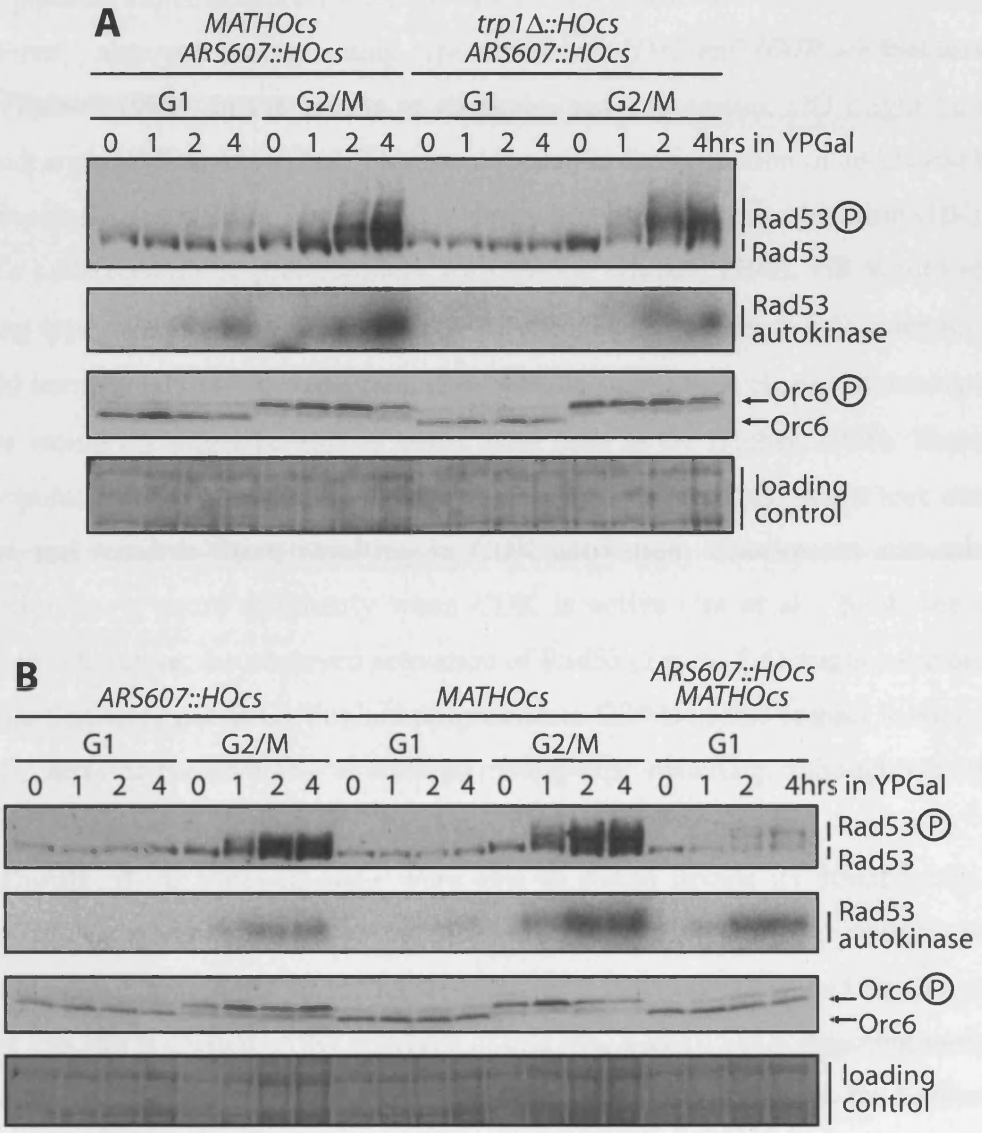

Figure 5.8: A DSB at *MAT* is stronger in inducing a checkpoint response than other sites but not sufficient for checkpoint activation in G1. **A:** Cells of strains YCZ100 (*MATHOcs ARS607::HOcs*) and YCZ127 (*trp1Δ::HOcs ARS607::HOcs*) were grown as described in Figure 5.3. TCA extracts were used for immunoblotting and Rad53 autokinase assay. Ponceau-S staining is included as a loading control. **B:** Cells of strains YCZ70 (*ARS607::HOcs*), YCZ102 (*MATHOcs*) and YCZ64 (*MATHOcs ARS607::HOcs*) were used as in A.

What makes a DSB at *MAT* special when compared to breaks at other locations? One feature that is unique to *MAT* is that it is able to recombine with the silent mating type loci *HML* and *HMR* (see section 1.2.3.2). The presence of *HML* and *HMR* provides three possible explanations for the observations described.

Firstly, although during mating-type switching, *HML* and *HMR* are inaccessible to HO (Haber, 1998), in the course of its prolonged expression, HO might be able to interact with *HML* and/or *HMR*. This would result in the formation of additional breaks.

Secondly, the DSB at *MAT* could undergo homologous recombination (HR). Since *MATa* cells recombine preferentially with *HMLα* (Haber, 1998), HR would result in mating type switching to *MATα*. Due to the chronic expression of HO, a repaired DSB would immediately be cleaved again. However, because of the change in mating type, α factor would no longer be able to arrest these cells in G1 (Haber, 1998). Therefore, a subpopulation of the cells, although maintaining a broken locus, might leak out of G1 arrest and traverse Start, resulting in CDK activation. Checkpoint activation and resection occur more efficiently when CDK is active (Ira et al., 2004; see section 1.2.3.6). Therefore, the observed activation of Rad53 (Figure 5.4) might have happened in cells that were not in G1 but had progressed to G2/M. In this respect it is of interest that G1 arrested cells are able to undergo mating-type switching, although with delayed kinetics (Aylon et al., 2004).

Thirdly, if the break at *MAT* were able to strand invade its donor locus, repair intermediates might be generated that are substrates for HO. One such possible pathway is outlined in Figure 5.9C. In such a scenario, after strand invasion and repair synthesis, a new HO site is created. After cleavage of this site, a small DNA fragment will remain associated with the invaded sequence. The other end will be available for another round of strand invasion, resulting in the cycle being repeated. Such a mechanism would lead to the accumulation of small, partially double-stranded fragments, that could potentially be good structures for checkpoint activation.

To determine the contribution of these possible mechanisms to the apparent checkpoint activation and DSB resection in G1, several experiments were performed.

In Southern blot based DSB assays (see Chapter 2, Material and Methods), break formation at *HML* and *HMR* was analysed. Two different strains, the 1HOcs strain (*ARS607::HOcs*) and the 2HOcs strain (*ARS607::HOcs MATHOcs*), arrested in both G1 and G2/M were used. Both *HML* and *HMR* were found to be cleaved by HO (Figure 5.9A, left and middle panels). However, as opposed to a non-silenced HOcs

(*ARS607::HOcs*, Figure 5.9A right panel), both *HML* and *HMR* were cut with much lower efficiency (Figure 5.9). Break formation occurred to a higher degree in G2/M arrested cells, possibly because of a less efficient NHEJ-mediated reverse reaction (Figure 5.9A, see above). Although *HML* was found not to be cut in G1 arrested cells, DSBs were detected at *HMR*. However, the efficiency of break formation was very low in G1 (~15% as opposed to ~60% in G2/M, Figure 5.9A). Together, this suggests that the silent mating-type loci can directly contribute to checkpoint activation following HO expression.

To determine the possible contribution of recombination to checkpoint activation, strains were constructed in which either *HML* or *HMR* were deleted. If recombination played a role, deletion of *HML* should have a stronger effect on checkpoint activation because it is the preferred donor for *MAT*a (Haber, 1998). Indeed, deletion of *HML* was found to completely abolish checkpoint activation in a 2cs strain (*ARS607::HOcs MATHOcs*, Figure 5.9B). In contrast, deletion of *HMR*, although cleaved with higher efficiency than *HML* (Figure 5.9A), caused only a mild reduction of activated Rad53 in α factor treated cells (Figure 5.9B). Checkpoint activation in G2/M appeared to be completely unaffected by either deletion (Figure 5.9B). These findings indicate that, although both cleavage of the donor loci and recombination may contribute to checkpoint activation under conditions of α factor arrest, recombination is more important.

To determine whether switching and consequential insensitivity to α factor were responsible for checkpoint activation in α factor treated cultures, the following experiment was performed. Strains were constructed that contained either *ARS607::HOcs* or both *ARS607::HOcs* and *MATHOcs*. In addition, these strains could be induced to express a stable version of Sic1 (Sic1Δnt) by the addition of galactose (Desdouets et al., 1998). Expression of Sic1 or Sic1Δnt results in a very specific and efficient inhibition of Clb-CDK (Schwob et al., 1994; Desdouets et al., 1998).

As shown in Figure 5.10A, Sic1 overexpression in cells that were arrested with α factor prevented Rad53 activation in strains with two HO recognition sites. Western blotting for Sic1Δnt (by virtue of its Myc-epitope tag at the C-terminus) confirmed its expression specifically after shift to galactose (Figure 5.10A). Furthermore, the small

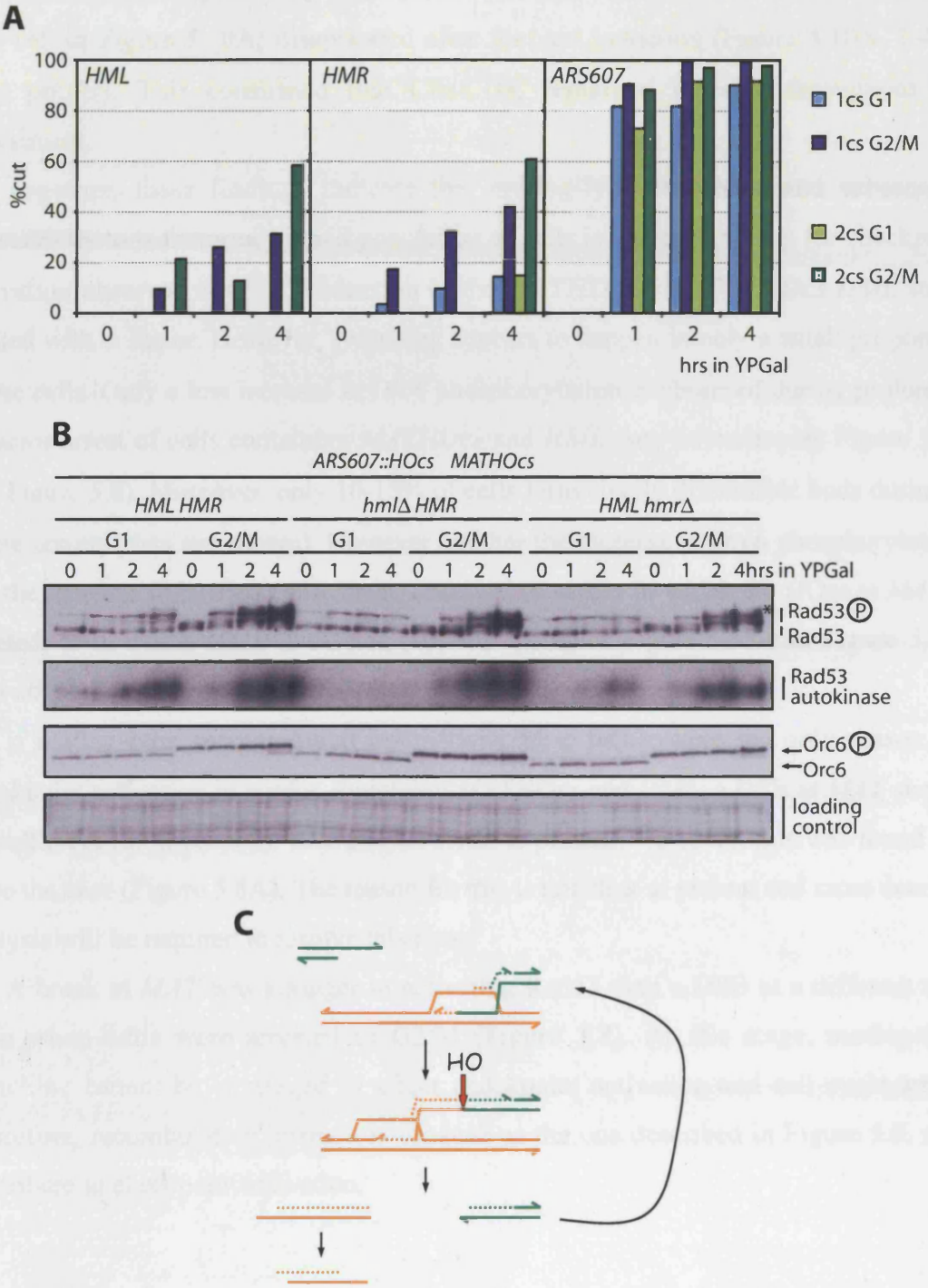

Figure 5.9: *HML* is required for a stronger checkpoint response to a DSB at *MAT*. Cells of the indicated strains were grown as described in Figure 5.3. **A:** Quantification of DSB formation at *HML* (left panel), *HMR* (middle panel) and *ARS607::HOcs* (right panel). Strains YCZ101 (1cs, *ARS607::HOcs*) and YCZ64 (2cs, *ARS607::HOcs MATHOcs*) were used. Both strains are wild-type for *HML* and *HMR*. 1cs, one cut site. 2cs, two cut sites. **B:** TCA extracts of strains YCZ64 (*ARS607::HOcs MATHOcs HML HMR*), YCZ147 (*ARS607::HOcs MATHOcs hmlΔ HMR*), and YCZ161 (*ARS607::HOcs MATHOcs HML hmrΔ*) were used for immunoblot analysis and Rad53 autokinase assay. Ponceau-S staining wasused as loading control. **C:** Speculative model for the mechanism of increased checkpoint activation in the presence of *HML* after DSB formation at *MAT*. See text for details.

fraction of phosphorylated Orc6 that is always observed in α factor arrested cultures (see t=0 in Figure 5.10A) disappeared after Sic1Δnt induction (Figure 5.10A, 1-4hrs time points). This confirmed that Clb-CDK remained inactive throughout the experiment.

Together, these findings indicate that mating-type switching and subsequent insensitivity to α factor in a small population of cells is the main reason for checkpoint activation observed after HO induction in the *MATHOcs ARS607::HOcs HML* strain treated with α factor. However, switching appears to happen in only a small proportion of the cells. Only a low increase in Orc6 phosphorylation is observed during prolonged α factor arrest of cells containing *MATHOcs* and *HML* (see for examples Figure 5.5F and Figure 5.8). Moreover, only 10-15% of cells form clearly discernible buds during α factor arrests (data not shown). However, neither the increase in Orc6 phosphorylation, nor the increase in budded cells can be observed in strains in which the HOcs at *MAT* is deleted, or in which *HML* is deleted (see for examples Figure 5.5F and Figure 5.9B, data not shown).

If mating-type switching and insensitivity to α factor were the only reason for checkpoint activation in strains containing *MATHOcs* and *HML*, a DSB at *MAT* should be sufficient for checkpoint activation if *HML* is present. However, this was found not to be the case (Figure 5.8A). The reason for this is not clear at present and more detailed analysis will be required to resolve this issue.

A break at *MAT* was stronger in activating Rad53 than a DSB at a different site, even when cells were arrested in G2/M (Figure 5.8). At this stage, mating-type switching cannot be envisaged to affect checkpoint activation and cell cycle arrest. Therefore, recombination intermediates, such as the one described in Figure 5.9, may contribute to checkpoint activation.

5.2.7 Cln-CDK can support checkpoint activation

In previous studies, the role of CDK in checkpoint activation in response to DSB damage had been addressed by inactivation of CDK in G2/M arrested cells (Aylon et al., 2004; Ira et al., 2004). At this stage, only Clb-type cyclins are available for binding Cdc28 (Nasmyth, 1996). It was thus concluded that checkpoint activation specifically required Clb-CDK. However, these experiments did not address whether Cln-CDK can support checkpoint activation in response to DSBs as well.

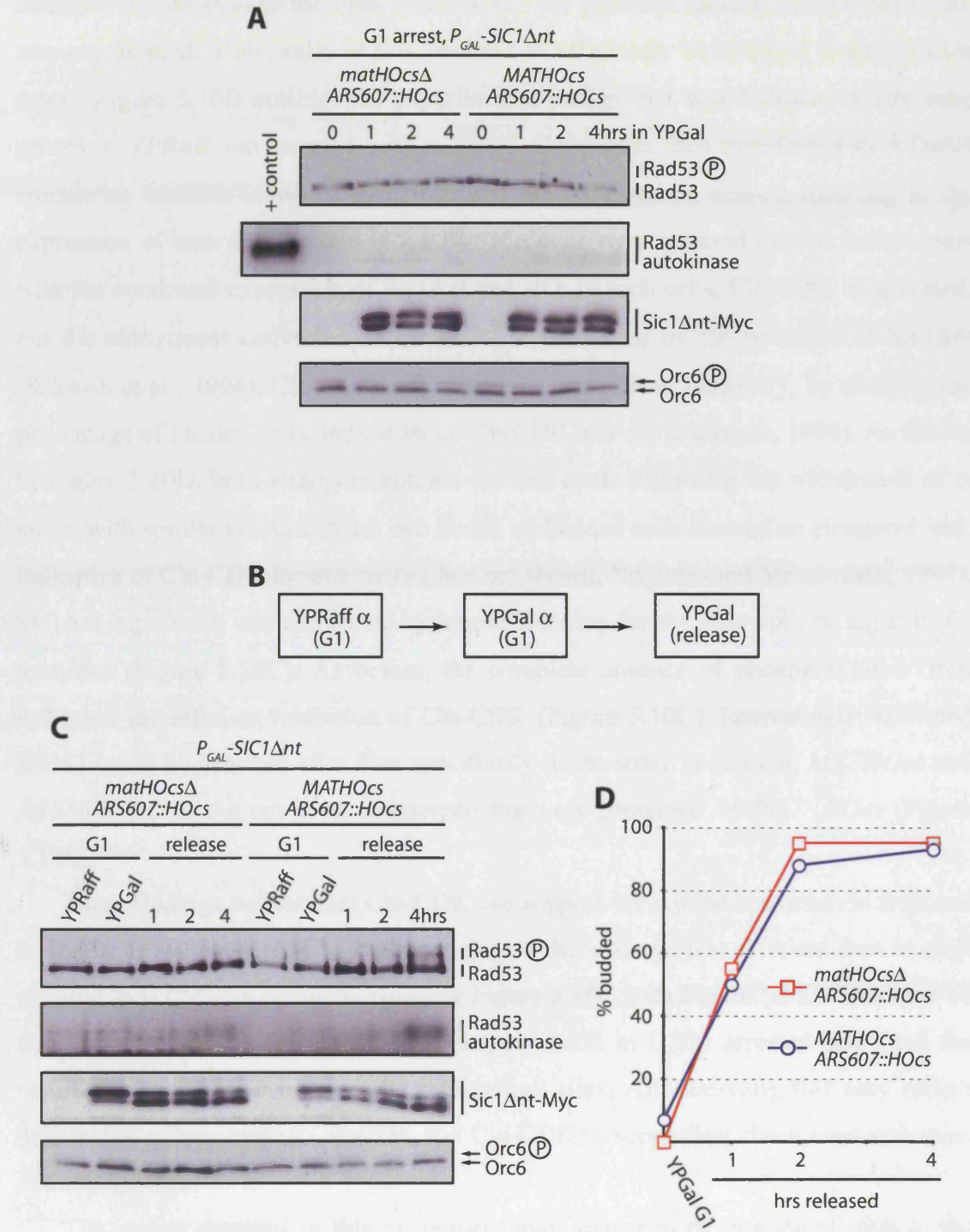

Figure 5.10: Characterisation of the effect of Clb-CDK inhibition on checkpoint activation. **A:** Cells of strain YCZ180 (*matHOcsΔ ARS607::HOcs* P_{GAL}*-SIC1Δnt bar1Δ hmrΔ*) and YCZ186 (*MATHOcs ARS607::HOcs* P_{GAL}*-SIC1Δnt bar1Δ hmrΔ*) grown in YPRaff and arrested in G1 with α factor. Cells were then transferred to α factor-containing YPGal medium to induce expression of *SIC1Δnt*. **B-D:** Cells of strain YCZ189 (*matHOcsΔ ARS607::HOcs* P_{GAL}*-SIC1Δnt hmrΔ*) and strain YCZ190 (*MATHOcs ARS607::HOcs* P_{GAL}*-SIC1Δnt hmrΔ*) were grown in YPRaff and arrested in G1 with α factor. Cells were then transferred to YPGal in the presence of α factor to induce expression of *SIC1Δnt* for 1hr. Cells were then released from G1 arrest.

As before, strains expressing Sic1Δnt were used to address this question. These strains were identical to the ones described in the previous section, except that *BAR1* was not deleted. Thus, cells of this strains can efficiently be released from α factor arrest. Figure 5.10B outlines the experimental design that was followed. Cells were grown in YPRaff and arrested with α factor. Cells were then transferred to α factor containing medium in which galactose was the only carbon source, resulting in the expression of both Sic1Δnt and HO. After 1hr, cells were released from α factor arrest with the continued expression of Sic1Δnt and HO. In such cells, Cln-CDK is activated, but the subsequent activation of Clb-CDK is prevented by the presence of Sic1Δnt (Schwob et al., 1994). Cln-CDK activation was determined indirectly, by charting the percentage of budded cells, indicative of Cln-CDK activity (Nasmyth, 1996). As shown in Figure 5.10D, both strains re-entered the cell cycle following the withdrawal of α factor with similar kinetics. After two hours, all budded cells showed an elongated bud, indicative of Cln-CDK hyperactivity (data not shown, Nugroho and Mendenhall, 1994). Sic1Δnt expression was confirmed by immunoblotting for the Myc-eptiope tag at its C-terminus (Figure 5.10C). As before, the complete absence of phosphorylated Orc6 indicated the efficient inhibition of Clb-CDK (Figure 5.10C). Interestingly, activated Rad53 could be detected after 4hrs specifically in the strain containing *MATHOcs* and *ARS607::HOcs*, but not in its counterpart that only contained *ARS607::HOcs* (Figure 5.10C).

These findings suggest that Cln-CDK can support checkpoint activation in response to DSBs. However, Rad53 activation appeared delayed and less efficient than in cells arrested in G2/M (for example, compare Figure 5.10C with Figure 5.5E). This may be due to the presence of a replicated sister chromatid in G2/M arrested cells, and the resulting two-fold increase in HO recognition sites. Alternatively, this may reflect differential efficiencies of Clb-CDK and Cln-CDK in supporting checkpoint activation to DSB damage.

The results obtained in this experiment may appear to be in contradiction to the results described in the previous section. If Cln-CDK can support checkpoint activation, why was activated Rad53 not observed in the previous experiment, when have switched mating type but were arrested due to overexpression of Sic1Δnt? In the experiment described in this section, the whole population of cells is released from α factor arrest and allowed to activate Cln-CDK. However, in the experiment from the previous section, only the subpopulation of cells that have switched (probably no more than

~15%) escape from α factor arrest and contain active Cln-CDK. Therefore, the lower efficiency of Cln-CDK to support checkpoint activation, in combination with the low number of cells that have escaped from the G1 arrest, may prevent the detection of activated Rad53 in the previous experiment.

5.2.8 Checkpoint activation and DSB resection are dose-dependent processes in G1

In a situation where both *HMR* and *HML* are deleted, two DSBs, one at *MAT* and one at *ARS607*, are insufficient for checkpoint activation in G1 (see above). Moreover, the formation of an additional DSB, by insertion of an HOcs at the *trp1* locus, did not result in detectable Rad53 activation in G1 arrested cells (data not shown). However, in strains that contained four HO recognition sites (*MATHOcs ARS607::HOcs trp1Δ::HOcs leu2Δ::HOcs*), activated Rad53 was detected in G1 arrested cells (Figure 5.11A). Since *HML* and *HMR* were deleted in this strain, checkpoint activation was not due to mating-type switching and subsequent insensitivity to α factor. Therefore, checkpoint activation in response to DSBs is possible in G1 in a dose-dependent manner.

Checkpoint activation after DSB formation may also have an element of dose dependency in G2/M. Rad53 activation appeared to be quicker when more breaks were induced (compare the 1hr time point in 1cs and 4cs strains in Figure 5.11A). Furthermore, virtually all Rad53 was hyperphosphorylated after 2hrs in the 4cs strain, whereas a large fraction of Rad53 molecules remained in the fast-migrating, hypo-phosphorylated, form in the 1cs strain (Figure 5.11A).

In addition to checkpoint activation, DSB resection was followed in this experiment (Figure 5.11B-F). A large increase in ssDNA formation was detected in G1 arrested cells of the 4cs strain when compared to their 1cs strain counterparts (Figure 5.11D). Similar to what was observed in the *dnl4Δ* strain arrested in G1 (see above), resection was specifically increased close to the DSB in the 4cs strain arrested in G2/M (0.3kb amplicon), but not further away from the break (Figure 5.11D). However, even at the site closest to the DSB, resection did not reach levels comparable to G2/M arrested cells (Figure 5.11B and F). Resection was also increased in G2/M arrested cells of the 4cs strain when compared to the 1cs strain (Figure 5.11E). Again, this effect was only apparent at the site closest to the DSB.

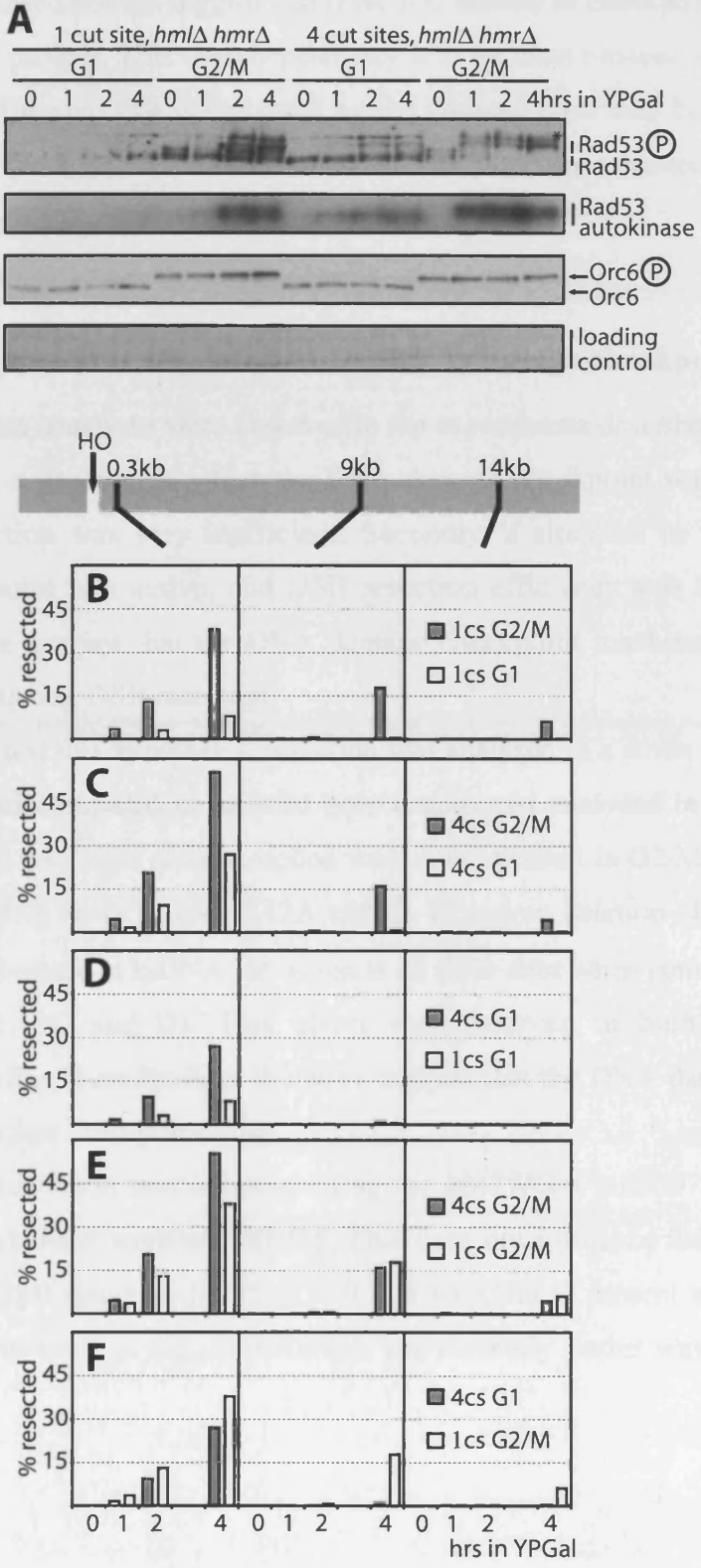

Figure 5.11: Checkpoint activation and DSB-resection are dose-dependent processes in G1. Cells of strains YCZ173 (1cs, *ARS607::HOcs matHOcsΔ hmlΔ hmrΔ*) and YCZ172 (2cs, *ARS607::HOcs hmlΔ hmrΔ*) were grown as described in Figure 5.3. **A:** TCA extracts were used for immunoblotting with the indicated antibodies and for Rad53 autokinase analysis. Ponceau-S staining was used as loading control. **B-F:** Resection at the DSB close to ARS607. Comparisons between the indicated strains and cell-cycle stages are shown. 1cs, one HO cut site; 4cs, four HO cut sites.

Together, these findings suggest that resection, similar to checkpoint activation, is a dose-dependent process. This dose dependency is at its most obvious at the G1 stage of the cell cycle. The step that is regulated by the damage dose may be the initiation of resection, since the dose-dependent increase in resection was confined to regions close to the broken ends.

5.2.9 DSB resection is regulated by the DNA damage checkpoint

Two different situations were observed in the experiments described in the previous section. Firstly, a situation in which the DNA damage checkpoint was inactive in G1, and DSB resection was very inefficient. Secondly, a situation in which the DNA damage checkpoint was active, and DSB resection efficiency was increased. These results therefore suggest that the DNA damage checkpoint machinery itself may be involved in regulating DSB resection.

To directly test this hypothesis, resection was analysed in a strain in which *RAD53* was deleted, and compared to its wild type counterpart analysed in parallel (Figure 5.12). Similar to wild type cells, resection was more efficient in G2/M cells than in G1 cells in the *rad53Δ* strain (Figure 5.12A and B). However, deletion of *RAD53* resulted in a ~2-4 fold decrease in ssDNA formation at all three sites when compared to the wild type (Figure 5.12C and D). This effect was observed in both G1 and G2/M synchronised cells. These findings therefore suggest that the DNA damage checkpoint does indeed regulate DSB processing.

However, this result was obtained using the *MATHOcs ARS607::HOcs* strain in which *HML* and *HMR* were not deleted. This does not influence the conclusion that Rad53 affects DSB resection in G2/M, but it is not clear at present whether a similar mechanism is at work in G1. Experiments are currently under way to address this question.

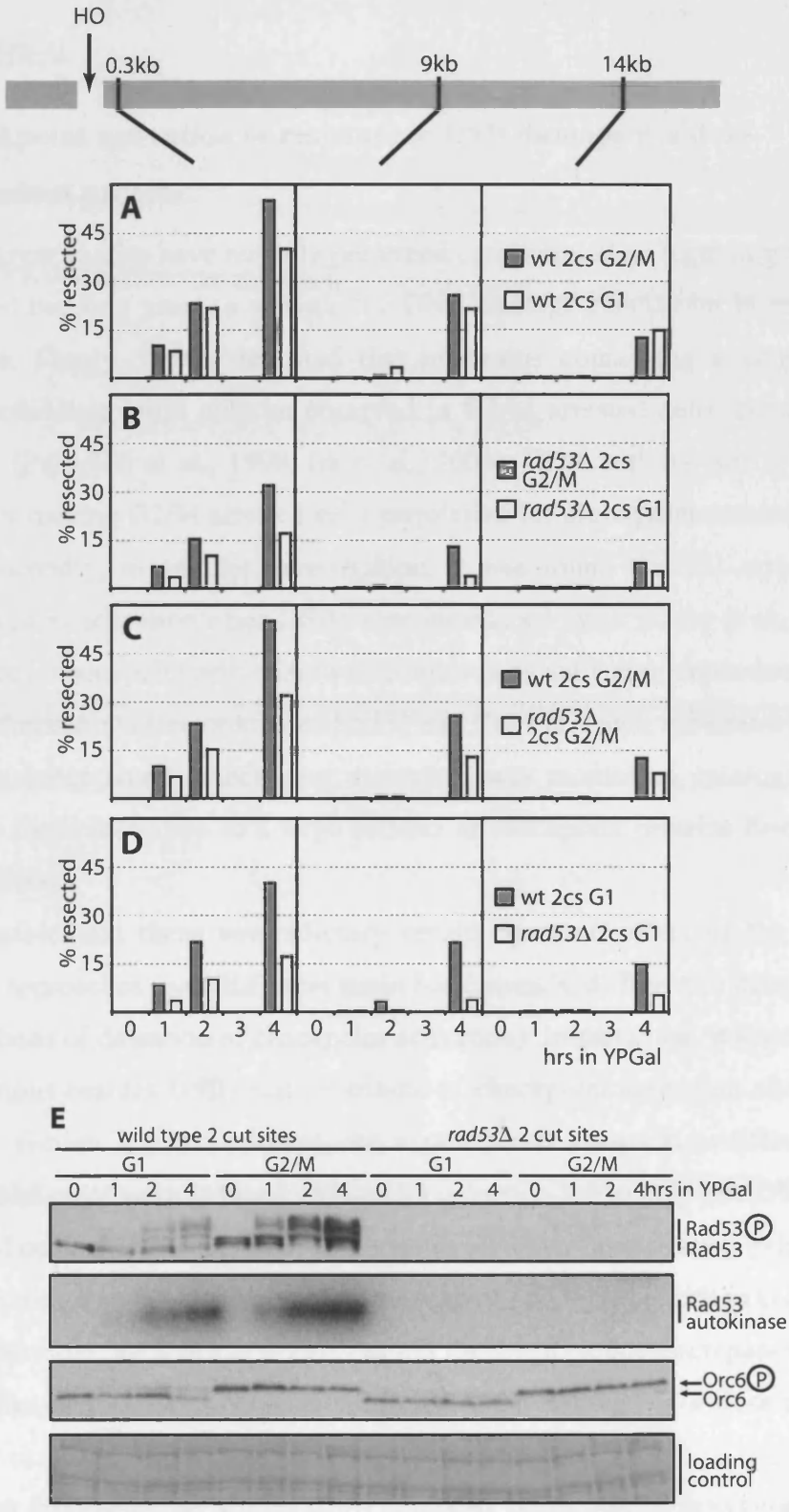

Figure 5.12: DSB resection may be regulated by the DNA damage checkpoint. Cells of strain YCZ64 (wild type) and YCZ134 (*rad53*Δ) were grown as described in Figure 5.3. **A-D:** Resection at *ARS607::HOcs*. The graphs show comparisons between the indicated strains and cell cycle stages. 2cs, two HOcs. **E:** TCA exracts were used for immunoblotting and Rad53 autokinase assay. Ponceau-S staining was used as loading control.

5.3 Discussion

5.3.1 Checkpoint activation in response to DSB damage is a dose-dependent process

Two different studies have recently presented conflicting data regarding the ability of G1 arrested budding yeast to activate the DNA damage checkpoint in response to DSB damage. Firstly, it was reported that in strains containing a single HOcs, checkpoint activation could only be observed in G2/M arrested cells, but not in G1 arrested cells (Pellicioli et al., 1999; Ira et al., 2004). CDK activity was found to be responsible for making G2/M arrested cells permissive for checkpoint activation (Ira et al., 2004). Secondly, in another investigation, it was found that G1 arrested cells showed checkpoint activation when DSBs were introduced by IR (Lisby et al., 2004). In the former study, checkpoint activation was monitored by activation-dependent mobility shifts of the checkpoint effector kinases Rad53 and Chk1 and their substrates (Ira et al., 2004). In the latter study, checkpoint activation was monitored cytologically, by analysing the focus formation of a large number of checkpoint proteins fused to GFP (Lisby et al., 2004).

It is possible that these contradictory results were an effect of the different experimental approaches used (different strain backgrounds, different sources of DSBs, different methods of detection of checkpoint activation). In particular, it is conceivable that other lesions besides DSBs can contribute to checkpoint activation after IR (see Introduction, section 1.2.1). However, the experimental setups also differed in the numbers of DSBs that were induced. While HO induction led to only one DSB formed in G1 arrested cells, the IR doses that were used in the other investigation (~100Gy) are predicted to have led to the formation of an average of ~3 DSBs per cell in G1 (Lisby et al., 2004). Therefore, an alternative explanation for the apparent discrepancy between the two studies is that checkpoint activation to DSB damage is a dose-dependent process.

Indeed, by increasing the number of HO-induced DSBs, Rad53 activation could be induced in G1 arrested cells (Figure 5.11A). Therefore, G1 arrested cells are permissive for checkpoint activation in response to DSBs in G1. Different DSB doses appear to be required for checkpoint activation in G1 versus in G2/M cells, since strains containing only two DSBs showed activated Rad53 after HO induction in G2/M, whereas four breaks were required in G1 (Figure 5.11A). However, in G2/M arrested cells, DSB-

dependent checkpoint activation appears to be dose dependent as well. When more breaks were formed, Rad53 activation was faster and reached apparent completion at steady-state levels (Figure 5.11A). Since cells arrested in G2/M by nocodazole treatment contain replicated chromosomes, two DSBs is the minimal amount that can thus be induced by HO. Although often mentioned in the literature, it is therefore not clear whether a single DSB is sufficient for activating the DNA damage checkpoint. Similar to what is here shown for DSBs, other kinds of DNA damage, such as that induced by MMS and UV, are dose-dependent in their elicited checkpoint responses (see for examples Tercero et al., 2003; Zhang et al., 2003).

5.3.2 DSBs are not frequently processed into long tracts of ssDNA

Previous studies by other groups have provided evidence that DSB resection is a synchronous and efficient process that occurs at a rate of ~4kb/hr (Fishman-Lobell et al., 1992; Lee et al., 1998; Vaze et al., 2002). This rate of DSB processing was estimated by an indirect assay (Fishman-Lobell et al., 1992; Vaze et al., 2002). An HOcs was placed between two direct repeats, and the time was measured that was required for single strand annealing to occur (see section 1.2.3.5). Increasing the distance between the two repeats by ~4kb resulted in a delay by ~1hr (Fishman-Lobell et al., 1992; Vaze et al., 2002). The authors thus concluded that the DSB processing nucleases required ~1hr to resect 4kb.

In contrast, the quantification of ssDNA formation presented in this study did not support such high efficiencies of resection. Some molecules may indeed be processed with high resection rates, since ssDNA was detected in G2/M arrested cells at a site ~14kb distal from the DSB after 4hrs (see for example Figure 5.3C and Figure 5.11B). However, this happened only in a low percentage of cases (≤10%). Even at a site very close to the DSB (0.3kb), ssDNA formation only reached ~50% after 4hrs. Thus, in the majority of cases, resection occurred with low rates. Two situations may be able to explain the discrepancy between these results and the ones described earlier (Fishman-Lobell et al., 1992; Lee et al., 1998; Vaze et al., 2002).

Firstly, most models for 5'-3' resection predict the function of an exonuclease that degrades the 5' strand (see section 1.2.3.6 for a detailed description of 5'-3' resection). However, the enzymes that mediate this process have not yet been clearly identified. An alternative possibility is that resection is mediated by the action of an unidentified helicase together with a ssDNA-specific endonuclease. In such a model, ssDNA could

be available for SSA without requiring the degradation of the 5' strand (see Figure 1.7). Since all physical assays for the detection of ssDNA at DSBs, including the one presented in this study, require one of the strands to be degraded, these regions of ssDNA *in vivo* would not be detectable *in vitro*.

Secondly, a Rad52-dependent pathway for the repair of DSBs has recently been described that occurred in the absence of the RecA homologues Rad51 and Dmc1 in meiotic cells (Henry et al., 2006). These DSBs were able to recombine with internal chromosomal regions, apparently independently of ssDNA formation at the invaded locus. Recombination occurred at regions with limited homology to the DSB sites. These findings thus suggest the existence of novel recombination pathways that only require one of the ends to be resected. In the SSA assay that was used to determine the time required for resection, one of the repeats was very close to the DSB, while the distance between the DSB and the repeat on the other side was increased (Vaze et al., 2002). Thus, only the repeat close to the DSB would have to be resected if similar mechanisms were at work in vegetative cells.

In *S. cerevisiae* there are only ~150bp of homology between *MAT* and *HML/HMR* (Haber, 2002). Yet, mating-type switching is an extremely efficient recombination process (Haber, 2002). Therefore, extended resection over many kilobases does probably not represent a physiological requirement for HR.

Recently, a quantitative assay for the detection of ssDNA at eroded *cdc13-1* telomeres was presented (Booth et al., 2001; Maringele and Lydall, 2002, see sections 1.2.3.3 and 1.2.3.6). This assay showed that such telomeres were resected with rates comparable to the ones reported for DSB resection in this study (Booth et al., 2001; Maringele and Lydall, 2002). As outlined in the Introduction, processes occurring at unprotected telomeres may not directly relate to processes occurring at proper DSBs (see section 1.2.3.3 and 1.2.3.6). However, to date, this represents the only precedent in the literature for quantified 5'-3' resection.

5.3.3 Checkpoint activation does not correlate with long resection tracts

In cases in which DSBs cannot be repaired due to the absence of homologous donor regions and/or due to the continued expression of HO, checkpoint activation can be observed after ~1-2hrs (Pellicioli et al., 1999, Figure 5.3A and Figure 5.11A). Due to the estimated resection rates described above, it is widely believed that long tracts of

ssDNA (at least 4kb at each end of a DSB) are required for checkpoint activation (Vaze et al., 2002; Zou and Elledge, 2003). However, the quantifications presented in this study indicate much less ssDNA to be generated (see above). Even after 4hrs, when the majority of cells show checkpoint activation (Figure 5.3A and B, Figure 5.11A), only ~50% of the breaks were resected up to 0.3kb (Figure 5.3C and Figure 5.11B). Therefore, long tracts of resection do not seem to correlate with checkpoint activation.

These findings do not allow conclusions regarding the absolute requirement for ssDNA for checkpoint activation. However, they indicate that if DSB resection is required for checkpoint activation, less resection than previously estimated appears to be sufficient. Alternatively, if ssDNA at a DSB were generated by helicase/endonuclease activity (see above), large regions of ssDNA could be generated that would not be detected in this assay. Further studies will be required to clarify this issue.

5.3.4 New insights into the CDK regulation of resection and DNA damage checkpoint activation

Previous studies have analysed the influence of CDK inhibition on DSB resection and checkpoint activation in cells arrested in mitosis by treatment with nocodazole (Aylon et al., 2004; Ira et al., 2004). In these studies, it was found that inhibition of Clb-CDK by overexpression of the Clb-CDK inhibitor Sic1 (Schwob et al., 1994) compromised DSB resection and checkpoint activation. It was therefore concluded that Clb-CDK activity is required for both DSB resection and checkpoint activation in response to DSB damage. However, these studies did not address whether Cln-CDK was able to support either of the two processes.

Here, evidence was presented suggesting that checkpoint activation in response to DSB damage is possible in the presence of only Cln-CDK (Figure 5.10D). However, checkpoint activation required the formation of at least two DSBs (Figure 5.10D). In addition, Rad53 activation was delayed and less efficient when compared to a situation in G2/M when Clb-CDK is active and an equal number of DSBs was induced (compare Figure 5.10D and Figure 5.11A). This suggests that Cln-CDK is less efficient in supporting checkpoint activation than Clb-CDK. Since the strains that were used contained a wild type *HML* locus (although *HMR* was deleted), aborted recombination intermediates may also contribute to checkpoint activation in this case (see section 5.2.6). However, although mating-type switching may happen in such cells, this is not

likely to have an influence on checkpoint activation. Cells were only held in α factor arrest at the initial stages of the experiment and during the remainder of the experiment cell cycle arrest was due to Sic1, and thus independent of mating type. Therefore, insensitivity to α factor arrest is not expected to be an issue in this experiment.

It is not known how CDKs regulate checkpoint activation and DSB resection. Since resection efficiencies and checkpoint activation strength usually correlate (see Chapter 1, Introduction), the simplest explanation is that CDKs regulate checkpoint activation by regulating DSB resection (Ira et al., 2004). How is such regulation achieved? Two different mechanisms are possible that are not necessarily exclusive. Firstly, CDKs might regulate DSB resection by increasing the chance of the initiation of resection. Secondly, CDKs might control the rate of resection, allowing longer tracts of the 5' strand to be degraded once initiated.

It has been shown that NHEJ is inhibitory to DSB resection (Lee et al., 1998, see above). Furthermore, NHEJ is under negative control by CDK (Frank-Vaillant and Marcand, 2002; Ira et al., 2004). Therefore, it is possible that CDKs stimulate resection by downregulating NHEJ. Interestingly, the deletion of *DNL4*, the ligase specific for NHEJ (Schar et al., 1997; Teo and Jackson, 1997; Wilson et al., 1997), resulted in a dramatic increase in ssDNA formation in G1 arrested cells (Figure 5.7B and D). This effect was specific for the site closest to the DSB (0.3kb), where resection was increased to levels identical to G2/M arrested cells. At the other two sites (9kb and 14kb removed from the break), resection was only slightly increased (Figure 5.7B, D and E). In contrast, in G2/M cells, deletion of *DNL4* resulted in only a mild increase in resection. A similar increase was, however, observed at all three sites (Figure 5.7C). These findings suggest that CDKs stimulate resection by at least two different mechanisms: firstly, by downregulating NHEJ, and secondly, by increasing the rate of resection.

What are the phosphorylation targets of CDK in this process? With the exception of Rad50, all proteins that are involved in NHEJ contain CDK phosphorylation consensus sites, and are thus possible candidates for CDK regulation (data not shown). However, only Xrs2 has so far been shown to be a phosphoprotein *in vivo* (Usui et al., 1998; D'Amours and Jackson, 2001). Unfortunately, it is not known which kinase is responsible for phosphorylation of Xrs2, or indeed whether this phosphorylation is absent in G1. Furthermore, the biological significance of Xrs2 phosphorylation has not

been addressed. It is therefore not clear whether CDK phosphorylation of Xrs2 or other NHEJ proteins represents a mechanism regulating NHEJ and resection.

Recently, an attempt was made to characterise the *in vivo* targets of CDK in yeast (Ubersax et al., 2003). Interestingly, two potential nucleases were identified as substrates of CDK, Yen1 and Dna2. This makes them candidates for being involved in DSB processing. However, preliminary results suggest that deletion of *YEN1* does not affect ssDNA formation at *ARS607::HOcs* (data not shown). Thus, Yen1 is not likely to be a major factor in DSB resection. Work on *DNA2* is complicated by the fact that it is required for Okazaki fragment maturation (reviewed in Hubscher and Seo, 2001) and thus essential for viability (Budd and Campbell, 1995). Therefore, mutations in *DNA2* may not have been picked up in screens for recombination mutants. However, hypomorphic mutations of *DNA2* cause sensitivity to DNA damaging agents (Budd and Campbell, 2000). Importantly, Dna2 contains both helicase and endonuclease activities (Budd et al., 1995; Budd et al., 2000). Dna2 is thus a prime candidate for being involved in DSB resection if resection involved concerted helicase/endonuclease activity (see above). Further studies will be required to determine the factors that are regulated by CDK to stimulate DSB resection.

5.3.5 The DNA damage checkpoint machinery regulates DSB processing

The results presented in this study show that checkpoint activation in response to DSB damage is a dose-dependent process, especially in G1 (Figure 5.11A). In a similar manner, DSB resection was also found to be dose dependent (Figure 5.11B-F). These findings raised the possibility that some aspect of DSB resection was under checkpoint control. Indeed, deletion of *RAD53* resulted in large reduction in ssDNA formation in G2/M at all three tested loci (Figure 5.12C). Deletion of *RAD53* also caused strongly reduced ssDNA formation in G1 (Figure 5.12D). Unfortunately, the results obtained with the G1 arrested population are somewhat ambiguous due to the presence of the silent mating type loci in the strain used. Thus, cells have the possibility of switching mating type and leaking out of the G1 arrest induced by α factor (see above).

It will be of interest to determine whether the Rad53-dependent stimulation of DSB resection is dependent on its prior activation by the DNA damage checkpoint machinery. Interestingly, preliminary data indicates that deletion of *MEC1*, which is required for Rad53 activation (see Chapter 1, Introduction), results in similar resection defects as deletion of *RAD53* (data not shown). Therefore, it is very likely that Rad53

has to be activated by upstream factors in the DNA damage checkpoint machinery in order to stimulate ssDNA formation.

In contrast to G1 arrested cells containing only one DSB, cells with four DSBs contain activated Rad53 (see above, Figure 5.11A). This situation can therefore be used to distinguish between checkpoint activation dependent and checkpoint activation independent effects of Rad53 on DSB resection.

The finding that resection is checkpoint-regulated – and thus a dose dependent process – may explain another discrepancy between the two studies mentioned at the beginning of this discussion (see section 5.3.1). Ira et al. (2004) have found that a DSB induced by HO in G1 arrested cells is resected with very poor efficiencies. Similar results were observed in this study (Figure 5.3A and Figure 5.11A). In contrast, the other report (Lisby et al., 2004) found that Rpa1 readily formed foci in G1 cells after IR treatment, indicating that DSBs were resected. It is possible that IR-induced lesions other than DSBs are responsible for this inconsistency. However, as before, the results presented here suggest that differences in the DSB dose can sufficiently explain the conflicting results.

What is the biological significance of a mechanism in which an activated DNA damage checkpoint stimulates the formation of ssDNA at DSBs? In a case in which a DSB can be repaired by HR, checkpoint activation is not observed (Pellicioli et al., 1999). Therefore, checkpoint activation after induction of a low number of DSBs only occurs when the breaks cannot be repaired. Checkpoint activation requires ~1-2hrs (see for example Figure 5.11A), at which point ends are already processed (Frank-Vaillant and Marcand, 2002). Processed ends efficiently rule out repair by NHEJ (Frank-Vaillant and Marcand, 2002; Daley and Wilson, 2005). Therefore, at this point, DSB repair by conventional mechanisms is not possible anymore. Increasing ssDNA formation at these breaks can serve a two-fold purpose (Figure 5.13). Firstly, this may represent a positive feedback loop in checkpoint signalling and reinforce the arrested state. Thus, cells could make sure that stochastic inactivation of the checkpoint and re-entry into the cell cycle is prevented. Secondly, increased resection would improve the chances of uncovering homologies between the ends of a DSB, such as transposons and retroelements. Such uncovered regions of homology could then be used for repair by single strand annealing.

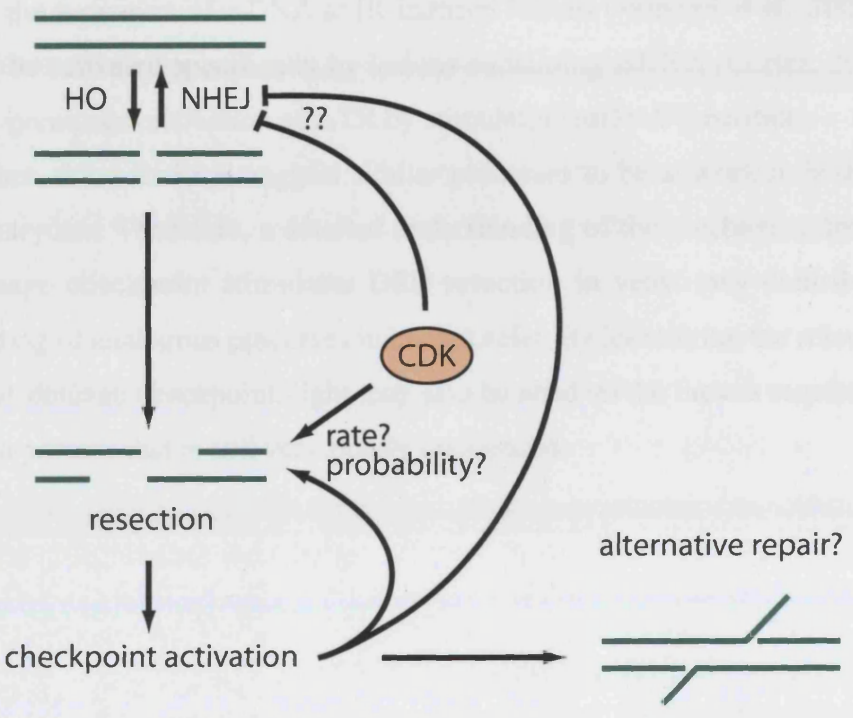

Figure 5.13: Model for the regulation of DSB processing. A DSB induced by HO can be directly religated by NHEJ. Due to the continued expression of HO in the experimental system used here, all religated breaks will again be cleaved soon after. This process will go back and forth until a break undergoes 5'-3' resection, at which point it will not be a substrate for NHEJ anymore. If the DSB dose is high enough and/or enough ssDNA is generated, DNA damage checkpoint activation ensues. This results in a stimulation of DSB resection by as yet unknown mechanisms. Two consequences are hypothesised to be the outcome. Firstly, in a positive feedback loop, checkpoint activation is reinforced by the additional ssDNA formation. Secondly, homologous regions between two ends can be used for alternative repair such as SSA.
In addition to the DNA damage checkpoint, CDKs regulate DSB processing. However, the mechanistic basis for this process is poorly understood.

A situation in which DNA damage checkpoint proteins regulate DSB processing as part of a positive feedback loop is not without precedent. Recently, it was shown that ATM is required for the activation of ATR after low doses of IR in human cells (Jazayeri et al., 2006). Furthermore, evidence was presented indicating that ATM stimulates the formation of ssDNA at IR-induced lesions (Jazayeri et al., 2006). ATR is thought to be activated specifically by lesions containing ssDNA (Cortez, 2005). Thus, ATM may permit the activation of ATR by stimulating ssDNA formation.

Together, these findings suggest similar processes to be at work in both yeast and higher eukaryotes. Therefore, a detailed understanding of the mechanism by which the DNA damage checkpoint stimulates DSB resection in yeast may contribute to our understanding of analogous processes in human cells. By identifying the relevant targets of the DNA damage checkpoint, light may also be shed on the factors required for DSB resection, a process that is still very poorly understood.

6 Conclusions

The maintenance of genomic stability is essential for viability. Therefore, sophisticated repair mechanisms have evolved to counteract DNA lesions. However, if lesions are not efficiently and quickly repaired, cells respond by activating a signalling cascade known as the DNA damage checkpoint machinery. This ultimately results in a variety of outcomes, including cell cycle arrest, the stabilisation of stalled replication forks, and the stimulation of repair processes. While the majority of the key players in checkpoint signalling are likely to be known, only limited understanding exists of the initial steps of damage recognition by the checkpoint machinery. Over the past years, evidence has accumulated supporting the idea that ssDNA is a key component in checkpoint activation. The investigations presented here were performed to gain more insight into the connection between ssDNA and DNA damage checkpoint activation. Three different approaches were taken.

Firstly, an attempt was made to generate ssDNA *in vivo* without generating strand breaks at the same time. It is not known whether ssDNA itself is sufficient for checkpoint activation because all checkpoint-inducing lesions contain strand breaks in addition to ssDNA. Therefore, in the study reported here, an attempt was made to induce the unwinding of a circular plasmid *in vivo*, thus generating only ssDNA while avoiding additional strand breaks. Two different enzymes, SV40 T-Ag and bacteriophage P4 gpα, were utilised to this end. Both enzymes encode both the origin recognition activity and replicative helicase in their respective replication systems (Fanning and Knippers, 1992; Ziegelin and Lanka, 1995). Subsequently, species-specific protein-protein interactions are required for replisome assembly in both systems (Brill and Stillman, 1989; Fanning and Knippers, 1992; Ziegelin and Lanka, 1995). Therefore, expression of these proteins in yeast cells harbouring plasmids containing their respective origins of replication should result in the unwinding of DNA, but not in the initiation of replication. However, no unwound DNA was detected after expression of either protein. Therefore, this approach did not prove successful.

Secondly, the effects of the degradation of RPA, the main single-stranded DNA binding complex in eukaryotes, was analysed. Several connections exist between checkpoint signalling and RPA (described in detail in the Introduction, Chapter 1). However, because all the three subunits of RPA are essential due to their requirement in

DNA replication (Brill and Stillman, 1991), analysis of null mutants has been impossible. A large number of hypomorphic mutants have been generated. However, no clear picture of the role of RPA in checkpoint signalling has emerged by using these (see Chapter 1, Introduction). In an attempt to generate mutants mimicking deletion mutants, temperature sensitive degron mutants were constructed for all three subunits of RPA in this study. In this system, the degradation of a protein of choice can be induced by temperature shift (Dohmen et al., 1994; Labib et al., 2000; Sanchez-Diaz et al., 2004). Induced degradation occurred to near-completion, and only a small fraction of the starting protein remained. Interestingly, cells with degraded RPA were able to finish bulk DNA replication. However, cells rapidly lost viability during replication and underwent a Rad9-dependent cell cycle arrest. These findings strongly indicate that replication with limiting amounts of RPA leads to the formation of irreversible DNA damage. Interestingly, checkpoint responses to replication stress appeared to remain intact after RPA degradation. However, degradation of RPA does not appear to result in a complete null phenotype, since cells were able to replicate most of their genome. Therefore, conclusions drawn from experiments carried out on these cells are not unambiguous. Nonetheless, these results raise the possibility of checkpoint activation pathways that are independent of long tracts of RPA-covered ssDNA.

Thirdly, a new assay, based on quantitative real-time PCR, was set up to quantify ssDNA formed at a site-specific DSB introduced by HO endonuclease. Using this assay, it was found that less ssDNA than previously estimated was generated. In G2/M arrested cells, even after 4hrs, only ~50% of the breaks were resected at a site that was just 300bp away from the DSB site. At this time, the majority of cells showed an activated DNA damage checkpoint. Therefore, these results again suggest that checkpoint activation is possible in the absence of long tracts of ssDNA. In the process of these investigations, it was also found that checkpoint activation to DSBs is a dose-dependent process. In G2/M arrested cells, increasing the amount of breaks resulted in faster and more quantitative activation of the downstream checkpoint kinase Rad53. Furthermore, in agreement with published results (Pellicioli et al., 1999), checkpoint activation was found not to be detectable when a low amount of DSBs was introduced in G1 arrested cells. However, after formation of at least four DSBs, checkpoint activation was detected in G1 arrested cells. These results therefore show that DNA damage checkpoint activation is possible in G1, but that higher doses are required than for checkpoint activation in G2/M. Interestingly, after the formation of a single DSB in

G1, ssDNA formation was found to be very inefficient, again in agreement with previously published results (Aylon et al., 2004; Ira et al., 2004). However, upon formation of a number of DSBs sufficient for checkpoint activation, the efficiency of resection was increased. These results suggested that the checkpoint itself might regulate DSB resection. Indeed, it was found that deletion of *RAD53* resulted in a reduction in ssDNA formation. The finding that both checkpoint activation and ssDNA were dose-dependent processes may also resolve a discrepancy between recently published studies which reported conflicting results regarding these issues (Aylon et al., 2004; Ira et al., 2004; Lisby et al., 2004).

In summary, the results presented here provide evidence that DNA damage checkpoint activation may occur independently of long tracts of RPA covered ssDNA. However, no conclusions regarding the absolute requirement for ssDNA in checkpoint activation can be drawn from the data. In addition, it is still not clear whether ssDNA can lead to checkpoint activation on its own. Further studies will be required to clarify this issue.

In the near future, experiments will be carried out to solve some of the questions raised by the studies presented here. The RPA-degron strains will be used to address whether degradation of RPA results in a deficiency in Okazaki fragment processing *in vivo*, as suggested by *in vitro* data (Bae et al., 2001). However, the main emphasis will be laid on further characterising the regulation of DSB resection. In particular, the checkpoint control of resection will be further analysed, and various checkpoint mutants will be compared. Furthermore, it will be determined, whether a single DSB is sufficient for checkpoint activation in G2/M. In the long term, it will be of interest to find the target proteins that are regulated by the DNA damage checkpoint to stimulate DSB resection. This may also provide valuable information about the enzymes that mediate general DSB processing. Lastly, it will be of interest to analyse replication in strains containing Rad53 activated by DSB damage in late G1. This system can be used to investigate the effects of the checkpoint response on DNA replication forks and origin firing in a situation in which fork progression is not affected by the checkpoint-inducing lesions.

Many fundamental cellular processes are well conserved in evolution. Recently, DSB-processing and checkpoint activation mechanisms reminiscent of the ones described here have been described in human cells (Jazayeri et al., 2006). In metazoans,

the DNA damage checkpoint and DNA repair are essential factors for genetic stability and in preventing tumour formation (Hoeijmakers, 2001; O'Driscoll and Jeggo, 2006). Therefore, the investigations presented here may also hold direct relevance for our understanding of these processes in human cells.

7 References

Adamczewski, J. P., Gannon, J. V., and Hunt, T. (1993). Simian virus 40 large T antigen associates with cyclin A and p33cdk2. J Virol *67*, 6551-6557.

Agarwal, R., Tang, Z., Yu, H., and Cohen-Fix, O. (2003). Two distinct pathways for inhibiting pds1 ubiquitination in response to DNA damage. J Biol Chem *278*, 45027-45033.

Alberghina, L., Rossi, R. L., Querin, L., Wanke, V., and Vanoni, M. (2004). A cell sizer network involving Cln3 and Far1 controls entrance into S phase in the mitotic cycle of budding yeast. J Cell Biol *167*, 433-443.

Alcasabas, A. A., Osborn, A. J., Bachant, J., Hu, F., Werler, P. J., Bousset, K., Furuya, K., Diffley, J. F., Carr, A. M., and Elledge, S. J. (2001). Mrc1 transduces signals of DNA replication stress to activate Rad53. Nat Cell Biol *3*, 958-965.

Alexiadis, V., Varga-Weisz, P. D., Bonte, E., Becker, P. B., and Gruss, C. (1998). In vitro chromatin remodelling by chromatin accessibility complex (CHRAC) at the SV40 origin of DNA replication. Embo J *17*, 3428-3438.

Amon, A., Surana, U., Muroff, I., and Nasmyth, K. (1992). Regulation of p34CDC28 tyrosine phosphorylation is not required for entry into mitosis in S. cerevisiae. Nature *355*, 368-371.

Antunez de Mayolo, A., Lisby, M., Erdeniz, N., Thybo, T., Mortensen, U. H., and Rothstein, R. (2006). Multiple start codons and phosphorylation result in discrete Rad52 protein species. Nucleic Acids Res *34*, 2587-2597.

Aparicio, O. M., Weinstein, D. M., and Bell, S. P. (1997). Components and dynamics of DNA replication complexes in S. cerevisiae: redistribution of MCM proteins and Cdc45p during S phase. Cell *91*, 59-69.

Aylon, Y., and Kupiec, M. (2003). The checkpoint protein Rad24 of Saccharomyces cerevisiae is involved in processing double-strand break ends and in recombination partner choice. Mol Cell Biol *23*, 6585-6596.

Aylon, Y., Liefshitz, B., and Kupiec, M. (2004). The CDK regulates repair of double-strand breaks by homologous recombination during the cell cycle. Embo J *23*, 4868-4875.

Bae, S. H., Bae, K. H., Kim, J. A., and Seo, Y. S. (2001). RPA governs endonuclease switching during processing of Okazaki fragments in eukaryotes. Nature *412*, 456-461.

Bahler, J., Wu, J. Q., Longtine, M. S., Shah, N. G., McKenzie, A., 3rd, Steever, A. B., Wach, A., Philippsen, P., and Pringle, J. R. (1998). Heterologous modules for efficient and versatile PCR-based gene targeting in Schizosaccharomyces pombe. Yeast *14*, 943-951.

Baker, T. A., Sekimizu, K., Funnell, B. E., and Kornberg, A. (1986). Extensive unwinding of the plasmid template during staged enzymatic initiation of DNA replication from the origin of the Escherichia coli chromosome. Cell *45*, 53-64.

Bakkenist, C. J., and Kastan, M. B. (2003). DNA damage activates ATM through intermolecular autophosphorylation and dimer dissociation. Nature *421*, 499-506.

Ball, H. L., Myers, J. S., and Cortez, D. (2005). ATRIP binding to replication protein A-single-stranded DNA promotes ATR-ATRIP localization but is dispensable for Chk1 phosphorylation. Mol Biol Cell *16*, 2372-2381.

Banecki, B., Kaguni, J. M., and Marszalek, J. (1998). Role of adenine nucleotides, molecular chaperones and chaperonins in stabilization of DnaA initiator protein of Escherichia coli. Biochim Biophys Acta *1442*, 39-48.

Bardin, A. J., and Amon, A. (2001). Men and sin: what's the difference? Nat Rev Mol Cell Biol *2*, 815-826.

Bartek, J., Falck, J., and Lukas, J. (2001). CHK2 kinase--a busy messenger. Nat Rev Mol Cell Biol *2*, 877-886.

Bashkirov, V. I., Bashkirova, E. V., Haghnazari, E., and Heyer, W. D. (2003). Direct kinase-to-kinase signaling mediated by the FHA phosphoprotein recognition domain of the Dun1 DNA damage checkpoint kinase. Mol Cell Biol *23*, 1441-1452.

Bates, A. D., and Maxwell, A. (1993). DNA topology (New York, IRL Press at Oxford University Press).

Baumer, M., Braus, G. H., and Irniger, S. (2000). Two different modes of cyclin clb2 proteolysis during mitosis in Saccharomyces cerevisiae. FEBS Lett *468*, 142-148.

Bell, S. P., and Dutta, A. (2002). DNA replication in eukaryotic cells. Annu Rev Biochem *71*, 333-374.

Belli, G., Gari, E., Piedrafita, L., Aldea, M., and Herrero, E. (1998). An activator/repressor dual system allows tight tetracycline-regulated gene expression in budding yeast. Nucleic Acids Res *26*, 942-947.

Bielinsky, A. K., and Gerbi, S. A. (1999). Chromosomal ARS1 has a single leading strand start site. Mol Cell *3*, 477-486.

Biswas, E. E., Chen, P. H., and Biswas, S. B. (2002). Modulation of enzymatic activities of Escherichia coli DnaB helicase by single-stranded DNA-binding proteins. Nucleic Acids Res *30*, 2809-2816.

Blankley, R. T., and Lydall, D. (2004). A domain of Rad9 specifically required for activation of Chk1 in budding yeast. J Cell Sci *117*, 601-608.

Blondel, M., Galan, J. M., Chi, Y., Lafourcade, C., Longaretti, C., Deshaies, R. J., and Peter, M. (2000). Nuclear-specific degradation of Far1 is controlled by the localization of the F-box protein Cdc4. Embo J *19*, 6085-6097.

Blow, J. J., and Dutta, A. (2005). Preventing re-replication of chromosomal DNA. Nat Rev Mol Cell Biol *6*, 476-486.

Bochkarev, A., Bochkareva, E., Frappier, L., and Edwards, A. M. (1999). The crystal structure of the complex of replication protein A subunits RPA32 and RPA14 reveals a mechanism for single-stranded DNA binding. Embo J *18*, 4498-4504.

Bochkarev, A., Pfuetzner, R. A., Edwards, A. M., and Frappier, L. (1997). Structure of the single-stranded-DNA-binding domain of replication protein A bound to DNA. Nature *385*, 176-181.

Boiteux, S., and Guillet, M. (2004). Abasic sites in DNA: repair and biological consequences in Saccharomyces cerevisiae. DNA Repair (Amst) *3*, 1-12.

Booth, C., Griffith, E., Brady, G., and Lydall, D. (2001). Quantitative amplification of single-stranded DNA (QAOS) demonstrates that cdc13-1 mutants generate ssDNA in a telomere to centromere direction. Nucleic Acids Res *29*, 4414-4422.

Boulton, S. J., and Jackson, S. P. (1996). Saccharomyces cerevisiae Ku70 potentiates illegitimate DNA double-strand break repair and serves as a barrier to error-prone DNA repair pathways. Embo J *15*, 5093-5103.

Boutros, R., Dozier, C., and Ducommun, B. (2006). The when and wheres of CDC25 phosphatases. Curr Opin Cell Biol *18*, 185-191.

Breeden, L. L. (2003). Periodic transcription: a cycle within a cycle. Curr Biol *13*, R31-38.

Briani, F., Deho, G., Forti, F., and Ghisotti, D. (2001). The plasmid status of satellite bacteriophage P4. Plasmid *45*, 1-17.

Brill, S. J., and Bastin-Shanower, S. (1998). Identification and characterization of the fourth single-stranded-DNA binding domain of replication protein A. Mol Cell Biol *18*, 7225-7234.

Brill, S. J., and Stillman, B. (1989). Yeast replication factor-A functions in the unwinding of the SV40 origin of DNA replication. Nature *342*, 92-95.

Brill, S. J., and Stillman, B. (1991). Replication factor-A from Saccharomyces cerevisiae is encoded by three essential genes coordinately expressed at S phase. Genes Dev *5*, 1589-1600.

Brush, G. S., Clifford, D. M., Marinco, S. M., and Bartrand, A. J. (2001). Replication protein A is sequentially phosphorylated during meiosis. Nucleic Acids Res *29*, 4808-4817.

Brush, G. S., and Kelly, T. J. (2000). Phosphorylation of the replication protein A large subunit in the Saccharomyces cerevisiae checkpoint response. Nucleic Acids Res *28*, 3725-3732.

Brush, G. S., Morrow, D. M., Hieter, P., and Kelly, T. J. (1996). The ATM homologue MEC1 is required for phosphorylation of replication protein A in yeast. Proc Natl Acad Sci U S A *93*, 15075-15080.

Bucking-Throm, E., Duntze, W., Hartwell, L. H., and Manney, T. R. (1973). Reversible arrest of haploid yeast cells in the initiation of DNA synthesis by a diffusible sex factor. Exp Cell Res *76*, 99-110.

Budd, M. E., and Campbell, J. L. (1995). A yeast gene required for DNA replication encodes a protein with homology to DNA helicases. Proc Natl Acad Sci U S A *92*, 7642-7646.

Budd, M. E., and Campbell, J. L. (2000). The pattern of sensitivity of yeast dna2 mutants to DNA damaging agents suggests a role in DSB and postreplication repair pathways. Mutat Res *459*, 173-186.

Budd, M. E., Choe, W., and Campbell, J. L. (2000). The nuclease activity of the yeast DNA2 protein, which is related to the RecB-like nucleases, is essential in vivo. J Biol Chem *275*, 16518-16529.

Budd, M. E., Choe, W. C., and Campbell, J. L. (1995). DNA2 encodes a DNA helicase essential for replication of eukaryotic chromosomes. J Biol Chem *270*, 26766-26769.

Byun, T. S., Pacek, M., Yee, M. C., Walter, J. C., and Cimprich, K. A. (2005). Functional uncoupling of MCM helicase and DNA polymerase activities activates the ATR-dependent checkpoint. Genes Dev *19*, 1040-1052.

Cannella, D., Roberts, J. M., and Fotedar, R. (1997). Association of cyclin A and cdk2 with SV40 DNA in replication initiation complexes is cell cycle dependent. Chromosoma *105*, 349-359.

Cao, L., Alani, E., and Kleckner, N. (1990). A pathway for generation and processing of double-strand breaks during meiotic recombination in S. cerevisiae. Cell *61*, 1089-1101.

Cary, R. B., Peterson, S. R., Wang, J., Bear, D. G., Bradbury, E. M., and Chen, D. J. (1997). DNA looping by Ku and the DNA-dependent protein kinase. Proc Natl Acad Sci U S A *94*, 4267-4272.

Chakravarthy, S., Park, Y. J., Chodaparambil, J., Edayathumangalam, R. S., and Luger, K. (2005). Structure and dynamic properties of nucleosome core particles. FEBS Lett *579*, 895-898.

Chan, R. K., and Otte, C. A. (1982). Physiological characterization of Saccharomyces cerevisiae mutants supersensitive to G1 arrest by a factor and alpha factor pheromones. Mol Cell Biol *2*, 21-29.

Chen, L., Trujillo, K., Ramos, W., Sung, P., and Tomkinson, A. E. (2001). Promotion of Dnl4-catalyzed DNA end-joining by the Rad50/Mre11/Xrs2 and Hdf1/Hdf2 complexes. Mol Cell *8*, 1105-1115.

Chen, L., Trujillo, K. M., Van Komen, S., Roh, D. H., Krejci, L., Lewis, L. K., Resnick, M. A., Sung, P., and Tomkinson, A. E. (2005). Effect of amino acid substitutions in the rad50 ATP binding domain on DNA double strand break repair in yeast. J Biol Chem *280*, 2620-2627.

Cheng, L., Hunke, L., and Hardy, C. F. (1998). Cell cycle regulation of the Saccharomyces cerevisiae polo-like kinase cdc5p. Mol Cell Biol *18*, 7360-7370.

Christianson, T. W., Sikorski, R. S., Dante, M., Shero, J. H., and Hieter, P. (1992). Multifunctional yeast high-copy-number shuttle vectors. Gene *110*, 119-122.

Clerici, M., Baldo, V., Mantiero, D., Lottersberger, F., Lucchini, G., and Longhese, M. P. (2004). A Tel1/MRX-dependent checkpoint inhibits the metaphase-to-anaphase transition after UV irradiation in the absence of Mec1. Mol Cell Biol *24*, 10126-10144.

Clerici, M., Mantiero, D., Lucchini, G., and Longhese, M. P. (2005). The Saccharomyces cerevisiae Sae2 protein promotes resection and bridging of double strand break ends. J Biol Chem *280*, 38631-38638.

Clerici, M., Mantiero, D., Lucchini, G., and Longhese, M. P. (2006). The Saccharomyces cerevisiae Sae2 protein negatively regulates DNA damage checkpoint signalling. EMBO Rep *7*, 212-218.

Clikeman, J. A., Khalsa, G. J., Barton, S. L., and Nickoloff, J. A. (2001). Homologous recombinational repair of double-strand breaks in yeast is enhanced by MAT heterozygosity through yKU-dependent and -independent mechanisms. Genetics *157*, 579-589.

Cohen-Fix, O., and Koshland, D. (1997). The anaphase inhibitor of Saccharomyces cerevisiae Pds1p is a target of the DNA damage checkpoint pathway. Proc Natl Acad Sci U S A *94*, 14361-14366.

Cortez, D. (2005). Unwind and slow down: checkpoint activation by helicase and polymerase uncoupling. Genes Dev *19*, 1007-1012.

Cortez, D., Guntuku, S., Qin, J., and Elledge, S. J. (2001). ATR and ATRIP: partners in checkpoint signaling. Science *294*, 1713-1716.

Costanzo, M., Nishikawa, J. L., Tang, X., Millman, J. S., Schub, O., Breitkreuz, K., Dewar, D., Rupes, I., Andrews, B., and Tyers, M. (2004). CDK activity antagonizes Whi5, an inhibitor of G1/S transcription in yeast. Cell *117*, 899-913.

Costanzo, V., and Gautier, J. (2003). Single-strand DNA gaps trigger an ATR- and Cdc7-dependent checkpoint. Cell Cycle *2*, 17.

Costanzo, V., Shechter, D., Lupardus, P. J., Cimprich, K. A., Gottesman, M., and Gautier, J. (2003). An ATR- and Cdc7-dependent DNA damage checkpoint that inhibits initiation of DNA replication. Mol Cell *11*, 203-213.

Cotta-Ramusino, C., Fachinetti, D., Lucca, C., Doksani, Y., Lopes, M., Sogo, J., and Foiani, M. (2005). Exo1 processes stalled replication forks and counteracts fork reversal in checkpoint-defective cells. Mol Cell *17*, 153-159.

Coverley, D., Kenny, M. K., Munn, M., Rupp, W. D., Lane, D. P., and Wood, R. D. (1991). Requirement for the replication protein SSB in human DNA excision repair. Nature *349*, 538-541.

Cox, M. M., Goodman, M. F., Kreuzer, K. N., Sherratt, D. J., Sandler, S. J., and Marians, K. J. (2000). The importance of repairing stalled replication forks. Nature *404*, 37-41.

D'Amours, D., and Amon, A. (2004). At the interface between signaling and executing anaphase--Cdc14 and the FEAR network. Genes Dev *18*, 2581-2595.

D'Amours, D., and Jackson, S. P. (2001). The yeast Xrs2 complex functions in S phase checkpoint regulation. Genes Dev *15*, 2238-2249.

D'Amours, D., and Jackson, S. P. (2002). The Mre11 complex: at the crossroads of dna repair and checkpoint signalling. Nat Rev Mol Cell Biol *3*, 317-327.

Daley, J. M., Palmbos, P. L., Wu, D., and Wilson, T. E. (2005). Nonhomologous end joining in yeast. Annu Rev Genet *39*, 431-451.

Daley, J. M., and Wilson, T. E. (2005). Rejoining of DNA double-strand breaks as a function of overhang length. Mol Cell Biol *25*, 896-906.

Davey, M. J., Jeruzalmi, D., Kuriyan, J., and O'Donnell, M. (2002). Motors and switches: AAA+ machines within the replisome. Nat Rev Mol Cell Biol *3*, 826-835.

de la Torre-Ruiz, M., and Lowndes, N. F. (2000). The Saccharomyces cerevisiae DNA damage checkpoint is required for efficient repair of double strand breaks by non-homologous end joining. FEBS Lett *467*, 311-315.

de la Torre-Ruiz, M. A., Green, C. M., and Lowndes, N. F. (1998). RAD9 and RAD24 define two additive, interacting branches of the DNA damage checkpoint pathway in budding yeast normally required for Rad53 modification and activation. Embo J *17*, 2687-2698.

Dean, F. B., Bullock, P., Murakami, Y., Wobbe, C. R., Weissbach, L., and Hurwitz, J. (1987). Simian virus 40 (SV40) DNA replication: SV40 large T antigen unwinds DNA containing the SV40 origin of replication. Proc Natl Acad Sci U S A *84*, 16-20.

Desany, B. A., Alcasabas, A. A., Bachant, J. B., and Elledge, S. J. (1998). Recovery from DNA replicational stress is the essential function of the S-phase checkpoint pathway. Genes Dev *12*, 2956-2970.

Desdouets, C., Santocanale, C., Drury, L. S., Perkins, G., Foiani, M., Plevani, P., and Diffley, J. F. (1998). Evidence for a Cdc6p-independent mitotic resetting event involving DNA polymerase alpha. Embo J *17*, 4139-4146.

Diaz Orejas, R., Ziegelin, G., Lurz, R., and Lanka, E. (1994). Phage P4 DNA replication in vitro. Nucleic Acids Res *22*, 2065-2070.

Diffley, J. F. (2004). Regulation of early events in chromosome replication. Curr Biol *14*, R778-786.

Diffley, J. F., Cocker, J. H., Dowell, S. J., and Rowley, A. (1994). Two steps in the assembly of complexes at yeast replication origins in vivo. Cell *78*, 303-316.

Diffley, J. F., and Labib, K. (2002). The chromosome replication cycle. J Cell Sci *115*, 869-872.

Dodson, G. E., Shi, Y., and Tibbetts, R. S. (2004). DNA replication defects, spontaneous DNA damage, and ATM-dependent checkpoint activation in replication protein A-deficient cells. J Biol Chem *279*, 34010-34014.

Dohmen, R. J., Wu, P., and Varshavsky, A. (1994). Heat-inducible degron: a method for constructing temperature-sensitive mutants. Science *263*, 1273-1276.

Donovan, S., and Diffley, J. F. (1996). Replication origins in eukaroytes. Curr Opin Genet Dev *6*, 203-207.

Donovan, S., Harwood, J., Drury, L. S., and Diffley, J. F. (1997). Cdc6p-dependent loading of Mcm proteins onto pre-replicative chromatin in budding yeast. Proc Natl Acad Sci U S A *94*, 5611-5616.

Douki, T., Court, M., Sauvaigo, S., Odin, F., and Cadet, J. (2000). Formation of the main UV-induced thymine dimeric lesions within isolated and cellular DNA as measured by high performance liquid chromatography-tandem mass spectrometry. J Biol Chem *275*, 11678-11685.

Downs, J. A., Lowndes, N. F., and Jackson, S. P. (2000). A role for Saccharomyces cerevisiae histone H2A in DNA repair. Nature *408*, 1001-1004.

Drablos, F., Feyzi, E., Aas, P. A., Vaagbo, C. B., Kavli, B., Bratlie, M. S., Pena-Diaz, J., Otterlei, M., Slupphaug, G., and Krokan, H. E. (2004). Alkylation damage in DNA and RNA--repair mechanisms and medical significance. DNA Repair (Amst) *3*, 1389-1407.

Drury, L. S., Perkins, G., and Diffley, J. F. (2000). The cyclin-dependent kinase Cdc28p regulates distinct modes of Cdc6p proteolysis during the budding yeast cell cycle. Curr Biol *10*, 231-240.

Dudasova, Z., Dudas, A., and Chovanec, M. (2004). Non-homologous end-joining factors of Saccharomyces cerevisiae. FEMS Microbiol Rev *28*, 581-601.

Duncker, B. P., Shimada, K., Tsai-Pflugfelder, M., Pasero, P., and Gasser, S. M. (2002). An N-terminal domain of Dbf4p mediates interaction with both origin recognition complex (ORC) and Rad53p and can deregulate late origin firing. Proc Natl Acad Sci U S A *99*, 16087-16092.

Duntze, W., Stotzler, D., Bucking-Throm, E., and Kalbitzer, S. (1973). Purification and partial characterization of -factor, a mating-type specific inhibitor of cell reproduction from Saccharomyces cerevisiae. Eur J Biochem *35*, 357-365.

Elford, H. L. (1968). Effect of hydroxyurea on ribonucleotide reductase. Biochem Biophys Res Commun *33*, 129-135.

Ellison, V., and Stillman, B. (2003). Biochemical characterization of DNA damage checkpoint complexes: clamp loader and clamp complexes with specificity for 5' recessed DNA. PLoS Biol *1*, E33.

Erdile, L. F., Heyer, W. D., Kolodner, R., and Kelly, T. J. (1991). Characterization of a cDNA encoding the 70-kDa single-stranded DNA-binding subunit of human replication protein A and the role of the protein in DNA replication. J Biol Chem *266*, 12090-12098.

Fairman, M. P., and Stillman, B. (1988). Cellular factors required for multiple stages of SV40 DNA replication in vitro. Embo J *7*, 1211-1218.

Falck, J., Coates, J., and Jackson, S. P. (2005). Conserved modes of recruitment of ATM, ATR and DNA-PKcs to sites of DNA damage. Nature *434*, 605-611.

Fanning, E., and Knippers, R. (1992). Structure and function of simian virus 40 large tumor antigen. Annu Rev Biochem *61*, 55-85.

Feng, W., Collingwood, D., Boeck, M. E., Fox, L. A., Alvino, G. M., Fangman, W. L., Raghuraman, M. K., and Brewer, B. J. (2006). Genomic mapping of single-stranded DNA in hydroxyurea-challenged yeasts identifies origins of replication. Nat Cell Biol *8*, 148-155.

Ferreira, M. F., Santocanale, C., Drury, L. S., and Diffley, J. F. (2000). Dbf4p, an essential S phase-promoting factor, is targeted for degradation by the anaphase-promoting complex. Mol Cell Biol *20*, 242-248.

Firmenich, A. A., Elias-Arnanz, M., and Berg, P. (1995). A novel allele of Saccharomyces cerevisiae RFA1 that is deficient in recombination and repair and suppressible by RAD52. Mol Cell Biol *15*, 1620-1631.

Fishman-Lobell, J., Rudin, N., and Haber, J. E. (1992). Two alternative pathways of double-strand break repair that are kinetically separable and independently modulated. Mol Cell Biol *12*, 1292-1303.

Flensburg, J., and Calendar, R. (1987). Bacteriophage P4 DNA replication. Nucleotide sequence of the P4 replication gene and the cis replication region. J Mol Biol *195*, 439-445.

Foiani, M., Pellicioli, A., Lopes, M., Lucca, C., Ferrari, M., Liberi, G., Muzi Falconi, M., and Plevani, P. (2000). DNA damage checkpoints and DNA replication controls in Saccharomyces cerevisiae. Mutat Res *451*, 187-196.

Foster, S. S., Zubko, M. K., Guillard, S., and Lydall, D. (2006). MRX protects telomeric DNA at uncapped telomeres of budding yeast cdc13-1 mutants. DNA Repair (Amst) *5*, 840-851.

Frank-Vaillant, M., and Marcand, S. (2001). NHEJ regulation by mating type is exercised through a novel protein, Lif2p, essential to the ligase IV pathway. Genes Dev *15*, 3005-3012.

Frank-Vaillant, M., and Marcand, S. (2002). Transient stability of DNA ends allows nonhomologous end joining to precede homologous recombination. Mol Cell *10*, 1189-1199.

Frei, C., and Gasser, S. M. (2000). The yeast Sgs1p helicase acts upstream of Rad53p in the DNA replication checkpoint and colocalizes with Rad53p in S-phase-specific foci. Genes Dev *14*, 81-96.

Friedberg, E. C. (2006). DNA repair and mutagenesis, 2nd edn (Washington, D.C., ASM Press).

Gai, D., Zhao, R., Li, D., Finkielstein, C. V., and Chen, X. S. (2004). Mechanisms of conformational change for a replicative hexameric helicase of SV40 large tumor antigen. Cell *119*, 47-60.

Gardner, R., Putnam, C. W., and Weinert, T. (1999). RAD53, DUN1 and PDS1 define two parallel G2/M checkpoint pathways in budding yeast. Embo J *18*, 3173-3185.

Gardner, R. D., and Burke, D. J. (2000). The spindle checkpoint: two transitions, two pathways. Trends Cell Biol *10*, 154-158.

Garvik, B., Carson, M., and Hartwell, L. (1995). Single-stranded DNA arising at telomeres in cdc13 mutants may constitute a specific signal for the RAD9 checkpoint. Mol Cell Biol *15*, 6128-6138.

Gasch, A. P., Huang, M., Metzner, S., Botstein, D., Elledge, S. J., and Brown, P. O. (2001). Genomic expression responses to DNA-damaging agents and the regulatory role of the yeast ATR homolog Mec1p. Mol Biol Cell *12*, 2987-3003.

Ghaemmaghami, S., Huh, W. K., Bower, K., Howson, R. W., Belle, A., Dephoure, N., O'Shea, E. K., and Weissman, J. S. (2003). Global analysis of protein expression in yeast. Nature *425*, 737-741.

Giannattasio, M., Lazzaro, F., Plevani, P., and Muzi-Falconi, M. (2005). The DNA damage checkpoint response requires histone H2B ubiquitination by Rad6-Bre1 and H3 methylation by Dot1. J Biol Chem *280*, 9879-9886.

Gibson, D. G., Aparicio, J. G., Hu, F., and Aparicio, O. M. (2004). Diminished S-phase cyclin-dependent kinase function elicits vital Rad53-dependent checkpoint responses in Saccharomyces cerevisiae. Mol Cell Biol *24*, 10208-10222.

Gilbert, C. S., Green, C. M., and Lowndes, N. F. (2001). Budding yeast Rad9 is an ATP-dependent Rad53 activating machine. Mol Cell *8*, 129-136.

Glotzer, M., Murray, A. W., and Kirschner, M. W. (1991). Cyclin is degraded by the ubiquitin pathway. Nature *349*, 132-138.

Gluzman, Y., Sambrook, J. F., and Frisque, R. J. (1980). Expression of early genes of origin-defective mutants of simian virus 40. Proc Natl Acad Sci U S A *77*, 3898-3902.

Grandin, N., Bailly, A., and Charbonneau, M. (2005). Activation of Mrc1, a mediator of the replication checkpoint, by telomere erosion. Biol Cell *97*, 799-814.
Gray, J. V., Petsko, G. A., Johnston, G. C., Ringe, D., Singer, R. A., and Werner-Washburne, M. (2004). "Sleeping beauty": quiescence in Saccharomyces cerevisiae. Microbiol Mol Biol Rev *68*, 187-206.
Green, C. M., Erdjument-Bromage, H., Tempst, P., and Lowndes, N. F. (2000). A novel Rad24 checkpoint protein complex closely related to replication factor C. Curr Biol *10*, 39-42.
Grenon, M., Gilbert, C., and Lowndes, N. F. (2001). Checkpoint activation in response to double-strand breaks requires the Mre11/Rad50/Xrs2 complex. Nat Cell Biol *3*, 844-847.
Guldener, U., Heck, S., Fielder, T., Beinhauer, J., and Hegemann, J. H. (1996). A new efficient gene disruption cassette for repeated use in budding yeast. Nucleic Acids Res *24*, 2519-2524.
Haber, J. E. (1998). Mating-type gene switching in Saccharomyces cerevisiae. Annu Rev Genet *32*, 561-599.
Haber, J. E. (2002). Uses and abuses of HO endonuclease. Methods Enzymol *350*, 141-164.
Haghnazari, E., and Heyer, W. D. (2004). The DNA damage checkpoint pathways exert multiple controls on the efficiency and outcome of the repair of a double-stranded DNA gap. Nucleic Acids Res *32*, 4257-4268.
Hardy, C. F., Dryga, O., Seematter, S., Pahl, P. M., and Sclafani, R. A. (1997). mcm5/cdc46-bob1 bypasses the requirement for the S phase activator Cdc7p. Proc Natl Acad Sci U S A *94*, 3151-3155.
Harper, J. W., Burton, J. L., and Solomon, M. J. (2002). The anaphase-promoting complex: it's not just for mitosis any more. Genes Dev *16*, 2179-2206.
Harrison, J. C., and Haber, J. E. (2006). Surviving the Breakup: The DNA Damage Checkpoint. Annu Rev Genet.
Hartwell, L. H., Culotti, J., and Reid, B. (1970). Genetic control of the cell-division cycle in yeast. I. Detection of mutants. Proc Natl Acad Sci U S A *66*, 352-359.
Hartwell, L. H., and Weinert, T. A. (1989). Checkpoints: controls that ensure the order of cell cycle events. Science *246*, 629-634.
Heid, C. A., Stevens, J., Livak, K. J., and Williams, P. M. (1996). Real time quantitative PCR. Genome Res *6*, 986-994.
Heller, R. C., and Marians, K. J. (2005). The disposition of nascent strands at stalled replication forks dictates the pathway of replisome loading during restart. Mol Cell *17*, 733-743.
Heller, R. C., and Marians, K. J. (2006). Replication fork reactivation downstream of a blocked nascent leading strand. Nature *439*, 557-562.
Henchoz, S., Chi, Y., Catarin, B., Herskowitz, I., Deshaies, R. J., and Peter, M. (1997). Phosphorylation- and ubiquitin-dependent degradation of the cyclin-dependent kinase inhibitor Far1p in budding yeast. Genes Dev *11*, 3046-3060.
Henricksen, L. A., Umbricht, C. B., and Wold, M. S. (1994). Recombinant replication protein A: expression, complex formation, and functional characterization. J Biol Chem *269*, 11121-11132.
Henry, J. M., Camahort, R., Rice, D. A., Florens, L., Swanson, S. K., Washburn, M. P., and Gerton, J. L. (2006). Mnd1/Hop2 facilitates Dmc1-dependent interhomolog crossover formation in meiosis of budding yeast. Mol Cell Biol *26*, 2913-2923.
Herrmann, G., Lindahl, T., and Schar, P. (1998). Saccharomyces cerevisiae LIF1: a function involved in DNA double-strand break repair related to mammalian XRCC4. Embo J *17*, 4188-4198.

Hiasa, H., and Marians, K. J. (1996). Two distinct modes of strand unlinking during theta-type DNA replication. J Biol Chem *271*, 21529-21535.

Hoeijmakers, J. H. (2001). Genome maintenance mechanisms for preventing cancer. Nature *411*, 366-374.

Huang, M., Zhou, Z., and Elledge, S. J. (1998a). The DNA replication and damage checkpoint pathways induce transcription by inhibition of the Crt1 repressor. Cell *94*, 595-605.

Huang, W., Feaver, W. J., Tomkinson, A. E., and Friedberg, E. C. (1998b). The N-degron protein degradation strategy for investigating the function of essential genes: requirement for replication protein A and proliferating cell nuclear antigen proteins for nucleotide excision repair in yeast extracts. Mutat Res *408*, 183-194.

Hubner, S., Xiao, C. Y., and Jans, D. A. (1997). The protein kinase CK2 site (Ser111/112) enhances recognition of the simian virus 40 large T-antigen nuclear localization sequence by importin. J Biol Chem *272*, 17191-17195.

Hubscher, U., and Seo, Y. S. (2001). Replication of the lagging strand: a concert of at least 23 polypeptides. Mol Cells *12*, 149-157.

Huyen, Y., Zgheib, O., Ditullio, R. A., Jr., Gorgoulis, V. G., Zacharatos, P., Petty, T. J., Sheston, E. A., Mellert, H. S., Stavridi, E. S., and Halazonetis, T. D. (2004). Methylated lysine 79 of histone H3 targets 53BP1 to DNA double-strand breaks. Nature *432*, 406-411.

Iftode, C., Daniely, Y., and Borowiec, J. A. (1999). Replication protein A (RPA): the eukaryotic SSB. Crit Rev Biochem Mol Biol *34*, 141-180.

Ira, G., Pellicioli, A., Balijja, A., Wang, X., Fiorani, S., Carotenuto, W., Liberi, G., Bressan, D., Wan, L., Hollingsworth, N. M., *et al.* (2004). DNA end resection, homologous recombination and DNA damage checkpoint activation require CDK1. Nature *431*, 1011-1017.

Ishimi, Y. (1992). Preincubation of T antigen with DNA overcomes repression of SV40 DNA replication by nucleosome assembly. J Biol Chem *267*, 10910-10913.

Ishimi, Y. (1997). A DNA helicase activity is associated with an MCM4, -6, and -7 protein complex. J Biol Chem *272*, 24508-24513.

Ivanov, E. L., and Haber, J. E. (1995). RAD1 and RAD10, but not other excision repair genes, are required for double-strand break-induced recombination in Saccharomyces cerevisiae. Mol Cell Biol *15*, 2245-2251.

Ivanov, E. L., Sugawara, N., Fishman-Lobell, J., and Haber, J. E. (1996). Genetic requirements for the single-strand annealing pathway of double-strand break repair in Saccharomyces cerevisiae. Genetics *142*, 693-704.

Ivanov, E. L., Sugawara, N., White, C. I., Fabre, F., and Haber, J. E. (1994). Mutations in XRS2 and RAD50 delay but do not prevent mating-type switching in Saccharomyces cerevisiae. Mol Cell Biol *14*, 3414-3425.

Jackson, L. P., Reed, S. I., and Haase, S. B. (2006). Distinct mechanisms control the stability of the related S-phase cyclins Clb5 and Clb6. Mol Cell Biol *26*, 2456-2466.

Jacobs, C. W., Adams, A. E., Szaniszlo, P. J., and Pringle, J. R. (1988). Functions of microtubules in the Saccharomyces cerevisiae cell cycle. J Cell Biol *107*, 1409-1426.

Jazayeri, A., Falck, J., Lukas, C., Bartek, J., Smith, G. C., Lukas, J., and Jackson, S. P. (2006). ATM- and cell cycle-dependent regulation of ATR in response to DNA double-strand breaks. Nat Cell Biol *8*, 37-45.

Jia, X., Weinert, T., and Lydall, D. (2004). Mec1 and Rad53 inhibit formation of single-stranded DNA at telomeres of Saccharomyces cerevisiae cdc13-1 mutants. Genetics *166*, 753-764.

Johnson, A., and O'Donnell, M. (2005). Cellular DNA replicases: components and dynamics at the replication fork. Annu Rev Biochem *74*, 283-315.

Jorgensen, P., and Tyers, M. (2004). How cells coordinate growth and division. Curr Biol *14*, R1014-1027.

Kanoh, Y., Tamai, K., and Shirahige, K. (2006). Different requirements for the association of ATR-ATRIP and 9-1-1 to the stalled replication forks. Gene.

Kantake, N., Sugiyama, T., Kolodner, R. D., and Kowalczykowski, S. C. (2003). The recombination-deficient mutant RPA (rfa1-t11) is displaced slowly from single-stranded DNA by Rad51 protein. J Biol Chem *278*, 23410-23417.

Katou, Y., Kanoh, Y., Bando, M., Noguchi, H., Tanaka, H., Ashikari, T., Sugimoto, K., and Shirahige, K. (2003). S-phase checkpoint proteins Tof1 and Mrc1 form a stable replication-pausing complex. Nature *424*, 1078-1083.

Kawamoto, T., Araki, K., Sonoda, E., Yamashita, Y. M., Harada, K., Kikuchi, K., Masutani, C., Hanaoka, F., Nozaki, K., Hashimoto, N., and Takeda, S. (2005). Dual roles for DNA polymerase eta in homologous DNA recombination and translesion DNA synthesis. Mol Cell *20*, 793-799.

Kegel, A., Sjostrand, J. O., and Astrom, S. U. (2001). Nej1p, a cell type-specific regulator of nonhomologous end joining in yeast. Curr Biol *11*, 1611-1617.

Keogh, M. C., Kim, J. A., Downey, M., Fillingham, J., Chowdhury, D., Harrison, J. C., Onishi, M., Datta, N., Galicia, S., Emili, A., *et al.* (2006). A phosphatase complex that dephosphorylates gammaH2AX regulates DNA damage checkpoint recovery. Nature *439*, 497-501.

Kerr, C., and Sadowski, P. D. (1972a). Gene 6 exonuclease of bacteriophage T7. I. Purification and properties of the enzyme. J Biol Chem *247*, 305-310.

Kerr, C., and Sadowski, P. D. (1972b). Gene 6 exonuclease of bacteriophage T7. II. Mechanism of the reaction. J Biol Chem *247*, 311-318.

Kim, H. S., and Brill, S. J. (2001). Rfc4 interacts with Rpa1 and is required for both DNA replication and DNA damage checkpoints in Saccharomyces cerevisiae. Mol Cell Biol *21*, 3725-3737.

Kim, H. S., and Brill, S. J. (2003). MEC1-dependent phosphorylation of yeast RPA1 in vitro. DNA Repair (Amst) *2*, 1321-1335.

Kim, S. M., Kumagai, A., Lee, J., and Dunphy, W. G. (2005). Phosphorylation of Chk1 by ATM- and Rad3-related (ATR) in Xenopus egg extracts requires binding of ATRIP to ATR but not the stable DNA-binding or coiled-coil domains of ATRIP. J Biol Chem *280*, 38355-38364.

Kim, S. T., Lim, D. S., Canman, C. E., and Kastan, M. B. (1999). Substrate specificities and identification of putative substrates of ATM kinase family members. J Biol Chem *274*, 37538-37543.

Knop, M., Siegers, K., Pereira, G., Zachariae, W., Winsor, B., Nasmyth, K., and Schiebel, E. (1999). Epitope tagging of yeast genes using a PCR-based strategy: more tags and improved practical routines. Yeast *15*, 963-972.

Kondo, T., Wakayama, T., Naiki, T., Matsumoto, K., and Sugimoto, K. (2001). Recruitment of Mec1 and Ddc1 checkpoint proteins to double-strand breaks through distinct mechanisms. Science *294*, 867-870.

Kornberg, A., and Baker, T. (1992). DNA replication, 2nd edn (New York, W.H. Freeman).

Kowalczykowski, S. C. (2000). Initiation of genetic recombination and recombination-dependent replication. Trends Biochem Sci *25*, 156-165.

Kunkel, T. A., and Erie, D. A. (2005). DNA mismatch repair. Annu Rev Biochem *74*, 681-710.

Kunz, B. A., Straffon, A. F., and Vonarx, E. J. (2000). DNA damage-induced mutation: tolerance via translesion synthesis. Mutat Res *451*, 169-185.

Labib, K., and Diffley, J. F. (2001). Is the MCM2-7 complex the eukaryotic DNA replication fork helicase? Curr Opin Genet Dev *11*, 64-70.

Labib, K., Diffley, J. F., and Kearsey, S. E. (1999). G1-phase and B-type cyclins exclude the DNA-replication factor Mcm4 from the nucleus. Nat Cell Biol *1*, 415-422.

Labib, K., Tercero, J. A., and Diffley, J. F. (2000). Uninterrupted MCM2-7 function required for DNA replication fork progression. Science *288*, 1643-1647.

Lee, S. E., Moore, J. K., Holmes, A., Umezu, K., Kolodner, R. D., and Haber, J. E. (1998). Saccharomyces Ku70, mre11/rad50 and RPA proteins regulate adaptation to G2/M arrest after DNA damage. Cell *94*, 399-409.

Lee, S. E., Pellicioli, A., Malkova, A., Foiani, M., and Haber, J. E. (2001). The Saccharomyces recombination protein Tid1p is required for adaptation from G2/M arrest induced by a double-strand break. Curr Biol *11*, 1053-1057.

Lee, S. E., Pellicioli, A., Vaze, M. B., Sugawara, N., Malkova, A., Foiani, M., and Haber, J. E. (2003). Yeast Rad52 and Rad51 recombination proteins define a second pathway of DNA damage assessment in response to a single double-strand break. Mol Cell Biol *23*, 8913-8923.

Lengronne, A., Pasero, P., Bensimon, A., and Schwob, E. (2001). Monitoring S phase progression globally and locally using BrdU incorporation in TK(+) yeast strains. Nucleic Acids Res *29*, 1433-1442.

Leroy, C., Lee, S. E., Vaze, M. B., Ochsenbien, F., Guerois, R., Haber, J. E., and Marsolier-Kergoat, M. C. (2003). PP2C phosphatases Ptc2 and Ptc3 are required for DNA checkpoint inactivation after a double-strand break. Mol Cell *11*, 827-835.

Leu, J. Y., and Roeder, G. S. (1999). The pachytene checkpoint in S. cerevisiae depends on Swe1-mediated phosphorylation of the cyclin-dependent kinase Cdc28. Mol Cell *4*, 805-814.

Lew, D. J. (2000). Cell-cycle checkpoints that ensure coordination between nuclear and cytoplasmic events in Saccharomyces cerevisiae. Curr Opin Genet Dev *10*, 47-53.

Li, J. J., and Kelly, T. J. (1984). Simian virus 40 DNA replication in vitro. Proc Natl Acad Sci U S A *81*, 6973-6977.

Li, J. J., and Kelly, T. J. (1985). Simian virus 40 DNA replication in vitro: specificity of initiation and evidence for bidirectional replication. Mol Cell Biol *5*, 1238-1246.

Li, L., and Zou, L. (2005). Sensing, signaling, and responding to DNA damage: organization of the checkpoint pathways in mammalian cells. J Cell Biochem *94*, 298-306.

Liku, M. E., Nguyen, V. Q., Rosales, A. W., Irie, K., and Li, J. J. (2005). CDK phosphorylation of a novel NLS-NES module distributed between two subunits of the Mcm2-7 complex prevents chromosomal rereplication. Mol Biol Cell *16*, 5026-5039.

Lipford, J. R., and Bell, S. P. (2001). Nucleosomes positioned by ORC facilitate the initiation of DNA replication. Mol Cell *7*, 21-30.

Lisby, M., Barlow, J. H., Burgess, R. C., and Rothstein, R. (2004). Choreography of the DNA damage response: spatiotemporal relationships among checkpoint and repair proteins. Cell *118*, 699-713.

Lisby, M., and Rothstein, R. (2004). DNA damage checkpoint and repair centers. Curr Opin Cell Biol *16*, 328-334.

Liu, Y., Vidanes, G., Lin, Y. C., Mori, S., and Siede, W. (2000). Characterization of a Saccharomyces cerevisiae homologue of Schizosaccharomyces pombe Chk1 involved in DNA-damage-induced M-phase arrest. Mol Gen Genet *262*, 1132-1146.

Liu, Y., and West, S. C. (2004). Happy Hollidays: 40th anniversary of the Holliday junction. Nat Rev Mol Cell Biol *5*, 937-944.

Llorente, B., and Symington, L. S. (2004). The Mre11 nuclease is not required for 5' to 3' resection at multiple HO-induced double-strand breaks. Mol Cell Biol *24*, 9682-9694.

Longhese, M. P., Clerici, M., and Lucchini, G. (2003). The S-phase checkpoint and its regulation in Saccharomyces cerevisiae. Mutat Res *532*, 41-58.

Longhese, M. P., Mantiero, D., and Clerici, M. (2006). The cellular response to chromosome breakage. Mol Microbiol *60*, 1099-1108.

Longhese, M. P., Neecke, H., Paciotti, V., Lucchini, G., and Plevani, P. (1996). The 70 kDa subunit of replication protein A is required for the G1/S and intra-S DNA damage checkpoints in budding yeast. Nucleic Acids Res *24*, 3533-3537.

Longhese, M. P., Paciotti, V., Fraschini, R., Zaccarini, R., Plevani, P., and Lucchini, G. (1997). The novel DNA damage checkpoint protein ddc1p is phosphorylated periodically during the cell cycle and in response to DNA damage in budding yeast. Embo J *16*, 5216-5226.

Longhese, M. P., Plevani, P., and Lucchini, G. (1994). Replication factor A is required in vivo for DNA replication, repair, and recombination. Mol Cell Biol *14*, 7884-7890.

Longtine, M. S., McKenzie, A., 3rd, Demarini, D. J., Shah, N. G., Wach, A., Brachat, A., Philippsen, P., and Pringle, J. R. (1998). Additional modules for versatile and economical PCR-based gene deletion and modification in Saccharomyces cerevisiae. Yeast *14*, 953-961.

Lopes, M., Cotta-Ramusino, C., Pellicioli, A., Liberi, G., Plevani, P., Muzi-Falconi, M., Newlon, C. S., and Foiani, M. (2001). The DNA replication checkpoint response stabilizes stalled replication forks. Nature *412*, 557-561.

Lou, Z., Minter-Dykhouse, K., Franco, S., Gostissa, M., Rivera, M. A., Celeste, A., Manis, J. P., van Deursen, J., Nussenzweig, A., Paull, T. T., *et al.* (2006). MDC1 maintains genomic stability by participating in the amplification of ATM-dependent DNA damage signals. Mol Cell *21*, 187-200.

Lovett, S. T. (2005). Filling the gaps in replication restart pathways. Mol Cell *17*, 751-752.

Lowndes, N. F., and Murguia, J. R. (2000). Sensing and responding to DNA damage. Curr Opin Genet Dev *10*, 17-25.

Lucca, C., Vanoli, F., Cotta-Ramusino, C., Pellicioli, A., Liberi, G., Haber, J., and Foiani, M. (2004). Checkpoint-mediated control of replisome-fork association and signalling in response to replication pausing. Oncogene *23*, 1206-1213.

Lupardus, P. J., Byun, T., Yee, M. C., Hekmat-Nejad, M., and Cimprich, K. A. (2002). A requirement for replication in activation of the ATR-dependent DNA damage checkpoint. Genes Dev *16*, 2327-2332.

Lydall, D., and Weinert, T. (1995). Yeast checkpoint genes in DNA damage processing: implications for repair and arrest. Science *270*, 1488-1491.

Ma, J. L., Lee, S. J., Duong, J. K., and Stern, D. F. (2006). Activation of the checkpoint kinase Rad53 by the phosphatidyl inositol kinase-like kinase Mec1. J Biol Chem *281*, 3954-3963.

Majka, J., Binz, S. K., Wold, M. S., and Burgers, P. M. (2006). RPA directs loading of the DNA damage checkpoint clamp to 5'-DNA junctions. J Biol Chem.

Maniar, H. S., Wilson, R., and Brill, S. J. (1997). Roles of replication protein-A subunits 2 and 3 in DNA replication fork movement in Saccharomyces cerevisiae. Genetics *145*, 891-902.

Marians, K. J. (2004). Mechanisms of replication fork restart in Escherichia coli. Philos Trans R Soc Lond B Biol Sci *359*, 71-77.

Maringele, L., and Lydall, D. (2002). EXO1-dependent single-stranded DNA at telomeres activates subsets of DNA damage and spindle checkpoint pathways in budding yeast yku70Delta mutants. Genes Dev *16*, 1919-1933.

Marston, A. L., and Amon, A. (2004). Meiosis: cell-cycle controls shuffle and deal. Nat Rev Mol Cell Biol *5*, 983-997.

McIlwraith, M. J., Vaisman, A., Liu, Y., Fanning, E., Woodgate, R., and West, S. C. (2005). Human DNA polymerase eta promotes DNA synthesis from strand invasion intermediates of homologous recombination. Mol Cell *20*, 783-792.

McInerny, C. J., Partridge, J. F., Mikesell, G. E., Creemer, D. P., and Breeden, L. L. (1997). A novel Mcm1-dependent element in the SWI4, CLN3, CDC6, and CDC47 promoters activates M/G1-specific transcription. Genes Dev *11*, 1277-1288.

McKee, A. H., and Kleckner, N. (1997). A general method for identifying recessive diploid-specific mutations in Saccharomyces cerevisiae, its application to the isolation of mutants blocked at intermediate stages of meiotic prophase and characterization of a new gene SAE2. Genetics *146*, 797-816.

McVey, D., Brizuela, L., Mohr, I., Marshak, D. R., Gluzman, Y., and Beach, D. (1989). Phosphorylation of large tumour antigen by cdc2 stimulates SV40 DNA replication. Nature *341*, 503-507.

McVey, D., Ray, S., Gluzman, Y., Berger, L., Wildeman, A. G., Marshak, D. R., and Tegtmeyer, P. (1993). cdc2 phosphorylation of threonine 124 activates the origin-unwinding functions of simian virus 40 T antigen. J Virol *67*, 5206-5215.

Melo, J., and Toczyski, D. (2002). A unified view of the DNA-damage checkpoint. Curr Opin Cell Biol *14*, 237-245.

Melo, J. A., Cohen, J., and Toczyski, D. P. (2001). Two checkpoint complexes are independently recruited to sites of DNA damage in vivo. Genes Dev *15*, 2809-2821.

Mendenhall, M. D., and Hodge, A. E. (1998). Regulation of Cdc28 cyclin-dependent protein kinase activity during the cell cycle of the yeast Saccharomyces cerevisiae. Microbiol Mol Biol Rev *62*, 1191-1243.

Milne, G. T., Jin, S., Shannon, K. B., and Weaver, D. T. (1996). Mutations in two Ku homologs define a DNA end-joining repair pathway in Saccharomyces cerevisiae. Mol Cell Biol *16*, 4189-4198.

Mimura, S., Seki, T., Tanaka, S., and Diffley, J. F. (2004). Phosphorylation-dependent binding of mitotic cyclins to Cdc6 contributes to DNA replication control. Nature *431*, 1118-1123.

Mitkova, A. V., Biswas, E. E., and Biswas, S. B. (2002). Cell cycle specific plasmid DNA replication in the nuclear extract of Saccharomyces cerevisiae: modulation by replication protein A and proliferating cell nuclear antigen. Biochemistry *41*, 5255-5265.

Moarefi, I. F., Small, D., Gilbert, I., Hopfner, M., Randall, S. K., Schneider, C., Russo, A. A., Ramsperger, U., Arthur, A. K., Stahl, H., and et al. (1993). Mutation of the cyclin-dependent kinase phosphorylation site in simian virus 40 (SV40)

large T antigen specifically blocks SV40 origin DNA unwinding. J Virol *67*, 4992-5002.

Mohr, I. J., Gluzman, Y., Fairman, M. P., Strauss, M., McVey, D., Stillman, B., and Gerard, R. D. (1989). Production of simian virus 40 large tumor antigen in bacteria: altered DNA-binding specificity and dna-replication activity of underphosphorylated large tumor antigen. Proc Natl Acad Sci U S A *86*, 6479-6483.

Moll, T., Tebb, G., Surana, U., Robitsch, H., and Nasmyth, K. (1991). The role of phosphorylation and the CDC28 protein kinase in cell cycle-regulated nuclear import of the S. cerevisiae transcription factor SWI5. Cell *66*, 743-758.

Moore, J. K., and Haber, J. E. (1996). Cell cycle and genetic requirements of two pathways of nonhomologous end-joining repair of double-strand breaks in Saccharomyces cerevisiae. Mol Cell Biol *16*, 2164-2173.

Moreau, S., Ferguson, J. R., and Symington, L. S. (1999). The nuclease activity of Mre11 is required for meiosis but not for mating type switching, end joining, or telomere maintenance. Mol Cell Biol *19*, 556-566.

Moreau, S., Morgan, E. A., and Symington, L. S. (2001). Overlapping functions of the Saccharomyces cerevisiae Mre11, Exo1 and Rad27 nucleases in DNA metabolism. Genetics *159*, 1423-1433.

Morrow, D. M., Tagle, D. A., Shiloh, Y., Collins, F. S., and Hieter, P. (1995). TEL1, an S. cerevisiae homolog of the human gene mutated in ataxia telangiectasia, is functionally related to the yeast checkpoint gene MEC1. Cell *82*, 831-840.

Moyer, S. E., Lewis, P. W., and Botchan, M. R. (2006). Isolation of the Cdc45/Mcm2-7/GINS (CMG) complex, a candidate for the eukaryotic DNA replication fork helicase. Proc Natl Acad Sci U S A *103*, 10236-10241.

Murray, A. W. (2004). Recycling the cell cycle: cyclins revisited. Cell *116*, 221-234.

Nairz, K., and Klein, F. (1997). mre11S--a yeast mutation that blocks double-strand-break processing and permits nonhomologous synapsis in meiosis. Genes Dev *11*, 2272-2290.

Nakada, D., Hirano, Y., and Sugimoto, K. (2004). Requirement of the Mre11 complex and exonuclease 1 for activation of the Mec1 signaling pathway. Mol Cell Biol *24*, 10016-10025.

Nakada, D., Hirano, Y., Tanaka, Y., and Sugimoto, K. (2005). Role of the C-Terminus of Mec1 Checkpoint Kinase in Its Localization to Sites of DNA Damage. Mol Biol Cell.

Nakada, D., Matsumoto, K., and Sugimoto, K. (2003). ATM-related Tel1 associates with double-strand breaks through an Xrs2-dependent mechanism. Genes Dev *17*, 1957-1962.

Nakamura, T. M., Du, L. L., Redon, C., and Russell, P. (2004). Histone H2A phosphorylation controls Crb2 recruitment at DNA breaks, maintains checkpoint arrest, and influences DNA repair in fission yeast. Mol Cell Biol *24*, 6215-6230.

Namiki, Y., and Zou, L. (2006). ATRIP associates with replication protein A-coated ssDNA through multiple interactions. Proc Natl Acad Sci U S A *103*, 580-585.

Nash, P., Tang, X., Orlicky, S., Chen, Q., Gertler, F. B., Mendenhall, M. D., Sicheri, F., Pawson, T., and Tyers, M. (2001). Multisite phosphorylation of a CDK inhibitor sets a threshold for the onset of DNA replication. Nature *414*, 514-521.

Nasmyth, K. (1996). At the heart of the budding yeast cell cycle. Trends Genet *12*, 405-412.

Nasmyth, K. (2001a). Disseminating the genome: joining, resolving, and separating sister chromatids during mitosis and meiosis. Annu Rev Genet *35*, 673-745.

Nasmyth, K. (2001b). A prize for proliferation. Cell *107*, 689-701.

Nasmyth, K. (2005). How do so few control so many? Cell *120*, 739-746.
Navas, T. A., Sanchez, Y., and Elledge, S. J. (1996). RAD9 and DNA polymerase epsilon form parallel sensory branches for transducing the DNA damage checkpoint signal in Saccharomyces cerevisiae. Genes Dev *10*, 2632-2643.
Neale, M. J., Pan, J., and Keeney, S. (2005). Endonucleolytic processing of covalent protein-linked DNA double-strand breaks. Nature *436*, 1053-1057.
Neecke, H., Lucchini, G., and Longhese, M. P. (1999). Cell cycle progression in the presence of irreparable DNA damage is controlled by a Mec1- and Rad53-dependent checkpoint in budding yeast. Embo J *18*, 4485-4497.
Nguyen, V. Q., Co, C., Irie, K., and Li, J. J. (2000). Clb/Cdc28 kinases promote nuclear export of the replication initiator proteins Mcm2-7. Curr Biol *10*, 195-205.
Nguyen, V. Q., Co, C., and Li, J. J. (2001). Cyclin-dependent kinases prevent DNA re-replication through multiple mechanisms. Nature *411*, 1068-1073.
Nugroho, T. T., and Mendenhall, M. D. (1994). An inhibitor of yeast cyclin-dependent protein kinase plays an important role in ensuring the genomic integrity of daughter cells. Mol Cell Biol *14*, 3320-3328.
O'Connell, M. J., and Cimprich, K. A. (2005). G2 damage checkpoints: what is the turn-on? J Cell Sci *118*, 1-6.
O'Driscoll, M., and Jeggo, P. A. (2006). The role of double-strand break repair - insights from human genetics. Nat Rev Genet *7*, 45-54.
Ooi, S. L., Shoemaker, D. D., and Boeke, J. D. (2001). A DNA microarray-based genetic screen for nonhomologous end-joining mutants in Saccharomyces cerevisiae. Science *294*, 2552-2556.
Osborn, A. J., and Elledge, S. J. (2003). Mrc1 is a replication fork component whose phosphorylation in response to DNA replication stress activates Rad53. Genes Dev *17*, 1755-1767.
Pacek, M., and Walter, J. C. (2004). A requirement for MCM7 and Cdc45 in chromosome unwinding during eukaryotic DNA replication. Embo J *23*, 3667-3676.
Paciotti, V., Clerici, M., Lucchini, G., and Longhese, M. P. (2000). The checkpoint protein Ddc2, functionally related to S. pombe Rad26, interacts with Mec1 and is regulated by Mec1-dependent phosphorylation in budding yeast. Genes Dev *14*, 2046-2059.
Palmbos, P. L., Daley, J. M., and Wilson, T. E. (2005). Mutations of the Yku80 C terminus and Xrs2 FHA domain specifically block yeast nonhomologous end joining. Mol Cell Biol *25*, 10782-10790.
Paques, F., and Haber, J. E. (1999). Multiple pathways of recombination induced by double-strand breaks in Saccharomyces cerevisiae. Microbiol Mol Biol Rev *63*, 349-404.
Parker, A. E., Clyne, R. K., Carr, A. M., and Kelly, T. J. (1997). The Schizosaccharomyces pombe rad11+ gene encodes the large subunit of replication protein A. Mol Cell Biol *17*, 2381-2390.
Parsons, A. B., Brost, R. L., Ding, H., Li, Z., Zhang, C., Sheikh, B., Brown, G. W., Kane, P. M., Hughes, T. R., and Boone, C. (2004). Integration of chemical-genetic and genetic interaction data links bioactive compounds to cellular target pathways. Nat Biotechnol *22*, 62-69.
Paulovich, A. G., and Hartwell, L. H. (1995). A checkpoint regulates the rate of progression through S phase in S. cerevisiae in response to DNA damage. Cell *82*, 841-847.

Paulovich, A. G., Margulies, R. U., Garvik, B. M., and Hartwell, L. H. (1997). RAD9, RAD17, and RAD24 are required for S phase regulation in Saccharomyces cerevisiae in response to DNA damage. Genetics *145*, 45-62.

Pellicioli, A., and Foiani, M. (2005). Signal transduction: how rad53 kinase is activated. Curr Biol *15*, R769-771.

Pellicioli, A., Lee, S. E., Lucca, C., Foiani, M., and Haber, J. E. (2001). Regulation of Saccharomyces Rad53 checkpoint kinase during adaptation from DNA damage-induced G2/M arrest. Mol Cell *7*, 293-300.

Pellicioli, A., Lucca, C., Liberi, G., Marini, F., Lopes, M., Plevani, P., Romano, A., Di Fiore, P. P., and Foiani, M. (1999). Activation of Rad53 kinase in response to DNA damage and its effect in modulating phosphorylation of the lagging strand DNA polymerase. Embo J *18*, 6561-6572.

Pickart, C. M., and Eddins, M. J. (2004). Ubiquitin: structures, functions, mechanisms. Biochim Biophys Acta *1695*, 55-72.

Pickart, C. M., and Fushman, D. (2004). Polyubiquitin chains: polymeric protein signals. Curr Opin Chem Biol *8*, 610-616.

Postow, L., Crisona, N. J., Peter, B. J., Hardy, C. D., and Cozzarelli, N. R. (2001). Topological challenges to DNA replication: conformations at the fork. Proc Natl Acad Sci U S A *98*, 8219-8226.

Prakash, S., Johnson, R. E., and Prakash, L. (2005). Eukaryotic translesion synthesis DNA polymerases: specificity of structure and function. Annu Rev Biochem *74*, 317-353.

Prakash, S., and Prakash, L. (2000). Nucleotide excision repair in yeast. Mutat Res *451*, 13-24.

Prinz, S., Amon, A., and Klein, F. (1997). Isolation of COM1, a new gene required to complete meiotic double-strand break-induced recombination in Saccharomyces cerevisiae. Genetics *146*, 781-795.

Ramsden, D. A., and Gellert, M. (1998). Ku protein stimulates DNA end joining by mammalian DNA ligases: a direct role for Ku in repair of DNA double-strand breaks. Embo J *17*, 609-614.

Raveh, D., Hughes, S. H., Shafer, B. K., and Strathern, J. N. (1989). Analysis of the HO-cleaved MAT DNA intermediate generated during the mating type switch in the yeast Saccharomyces cerevisiae. Mol Gen Genet *220*, 33-42.

Reed, S. I. (2003). Ratchets and clocks: the cell cycle, ubiquitylation and protein turnover. Nat Rev Mol Cell Biol *4*, 855-864.

Rouse, J. (2004). Esc4p, a new target of Mec1p (ATR), promotes resumption of DNA synthesis after DNA damage. Embo J *23*, 1188-1197.

Rouse, J., and Jackson, S. P. (2000). LCD1: an essential gene involved in checkpoint control and regulation of the MEC1 signalling pathway in Saccharomyces cerevisiae. Embo J *19*, 5801-5812.

Rouse, J., and Jackson, S. P. (2002a). Interfaces between the detection, signaling, and repair of DNA damage. Science *297*, 547-551.

Rouse, J., and Jackson, S. P. (2002b). Lcd1p recruits Mec1p to DNA lesions in vitro and in vivo. Mol Cell *9*, 857-869.

Rudner, A. D., and Murray, A. W. (2000). Phosphorylation by Cdc28 activates the Cdc20-dependent activity of the anaphase-promoting complex. J Cell Biol *149*, 1377-1390.

Sambrook, J., and Russell, D. W. (2001). Molecular cloning : a laboratory manual, 3rd edn (Cold Spring Harbor, N.Y., Cold Spring Harbor Laboratory Press).

Sancar, A., Lindsey-Boltz, L. A., Unsal-Kacmaz, K., and Linn, S. (2004). Molecular mechanisms of mammalian DNA repair and the DNA damage checkpoints. Annu Rev Biochem *73*, 39-85.

Sanchez, Y., Bachant, J., Wang, H., Hu, F., Liu, D., Tetzlaff, M., and Elledge, S. J. (1999). Control of the DNA damage checkpoint by chk1 and rad53 protein kinases through distinct mechanisms. Science *286*, 1166-1171.

Sanchez, Y., Desany, B. A., Jones, W. J., Liu, Q., Wang, B., and Elledge, S. J. (1996). Regulation of RAD53 by the ATM-like kinases MEC1 and TEL1 in yeast cell cycle checkpoint pathways. Science *271*, 357-360.

Sanchez-Diaz, A., Kanemaki, M., Marchesi, V., and Labib, K. (2004). Rapid depletion of budding yeast proteins by fusion to a heat-inducible degron. Sci STKE *2004*, PL8.

Sandler, S. J., and Marians, K. J. (2000). Role of PriA in replication fork reactivation in Escherichia coli. J Bacteriol *182*, 9-13.

Santocanale, C., and Diffley, J. F. (1998). A Mec1- and Rad53-dependent checkpoint controls late-firing origins of DNA replication. Nature *395*, 615-618.

Santocanale, C., Neecke, H., Longhese, M. P., Lucchini, G., and Plevani, P. (1995). Mutations in the gene encoding the 34 kDa subunit of yeast replication protein A cause defective S phase progression. J Mol Biol *254*, 595-607.

Schar, P., Herrmann, G., Daly, G., and Lindahl, T. (1997). A newly identified DNA ligase of Saccharomyces cerevisiae involved in RAD52-independent repair of DNA double-strand breaks. Genes Dev *11*, 1912-1924.

Schneider, J., and Fanning, E. (1988). Mutations in the phosphorylation sites of simian virus 40 (SV40) T antigen alter its origin DNA-binding specificity for sites I or II and affect SV40 DNA replication activity. J Virol *62*, 1598-1605.

Schollaert, K. L., Poisson, J. M., Searle, J. S., Schwanekamp, J. A., Tomlinson, C. R., and Sanchez, Y. (2004). A role for Saccharomyces cerevisiae Chk1p in the response to replication blocks. Mol Biol Cell *15*, 4051-4063.

Schwartz, M. F., Duong, J. K., Sun, Z., Morrow, J. S., Pradhan, D., and Stern, D. F. (2002). Rad9 phosphorylation sites couple Rad53 to the Saccharomyces cerevisiae DNA damage checkpoint. Mol Cell *9*, 1055-1065.

Schwob, E., Bohm, T., Mendenhall, M. D., and Nasmyth, K. (1994). The B-type cyclin kinase inhibitor p40SIC1 controls the G1 to S transition in S. cerevisiae. Cell *79*, 233-244.

Shi, Y., Dodson, G. E., Shaikh, S., Rundell, K., and Tibbetts, R. S. (2005). Ataxia-telangiectasia-mutated (ATM) is a T-antigen kinase that controls SV40 viral replication in vivo. J Biol Chem *280*, 40195-40200.

Shiloh, Y. (2003). ATM and related protein kinases: safeguarding genome integrity. Nat Rev Cancer *3*, 155-168.

Shimada, K., Pasero, P., and Gasser, S. M. (2002). ORC and the intra-S-phase checkpoint: a threshold regulates Rad53p activation in S phase. Genes Dev *16*, 3236-3252.

Shinozaki, K., and Okazaki, T. (1978). T7 gene 6 exonuclease has an RNase H activity. Nucleic Acids Res *5*, 4245-4261.

Shirahige, K., Hori, Y., Shiraishi, K., Yamashita, M., Takahashi, K., Obuse, C., Tsurimoto, T., and Yoshikawa, H. (1998). Regulation of DNA-replication origins during cell-cycle progression. Nature *395*, 618-621.

Shirayama, M., Toth, A., Galova, M., and Nasmyth, K. (1999). APC(Cdc20) promotes exit from mitosis by destroying the anaphase inhibitor Pds1 and cyclin Clb5. Nature *402*, 203-207.

Shou, W., Seol, J. H., Shevchenko, A., Baskerville, C., Moazed, D., Chen, Z. W., Jang, J., Charbonneau, H., and Deshaies, R. J. (1999). Exit from mitosis is triggered by Tem1-dependent release of the protein phosphatase Cdc14 from nucleolar RENT complex. Cell *97*, 233-244.

Shroff, R., Arbel-Eden, A., Pilch, D., Ira, G., Bonner, W. M., Petrini, J. H., Haber, J. E., and Lichten, M. (2004). Distribution and dynamics of chromatin modification induced by a defined DNA double-strand break. Curr Biol *14*, 1703-1711.

Sidorova, J. M., and Breeden, L. L. (1997). Rad53-dependent phosphorylation of Swi6 and down-regulation of CLN1 and CLN2 transcription occur in response to DNA damage in Saccharomyces cerevisiae. Genes Dev *11*, 3032-3045.

Sidorova, J. M., and Breeden, L. L. (2003). Rad53 checkpoint kinase phosphorylation site preference identified in the Swi6 protein of Saccharomyces cerevisiae. Mol Cell Biol *23*, 3405-3416.

Siede, W., Friedberg, A. S., and Friedberg, E. C. (1993). RAD9-dependent G1 arrest defines a second checkpoint for damaged DNA in the cell cycle of Saccharomyces cerevisiae. Proc Natl Acad Sci U S A *90*, 7985-7989.

Siede, W., Friedl, A. A., Dianova, I., Eckardt-Schupp, F., and Friedberg, E. C. (1996). The Saccharomyces cerevisiae Ku autoantigen homologue affects radiosensitivity only in the absence of homologous recombination. Genetics *142*, 91-102.

Sikorski, R. S., and Hieter, P. (1989). A system of shuttle vectors and yeast host strains designed for efficient manipulation of DNA in Saccharomyces cerevisiae. Genetics *122*, 19-27.

Skowyra, D., Craig, K. L., Tyers, M., Elledge, S. J., and Harper, J. W. (1997). F-box proteins are receptors that recruit phosphorylated substrates to the SCF ubiquitin-ligase complex. Cell *91*, 209-219.

Smith, G. C., Cary, R. B., Lakin, N. D., Hann, B. C., Teo, S. H., Chen, D. J., and Jackson, S. P. (1999). Purification and DNA binding properties of the ataxia-telangiectasia gene product ATM. Proc Natl Acad Sci U S A *96*, 11134-11139.

Smith, J., and Rothstein, R. (1995). A mutation in the gene encoding the Saccharomyces cerevisiae single-stranded DNA-binding protein Rfa1 stimulates a RAD52-independent pathway for direct-repeat recombination. Mol Cell Biol *15*, 1632-1641.

Smith, J., and Rothstein, R. (1999). An allele of RFA1 suppresses RAD52-dependent double-strand break repair in Saccharomyces cerevisiae. Genetics *151*, 447-458.

Smith, J., Zou, H., and Rothstein, R. (2000). Characterization of genetic interactions with RFA1: the role of RPA in DNA replication and telomere maintenance. Biochimie *82*, 71-78.

Smits, V. A., and Medema, R. H. (2001). Checking out the G(2)/M transition. Biochim Biophys Acta *1519*, 1-12.

Smogorzewska, A., and de Lange, T. (2004). Regulation of telomerase by telomeric proteins. Annu Rev Biochem *73*, 177-208.

Sogo, J. M., Lopes, M., and Foiani, M. (2002). Fork reversal and ssDNA accumulation at stalled replication forks owing to checkpoint defects. Science *297*, 599-602.

Soulier, J., and Lowndes, N. F. (1999). The BRCT domain of the S. cerevisiae checkpoint protein Rad9 mediates a Rad9-Rad9 interaction after DNA damage. Curr Biol *9*, 551-554.

Soustelle, C., Vedel, M., Kolodner, R., and Nicolas, A. (2002). Replication protein A is required for meiotic recombination in Saccharomyces cerevisiae. Genetics *161*, 535-547.

Stillman, B. W., and Gluzman, Y. (1985). Replication and supercoiling of simian virus 40 DNA in cell extracts from human cells. Mol Cell Biol *5*, 2051-2060.

Strack, B., Lessl, M., Calendar, R., and Lanka, E. (1992). A common sequence motif, -E-G-Y-A-T-A-, identified within the primase domains of plasmid-encoded I- and P-type DNA primases and the alpha protein of the Escherichia coli satellite phage P4. J Biol Chem *267*, 13062-13072.

Stucki, M., Clapperton, J. A., Mohammad, D., Yaffe, M. B., Smerdon, S. J., and Jackson, S. P. (2005). MDC1 directly binds phosphorylated histone H2AX to regulate cellular responses to DNA double-strand breaks. Cell *123*, 1213-1226.

Sugawara, N., Ira, G., and Haber, J. E. (2000). DNA length dependence of the single-strand annealing pathway and the role of Saccharomyces cerevisiae RAD59 in double-strand break repair. Mol Cell Biol *20*, 5300-5309.

Sugawara, N., Wang, X., and Haber, J. E. (2003). In vivo roles of Rad52, Rad54, and Rad55 proteins in Rad51-mediated recombination. Mol Cell *12*, 209-219.

Sullivan, C. S., and Pipas, J. M. (2002). T antigens of simian virus 40: molecular chaperones for viral replication and tumorigenesis. Microbiol Mol Biol Rev *66*, 179-202.

Sun, H., Treco, D., and Szostak, J. W. (1991). Extensive 3'-overhanging, single-stranded DNA associated with the meiosis-specific double-strand breaks at the ARG4 recombination initiation site. Cell *64*, 1155-1161.

Sun, Z., Fay, D. S., Marini, F., Foiani, M., and Stern, D. F. (1996). Spk1/Rad53 is regulated by Mec1-dependent protein phosphorylation in DNA replication and damage checkpoint pathways. Genes Dev *10*, 395-406.

Sun, Z., Hsiao, J., Fay, D. S., and Stern, D. F. (1998). Rad53 FHA domain associated with phosphorylated Rad9 in the DNA damage checkpoint. Science *281*, 272-274.

Sundin, O., and Varshavsky, A. (1980). Terminal stages of SV40 DNA replication proceed via multiply intertwined catenated dimers. Cell *21*, 103-114.

Sundin, O., and Varshavsky, A. (1981). Arrest of segregation leads to accumulation of highly intertwined catenated dimers: dissection of the final stages of SV40 DNA replication. Cell *25*, 659-669.

Sung, P. (1997). Function of yeast Rad52 protein as a mediator between replication protein A and the Rad51 recombinase. J Biol Chem *272*, 28194-28197.

Sutton, M. D., Smith, B. T., Godoy, V. G., and Walker, G. C. (2000). The SOS response: recent insights into umuDC-dependent mutagenesis and DNA damage tolerance. Annu Rev Genet *34*, 479-497.

Suzuki, K., Kodama, S., and Watanabe, M. (1999). Recruitment of ATM protein to double strand DNA irradiated with ionizing radiation. J Biol Chem *274*, 25571-25575.

Sweeney, F. D., Yang, F., Chi, A., Shabanowitz, J., Hunt, D. F., and Durocher, D. (2005). Saccharomyces cerevisiae Rad9 acts as a Mec1 adaptor to allow Rad53 activation. Curr Biol *15*, 1364-1375.

Szostak, J. W., Orr-Weaver, T. L., Rothstein, R. J., and Stahl, F. W. (1983). The double-strand-break repair model for recombination. Cell *33*, 25-35.

Tanaka, K., and Russell, P. (2001). Mrc1 channels the DNA replication arrest signal to checkpoint kinase Cds1. Nat Cell Biol *3*, 966-972.

Tanaka, K., and Russell, P. (2004). Cds1 phosphorylation by Rad3-Rad26 kinase is mediated by forkhead-associated domain interaction with Mrc1. J Biol Chem *279*, 32079-32086.

Tanaka, S., and Diffley, J. F. (2002a). Deregulated G1-cyclin expression induces genomic instability by preventing efficient pre-RC formation. Genes Dev *16*, 2639-2649.

Tanaka, S., and Diffley, J. F. (2002b). Interdependent nuclear accumulation of budding yeast Cdt1 and Mcm2-7 during G1 phase. Nat Cell Biol *4*, 198-207.

Tanaka, T. U. (2002). Bi-orienting chromosomes on the mitotic spindle. Curr Opin Cell Biol *14*, 365-371.

Teo, S. H., and Jackson, S. P. (1997). Identification of Saccharomyces cerevisiae DNA ligase IV: involvement in DNA double-strand break repair. Embo J *16*, 4788-4795.

Teo, S. H., and Jackson, S. P. (2000). Lif1p targets the DNA ligase Lig4p to sites of DNA double-strand breaks. Curr Biol *10*, 165-168.

Tercero, J. A., and Diffley, J. F. (2001). Regulation of DNA replication fork progression through damaged DNA by the Mec1/Rad53 checkpoint. Nature *412*, 553-557.

Tercero, J. A., Labib, K., and Diffley, J. F. (2000). DNA synthesis at individual replication forks requires the essential initiation factor Cdc45p. Embo J *19*, 2082-2093.

Tercero, J. A., Longhese, M. P., and Diffley, J. F. (2003). A central role for DNA replication forks in checkpoint activation and response. Mol Cell *11*, 1323-1336.

Thelen, M. P., Venclovas, C., and Fidelis, K. (1999). A sliding clamp model for the Rad1 family of cell cycle checkpoint proteins. Cell *96*, 769-770.

Tocchetti, A., Galimberti, G., Deho, G., and Ghisotti, D. (1999). Characterization of the oriI and oriII origins of replication in phage-plasmid P4. J Virol *73*, 7308-7316.

Toczyski, D. P., Galgoczy, D. J., and Hartwell, L. H. (1997). CDC5 and CKII control adaptation to the yeast DNA damage checkpoint. Cell *90*, 1097-1106.

Toh, G. W., and Lowndes, N. F. (2003). Role of the Saccharomyces cerevisiae Rad9 protein in sensing and responding to DNA damage. Biochem Soc Trans *31*, 242-246.

Toh, G. W., O'Shaughnessy, A. M., Jimeno, S., Dobbie, I. M., Grenon, M., Maffini, S., O'Rorke, A., and Lowndes, N. F. (2006). Histone H2A phosphorylation and H3 methylation are required for a novel Rad9 DSB repair function following checkpoint activation. DNA Repair (Amst) *5*, 693-703.

Tran, P. T., Erdeniz, N., Dudley, S., and Liskay, R. M. (2002). Characterization of nuclease-dependent functions of Exo1p in Saccharomyces cerevisiae. DNA Repair (Amst) *1*, 895-912.

Tran, P. T., Erdeniz, N., Symington, L. S., and Liskay, R. M. (2004). EXO1-A multi-tasking eukaryotic nuclease. DNA Repair (Amst) *3*, 1549-1559.

Tseng, H. M., and Tomkinson, A. E. (2002). A physical and functional interaction between yeast Pol4 and Dnl4-Lif1 links DNA synthesis and ligation in nonhomologous end joining. J Biol Chem *277*, 45630-45637.

Tsubouchi, H., and Ogawa, H. (1998). A novel mre11 mutation impairs processing of double-strand breaks of DNA during both mitosis and meiosis. Mol Cell Biol *18*, 260-268.

Tsubouchi, H., and Ogawa, H. (2000). Exo1 roles for repair of DNA double-strand breaks and meiotic crossing over in Saccharomyces cerevisiae. Mol Biol Cell *11*, 2221-2233.

Tyers, M., Tokiwa, G., Nash, R., and Futcher, B. (1992). The Cln3-Cdc28 kinase complex of S. cerevisiae is regulated by proteolysis and phosphorylation. Embo J *11*, 1773-1784.

Ubersax, J. A., Woodbury, E. L., Quang, P. N., Paraz, M., Blethrow, J. D., Shah, K., Shokat, K. M., and Morgan, D. O. (2003). Targets of the cyclin-dependent kinase Cdk1. Nature *425*, 859-864.

Umezu, K., Sugawara, N., Chen, C., Haber, J. E., and Kolodner, R. D. (1998). Genetic analysis of yeast RPA1 reveals its multiple functions in DNA metabolism. Genetics *148*, 989-1005.

Unsal-Kacmaz, K., and Sancar, A. (2004). Quaternary structure of ATR and effects of ATRIP and replication protein A on its DNA binding and kinase activities. Mol Cell Biol *24*, 1292-1300.

Usui, T., Ogawa, H., and Petrini, J. H. (2001). A DNA damage response pathway controlled by Tel1 and the Mre11 complex. Mol Cell *7*, 1255-1266.

Usui, T., Ohta, T., Oshiumi, H., Tomizawa, J., Ogawa, H., and Ogawa, T. (1998). Complex formation and functional versatility of Mre11 of budding yeast in recombination. Cell *95*, 705-716.

Valencia, M., Bentele, M., Vaze, M. B., Herrmann, G., Kraus, E., Lee, S. E., Schar, P., and Haber, J. E. (2001). NEJ1 controls non-homologous end joining in Saccharomyces cerevisiae. Nature *414*, 666-669.

Varshavsky, A. (1997). The N-end rule pathway of protein degradation. Genes Cells *2*, 13-28.

Vaze, M. B., Pellicioli, A., Lee, S. E., Ira, G., Liberi, G., Arbel-Eden, A., Foiani, M., and Haber, J. E. (2002). Recovery from checkpoint-mediated arrest after repair of a double-strand break requires Srs2 helicase. Mol Cell *10*, 373-385.

Vialard, J. E., Gilbert, C. S., Green, C. M., and Lowndes, N. F. (1998). The budding yeast Rad9 checkpoint protein is subjected to Mec1/Tel1- dependent hyperphosphorylation and interacts with Rad53 after DNA damage. Embo J *17*, 5679-5688.

Virshup, D. M., Kauffman, M. G., and Kelly, T. J. (1989). Activation of SV40 DNA replication in vitro by cellular protein phosphatase 2A. Embo J *8*, 3891-3898.

Virshup, D. M., Russo, A. A., and Kelly, T. J. (1992). Mechanism of activation of simian virus 40 DNA replication by protein phosphatase 2A. Mol Cell Biol *12*, 4883-4895.

Visintin, R., Craig, K., Hwang, E. S., Prinz, S., Tyers, M., and Amon, A. (1998). The phosphatase Cdc14 triggers mitotic exit by reversal of Cdk-dependent phosphorylation. Mol Cell *2*, 709-718.

Visintin, R., Hwang, E. S., and Amon, A. (1999). Cfi1 prevents premature exit from mitosis by anchoring Cdc14 phosphatase in the nucleolus. Nature *398*, 818-823.

Wach, A., Brachat, A., Alberti-Segui, C., Rebischung, C., and Philippsen, P. (1997). Heterologous HIS3 marker and GFP reporter modules for PCR-targeting in Saccharomyces cerevisiae. Yeast *13*, 1065-1075.

Wach, A., Brachat, A., Pohlmann, R., and Philippsen, P. (1994). New heterologous modules for classical or PCR-based gene disruptions in Saccharomyces cerevisiae. Yeast *10*, 1793-1808.

Waga, S., Bauer, G., and Stillman, B. (1994). Reconstitution of complete SV40 DNA replication with purified replication factors. J Biol Chem *269*, 10923-10934.

Waga, S., and Stillman, B. (1994). Anatomy of a DNA replication fork revealed by reconstitution of SV40 DNA replication in vitro. Nature *369*, 207-212.

Waga, S., and Stillman, B. (1998). The DNA replication fork in eukaryotic cells. Annu Rev Biochem *67*, 721-751.

Wakayama, T., Kondo, T., Ando, S., Matsumoto, K., and Sugimoto, K. (2001). Pie1, a protein interacting with Mec1, controls cell growth and checkpoint responses in Saccharomyces cerevisiae. Mol Cell Biol *21*, 755-764.

Walter, J., and Newport, J. (2000). Initiation of eukaryotic DNA replication: origin unwinding and sequential chromatin association of Cdc45, RPA, and DNA polymerase alpha. Mol Cell *5*, 617-627.

Walter, J., Sun, L., and Newport, J. (1998). Regulated chromosomal DNA replication in the absence of a nucleus. Mol Cell *1*, 519-529.

Walther, A. P., Bjerke, M. P., and Wold, M. S. (1999). A novel assay for examining the molecular reactions at the eukaryotic replication fork: activities of replication protein A required during elongation. Nucleic Acids Res *27*, 656-664.

Wang, H., Liu, D., Wang, Y., Qin, J., and Elledge, S. J. (2001). Pds1 phosphorylation in response to DNA damage is essential for its DNA damage checkpoint function. Genes Dev *15*, 1361-1372.

Wang, J. C. (2002). Cellular roles of DNA topoisomerases: a molecular perspective. Nat Rev Mol Cell Biol *3*, 430-440.

Wang, X., and Haber, J. E. (2004). Role of saccharomyces single-stranded DNA-binding protein RPA in the strand invasion step of double-strand break repair. PLoS Biol *2*, E21.

Ward, I. M., Minn, K., Jorda, K. G., and Chen, J. (2003). Accumulation of checkpoint protein 53BP1 at DNA breaks involves its binding to phosphorylated histone H2AX. J Biol Chem *278*, 19579-19582.

Weinert, T. A., and Hartwell, L. H. (1988). The RAD9 gene controls the cell cycle response to DNA damage in Saccharomyces cerevisiae. Science *241*, 317-322.

Weinert, T. A., and Hartwell, L. H. (1993). Cell cycle arrest of cdc mutants and specificity of the RAD9 checkpoint. Genetics *134*, 63-80.

Weinert, T. A., Kiser, G. L., and Hartwell, L. H. (1994). Mitotic checkpoint genes in budding yeast and the dependence of mitosis on DNA replication and repair. Genes Dev *8*, 652-665.

Weinreich, M., Palacios DeBeer, M. A., and Fox, C. A. (2004). The activities of eukaryotic replication origins in chromatin. Biochim Biophys Acta *1677*, 142-157.

Weinreich, M., and Stillman, B. (1999). Cdc7p-Dbf4p kinase binds to chromatin during S phase and is regulated by both the APC and the RAD53 checkpoint pathway. Embo J *18*, 5334-5346.

Weisshart, K., Pestryakov, P., Smith, R. W., Hartmann, H., Kremmer, E., Lavrik, O., and Nasheuer, H. P. (2004). Coordinated regulation of replication protein A activities by its subunits p14 and p32. J Biol Chem *279*, 35368-35376.

West, S. C. (2003). Molecular views of recombination proteins and their control. Nat Rev Mol Cell Biol *4*, 435-445.

White, C. I., and Haber, J. E. (1990). Intermediates of recombination during mating type switching in Saccharomyces cerevisiae. Embo J *9*, 663-673.

Willems, A. R., Schwab, M., and Tyers, M. (2004). A hitchhiker's guide to the cullin ubiquitin ligases: SCF and its kin. Biochim Biophys Acta *1695*, 133-170.

Wilson, T. E., Grawunder, U., and Lieber, M. R. (1997). Yeast DNA ligase IV mediates non-homologous DNA end joining. Nature *388*, 495-498.

Wilson, T. E., Topper, L. M., and Palmbos, P. L. (2003). Non-homologous end-joining: bacteria join the chromosome breakdance. Trends Biochem Sci *28*, 62-66.

Wiltzius, J. J., Hohl, M., Fleming, J. C., and Petrini, J. H. (2005). The Rad50 hook domain is a critical determinant of Mre11 complex functions. Nat Struct Mol Biol *12*, 403-407.

Winey, M., and O'Toole, E. T. (2001). The spindle cycle in budding yeast. Nat Cell Biol *3*, E23-27.

Wold, M. S. (1997). Replication protein A: a heterotrimeric, single-stranded DNA-binding protein required for eukaryotic DNA metabolism. Annu Rev Biochem *66*, 61-92.

Wold, M. S., and Kelly, T. (1988). Purification and characterization of replication protein A, a cellular protein required for in vitro replication of simian virus 40 DNA. Proc Natl Acad Sci U S A *85*, 2523-2527.

Wold, M. S., Li, J. J., and Kelly, T. J. (1987). Initiation of simian virus 40 DNA replication in vitro: large-tumor-antigen- and origin-dependent unwinding of the template. Proc Natl Acad Sci U S A *84*, 3643-3647.

Wolner, B., van Komen, S., Sung, P., and Peterson, C. L. (2003). Recruitment of the recombinational repair machinery to a DNA double-strand break in yeast. Mol Cell *12*, 221-232.

Wu, X., Shell, S. M., and Zou, Y. (2005). Interaction and colocalization of Rad9/Rad1/Hus1 checkpoint complex with replication protein A in human cells. Oncogene *24*, 4728-4735.

Wurtele, H., and Verreault, A. (2006). Histone post-translational modifications and the response to DNA double-strand breaks. Curr Opin Cell Biol *18*, 137-144.

Wysocki, R., Javaheri, A., Allard, S., Sha, F., Cote, J., and Kron, S. J. (2005). Role of Dot1-dependent histone H3 methylation in G1 and S phase DNA damage checkpoint functions of Rad9. Mol Cell Biol *25*, 8430-8443.

Wysocki, R., and Kron, S. J. (2004). Yeast cell death during DNA damage arrest is independent of caspase or reactive oxygen species. J Cell Biol *166*, 311-316.

Xiao, C. Y., Jans, P., and Jans, D. A. (1998). Negative charge at the protein kinase CK2 site enhances recognition of the SV40 large T-antigen NLS by importin: effect of conformation. FEBS Lett *440*, 297-301.

Xu, Y. J., Davenport, M., and Kelly, T. J. (2006). Two-stage mechanism for activation of the DNA replication checkpoint kinase Cds1 in fission yeast. Genes Dev *20*, 990-1003.

Zachariae, W., Schwab, M., Nasmyth, K., and Seufert, W. (1998). Control of cyclin ubiquitination by CDK-regulated binding of Hct1 to the anaphase promoting complex. Science *282*, 1721-1724.

Zegerman, P., and Diffley, J. F. (2003). Lessons in how to hold a fork. Nat Struct Biol *10*, 778-779.

Zhang, H., Taylor, J., and Siede, W. (2003). Checkpoint arrest signaling in response to UV damage is independent of nucleotide excision repair in Saccharomyces cerevisiae. J Biol Chem *278*, 9382-9387.

Zhao, X., Muller, E. G., and Rothstein, R. (1998). A suppressor of two essential checkpoint genes identifies a novel protein that negatively affects dNTP pools. Mol Cell *2*, 329-340.

Zhao, X., and Rothstein, R. (2002). The Dun1 checkpoint kinase phosphorylates and regulates the ribonucleotide reductase inhibitor Sml1. Proc Natl Acad Sci U S A *99*, 3746-3751.

Zhou, Z., and Elledge, S. J. (1993). DUN1 encodes a protein kinase that controls the DNA damage response in yeast. Cell *75*, 1119-1127.

Ziegelin, G., and Lanka, E. (1995). Bacteriophage P4 DNA replication. FEMS Microbiol Rev *17*, 99-107.

Ziegelin, G., Linderoth, N. A., Calendar, R., and Lanka, E. (1995). Domain structure of phage P4 alpha protein deduced by mutational analysis. J Bacteriol *177*, 4333-4341.

Ziegelin, G., Scherzinger, E., Lurz, R., and Lanka, E. (1993). Phage P4 alpha protein is multifunctional with origin recognition, helicase and primase activities. Embo J *12*, 3703-3708.

Zou, L., and Elledge, S. J. (2003). Sensing DNA damage through ATRIP recognition of RPA-ssDNA complexes. Science *300*, 1542-1548.

Zou, L., Liu, D., and Elledge, S. J. (2003). Replication protein A-mediated recruitment and activation of Rad17 complexes. Proc Natl Acad Sci U S A *100*, 13827-13832.